Localisation, Activity and Targeting of Bcr-Abl in Chronic Myeloid Leukaemia

Peixun Zhou

BSc Hons, MRes

A thesis submitted for the degree of Doctor of Philosophy to the

University of Glasgow

April 2011

Paul O'Gorman Leukaemia Research Centre

Institute of Cancer Sciences

College of Medical, Veterinary and Life Sciences

Abstract

Chronic myeloid leukaemia (CML) is a myeloproliferative disease of stem cell origin. It is characterised by the Philadelphia chromosome and Bcr-Abl oncoprotein which is a constitutively activated tyrosine kinase that is causative in CML. Treatment of CML was revolutionized by tyrosine kinase inhibitors (TKIs) in the last decade. TKIs target Bcr-Abl and block its tyrosine kinase activity. Despite the success of TKI in eliminating differentiated CML cells, primitive quiescent CML stem cells still resist or persist with TKI treatment. In this study, several strategies have been investigated towards elimination of TKI-insensitive primitive CML stem cells.

At first, the effect of nuclear entrapment of Bcr-Abl protein in CML cells was studied. Although Bcr-Abl protein is located in the cytoplasm of CML cells, TKIs, such as imatinib mesylate (IM), can induce the nuclear translocation of Bcr-Abl. Nuclear Bcr-Abl tyrosine kinase is capable of inducing apoptosis after drug washout, and leptomycin B (LMB) can trap translocated Bcr-Abl in the nucleus. Primary CML $CD34^+$ cells were treated with IM and LMB either continuously or sequentially. It was found that neither regimen significantly increased the anti-proliferative effect of IM in primary CML $CD34^+$ cells. It was also observed that the majority of Bcr-Abl was still retained in the cytoplasm of CML cells treated with IM and LMB, suggesting other mechanisms apart from its tyrosine kinase activity retained Bcr-Abl protein in the cytoplasm of CML cells. Next the subcellular distribution of Bcr-Abl was investigated in TKI-insensitive CML progenitors which survived 12-Day treatment of a potent TKI dasatinib (150nM).

It was demonstrated that about 50% of Bcr-Abl was still retained in the cytoplasm of TKI-insensitive primary CML progenitors, although there was a significant increase in nuclear Bcr-Abl level in these survived cells compared to the no drug control (NDC). It was hypothesised that the cytoplasmic retention of Bcr-Abl was caused by its cytoplasmic binding partners, and it was found that a proportion of Bcr-Abl protein was associated with 14-3-3 proteins in the surviving cells, indicating the cytoplasmic retention of Bcr-Abl might be due to its binding with 14-3-3 proteins.

In addition, due to the rapid nature of kinase inhibition and nuclear transportation, studies are required to measure the earliest time-point of inhibition of Bcr-Abl tyrosine kinase by IM. The common method to do this is to employ p-CrkL which has been widely used as a surrogate marker of Bcr-Abl tyrosine kinase activity, but the accuracy of p-CrkL as an indicator of Bcr-Abl tyrosine kinase status at early time-points during *in vitro* TKI treatment has not been examined. It was demonstrated that p-CrkL was not a reliable indicator of Bcr-Abl kinase activity within 24 hours of IM treatment *in vitro* and indicated that the early responses to IM and dasatinib were different. It was also observed that there was a rapid and active dephosphorylation of Bcr-Abl within 1 hour of TKI treatment, driven at least in part by protein tyrosine phosphatase activity.

Furthermore, a farnesyltransferase inhibitor (FTI) BMS-214662 preferentially induces apoptosis in CML stem and progenitor cells compared to their normal counterparts, but another similar FTI BMS-225975 does not. However, the mechanism of action of

BMS-214662 in inducing apoptosis of CML cells is not clear. When BMS-214662 was used as a negative control in the p-CrkL study, it was unexpectedly observed that the drug accumulated Bcr-Abl protein in CML cells. Thus, it was hypothesised that BMS-214662 may function as a proteasome inhibitor, which could result in accumulation of Bcr-Abl protein and further elevation of intracellular ROS level, leading to apoptosis of CML cells. Although BMS-214662 treatment induced accumulation of total ubiquitinated proteins and specifically Bcr-Abl protein in K562 cells, BMS-225975 had very similar effects, and this might result from the common mechanism of BMS-214662 and BMS-225975, which is their FTI activity. On the other hand, BMS-214662 induced significantly higher levels of intracellular ROS in both proliferating and non-proliferating K562 cells with respect to BMS-225975, indicating the production of ROS may be involved in the non-FTI mechanism of action of BMS-214662. However it was concluded that BMS-214662 was not a proteasome inhibitor like bortezomib.

Finally, the use of synthetic low density lipoprotein (sLDL) as a vehicle for drug delivery to overcome the insufficient intracellular drug concentration in CML stem cells was investigated. Uptake and internalization of unloaded sLDL particles by CML cell line K562 and for the first time by CML stem cells was observed, demonstrating the targeting potential of sLDL particles in CML when they are loaded with drugs.

Overall, this study provides further understanding of CML treatment and identifies some alternative strategies to target CML stem cells that may be used in combination with TKI to enhance the eradication of this stem cell-driven disease.

Table of Contents

List of Figures

List of Tables

Related Publications

Allan EK, Hamilton A, Hatziieremia S, **Zhou P**, Jorgensen HG, Vigneri P, et al. Nuclear entrapment of BCR-ABL by combining imatinib mesylate with leptomycin B does not eliminate $CD34^+$ chronic myeloid leukaemia cells. Leukemia 2009;23(5):1006-8.

Zhou P, Hatziieremia S, Elliott MA, Scobie L, Crossan C, Michie AM, et al. Uptake of synthetic Low Density Lipoprotein by leukemic stem cells — a potential stem cell targeted drug delivery strategy. Journal of controlled release 2010 20;148(3):380-7.

Zhou P, Hatziieremia S, Elliott MA, Holyoake TL, Halbert GW, Jorgensen HG. Synthetic low density lipoprotein uptake by leukaemic haemopoietic stem cells. Scottish Society for Experimental Medicine and Scottish Lipid Discussion Group 2009. No published abstracts [Oral Presentations]

Zhou P, Holyoake TL, Mountford JC, Jorgensen HG. p-CrkL is not a surrogate of Bcr-Abl activity in vitro at short time-points. British Journal of Haematology 2010;149:77. [Poster]

Zhou P, Hatziieremia S, Elliott MA, Abraham S, Holyoake TL, Halbert GW, et al. Uptake of synthetic low density lipoprotein by leukaemic stem cells - a potential targeted drug delivery strategy. British Journal of Haematology 2010;149:76. [Poster]

Leitch C, Shah M, Gallipoli P, **Zhou P**, Yule M, Holyoake TL, et al. JAK2 is a relevant target in chronic myeloid leukaemia. British Journal of Haematology 2010;149:77. [Poster]

Zhou P, Holyoake T, Mountford J, Jorgensen H. p-CrkL Is Not A Surrogate of Bcr-Abl Activity in Vitro at Short Time-Points. Haematologica-the Hematology Journal 2010;95:336. [Poster]

Acknowledgements

This thesis would not have been possible without the essential help from many individuals. Firstly, I owe my deepest gratitude to my principal supervisor Dr. Heather Jørgensen and my co-supervisor Dr Jo Mountford who have given me enormous help, guidance and support from the beginning to the end of the PhD project. This thesis would not have completed without their patience and encouragement.

I would like to show my gratitude to Elaine Allan who helped me carry out some of the research shown in this thesis, Professor Tessa Holyoake for her invaluable support, Dr. Ashley Hamilton and Dr. Alan Hair for their technical support, Dr. Vignir Helgason and Dr. Sheela Abraham for their useful advices. I also would like to thank all my colleagues at the Paul O'Gorman Leukaemia Research Centre who helped me in any respect during the PhD project.

In addition, it is an honour for me to thank my family and friends for their selfless support. Finally, I would like to thank the Glasgow Royal Infirmary Endowment Fund and University of Glasgow for funding this research.

Author’s Declaration

I declare that all data presented in this thesis is my own work, unless otherwise stated.

Abbreviations

5-FU	5-fluorouracil
7-AAD	7-Amino-actinomycin D
ABC	ATP binding cassette
Abl	Abelson kinase
ALL	Acute lymphoid leukaemia
AML	Acute myeloid leukaemia
AP	Accelerated phase
ATP	Adenosine triphosphate
Bad	Bcl-2 associated death promoter
Bap-1	Bcr-associated protein 1
BC	Blast crisis
BCA	Bicinchoninic acid
Bcl-2	B-cell lymphoma-2
Bcl-xL	B-cell lymphoma-extra large
Bcr-Abl	Bcr-Abl fusion gene
Bcr-Abl	Breakpoint cluster region-abelson
BMT	Bone marrow transplantation
bp	base pair
BSA	Bovine serum albumin
CaLB	Calcium dependent lipid binding domain
Cbl	Casitas B-lineage lymphoma
CCgR	Complete cytogenetic response
cDNA	complementary DNA
CESE	Carboxyeosin succinimidyl ester
CFC	Colony-forming cell
CHR	Complete haematologic response
CLP	Common lymphoid progenitor
CML	Chronic myeloid leukaemia

CMP	Common myeloid progenitor
CMR	Complete molecular response
CP	Chronic phase
CrkL	v-Crk avian sarcoma virus CT10 oncogene homolog-like
CSC	Cancer stem cell
CTxB	Cholera toxin subunit B
DAPI	4,6-diamidino-2-phenylindole
DCF	2',7'-dichlorofluorescein
DCFDA	2'-7'-Dichlorofluorescin diacetate
D-FISH	Double-fusion FISH
dH_2O	distilled water
DiO	Dioctadecyloxacarbocyanine
DMSO	Dimethyl sulpoxide
DNA	Deoxyribonucleic acid
DOX	Doxorubicin
FABD	F-actin binding domain
F-actin	Filament-actin
FCS	Foetal calf serum
FDA	Food and Drug Administration
FISH	Fluorescence in situ hybridization
FITC	Fluorescein isothiocyanate
FOXO3a	Forkhead box O3a
FTI	Farnesyltransferase inhibitor
FSC	Forward scatter
GAP	GTPase activation protein
GAPDH	Glyceraldehyde-3-phosphate dehydrogenase
G-CSF	Granulocyte colony-stimulating factor
GDP	Guanosine diphosphate
GEF	Guanine nucleotide exchange factor
GFs	Growth factors

GM1	Monosialotetrahexosylganglioside
GM-CSF	Granulocyte macrophage colony-stimulating factor
GMP	Granulocyte-macrophage progenitor
G-protein	Guanosine-nucleotide-binding protein
Grb2	Growth factor receptor bound protein 2
GTP	Guanosine triphosphate
GTPase	Guanosine triphosphatase
Hck	Haemopoietic cell kinase
hOCT1	human organic cation transporter
HRP	Horseradish peroxidise
HSC	Haemopoietic stem cell
IFN-α	Interferon-alpha
IGF-IR	Type 1 insulin-like growth factor receptor
IL1RAP	IL-1 receptor accessory protein
IL-3	Interleukin-3
IL-6	Interleukin-6
IM	Imatinib mesylate
IP	Immunoprecipitation
JAK	Janus kinase
JNK	c-Jun N-terminal kinase
kDa	KiloDalton
LDL	Low density lipoprotein
LDLR	Low density lipoprotein receptor
LMB	Leptomycin B
LREC	Local Research Ethics Committee
LSC	Leukaemic stem cell
LTC-IC	Long-Term Culture-Initiating Cell
LT-HSC	long-term HSC
MAPK	Mitogen activated protein kinase
M-bcr	Major break point cluster region

m-bcr	minor break point cluster region
MCgR	Major cytogenetic response
mCgR	Minor cytogenetic response
Mcl-1	Myeloid cell leukaemia-1
MDM2	Murine double minute 2
MEP	Megakaryocyte-erythroid progenitor
MFI	Mean fluorescence intensity
MMR	Major molecular response
MNC	Mononuclear cells
MPP	Multipotent progenitor
mRNA	messenger RNA
NDC	No drug control
NES	Nuclear export signal
NHL	non-Hodgkin's Lymphoma
NLS	Nuclear localisation signal
NOD/SCID	Nonobese diabetic/severe combined immunodeficient
PBS	Phosphate buffered saline
PCgR	Partial cytogenetic response
PCR	Polymerase chain reaction
p-CrkL	Phosphorylated CrkL
PDGF-R	Platelet-derived growth factor receptors
PGFs	Physiological growth factors
Ph	Philadelphia
PH domain	Pleckstrin homology domain
PHR	Partial haematologic response
PI	Propidium iodine
PI3K	Phosphatidylositol 3-kinase
PKCβ	Protein kinase Cβ
PLCγ	Phospholipase Cγ
PP2A	Protein phosphatase 2A

PTP1B	Protein tyrosine phosphatase 1B
PTP	Protein tyrosine phosphatase
PTK	Protein tyrosine kinase
p-Tyr	Phosphorylated tyrosine
p-Tyr Bcr-Abl	tyrosine phosphorylated Bcr-Abl
PVDF	Polyvinylidene fluoride
qRT-PCR	quantitative reverse transcription PCR
Ras	Rat sarcoma
RNA	Ribonucleic acid
ROS	Reactive oxygen species
Rpm	Revolutions per minute
RT	Reverse transcription
RTK	Receptor tyrosine kinase
SCF	Stem cell factor
SCT	Stem cell transplantation
SDS-PAGE	Sodium dodecyl sulphate-polyacrylamide gel electrophoresis
SFM	Serum free medium
SH	Src homology
Shc	Src homology-containing
siRNA	small interfering RNA
sLDL	synthetic low density lipoprotein
SL-IC	SCID leukaemia-initiating cell
SOS	Son of sevenless
SRC	SCID-repopulating cell
SSC	Side scatter
SSG	Sodium Stibogluconate
ST-HSC	Short-term HSC
STAT	Signal transducers and activators of transcription
Syp	Synaptophysin
TK	Tyrosine kinase

TKI	Tyrosine kinase inhibitor
Ub	Ubiquitin
WB	Western blotting
WCL	Whole cell lysate
WCC	white cell count

1 Introduction

1.1 Haemopoiesis and haemopoietic stem cells

Haemopoiesis is the production of blood cells as a result of differentiation of haemopoietic stem cells (HSCs) (1;2). HSCs are multipotent cells which are capable of both self-renewal and differentiation into all types of blood cells by a hierarchically progressive lineage commitment of haemopoietic stem and progenitor cells (Figure 1-1). In addition, HSCs reside in the bone marrow, and account for no more than 0.05% of bone marrow cells (1). Since most mature blood cells are terminally differentiated and short-lived in blood circulation, it is essential to generate functional blood cells to maintain the haemopoietic system in a steady state through the proliferation and differentiation of haemopoietic stem and progenitor cells (2). Furthermore, about 1.5×10^6 blood cells are continuously generated every second in an adult human (3).

The balance between self-renewal and differentiation is regulated to maintain the HSC pool while generating sufficient progeny, and this can be achieved by asymmetrical cell division where one HSC gives rise to an identical daughter cell and a differentiated progeny (4). In addition, HSC can also divide symmetrically to generate two identical daughter cells or two differentiated progeny (4). The fate of HSCs is thought to be regulated by factors in their bone marrow microenvironment, i.e. stem cell niche (5).

HSC function is usually assessed *in vitro* by colony-forming cell (CFC) and long-term culture initiating-cell (LTC-IC) assays or *in vivo* by bone marrow engraftment of non-obese diabetic/severe combined immunodeficient (NOD/SCID) mice (6). CFC assays detect multipotent and committed progenitors, while LTC-IC assays detect more primitive progenitors which are able to form colonies after 5-8 weeks culture on a stromal feeder layer (7;8). SCID-repopulation cells (SRCs) are capable of reconstituting NOD/SCID mice with a singe cell and are more primitive than most CFC or LTC-IC (9).

Based on their ability to reconstitute the haemopoietic system of lethally irradiated mice, HSCs can be separated into three distinct groups: long-term HSCs (LT-HSCs) which are able to generate all types of blood cells for the lifetime of the animals and reconstitute secondary hosts; short-term HSCs (ST-HSCs) which derive from LT-HSCs but can only reconstitute myeloid and/or lymphoid lineages for a limited period of time; multipotent progenitors (MPPs), which are generated by ST-HSCs, have no detectable self-renewal capacity and only transiently reconstitute lethally irradiated mice (10;11). MPPs can differentiate into common myeloid progenitors (CMPs) or common lymphoid progenitors (CLPs) which then give rise to myeloid or lymphoid lineage, respectively (12;13).

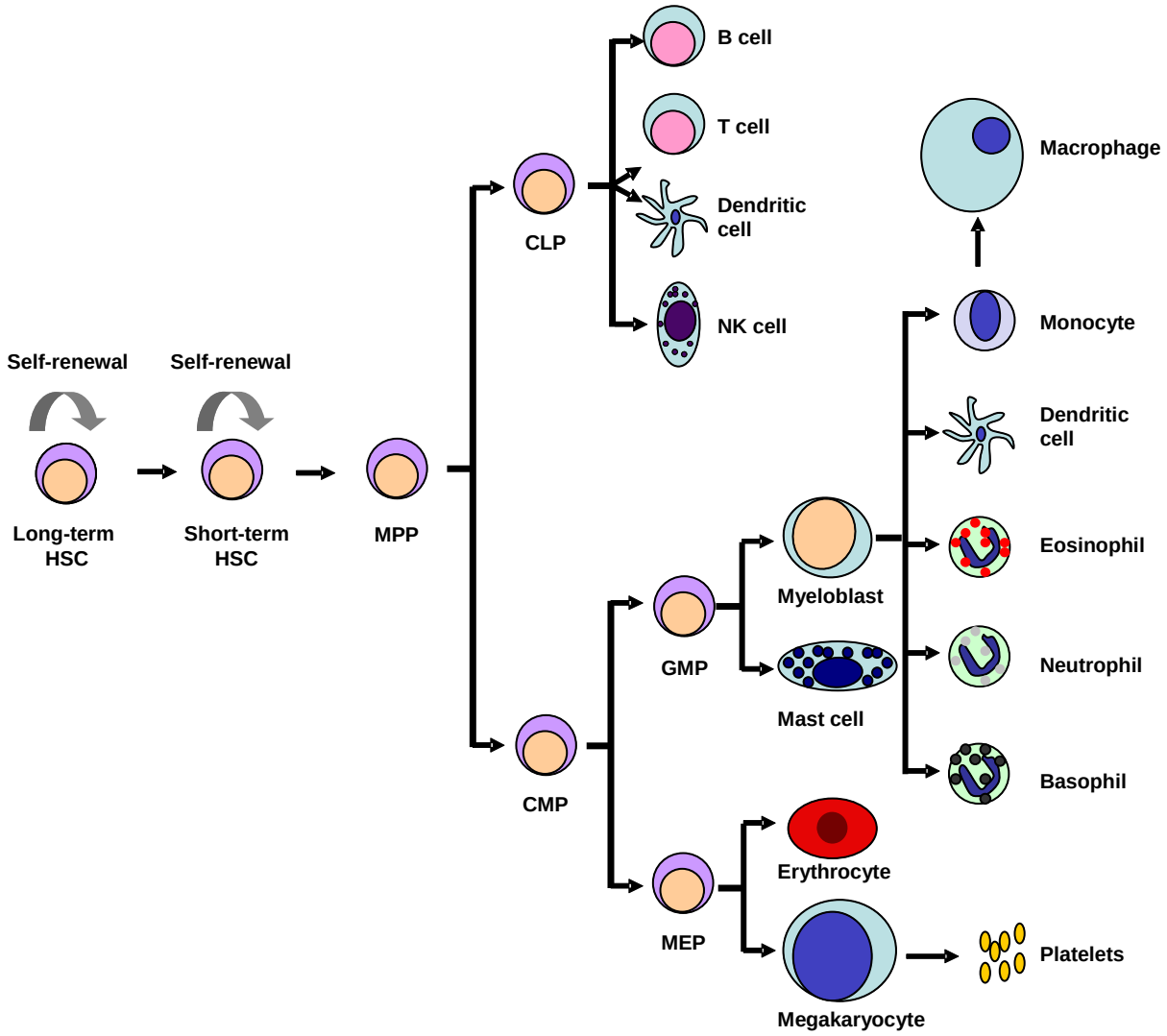

Figure 1-1: The model of haemopoietic hierarchy.

Long-term and short-term HSCs have self-renewal capacity, which is lost in MPPs. The multi-potent progenitors differentiate into CLPs or CMPs, which give rise to mature cells after several differentiation steps. MEP: megakaryocyte-erythroid progenitor, GMP: granulocyte-macrophage progenitor. Adapted from Passegue *et al*., 2003 (14)

There is evidence to suggest that the majority of HSCs are out of cell cycle and in a quiescent state (in G_0 phase of the cell cycle), as illustrated by the resistance of murine primitive haemopoietic cells to a anti-mitotic drug, 5-fluorouracil (5-FU) (15). It was also found that primitive human haemopoietic progenitors could remain in culture as single cells for more than 14 days and only started to divide with stimulation of some growth factors (16). Furthermore, it was estimated by mathematical modelling that HSCs only divide once every year, and each HSC could divide about 70 times in its lifetime (17). Thus, it is thought that at steady state homeostasis only a small fraction of HSCs are in cell cycle and repopulate the haemopoietic system (18) to ensure the stem cell pool is not exhausted throughout life. In addition, cell cycle arrest in G_0 also allows cells to repair any DNA damage and maintain genomic stability (19).

Cell surface antigens can be used to distinguish HSCs from differentiated cells in a heterogeneous haemopoietic population. CD34 is a widely used cell surface marker to identify HSCs, since the most primitive haemopoietic cells are contained in the $CD34^+$ population. The frequency of LTC-IC in an enriched $CD34^+$ population is 200-400 times higher than in total human bone marrow mononuclear cells (8). In addition, human bone marrow $CD34^+$ compartment contains primitive HSCs which are capable of generating all haemopoietic lineages (20). Furthermore, purified mobilized peripheral blood $CD34^+$ cells are capable of reconstituting the whole haemopoietic system after human allogeneic transplantation (21). $CD34^+$ cells represent about 1.5% of normal human bone marrow mononuclear cells (22), and the level of CD34 expression decreases progressively along with increased differentiation of these cells

(23). CD34 is a 115 kiloDaltons (kDa) transmembrane glycoprotein which may be involved in cell localisation, adhesion and signal transduction of haemopoietic stem and progenitor cells, but the understanding of its precise function is limited (22;24).

However, haemopoietic $CD34^+$ population is heterogeneous, and it contains primitive and committed haemopoietic progenitors (25). Thus, other cell surface markers are used together with CD34 to identify more primitive progenitors (26). It was found that SRCs are exclusively $CD34^+CD38^-$, and the frequency was calculated as 1 SRC in 617 $CD34^+CD38^-$ cells by limiting dilution analysis (26). $CD34^+CD38^-$ cells are capable of repopulating lethally irradiated mice in a continuous and multi-lineage manner (26;27), while $CD34^+CD38^+$ cord blood cells repopulate lethally irradiated mice rapidly but only transiently (27). CD38 is a transmembrane glycoprotein, and its expression on the cell surface is elevated in correlation with increased differentiation (28). CD38 is expressed in more than 90% of $CD34^+$ cells, and $CD34^+CD38^-$ cells represent about 0.05% of bone marrow or cord blood mononuclear cells (28). $CD34^+CD38^-$ cells are mainly quiescent in the absence of cytokine stimulation (28;29). After transplantation into irradiated mice, human $CD34^+CD38^-$ cells are located at the stem cell niche in a quiescent state, and these cells can engraft secondary recipient mice (30). Overall, the primitive HSCs are within the $CD34^+CD38^-$ compartment.

In addition, human $CD34^+CD38^-$ cells can be further fractionated based on cell-surface HLA-DR expression. Human bone marrow $CD34^+CD38^-$ HLA-DR^+ cells can

differentiate into all lineages of haemopoietic system, while the more primitive $CD34^{+}CD38^{-}$ HLA-DR^{-} cells can generate not only all haemopoietic lineages but also stromal cells which can support HSCs in the bone marrow microenvironment (20). In addition, CD133 (also known as AC133 or Prominin 1) is another cell surface marker to identify human HSCs (31). CD133 is a 5-transmembrane glycoprotein, and can be present on the cell surface of CD34 bright haemopoietic progenitors (31). Enriched human mobilized peripheral $CD133^{+}$ cells effectively engraft NOD/SCID mice, as well as secondary recipient mice (32). Purified human $CD133^{+}$ cells contain more primitive progenitors than $CD34^{+}$ cells as demonstrated by LTC-IC assay (33). Human $CD34^{+}CD133^{+}$ haemopoietic cells have a higher engraftment capacity of NOD/SCID mice than $CD34^{+}CD133^{-}$ cells (34), indicating $CD34^{+}CD133^{+}$ cells are more primitive than $CD34^{+}CD133^{-}$ cells.

1.1.1 Leukaemic stem cells

The hypothesis of cancer stem cells (CSCs) describes the existence of a small subset of cancer cells which are likely responsible for tumourigenesis, metastasis and disease relapse (35). CSCs have characteristics of normal stem cells, especially extensive self-renewal capability (35).

The leukaemic stem cell (LSC) is a paradigm of CSC model. Early studies suggested that only a small fraction of leukaemic cells was able to proliferate extensively *in vitro* and *in vivo* (14). Park *et al*. demonstrated that about 1 in 100-10,000 leukaemic cells form colonies in CFC assay *in vitro* (36), and only 1-4% of leukaemic cells formed

colonies in spleen after murine transplantation (37). These clonogenic leukaemic cells were thought to be LSCs (14). In 1997, Bonnet and Dick showed that a tiny proportion of human acute myeloid leukaemia (AML) blasts were capable of engrafting NOD/SCID mice, and producing a disease same as human AML (38). These cells were defined as SCID leukaemia-initiating cells (SL-ICs) and they were exclusively $CD34^{+}CD38^{-}$ in every patient, which is very similar to the phenotype of normal SRCs (38). In addition, these SL-ICs have great self-renewal capacity as assessed by successful engraftment of secondary recipient mice (38). These observations suggest that leukaemic transformations occur in primitive normal haemopoietic cells, which then give rise to leukaemia through clonal expansion (38). On the other hand, the leukaemic transformation may also occur in committed normal progenitors which then regain self-renewal capability and initiate leukaemias (14) (Figure 1-2).

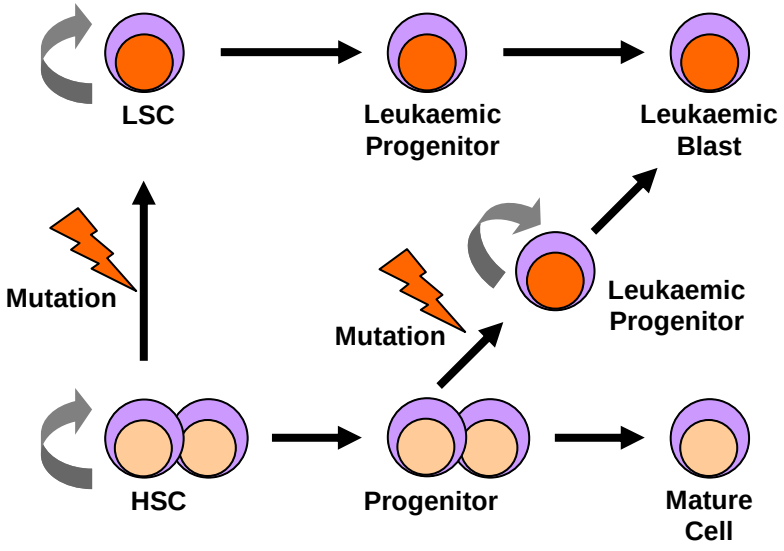

Figure 1-2: Model of leukaemic stem cell transformation.

Leukaemogenesis can occur in HSCs which give rise to a LSC with self-renewal capability. Alternatively, it can happen in progenitor cells which then reacquire self-renewal capacity. Adapted from Passegue *et al*., 2003 (14)

1.2 Chronic myeloid leukaemia

Chronic myeloid leukaemia (CML) is a clonal myeloproliferative disease of stem cell origin (39). The Bcr-Abl protein is present in multiple haemopoietic lineages including myeloid, erythroid, B-lymphoid and occasionally T-lymphoid cells in most CML patients, suggesting the *Bcr-Abl* oncogene is formed in HSCs (14). By studying female patients with X chromosome linked heterozygous alleles, CML was demonstrated to be a clonal disease with origin in a single multipotent stem cell (39;40).

The incidence of CML each year is 1 to 2 cases per one hundred thousand of the population, and it affects all age groups with median age of onset about 45-55 years (2;41). It accounts for about 20% of leukaemias in adults (41). CML is characterised by the presence of the Philadelphia (Ph) chromosome and *Bcr-Abl* oncogene. The reciprocal translocation between the long arms of chromosomes 9 and 22, t(9;22)-(q34;q11), results in a shortened chromosome 22, which is termed the Philadelphia (Ph) chromosome (Figure 1-3)(42;43). It is found in 95% of CML patients, and in 5% of children and 15-30% of adults with acute lymphoid leukaemia (ALL) (41). In addition, it is also present in 2% of patients with recently diagnosed AML (41).

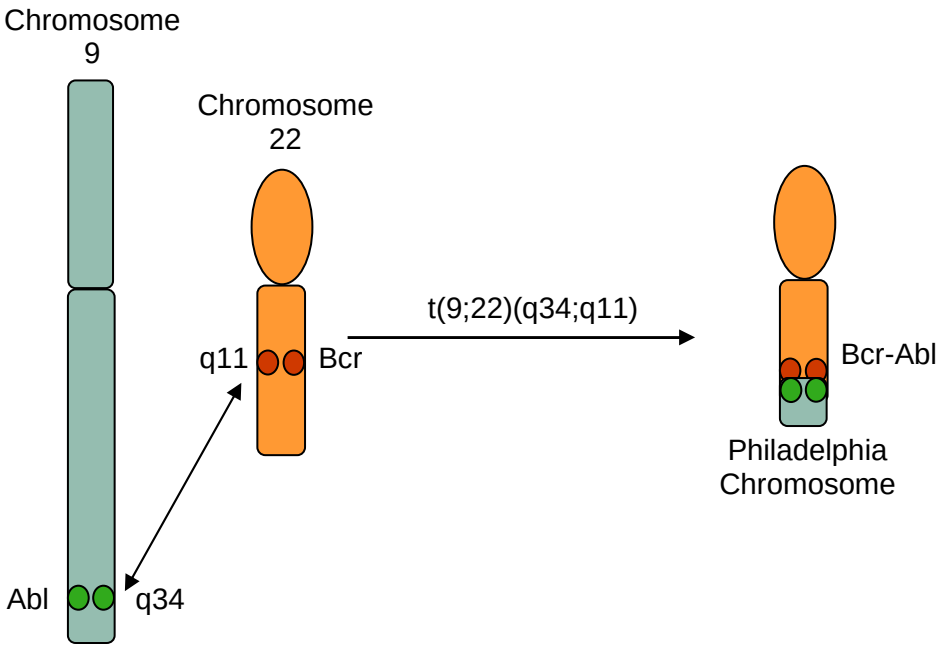

Figure 1-3: Formation of the Philadelphia chromosome and *Bcr-Abl* oncogene.

The reciprocal translocation between long arms of chromosome 9 and 22 results in a fused oncogene *Bcr-Abl* and a shortened chromosome 22, the Philadelphia chromosome. Adapted from Smith *et al*., 2003 (2).

The reciprocal translocation results in a fusion gene *Bcr-Abl* on the Ph chromosome (44). The fusion gene product, Bcr-Abl protein, significantly affects cell growth, turnover, differentiation, apoptosis and adhesion (44). The *Abl* (Abelson kinase) gene located on chromosome 9 has 11 exons and is 230 kilobase (kb). The breakpoint in *Abl* gene is usually upstream of exon 2 (41). In most cases, *Abl* gene exons 2 to 11 are translocated to the major break point cluster region(M-bcr) of the *Bcr* gene on chromosome 22, forming a hybrid *Bcr-Abl* gene. It is then transcribed into an 8.5 kb chimeric messenger ribonucleic acid (mRNA) with an e14a2 or e13a2 (also known as

b3a2 or b2a2) junction, and then mRNA is translated into a $p210^{Bcr\text{-}Abl}$ fusion protein (41;44;45). In rare cases of CML and in common cases of Ph positive ALL, the breakpoint of chromosome 22 occurs in a minor break point cluster region (m-bcr), and results in a e1a2 junction mRNA and a 190 kDa Bcr-Abl fusion protein, which is termed as $p190^{Bcr\text{-}Abl}$ (41;44). In very rare cases of CML, a third breakpoint is detected downstream of the M-bcr between exons e19 and e20 of *Bcr* gene, it is termed µ-bcr. Its transcription product is a mRNA with e19a2 junction and its final product is a 230 kDa Bcr-Abl protein which is termed $p230^{Bcr\text{-}Abl}$ (41;44) (Figure 1-4).

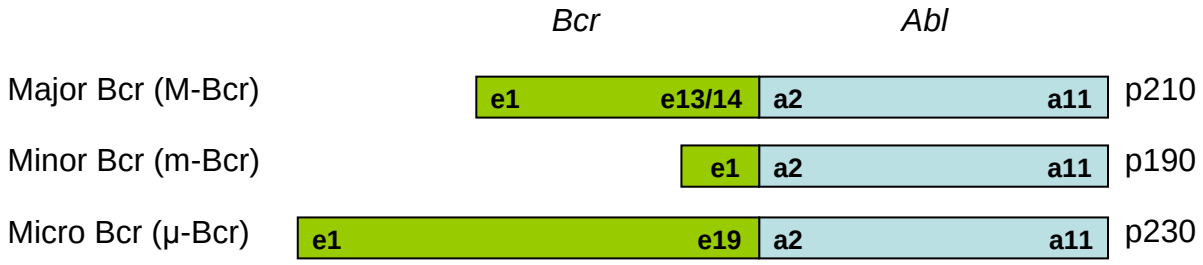

Figure 1-4: Three forms of *Bcr-Abl* oncogene.

Adapted from Franklin *et al*., 1999 (41).

CML is characterized by a triphasic clinical course (45), comprising initial chronic phase (CP), secondary accelerated phase (AP) and terminal blast crisis (BC) (41). About 85% of CML patients are diagnosed in CP, with common symptoms at presentation being abdominal fullness, anaemia, bleeding, fatigue, leukocytosis, purpura, splenomegaly, thrombocytosis and weight loss (41;46). CP CML features abnormal elevation of the number of myeloid progenitor and mature cells in the blood

and bone marrow (4;46;47). Bcr-Abl^{+} CML is diagnosed and monitored by the presence of Ph chromosome with cytogenetics, visualization of *Bcr-Abl* oncogene by double-fusion fluorescent in situ hybridization (D-FISH), or detection of Bcr-Abl mRNA with quantitative reverse-transcription polymerase chain reaction (qRT-PCR) (48;49).

The diagnostic criteria for AP and BC CML defined by the World Health Organisation are listed in the following table (Table 1-1). If left untreated, CP CML progresses to AP and BC about 3-5 years after onset (50). However, transformation of AP into BC can happen in several weeks or months (2). In the later stages, differentiation is blocked and non-functional immature blast cells accumulate in the blood and bone marrow, resembling acute leukaemias (2;47). Most patients acquire additional cytogenetic abnormality while progressing into BC CML (51), and the BC transformation can be myeloid, lymphoid or both lineages with very poor prognosis (2). The median survival time for myeloid and lymphoid BC CML is 4-5 months and 12 months, respectively (2).

AP CML (Diagnosed if one or more of the following present)
● 10 to 19% of peripheral blood white cells or bone marrow cells are blasts ● Peripheral blood basophils ≥20% ● Persistent thrombocytopenia (100 x 10^9/L) unrelated to therapy, or persistent thrombocytosis (1000 x 10^9/L) unresponsive to therapy ● Increasing spleen size and increasing WC count unresponsive to therapy ● Cytogenetic evidence of clonal evolution
BC CML (Diagnosed if one or more of the following present)
● ≥20% of peripheral blood white cells or bone marrow cells are blasts ● Extramedullary blast proliferation ● Large foci or clusters of blasts in BM biopsy

Table 1-1: Criteria for the diagnosis of AP and BC CML.

Adapted from Vardiman *et al*., 2002 (52)

1.2.1 The causal relationship between Bcr-Abl and CML

Bcr-Abl is thought to play an essential role in the leukaemic transformation of haemopoietic cells and in the pathogenesis of CML (44). Nowell and Hungerford described that an abnormally short chromosome in 1960, which was lately named Ph chromosome, was consistently present in seven patients with chronic granulocytic leukaemia but not in normal cells of those patients or cells of other leukaemias, suggesting there was a causal relationship between Ph chromosome and chronic granulocytic leukaemia (53). Then Rowley discovered in 1973 that the Ph chromosome was a hybrid of chromosome 9 and 22 (54), and the fusion gene *Bcr-Abl*

was revealed on the Ph chromosome in 1980s (55). In 1990, Elefanty *et al*. introduced Bcr-Abl bearing retrovirus into bone marrow cells, and reconstituted lethally irradiated mice with these cells, resulting in a mild CML-like syndrome among several haemopoietic neoplasms (56). In the same year, introduction of Bcr-Abl by retrovirus into murine haemopoietic stem cells was employed to reconstitute lethally irradiated mice, and a myeloproliferative syndrome similar to human CP CML was developed prominently among half of recipient mice (57). Several years later, an improved method produced a human CML-like myeloproliferative disease in all recipient mice after transplantation of bone marrow cells with virally transfected Bcr-Abl, and it is transplantable to secondary recipients (58). In addition, Bcr-Abl is associated with emergence of additional genomic abnormality and progression of CP CML into BC (59;60). Therefore, the leukaemogenic nature of Bcr-Abl makes it a therapeutic target in treating CML (2).

1.3 Structures and functions of Bcr, c-Abl and Bcr-Abl

1.3.1 Bcr

Bcr is a 160 kDa protein with several structural and functional domains (61). There is a coiled-coil oligomerization domain in the N-terminus of Bcr (62). This domain enables Bcr to form a homotetramer. Downstream of the coiled-coil domain, there is a Src homology (SH) 2 binding domain (63). This domain is able to interact with the SH2 domain on c-Abl in a phosphotyrosine independent manner (63). In addition, there is a serine/threonine kinase located in the N-terminus encoded by the first exon

of *Bcr* (64). Located in the C-terminal of Bcr is a GTPase activating domain, which can increase the guanosine triphosphate (GTP) hydrolysis rate of a $p21^{Rac}$ GTP binding protein (G protein) (65). Also in the C-terminal of Bcr, there is a domain homologous to guanine nucleotide exchange factors (GEFs) of $p21^{Rho/Rac}$ family of G proteins (66). There is also a pleckstrin homology domain (PH domain) and a calcium dependent lipid binding (CaLB) domain in the Bcr protein (61) (Figure 1-5A). Having different types of structural and functional properties, Bcr protein may be involved in different signalling pathways and serve as the cross point of these pathways, but the understanding of the biological function of Bcr protein is limited (49;61).

1.3.2 Abl

C-Abl protein is a 145 kDa non-receptor tyrosine kinase (41). There are two splice variants of c-Abl, encoding two proteins with their difference in the first exon (1a and 1b). C-Abl 1b is slightly longer than 1a and contains a myristoyl group at its N-terminus, and this myristoyl group links c-Abl 1b with lipid membrane (67). Located in the N-terminus of c-Abl are three SH domains: SH3, SH2 and SH1. The SH3 domain binds to proline-rich (PxxP) motifs (68;69), and negatively regulates c-Abl tyrosine kinase activity (41). C-Abl tyrosine kinase can be activated by deletion of the SH3 domain (70). The SH2 domain binds to phosphotyrosine residues in a sequence specific manner (68;69). The phosphotyrosine binding ability and transforming potential of activated Abl is reduced by point mutations in the SH2 domain (71). The following SH1 domain carries a tyrosine kinase (68). Downstream there are three proline-rich sequences which can interact with SH3-containing proteins (69). Towards

the C-terminus of c-Abl are three nuclear localisation signals (NLSs) and a nuclear export signal (NES), enabling it to shuttle between cell nucleus and cytoplasm (49;72). Located in the C-terminus are DNA and actin binding domains (49;73) (Figure 1-5B).

C-Abl is mainly located in the cytoplasm of human haemopoietic cells with a low-level presence in the nucleus (74), whereas it is largely present in the nucleus of fibroblasts (75). The tyrosine kinase activity of c-Abl is tightly regulated *in vivo*, and its activity is very low in normal context (76). C-Abl can be activated by cell cycle progression, DNA damage and integrin mediated adhesion (68). C-Abl tyrosine kinase is increased during cell cycle progression to S phase (68). Activated c-Abl phosphorylates C-terminal domain of RNA polymerase II and enhances transcription (68;77). In addition, c-Abl is activated in response to DNA damage and induces cell cycle arrest or apoptosis (78). Furthermore, integrin mediated adhesion can induce transient cytoplasmic translocation and activation of c-Abl in fibroblasts, which then activates mitogen activated protein kinase (MAPK) cascade (79;80).

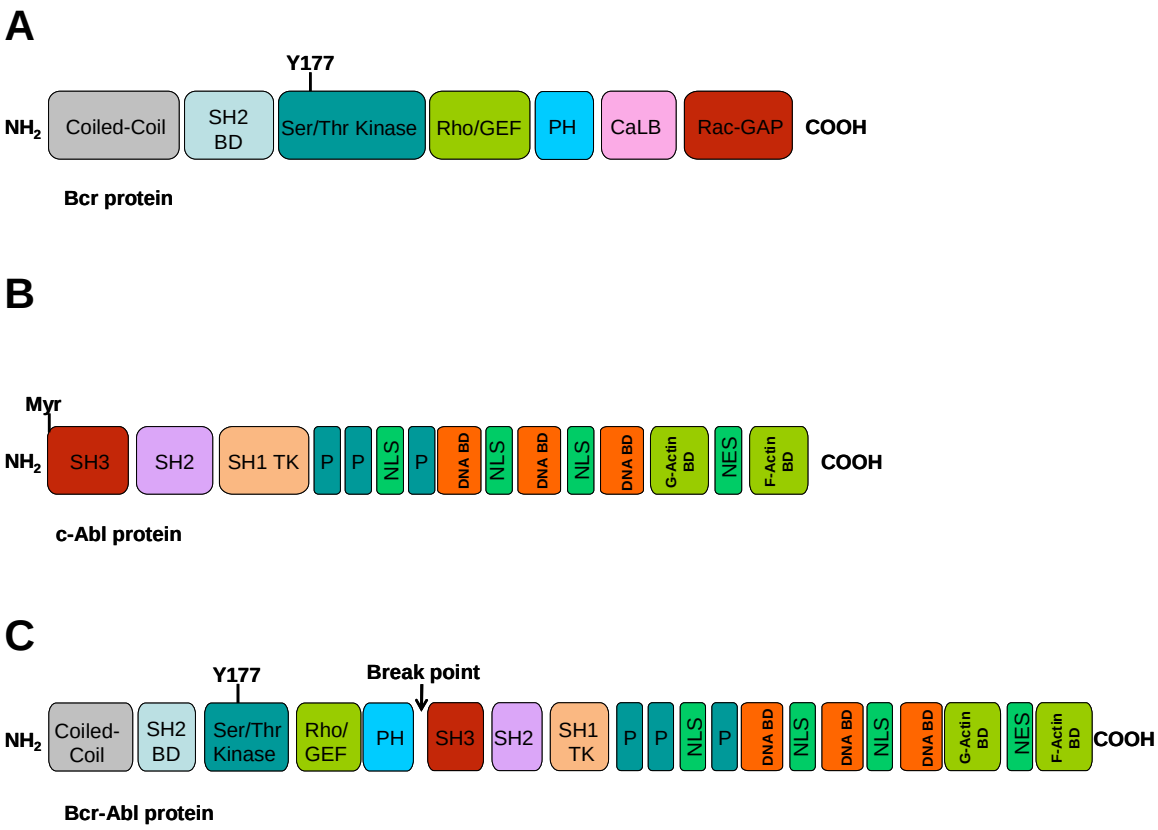

Figure 1-5: The structural and functional domains of Bcr, c-Abl and Bcr-Abl proteins.

(A) In Bcr, the coiled-coil oligomerization domain resides at the N-terminus. This is followed by a SH2 binding domain. Then there is a serine/threonine kinase domain, a Rho guanine nucleotide exchange factor (Rho-GEF) domain, a pleckstrin homology domain (PH domain), a calcium dependent lipid binding (CaLB) domain and a Rac GTPase activating protein (Rac-GAP) domain. (B) In c-Abl, there is a myristoyl group (in c-Abl 1b but not 1a), a Src homology 3 (SH3) domain, a SH2 domain and a SH1 tyrosine kinase (TK) domain at the N-terminus, followed by several proline-rich domains (P) and three nuclear localisation signals (NLSs). At the C-terminus there are DNA- and actin-binding domains and a nuclear export signal (NES). (C) Bcr-Abl contains the first five domains of Bcr and all the c-Abl domains except the N-terminus

encoded by its first exon. Adapted from Smith *et al.,* 2003 (2) and Deininger *et al.,* 2003 (49).

1.3.3 Bcr-Abl

The p210 Bcr-Abl protein forms dimers or tetramers *in vivo* that autophosphorylate each other (81). Fusion of Bcr to c-Abl inhibits the latter's SH3 kinase regulatory domain, resulting in constitutive activation of the Abl tyrosine kinase in Bcr-Abl (41). Two domains of Bcr are thought to be essential for Abl tyrosine kinase activation and transforming potential of the Bcr-Abl oncoprotein: amino acids 1-63 and 176-242 (62). The first domain is the coiled-coil oligomerization domain, and it is involved in the deregulation of Abl tyrosine kinase and enhancement of filament (F)-actin binding ability of Abl (82). Mutations in the oligomerization domain abolished the transforming activity of Bcr-Abl protein (62). Disruption of the Bcr-Abl tetramer by a competitive peptide of the coiled-coil oligomerization domain of Bcr efficiently inhibited tyrosine kinase activity and transforming function of Bcr-Abl protein (83). The second critical domain for kinase activation and transforming potential is the SH2 binding domain of Bcr (62), which deregulates tyrosine kinase by binding to Abl SH2 domain (63). On the other hand, Abl tyrosine kinase impairs Bcr serine/threonine kinase by phosphorylating Y360 residue on Bcr and Bcr-Abl (84). A deleted form of Bcr which cannot be tyrosine phosphorylated, inhibits tyrosine kinase activity of active c-Abl and Bcr-Abl, suggesting tyrosine phosphorylation of Bcr abolishes its inhibitory activity (85).

Bcr-Abl can interact and/or phosphorylate many proteins, making Bcr-Abl involved in diverse intracellular signalling pathways, including Ras-MAPK, PI3K-Akt, and JAK-STAT pathways (44;86) (Figure 1-6 and Table 1-2). Bcr-Abl was found to bind several adaptor proteins, such as growth factor receptor bound protein 2 (Grb2), v-Crk avian sarcoma virus CT10 oncogene homologue-like (CrkL) protein and Src homology-containing (Shc) protein (41). Grb2 is an SH2/3 domain-containing adaptor protein. The SH2 domain of Grb2 interacts with the phosphorylated Y177 residue located in the N-terminal part of Bcr-Abl (84). Y177F mutation impaired binding of Bcr-Abl with Grb2, and inhibited Ras signalling which can be activated by wild type Bcr-Abl (87). Interaction with Grb2 is essential for the transforming ability of Bcr-Abl. The Y177F Bcr-Abl mutant was not able to transform Rat1 fibroblasts and murine bone marrow cells (87).

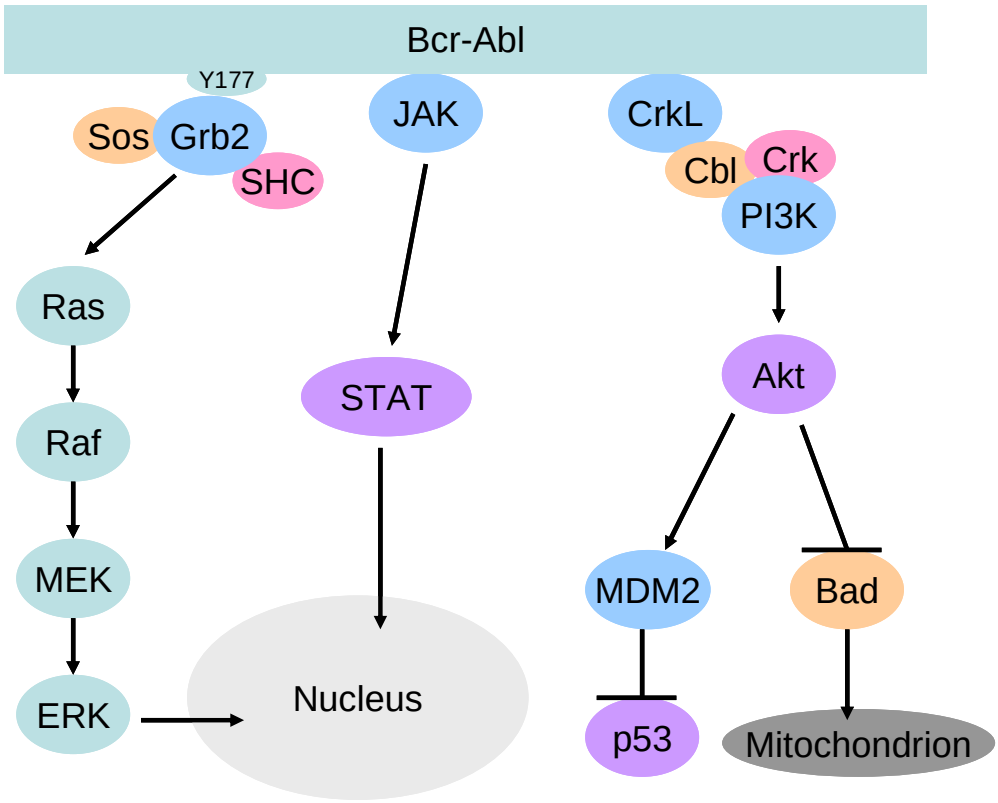

Figure 1-6: Major signalling pathways activated by Bcr-Abl protein in CML cells.

IL-3 activates these signalling pathways (PI3K-Akt, Ras-Raf-MEK-ERK and JAK-STAT) in Bcr-Abl$^-$ cells to promote growth, survival and differentiation. In CML cells, these pathways can be activated by Bcr-Abl in the absence of IL-3, leading to cell proliferation and survival.

Substrate	Full Name	Function	Reference
Akt	Protein kinase B	Serine/Threonine kinase	(88)
Bad	Bcl-2-associated death promoter	Pro-apoptotic	(89)
Bap-1	Bcr-associated protein 1	14-3-3 protein	(61)
Bcl-XL	B-cell lymphoma-extra large	Anti-apoptotic	(90)
Cbl	Casitas B-lineage lymphoma	E3-ubiquitin ligase	(91)
Crk	Avian sarcoma virus CT10 oncogene homologue	Adaptor molecule	(92)
CrkL	Crk-like protein	Adaptor molecule	(93)
Fak	Focal adhesion kinase	Cytoskeleton	(94)
Grb2	Growth factor receptor bound protein 2	Adaptor molecule	(87)
PI3K	Phosphatidylinositol 3-kinase	Phospholipid kinase	(95)
PLCγ	Phospholipase Cγ	Phospholipase	(96)
Raf	Ras-activated factor	Serine/Threonine kinase	(97)
Ras	Rat sarcoma	Small G-protein	(98)
Ras-GAP	Ras GTPase-activating protein	Ras-GTPase activating	(99)
Shc	Src homology containing protein	Adaptor molecule	(100)
SOS	Son of sevenless	Guanine nucleotide exchange factor	(101)
STAT1/5	Signal transducer and activator of transcription	Transcriptional activator	(102;103)
Syp	Synaptophysin	Protein phosphatase	(104)

Table 1-2: Examples of an extensive group of Bcr-Abl tyrosine kinase substrates.

Adapted from Raitano *et al.,* 1997 (68) and Smith *et al.,* 2003 (2).

Binding of Grb2 to Bcr-Abl links it with Rat sarcoma (Ras) cascade. Activation of Ras protein results in subsequent activation of Raf, MEK and ERK, leading to activation of gene transcription (105). Ras regulates cell proliferation and differentiation, and plays a central role in the pathogenesis of CML (41;106). Impairment of Ras signalling by dissociation of Grb2/SOS complex inhibits proliferation of primary CML cells and Bcr-Abl^+ cell lines (107).

Bcr-Abl protects CML cells from apoptosis. Expression of Bcr-Abl in haemopoietic cell lines elevates anti-apoptotic signals, such as B-cell lymphoma-2 (Bcl-2), B-cell lymphoma-extra large (Bcl-xL) and myeloid cell leukaemia-1 (Mcl-1) (88;90;108). CML $CD34^+$ cells are more resistant to a range of cytotoxic agents compared with their normal counterparts (109). Expression of Bcr-Abl in murine Bcr-Abl^- cell lines confers significantly increased resistance to cytotoxic agents compared with their parental cell lines (109). HL60 is a human Bcr-Abl^- promyelocytic cell line which is very sensitive to apoptosis inducing agents, while expression of Bcr-Abl in HL60 cells makes them very resistant to apoptosis induced by a range of cytotoxic agents (90).

Furthermore, Bcr-Abl can activate Phosphoinositide 3-kinase (PI3K)-Akt and Janus kinase (JAK)-signal transducers and activators of transcription (STAT) pathways to inhibit apoptosis. PI3K is a heterodimer containing an 85 KDa regulatory subunit and a 110 KDa catalytic subunit (68). The regulatory subunit is tyrosine phosphorylated in Bcr-Abl^+ cells, and PI3K activity is elevated in Bcr-Abl expressing fibroblasts and haemopoietic cells (68). Activation of PI3K by Bcr-Abl is mediated by adaptor proteins

CrkL, Crk and Cbl (2). Then a downstream serine/threonine kinase Akt (also known as protein kinase B) is activated which phosphorylates the pro-apoptotic protein Bcl-2 associated death promoter (Bad), leading to dissociation of Bad from anti-apoptotic signals (such as Bcl-xL) and suppression of apoptosis (110). Activated Akt also inhibit the tumour suppressor p53 via activation of murine double minute 2 (MDM2) protein, leading to cell survival (111). In addition, there is constitutive activation of JAK and STAT in Bcr-Abl$^+$ primary cells and cell lines (112;113). In the normal cellular context, cytokine stimulation activates JAKs which then phosphorylate and activate STATs. Activated STATs translocate to the nucleus and upregulate gene transcription (114). Activated STAT5 is involved in the malignant transformation of Bcr-Abl$^+$ cells (112;115;116). Activation of STAT5 by Bcr-Abl upregulates anti-apoptotic protein Bcl-xL, leading to suppression of apoptosis (117;118). However, activation of STAT5 is not always induced by activated JAKs in CML cells, as Bcr-Abl can phosphorylate STAT5 via haemopoietic cell kinase (Hck) (119).

Bcr-Abl transforms haemopoietic cell lines into interleukin (IL)-3 independence *in vitro* (59;120). The proliferation of Bcr-Abl$^+$ quiescent CML cells can be initiated without any added growth factor (121), but normal quiescent haemopoietic cells can not (16). Bcr-Abl also promotes IL-3 and granulocyte colony-stimulating factor (G-CSF) secretion and autocrine proliferation in CML stem and progenitor cells (122;123). IL-3 and G-CSF are growth factors which regulate proliferation, differentiation and survival of haemopoietic cells by activating intracellular signalling pathways including Ras-MAPK, PI3K-Akt, and JAK-STAT (86;124). Normal haemopoietic primitive cells are

dependent on growth factors to proliferate and survive (18). The aberrant autocrine production of IL-3 and G-CSF in CML stem and progenitor cells may confer them with a proliferative advantage compared with their normal counterparts (121;123).

Furthermore, Bcr-Abl alters cellular adhesion of CML primitive cells within their bone marrow microenvironment. Normal haemopoietic progenitors interact with their bone marrow microenvironment via integrin mediated adhesion (125), which negatively regulates their proliferation (126). Abnormal circulation of immature CML progenitors in the peripheral blood and the proliferative advantage of CML progenitors may be explained by their altered adhesion with the bone marrow microenvironment (127;128). Primary CML progenitors have reduced adhesion with bone marrow stromal cells and the extracellular matrix glycoprotein fibronectin *in vitro* (129;130). However, this is controversial as Bcr-Abl transfected human and murine haemopoietic cell lines have increased adhesive interaction with stromal cells and fibronectin (131;132). In addition, it was suggested that restoration of normal haemopoiesis by interferon-alpha (IFN-α) in some CML patients may be due to recovery of adhesion of CML progenitors to the bone marrow stroma (133).

In summary, the constitutively activated tyrosine kinase of Bcr-Abl promotes cell proliferation, inhibits apoptosis, transforms haemopoietic cells into growth factor independence and alters cellular adhesion, which is the driving force of leukaemogenesis of CML.

1.4 Treatment of CML

1.4.1 Conventional therapies (pre-tyrosine kinase inhibitor era)

Whole body or splenic radiation was the major treatment of CML until the 1950s, which was palliative and did not improve overall survival (45). Then busulfan was employed from the 1950s and it could maintain partial haematologic response (PHR, defined in Table 1-3) in most CML patients with serious side-effects (45;134). Hydroxyurea, an inhibitor of DNA synthesis and cell cycle, was introduced to treat CML in the 1970s (135). Hydroxyurea can rapidly control blood cell count and achieve complete haematologic response (CHR) in 50-80% of CML patients, but cytogenetic responses are rare (136;137). It is effective in CML patients resistant to busulfan treatment (135). However, both busulfan and hydroxyurea cannot block disease progression into BC where median survival remained to be 3 to 6 years (45).

Allogeneic bone marrow transplantation (BMT) or stem cell transplantation (SCT) is the only curative therapy for CML in suitable patients (2). Allogeneic SCT with peripheral blood $CD34^+$ progenitor cells can fully reconstitute the haemopoietic system of recipients (21). HLA matched donors receive G-CSF to mobilize their HSCs into peripheral blood. When 1-2% of blood cells are $CD34^+$, and after leukapheresis, $CD34^+$ cells are enriched by a CD34 specific monoclonal antibody for allogeneic transplantation (21). Haemopoietic engraftment by peripheral blood $CD34^+$ cells is stable, faster to recover all haemopoietic lineages, and the stem cell collection procedure itself is more comfortable for the donor than bone marrow harvest under

general anaesthetic (21). Five-year survival after allogeneic BMT or SCT is up to 72% in low-risk CML patients but is associated with at least 20% transplantation–related mortality, while there is only around 20% survival in high-risk patients with transplantation–related mortality as high as 73% (138). The high mortality rate is usually caused by graft-versus-host disease and opportunistic infections (137). 30-70% of CML patients achieved long-term disease-free survival after allogeneic SCT (45). However, only about 20% of CML patients are suitable for allogeneic transplantation due to limitations of age, fitness and matched donor availability (139).

A human cytokine, IFN-α, became the first line therapy of CML patients who were not eligible for allogeneic SCT in the 1980s (140). IFN-α can achieve CHR in 46-80% of CML patients, partial cytogenetic response (PCgR) in 11-16% of patients and complete cytogenetic response (CCgR) in 13-32% of patients (45). IFN-α achieves durable CCgR in a subset of CML patients and is superior to busulfan and hydroxyurea in patient survival (140). However, IFN-α therapy results in a high possibility of neurotoxicity as well as some other intolerable side effects in older patients (45). Combination of IFN-α and cytarabine (or cytosine arabinoside, Ara-C) significantly improved cytogenetic response rates and survival time of CP CML patients compared with IFN-α alone (141;142). IFN-α plus cytarabine then became the standard therapy for those CML patients who were unsuitable for transplantation (142;143).

Response	Criteria
Complete haematologic response (CHR)	Complete normalization of peripheral blood count: ● Leukocyte count <10 x 10^9 cells/L ● Platelet count <450 x 10^9 cells/L ● No immature cells in the peripheral blood ● No sings or symptoms of disease including splenomegaly
Partial haematologic response (PHR)	Same as those for CHR, except ● Persistence of immature cells, or ● Platelet count <50% of the pre-treatment count but >450 x 10^9 cells/L, or ● persistent splenomegaly but >50% of the pre-treatment extent
Complete cytogenetic response (CCgR)	No Ph^+ cells detectable by cytogenetics in the bone marrow
Partial cytogenetic response (PCgR)	1-34% Ph^+ cells detectable in the bone marrow
Major cytogenetic response (MCgR)	<35% Ph^+ cells detectable in the bone marrow (includes CCgR and PCgR)
Minor cytogenetic response (mCgR)	35-90% Ph^+ cells detectable in the bone marrow
Complete molecular response (CMR)	● Undetectable Bcr-Abl transcript by qRT-PCR, or ● ≥4.5 log reduction compared to starting level
Major molecular response (MMR)	● ≥3 log reduction of Bcr-Abl transcript, or ● <0.1% Bcr-Abl transcript by qRT-PCR

Table 1-3: Criteria of treatment responses in CML.

1.4.2 Tyrosine kinase inhibitors (TKI) – imatinib

As the understanding of the molecular biology of CML progressed further, Bcr-Abl became an attractive therapeutic target for CML. Imatinib mesylate (IM; Glivec® or Gleevec®, Novartis, Basel, Switzerland. Figure 1-7) is an Abl TKI, and it inhibits the kinase activity of Abl, c-Kit and platelet-derived growth factor receptors (PDGF-R) (44;144). IM competes with adenosine triphosphate (ATP) for the enzymatic binding site of Abl, and blocks Abl tyrosine kinase activity (44) (Figure 1-8). IM was developed by random screen of a large number of synthesized ATP-competitive 2-phenylaminopyrimidine compounds for TKI activity, and CGP57148 (later known as STI571 and IM) emerged as a potent inhibitor of Abl tyrosine kinase (145). The activation loop in the enzymatic site of Abl controls its kinase activity by switching between active and inactive conformations. IM binds to Abl only when it is in the inactive state and prevents it from changing into the active conformation (146).

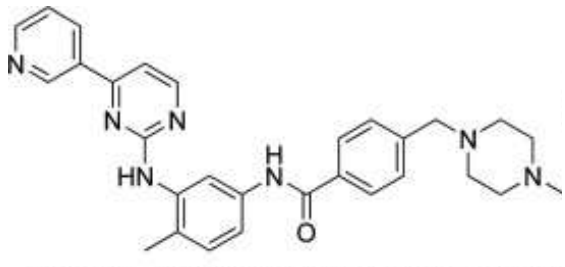

Figure 1-7: Structure of IM (147).

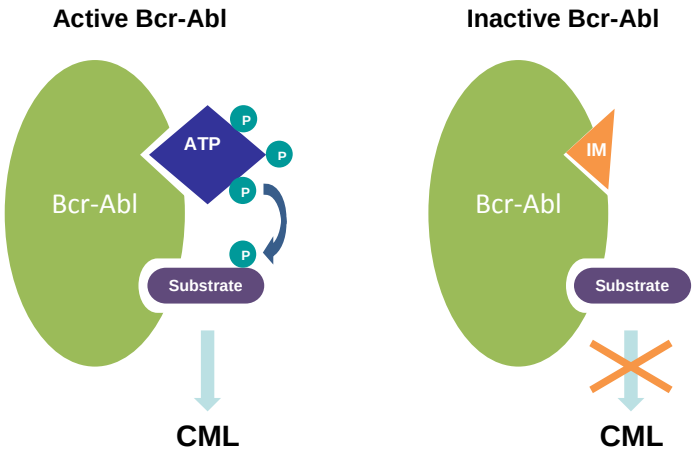

Figure 1-8: Mechanism of action of IM on Bcr-Abl.

ATP binding is essential for Bcr-Abl to phosphorylate substrates and subsequently activate downstream pathways that promote cell survival, proliferation and regulation. IM can bind to the inactive state of Bcr-Abl at its ATP binding site, and inhibit the phosphorylation of substrates that would activate downstream signalling and lead to CML.

IM inhibits proliferation and causes apoptosis in Bcr-Abl$^+$ cell lines and CML progenitors *in vitro* and *in vivo*, with very low toxicity to Bcr-Abl negative cell lines and normal progenitors, demonstrating the specificity of this drug against Bcr-Abl$^+$ cells (145;148). In June 1998 IM was taken into a phase I clinical trial with CP CML patients who failed IFN-α treatment, and 98% of these patients achieved CHR within four weeks at 300mg or more IM once daily (149). Side effects with IM treatment were mild, including nausea, myalgias, oedema, and diarrhoea (149). A daily dose of 400mg IM or more was recommended for future studies. A peak plasma

concentration of 4.6μM and a tough concentration of 1.46μM were achieved with this dose at steady-state (149). At the phase II clinical trial, IM was administered orally at 400mg daily to CP CML patients who had failed IFN-α treatment (150). About 95% patients achieved CHR and 60% achieved major cytogenetic response (MCgR) (150). AP and BC CML patients were treated with 400mg or 600mg IM daily, and achieved higher response rates and longer survival time than conventional treatments (151;152).

In June 2000, the phase III International Randomized Study of Interferon and STI571 (IRIS) study was initiated with newly diagnosed CP CML patients and compared IM treatment with IFN-α plus cytarabine (153;154). After a median of 18 months follow-up, 76.2% patients treated with IM achieved CCgR, while only 14.5% patients treated with IFN-α plus cytarabine achieved CCgR (153;154). IM was shown to be superior to IFN-α plus cytarabine in treating newly diagnosed CP CML, and subsequently most patients in the IFN-α plus cytarabine treatment arm crossed over to the IM arm (153;154). In May 2001, IM was rapidly approved by the United States Food and Drug Administration (FDA) for treatment of Ph^+ CML (153). After six years follow-up of the IM arm in the IRIS study, the estimated total survival rate was 88%, or 95% when counting CML-related deaths only, and the cumulative best rate of CCgR was 83% (155). Owing to the efficacy and low toxicity of IM, it is now considered as the first-line treatment for newly diagnosed CP CML (153-155).

However, resistance developed against IM. It was shown that the approximate relapse rate was 17% after 60 months of IM treatment, and about 7% of all patients treated with IM entered AP or BC (143). About 20-25% of patients treated with IM never achieved CCgR (156). Resistance to IM can be described as primary or acquired. Primary resistance is where there is no initial response to IM, and it is defined as a failure to achieve CHR within 3 months, cytogenetic response within 6 months, PCgR within 12 months or CCgR within 18 months of treatment (157;158). Acquired resistance is loss of established CHR, or CCgR, or progression to AP or BC (157). Acquired resistance to IM is often mediated by point mutations in the kinase domain of Bcr-Abl (159).

1.4.2.1 p-CrkL as a surrogate marker of Bcr-Abl kinase inhibition by TKI

Phosphorylated CrkL (p-CrkL) is commonly used as a surrogate marker for Bcr-Abl tyrosine kinase activity (160-163). It was firstly identified in 1994 that a 39 kDa protein was consistently tyrosine phosphorylated in peripheral blood neutrophils from all 18 chronic phase CML patients screened, but not in normal controls (93). It was also found that the same protein was tyrosine phosphorylated in Bcr-Abl$^+$ cell lines, such as K562 and BV173 (93). Later this 39 kDa protein was identified as CrkL after protein purification (93). The *CrkL* gene had been discovered in 1993; it is located on chromosome 22 and centromeric to the *Bcr* gene (164). Its protein product is very similar to the product of a viral oncogene *v-Crk* which is from avian sarcoma virus CT10, and CrkL is 60% homologous to Crk that is the human homolog of *v-Crk* (164). CrkL protein contains a SH2 domain and two tandem SH3 domains without having

any catalytic domain (164). It was revealed that CrkL interacted with Abl directly (93). It was also found that CrkL was tyrosine phosphorylated by Abl and Bcr-Abl in transfected COS-1 cells and complexed with both of them in K562 and transfected COS-1 cells (165;166). Subsequently, it was identified that Bcr-Abl phosphorylated CrkL on tyrosine 207 (167).

p-CrkL has been used as a marker to assess the effect of IM on inhibition of Abl kinase activity in patient samples by Western blotting (149;160). A method was developed to detect the level of p-CrkL in $CD34^+$ CML progenitor cells using intracellular flow cytometry (161). This method takes much less time than Western blotting, but more importantly requires as few as 10^4 cells for each test, while Western blotting requires more than 10^5 cells, making the flow cytometry method a preferred choice with rare stem cell populations (161). A further validation of the flow cytometry method was reported in 2009, it showed that p-CrkL and total tyrosine phosphorylation are reduced to the same levels in K562 cells with 48 hours of IM treatment (162). However, a direct comparison of p-CrkL and Bcr-Abl tyrosine kinase activity has not been made, especially at short time-points (≤24h).

1.4.3 Second generation TKI – nilotinib and dasatinib

Second generation TKI drugs have emerged to target Bcr-Abl in order to overcome IM resistance. Nilotinib (Tasigna®; formerly AMN107, Novartis, Basel, Switzerland) (Figure 1-9) is a rationally designed and orally available specific inhibitor of Abl tyrosine kinase (168). Apart from Abl kinase, nilotinib also inhibits the activity of c-kit

and PDGF-R (169). Nilotinib was designed to have higher binding affinity than IM to the ATP binding site on the kinase domain of Abl (168). Nilotinib binds to the inactive conformation of Abl kinase, and blocks its tyrosine kinase activity (170;171).

Nilotinib inhibits 32 out of 33 IM-resistant Bcr-Abl mutants except the T315I mutation (168). Nilotinib exhibits ≥20-time more potency than IM in IM sensitive and insensitive Bcr-Abl$^+$ cell lines (170;172;173). Although nilotinib is much more effective than IM in Bcr-Abl$^+$ cell lines, nilotinib and IM are equally potent in human primary CD34$^+$ CML cells, and only have anti-proliferative effect instead of eradicating these cells (172). Nonetheless, clinical studies have demonstrated the effectiveness and safety of nilotinib in IM resistant or intolerant CML patients (174;175), leading to the approval of nilotinib by FDA for treating adult Ph$^+$ CP and AP CML patients who are resistant to or intolerant of prior therapy including IM, and subsequently newly diagnosed adult Ph$^+$ CP CML patients (176).

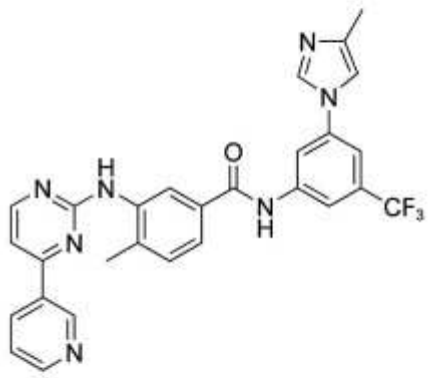

Figure 1-9: Structure of nilotinib (147).

Dasatinib (Sprycel®; formerly BMS-354825, Bristol-Myers Squibb, Princeton, USA) (Figure 1-10) is a dual Src/Abl tyrosine kinase inhibitor (177). It also targets c-kit and PDGF-R (177). Dasatinib is an orally administrated drug and is 325-fold more potent than IM in cells expressing wild-type Bcr-Abl protein (173). Almost all Bcr-Abl kinase domain mutations can be inhibited by dasatinib except the T315I mutation (159;173). Dasatinib binds to both active and inactive conformations of Abl kinase, rendering it much higher binding affinity than IM (159).

Clinical trials demonstrated the efficacy of dasatinib in all phases of IM resistant or intolerant CML patients, and it is well tolerated (178-180). Dasatinib was approved by FDA for treatment of adult Ph^+ CML and ALL patients who are resistant to or intolerant of prior therapy (such as IM), as well as newly diagnosed adult Ph^+ CP CML patients (181). However, dasatinib is not able to eliminate the primitive quiescent CML stem cell population (163). For this reason, although both nilotinib and dasatinib have improved effects in suppressing CML than IM, they are still not able to cure CML.

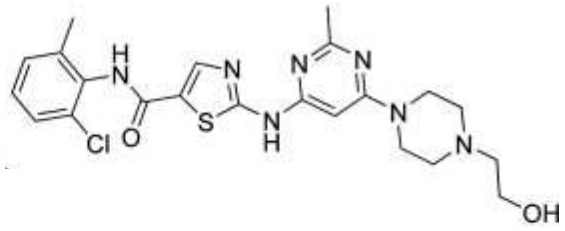

Figure 1-10: Structure of dasatinib (147).

1.5 Mechanisms of TKI resistance and CML stem cell persistence

Although most CML patients treated with IM are able to achieve CCgR, many of them still have detectable level of *Bcr-Abl* transcripts, and only 4% of patients treated with standard-dose IM have achieved complete molecular response (CMR) (143;156). After withdrawal of IM, about half of CML patients with durable CMR have disease relapse, whilst the other half remain in CMR for at least seven years (182). However, Bcr-Abl DNA is still detectable by highly sensitive PCR in the vast majority of these patients with stable CMR after IM is withdrawn (182). The disease relapse and minimal residual disease indicate that CML is not cured by IM. Resistance of CML to TKI can be described as Bcr-Abl independent or dependent (e.g. point mutations) (157).

1.5.1 Bcr-Abl independent resistance

Bcr-Abl independent resistance can be due to acquisition of additional oncogenic mutations, at which point Bcr-Abl becomes an irrelevant target (157). Aberrant growth factor secretion is another possible mechanism of resistance to TKI. Adaptive autocrine and paracrine secretion of granulocyte macrophage colony-stimulating factor (GM-CSF) activates anti-apoptotic JAK2/STAT5 pathway in a Bcr-Abl independent way in primary CML progenitors, and contributes to the resistance of CML cells to TKI treatment *in vivo* (183). Inhibition of JAK2 by AG490 abolishes the resistance mediated by GM-CSF (183), indicating the combination of TKI and JAK2 inhibitor is a potential method to eradicate CML. In addition, the frequency and level

of expression of type 1 insulin-like growth factor receptor (IGF-IR) is much higher in BC CML patients than in CP and AP, and inhibition of IGF-IR partially overcomes CML resistance to IM (184). Thus, targeting IGF-IR may facilitate TKI in treating CML in advanced stages (184).

Autophagy is another possible mechanism for CML cells to survive under TKI treatment. Autophagy is a pathway which degrades proteins or organelles to maintain cellular homeostasis, and also generates energy under starvation or other cellular stress (185). IM induces autophagy in CML cell lines and primary CML cells (186). Blockage of autophagy increases IM induced apoptosis in CML cells (185). Importantly, combination of autophagy inhibitor chloroquine and TKIs significantly induces apoptosis in CML progenitor and stem cells (186). This indicates that autophagy serves as a survival mechanism in CML cells with TKI treatment, and autophagy inhibition potentiates apoptosis induced by TKI in primitive CML cells (186).

1.5.2 Bcr-Abl dependent resistance

The possible mechanisms of Bcr-Abl dependent resistance are Bcr-Abl kinase domain point-mutations, *Bcr-Abl* gene amplification, Bcr-Abl protein over-expression and drug efflux (157). The major cause of resistance to IM is point-mutations in the kinase domain of Bcr-Abl protein (187). Almost all Bcr-Abl kinase domain mutants can be inhibited by second-generation TKIs, except the T315I mutant (188). Threonine 315, located at the Abl kinase domain, forms a pivotal hydrogen bond with TKI (187).

Mutation at this site disrupts the binding of TKI with Bcr-Abl. CML patients harbouring T351I Bcr-Abl mutant are associated with poor clinical prognosis (189).

1.5.2.1 Drug Efflux

One possible mechanism of TKI resistance is drug efflux, which pumps out intracellular drugs typically by ATP binding cassette (ABC) transporters. ABC transporters are involved in multi-drug resistance in cancer chemotherapy (190). Drug efflux may lead to sub-optimal intracellular TKI concentration and insufficient inhibition of Bcr-Abl kinase activity.

It was shown that overexpression of an ABC transporter ABCB1 (MDR1, p-glycoprotein) in Bcr-Abl$^+$ cell lines conferred partial resistance to IM (191). However, the activity of ABCB1 in primary CML CD34$^+$ cells is very low, and inhibition of ABCB1 was not able to increase intracellular IM level (192). In addition, it was suggested that another ABC transporter ABCG2 (BCRP) was involved in the efflux of intracellular IM in ABCG2-overexpressing cell lines (193). ABCG2 transduced human BC CML cell line K562 cells become insensitive to IM and nilotinib treatments, and both TKIs associate with ABCG2 at its substrate binding sites (194). Although functional ABCG2 is overexpressed in CML CD34$^+$ cells, IM inhibits ABCG2 activity in this primitive CML population and is not a substrate of ABCG2 (195). This indicates that ABCG2 is not a regulator of intracellular IM concentration in primitive CML cells (195). Furthermore, nilotinib inhibits the activity of a range of transporters, including ABCB1, ABCG2 and the influx transporter human organic cation transporter 1

(hOCT1) in CML cell lines and CML $CD34^+$ cells (196;197). The uptake and efflux of nilotinib is not modulated by these transporters in CML cells (197). Taken together, drug efflux is unlikely a mechanism of CML stem cell resistance to IM and nilotinib.

1.5.2.2 Cytoplasmic retention of Bcr-Abl

The NLS and NES-containing protein c-Abl may be present both in the nucleus and cytoplasm (49;72). Although there are three NLSs present in the Bcr-Abl protein, Bcr-Abl is located in the cytoplasm of transformed fibroblasts (73;198). In addition, it was demonstrated that Bcr-Abl was localised to the cytoplasm of CML cell lines and primary cells (74). Export of NES-containing proteins from the nucleus is facilitated by the NES receptor CRM1/exportin-1 (199). CRM1/exportin-1 can be inactivated by a cytotoxin called leptomycin B (LMB), resulting in the inhibition of NES dependent protein export from the nucleus (72;199). In Bcr-Abl transfected fibroblasts, LMB treatment could not trap Bcr-Abl in the nucleus, showing that Bcr-Abl was not imported into the cell nucleus despite its NLS domains (198). However, in fibroblasts transfected with kinase–defective Bcr-Abl, about 30-35% kinase–defective Bcr-Abl was accumulated in the cell nucleus by LMB (198). In addition, IM could induce Bcr-Abl nuclear localisation and result in Bcr-Abl nuclear entrapment with LMB (198). The nuclear fraction of Bcr-Abl was demonstrated to correlate with increased IM concentration and incubation time, reaching a plateau with 10μM IM at about 25-35% (198). This indicates that inhibition of Bcr-Abl tyrosine kinase can induce nuclear transportation of Bcr-Abl protein, and the kinase activity of Bcr-Abl plays a role in its cytoplasmic retention.

Nuclear Abl kinase can be activated by DNA damage, subsequently inducing activation of protein p73 which is functionally homologous to the tumour suppressor protein p53. The activation of Abl and p73 is involved in DNA damage-induced apoptosis (200). It was demonstrated that nuclear Bcr-Abl kinase could induce cell apoptosis in transformed fibroblasts and K562 cells. Bcr-Abl expressing cells were treated with both IM and LMB to trap Bcr-Abl inside the nucleus, and then cells were washed extensively to get rid of IM to recover the tyrosine kinase activity of Bcr-Abl. After that cells were incubated with LMB alone. With this protocol, the apoptotic rate of Bcr-Abl expressing cells was about 70-80% higher than untransfected cells (198;200). These observations provided a new strategy for killing Bcr-Abl$^+$ cells. Interestingly, only about 20-25% of total Bcr-Abl accumulated in the nucleus of K562 cells treated with both IM and LMB, indicating that there were other mechanisms besides tyrosine kinase activity holding Bcr-Abl in the cytoplasm (198).

1.5.2.3 Quiescent CML stem cells

The quiescent (viable and non-dividing) CML stem cell population is insensitive to TKI treatment (201). IM and nilotinib have an anti-proliferative effect in the CML stem cell population, resulting in an accumulation of quiescent CML stem cells (172;201). Although dasatinib can target the committed CML stem cells, the quiescent CML stem cell population is still insensitive to this drug (163). In addition, the quiescent CML CD34$^+$ cells are resistant/persistent to a range of cytotoxic agents, including Ara-C, arsenic, PI-3K inhibitor LY294002 and et al. (202;203). Thus, eradication of this primitive Ph$^+$ stem cell population becomes an interesting research focus (157).

In addition, primitive CML $CD34^{+}38^{-}$ cells (approximating the *in vivo* quiescent stem cell pool) had significantly higher levels of *Bcr-Abl* mRNA transcript and Bcr-Abl protein compared to mature mononuclear cells (MNC) (163). Additionally, total phosphotyrosine and p-CrkL levels are increased in CML $CD34^{+}38^{-}$ cells with respect to MNC population. The level of p-CrkL is significantly elevated in CML $CD34^{+}38^{-}$ cells compared to bulk CML $CD34^{+}$ cells, indicating higher Bcr-Abl tyrosine kinase activity in $CD34^{+}38^{-}$ cells than CML MNC and bulk $CD34^{+}$ cells (163). Therefore, sufficient inhibition of Bcr-Abl tyrosine kinase in quiescent CML stem cells is required to eradicate them.

Type of Resistance	**Possible Mechanisms**
Bcr-Abl Dependent	Bcr-Abl kinase domain mutations Bcr-Abl gene amplification Bcr-Abl protein over-expression Drug efflux Cytoplasmic retention of Bcr-Abl CML stem cell persistence
Bcr-Abl Independent	Additional oncogenic mutations Aberrant growth factor secretion Autophagy

Table 1-4: Possible mechanisms of TKI resistance.

1.6 Novel treatment approaches

1.6.1 Farnesyltransferase inhibitors and CML

Ras (also known as $p21^{Ras}$) is a G or guanosine-nucleotide-binding protein. Ras is active when bound with guanosine triphosphate (GTP) and inactive with guanosine diphosphate (GDP). The *Ras* family contains H-*Ras*, K-*Ras* and N-*Ras* genes, the molecular weight of their protein products are 21 kDa (204). Ras proteins regulate several signalling pathways, among which the Ras-Raf-MEK-ERK signalling cascade is the pivotal one. In normal cellular context, this cascade is activated by binding of external stimuli to receptor tyrosine kinases (RTKs), leading to the dimerization of the RTKs and phosphorylation of an adaptor protein Grb2 (105). Subsequently, phosphorylated Grb2 brings a guanosine nucleotide exchange factor SOS (Son of Sevenless) to the membrane bound inactive Ras-GDP, and converts it into active Ras-GTP, leading to the sequential activation of Raf, MEK and ERK (105). Activated ERK then translocates into the cell nucleus resulting in phosphorylation of many transcription factors and transcription of genes involved in cell proliferation, differentiation and survival (105). Ras activity is regulated by opposite effects of GEFs and GAPs (205). GAPs enhance the intrinsic GTPase activity of Ras, resulting in increased GTP hydrolysis rate. Thus, GAPs negatively regulate Ras activity. On the other hand, GEFs facilitate exchange of Ras-GDP to Ras-GTP, making more active form of Ras protein. Therefore, GEFs are activators of Ras signalling (205).

Ras signalling is a critical pathway activated by Bcr-Abl protein. Experiments have demonstrated that inactivation of Ras signalling impaired the leukaemic transformation ability of Bcr-Abl protein (106). It was reported that the proliferation of a Bcr-Abl^{+} CML cell line BV173 was blocked by knock down of Ras. It was shown that inactivation of Ras dramatically reduced the number of colonies formed in soft agar assays with Bcr-Abl expressing Rat-1 fibroblasts (106). In addition, the transformation ability of Bcr-Abl in mouse bone marrow cells was completely inhibited by co-expression of inactive Ras (106). These observations show that Ras plays an essential role in the Bcr-Abl transformation, which makes Ras a potential therapeutic target in treating CML.

Cytosolic Ras protein is post-translationally modified to enable its membrane association, which is critical for the signalling functions of Ras (206). The post-translational modifications of Ras include farnesylation, proteolysis and carboxyl methylation (207). The first step in this process is addition of a 15-carbon farnesyl group to the cysteine residue of Ras C-terminal CAAX consensus sequence (C is cysteine, A is any aliphatic amino acid and X is any amino acid). Subsequently, the C-terminal tripeptide AAX is removed by proteolysis. Finally, the new C-terminal farnesylcysteine residue is carboxyl methylated (208;209). Among these three steps, farnesylation of the C-terminal cysteine residue of Ras by farnesyltransferase is the key step of this process (208). Therefore, inhibition of the farnesyltransferase activity prevents membrane association of cytosolic Ras and its signalling function.

Based on this, a range of farnesyltransferase inhibitors (FTI) were developed to inhibit the farnesyltransferase activity and intended to block the Ras signalling pathway. These FTIs have potential applications in a wide range of tumours, since mutant forms of Ras with constitutive activity are involved in about 90% of pancreatic adenocarcinoma, 50% of colon adenocarcinoma, 30% of myeloid leukemia and many other types of human tumours (210). More importantly, our previous study revealed that lonafarnib, a FTI, sensitized primitive quiescent CML cells to IM treatment *in vitro* (202).

1.6.2 BMS-214662

BMS-214662 is a potent FTI, which was developed as an inhibitor of Ras signalling pathway (Figure 1-11)(206). BMS-214662 has slightly lower FTI activity than another FTI, BMS-225975, as measured by *in vitro* kinase assay and in cell lines with mutant Ras (211). However, BMS-214662 exhibits potent apoptotic effects in tumour cells *in vivo*, whereas BMS-225975 only has cytostatic effects in the same context (211). This indicates BMS-214662 may induce apoptosis in tumour cells by a novel mechanism of action apart from its FTI activity. In addition, previous research demonstrated that BMS-214662, but not BMS-225975, selectively induced apoptosis in quiescent CML stem and progenitor cells in respect to their normal counterparts, making BMS-214662 a potential drug to eradicate CML (212). BMS-214662 induces apoptosis in primary CML stem and progenitor cells via the activation of protein kinase C β (PKCβ) and the intrinsic apoptotic pathway including generation of reactive oxygen species (ROS) and release of cytochrome c from the mitochondria (213). However, the exact

mechanism of how BMS-214662 activates the intrinsic apoptotic pathway is still not clear.

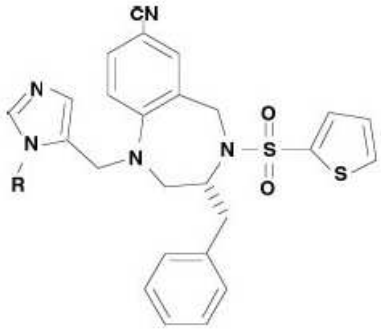

	R=
BMS-214662	H
BMS-225975	CH3

Figure 1-11: The structure of BMS-214662 and BMS-225975.

Adopted from Manne *et al*., 2004 (211).

1.6.3 Protein tyrosine phosphatases

Protein tyrosine phosphatases (PTPs) modulate signalling pathways mediated by protein tyrosine kinases (PTKs) and cytokines (214). Most of PTPs negatively regulate these signalling pathways, apart from a few PTPs like SHP2 and CD45, which increase immune response and cytokine signalling (214). SHP1 and SHP2 are SH2 domain-containing, non-receptor PTPs (215). They both have two tandem SH2 domains at the N-terminus, then a catalytic domain and an inhibitory C-terminus (215). Although SHP1 and SHP2 are structurally similar, they have different functions and expression patterns. SHP1 is highly expressed in haemopoietic cells, and negatively regulates cell signalling mediated by a range of cytokine receptors (215). However, SHP2 is widely expressed and promotes cell signalling pathways leading to differentiation, proliferation, and migration (215).

Phosphorylation of Bcr-Abl is regulated by PTPs. Bcr-Abl enhances expression of SET via JAK2 kinase (216;217). SET is an inhibitor of tumour suppressor protein phosphatase 2A (PP2A) (218), and PP2A is a serine/threonine phosphatase which activates SHP1 (217). The tyrosine phosphatase SHP1 associates with and dephosphorylates Bcr-Abl (217). Thus, Bcr-Abl maintains its tyrosine phosphorylated status by inhibiting SHP1 through SET-PP2A-SHP1 pathway. Inhibition of SHP1 by Bcr-Abl renders proliferative advantage to Bcr-Abl$^+$ cells, as it was shown that defect of *SHP1* gene was associated with hyperproliferation of haemopoietic cells in mice (219). In addition, expression of SHP1 is decreased in primary CML cells along with disease progression, which may explain resistance of advanced CML to TKI treatment (214).

Activation of PP2A and SHP1 becomes a potential therapeutic strategy in TKI-insensitive CML. PP2A activation leads to Bcr-Abl tyrosine dephosphorylation and its proteasomal degradation via SHP1 (217). Besides Bcr-Abl, SHP1 also associates with and dephosphorylates JAK2 kinase (220), and triggers proteasomal degradation of JAK kinases (221). JAK2 plays a critical role in Bcr-Abl mediated cell signalling (222;223). In addition, the substrates of PP2A include MAPK, STAT5, Akt, Myc and Bad. Down-regulation of SET and overexpression of PP2A in a Bcr-Abl$^+$ cell line inhibited phosphorylation of MAPK, STAT5 and Akt, reduced Myc expression and elevated the level of pro-apoptotic Bad (217). Activation of PP2A inhibits proliferation and clonogenic potential of Bcr-Abl$^+$ cells, and induces apoptosis greatly in these cells

(217). Overall, activation of PP2A and SHP1 inhibits Bcr-Abl and JAK2 kinase activity, as well as their downstream signalling, and impairs the leukaemogenic potential of Bcr-Abl.

Protein tyrosine phosphatase 1B (PTP1B) is another PTP which can dephosphorylate Bcr-Abl. Similar as SHP1, PTP1B is an intracellular PTP and a negative modulator of tyrosine kinases (224). PTP1B is able to associate with and dephosphorylate Bcr-Abl *in vivo* (225). PTP1B negatively regulates signalling and transformation mediated by Bcr-Abl *in vitro* and *in vivo* (225;226).

1.6.4 Disruption of association of Bcr-Abl and its binding partners

Since there are other mechanisms besides tyrosine kinase retaining Bcr-Abl in the cytoplasm (198), impairment of these mechanisms may induce nuclear localisation of Bcr-Abl and enhance apoptosis of CML cells. Cytoplasmic binding partners of Bcr-Abl may be involved in its cytoplasmic retention, and disruption of their association could potentially induce nuclear translocation of Bcr-Abl protein.

1.6.4.1 Bcr-Abl and actin

In the Bcr-Abl fusion protein, Bcr not only activates the tyrosine kinase activity of Abl, but also enhance the F-actin binding ability of Abl (82). The F-actin binding domain of Abl and Bcr-Abl protein is located in their C-terminal end (73). It was shown that Bcr-Abl with defective F-actin binding ability had decreased transforming potential, but was not able to abolish dependence of Ba/F3 cells on IL-3 (73). In transfected COS

cells, wild type Bcr-Abl co-localises with F-actin, but F-actin binding domain (FABD) deleted Bcr-Abl mutant does not (227). The FABD-deleted Bcr-Abl is located in the cytoplasm diffusely with punctation (227). Treatment with IM does not induce nuclear localisation of FABD-deleted Bcr-Abl (227). However, it is not clear whether FABD-deleted Bcr-Abl translocates to the nucleus with IM treatment, as Bcr-Abl may shuttle back to the cytoplasm very quickly in the absence of LMB.

1.6.4.2 Bcr-Abl and 14-3-3

14-3-3 proteins are highly conserved and ubiquitously expressed 28-33 kDa proteins involved in a wide variety of cellular processes in eukaryotes (228;229). There are seven major members in the mammalian 14-3-3 family (β, γ, ε, σ, ζ, τ and η), and these members form homodimers and heterodimers. 14-3-3 proteins have phospho-serine and phospho-threonine binding activities (229). By interacting with a wide range of proteins, 14-3-3 proteins are involved in cellular processes including signal transduction, apoptosis, metabolism, protein trafficking, cell cycle regulation and DNA damage/oxidative stress responses (228;229). 14-3-3 dimers function as adaptor molecules in signalling to allow un-complexed proteins to associate with each other indirectly (230).

14-3-3 proteins are involved in regulating nucleocytoplasmic shuttling of c-Abl. There is a consensus 14-3-3 binding site between the second and third NLSs of c-Abl protein (231). It was revealed that 14-3-3 proteins (β, γ, σ, ε, ζ and η) interacted with c-Abl at this site and sequestered c-Abl in the cytoplasm, as binding with 14-3-3

masks the NLSs of c-Abl (231). In addition, it was found that upon exposure to oxidative stress and DNA damage, activated JNK phosphorylated 14-3-3 (on Serine 184) and resulted in the release of c-Abl from 14-3-3, hence nuclear translocation of c-Abl (231). Phosphorylation of c-Abl at Thr735 is crucial for its binding with 14-3-3 proteins (231), and Thr735 phosphorylation is independent of DNA damage and subcellular localisation of c-Abl, and has no effect on the tyrosine kinase activity of c-Abl (231).

Furthermore, the N-terminal region of Bcr protein encoded by the first exon is associated with a member of 14-3-3 family, Bcr-associated protein 1 (Bap-1) (61). Bcr-Abl protein also interacts with Bap-1 (61). In addition, 14-3-3 β binds to the serine/threonine kinase domain of Bcr (232), and other 14-3-3 isoforms were found to interact with Bcr as well, including 14-3-3 γ, ε, ζ, τ, and η (233). 14-3-3 ζ, 80% of amino acid sequence identical to Bap-1, was revealed to be associated with both Bcr and Bcr-Abl proteins (61).

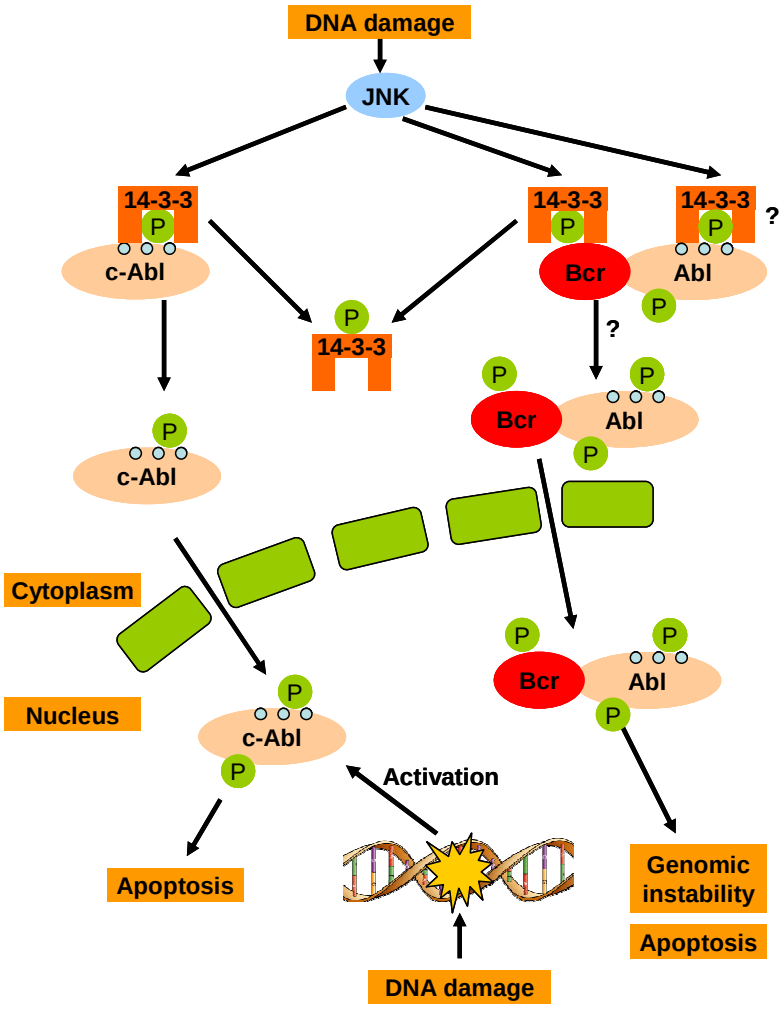

Figure 1-12: Nuclear translocation of c-Abl and Bcr-Abl in response to DNA damage.

Following genotoxic stress, activated JNK phosphorylates 14-3-3 and disrupts 14-3-3/c-Abl complex, leading to nuclear translocation of c-Abl. Then DNA damage activates the tyrosine kinase activity of c-Abl and results in apoptosis. Bcr-Abl can also be induced into the nucleus in response to genotoxic stress, which may enhance genomic instability in Bcr-Abl$^+$ cells. NLSs are indicated as little blue ovals on Abl. Adapted from Yoshida *et al*., 2005 (231) and Pendergast 2005 (234).

1.6.5 Novel stem cell targeted drug delivery

Stem cell targeted TKI delivery may be used in order to overcome the elevated expression and activity of Bcr-Abl kinase in CML stem cells (163). Low density lipoprotein (LDL), the major transporter of cholesterol in human plasma (235), could be an interesting drug delivery vector to primary haemopoietic stem cells. LDL particles are spherical and have a diameter of 22 nanometres (236). A LDL particle contains a core of about 1500 esterified cholesterol molecules surrounded by a shell of phospholipids, unesterified cholesterol and apoprotein B (237;238). Circulating LDL is taken up by cell surface receptors, then internalized and degraded to release cholesterol (Figure 1-13). Uptake of LDL is elevated in gynaecological cancer cells compared to normal cells (239). LDL receptor (LDLR) activity and cellular LDL uptake is markedly increased in primary peripheral blood and bone marrow AML and BC CML cells with respect to their healthy counterparts (237). Thus, LDL may be used as a selective drug delivery vehicle targeting CML stem cells.

However, as natural LDL is extracted from serum, it has limited availability, as well as issues of genetic and batch-to-batch variation. Synthetic LDL (sLDL) is physicochemically and biologically equivalent to natural LDL (240;241). It can be routinely produced (242), and does not have the issues associated with natural LDL. Furthermore, sLDL has been shown to incorporate drugs (243;244), demonstrating the competence of sLDL as a drug delivery vector. The effectiveness of sLDL as a drug delivery vehicle in CML stem cells had not been investigated yet.

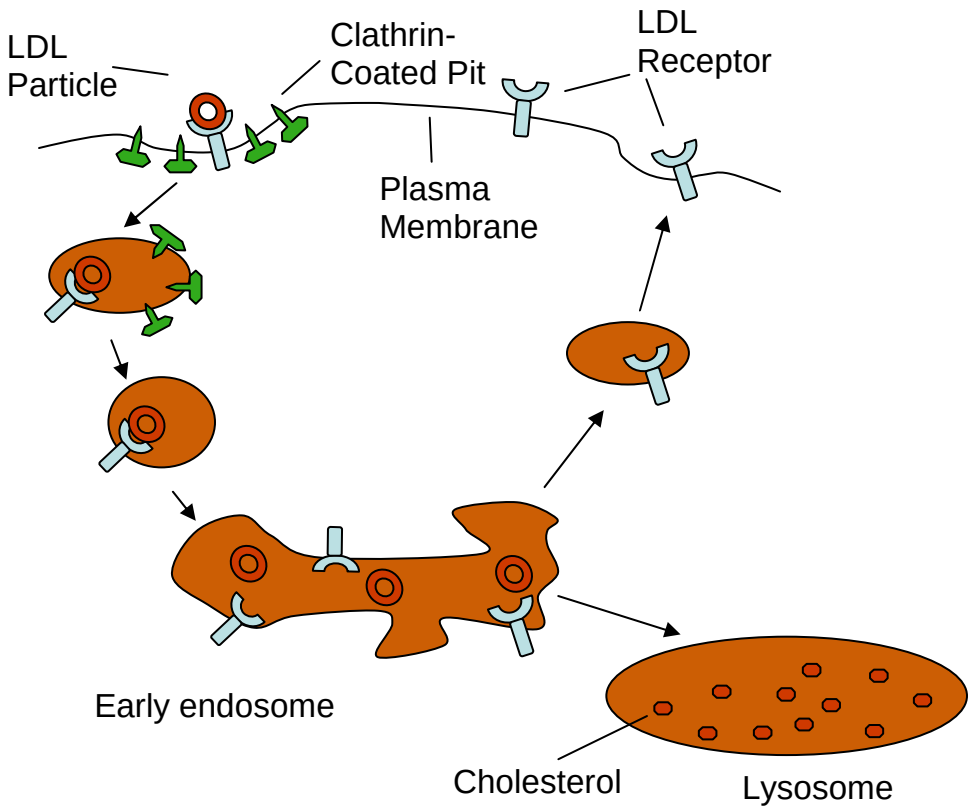

Figure 1-13: Internalization of LDL particles via receptor mediated endocytosis.

LDL particles circulating in the blood are taken up by LDL receptors in clathrin-coated pits on cell surface. These pits are internalized and form coated vesicles which fuse and form endosomes. In the acidic environment of endosomes, LDL particles are separated from their receptors and delivered to lysosomes, where they are degraded to release free cholesterol. LDL receptors are then recycled to the plasma membrane by transport vesicles. Adapted from Brown and Goldstein 1986 (236).

1.7 Aims

The following aims are addressed in this thesis:

1. To investigate the efficacy of nuclear entrapment of Bcr-Abl to induce apoptosis in CML cells;
2. To visualize the subcellular localisation of Bcr-Abl protein in CML progenitors which survive long-term TKI treatment, and to assess with which proteins Bcr-Abl is co-localised;
3. To determine if p-CrkL is an accurate surrogate marker of Bcr-Abl tyrosine kinase activity especially at short time points;
4. To investigate the mechanism of action of the putative farnesyltransferase inhibitor, BMS-214662 in CML cells;
5. To assess the efficacy of sLDL as a drug delivery vehicle to target primitive CML cells.

2 Methods and Materials

2.1 Methods

2.1.1 Cell Culture

2.1.1.1 Culture of cell lines

CML blast crisis cell lines K562 and KCL22, AML cell line HL60, murine cell lines Ba/F3 wild type and Ba/F3 Bcr-Abl were cultured in $RPMI^{++}$ (2.3.7.1). Cells were grown at 37°C with 5% CO_2 in tissue culture flasks. Cells were fed every one or two days to maintain a density of 2-10 x 10^5 cells/mL. 10ng/mL IL-3 was added to Ba/F3 wild type cell culture medium as these cells are IL-3 dependent.

2.1.1.2 Cell counting and trypan blue dye exclusion

The number of cells was counted with a haemocytometer. 10µL of cells were loaded into one side of the chamber in the haemocytometer, and at least 100 cells were counted to give a statistically significant count. For assessment of cell viability, trypan blue dye exclusion method was used. Trypan blue is a vital dye which can penetrate through the membrane of dead cells but not viable cells. Thus, dead cells can be distinguished with their blue colour under a microscope. At first, trypan blue solution was diluted 1 in 10 in PBS, and 90µL of such dilution was mixed with 10µL cells giving a dilution factor of 10. Then 10µL of the mixture was loaded into the

haemocytometer and at least 100 cells were counted. Cells without blue staining were counted as viable cells.

2.1.1.3 CML sample collection and enrichment

The research was approved by the Greater Glasgow and Clyde Health Board Local Research Ethics Committee (LREC) and all human participants gave written informed consent. Leukapheresis samples from newly diagnosed untreated patients with chronic phase CML were enriched to more than 90% $CD34^+$ progenitors by positive selection with CliniMACS and cryopreserved routinely in the lab. Enriched $CD34^+$ samples were validated by Ms Elaine Allan to be Ph^+ by D-FISH.

2.1.1.4 Cell sorting

Cell sorting was performed by technicians. Briefly, $CD34^+$ enriched cells were stained with anti-human anti-CD34-APC and anti-CD38-PE antibodies for 15 minutes in the dark. Then stained cells were sorted by using a BD FACS Aria into two populations: $CD34^+38^{hi/+}$ and $CD34^+38^{low/-}$. The $CD34^+38^{low/-}$ fraction approximates the most primitive quiescent stem cell pool (less than 5% total $CD34^+$ cells).

2.1.1.5 Cryopreservation of cells

Primary CML $CD34^+$ cells and cell lines were cryopreserved in liquid nitrogen for long-term storage. Newly selected CML $CD34^+$ cells were suspended in 4.5% human albumin (ALBA®) and aliquoted in cryotubes, then an equal volume of 20% dimethyl sulphoxide (DMSO) in 4.5% ALBA® was added to give a final DMSO concentration of 10%. Cell lines in exponential growth phase were collected and resuspended with

10% DMSO in foetal calf serum (FCS) (5-10 x 10^6 cells/mL), and were aliquoted into cryotubes. The cryotubes were then transferred into a Mr. Frosty freezing container and kept in a -80°C freezer overnight to achieve a -1°C per minute cooling rate then transferred to liquid nitrogen for long-term storage.

2.1.1.6 Recovery of frozen cells

Primary $CD34^+$ cells were removed from liquid nitrogen and immediately thawed at 37°C in a water bath until the ice crystals had disappeared. The cells were transferred to a 15mL sterile tube and recovered by slowly adding 10mL of warm DAMP solution (2.3.7.2) drop-wise over a 20-minute period with a pastette. This step was performed at room temperature to enhance the activity of the DNase I, with gentle shaking to prevent clumping of the cells. After centrifugation at 120 x g for 10 minutes, the supernatant was carefully removed without disturbing the pellet, and then the pellet was loosened by flicking the tube. The pellet was washed twice more in DAMP to get rid of all DMSO. The CML cells were resuspended in SFM + 5GFs medium (2.3.7.4) and plated in a $25cm^3$ non-adherent tissue culture flask at 5 x 10^5 cells/mL for overnight recovery. Then the recovered cells were plated in SFM + PGFs medium (2.3.7.5) when the experiment required.

Cell lines were thawed in a 37°C water bath and recovered slowly as above but in $RPMI^{++}$ instead of DAMP. The cells were then washed twice with $RPMI^{++}$ and resuspended in 20mL of $RPMI^{++}$. Finally cells were plated in a $75cm^3$ tissue culture flask (2 x 10^5 cells/mL unless otherwise stated).

2.1.2 Flow Cytometry

Flow cytometry is able to characterize individual cells with fluorochrome-labelled antibodies. It supplies excitation energy with lasers and detects fluorescent emissions with a range of filters and detectors. It can also measure the size of a cell using forward scatter (FSC), and the granularity of a cell using side scatter (SSC).

2.1.2.1 Surface antibody staining

1 x 10^5 primary cells were collected and washed in PBS/2% FCS (2mL FCS with 98mL PBS; 120 x g for 10 minutes). The washed cells were resuspended in 100μL PBS/2% FCS with appropriate antibody solution. Then the cells were incubated in the dark for 15 minutes. After incubation, the cells were washed twice in PBS/2% FCS (120 x g for 10 minutes), and analysed by FACS immediately, or kept at 4°C until analysis. Appropriate isotype controls were used as negative controls.

2.1.2.2 Intracellular antibody staining

1 x 10^5 cells were washed with PBS and resuspended in 100μL of fixing reagent (Reagent A of Fix & Perm® kit) and incubated for 15 minutes. The fixed cells were then washed with PBS/1% BSA (1g BSA in 100mL PBS), and supernatant was completely removed. Appropriate volume of primary antibody was diluted (e.g. anti-p-CrkL; 1:10 dilution) in the permeabilising reagent (Reagent B of Fix & Perm® kit), and the cell pellet was resuspended in the primary antibody dilution. The cells were then incubated for 45 minutes at room temperature in the dark. After incubation, cells were washed twice in PBS/1% BSA (120 x g for 10 minutes) to get rid of excessive primary

antibody. Then the cells were resuspended with 100μL appropriate secondary antibody (e.g. anti-rabbit IgG FITC-conjugate; 1:50 dilution in PBS/1% BSA) and incubated at room temperature for 30 minutes in the dark. Finally cells were washed twice in PBS and analysed by flow cytometry. A matched isotype control was used instead of primary antibody in a separate sample as a negative control.

2.1.2.3 Viability analysis with Annexin V and Via-Probe

Cell viability was assessed by flow cytometry with Annexin V and Via-Probe staining. One of the features of early apoptosis is the translocation of phosphatidylserine from the inner layer of plasma membrane to the outer layer, where the cell surface phosphatidylserine is available for binding by Annexin V before the integrity of plasma membrane has been lost. In addition, cells continue to bind Annexin V after loss of plasma membrane integrity in late apoptosis. Via-Probe^{TM} (7-Amino-actinomycin D; 7-AAD) is a dye of nucleic acid. Late apoptotic cells are stained with 7-AAD as the integrity of plasma membrane is lost. Staining cells simultaneously with Annexin V-FITC (green fluorescence) and 7-AAD (far red fluorescence) enables distinguishing of viable, early apoptotic and late apoptotic (or necrotic cells) by flow cytometry (Annexin V^- $7AAD^-$, Annexin V^+ $7AAD^-$ and Annexin V^+ $7AAD^+$, respectively) (Figure 2-1).

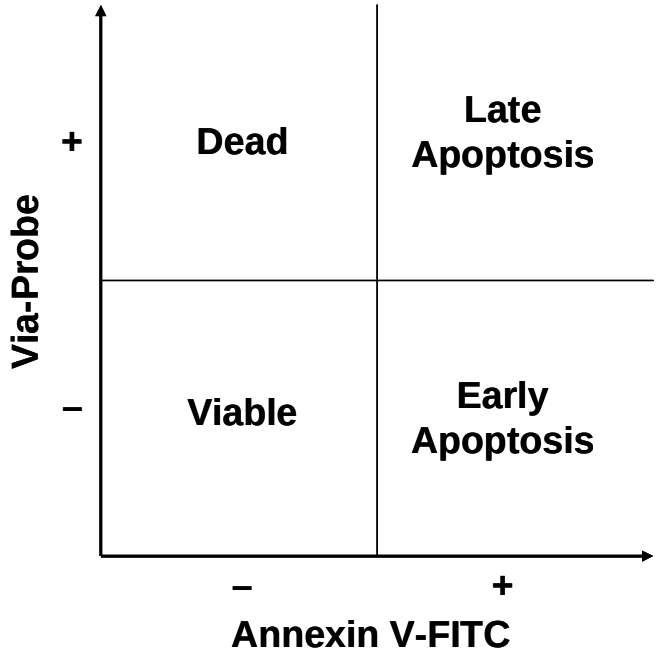

Figure 2-1: Assessment of cell viability by flow cytometry with Annexin V and Via-Probe staining.

For detection of viability, cells were collected at the stated times of drug exposure and pelleted by centrifugation (120 x g for 10 minutes). After that, pellets were resuspended in 85μL Annexin V Binding Buffer (1X) with 5μL Annexin V and 10μL Via-Probe^{TM} (100μL in total per 1 x 10^5 cells). Cells were then incubated in the dark for 15 minutes at room temperature. After incubation, 400μL 1X Annexin V Binding Buffer was added to each sample, and analysed immediately by flow cytometry.

2.1.3 Western blotting

2.1.3.1 Protein lysate preparation

Western blotting was used to separate, detect and quantify specific proteins from cell lysate. NP-40 lysis buffer (2.3.7.6) was prepared prior to use and kept on ice. Cells were taken from culture and washed twice with ice-cold PBS (120 x g for 5 minutes) in 1.5mL eppendorf tubes. Alternatively, cells taken from culture were pelleted rapidly at 21,000 x g for 30 seconds at 4°C. After removal of supernatant, the NP-40 lysis buffer was added to the cell pellets (2 x 10^5 cells/50μL) and mixed up by pipetting up and down at least five times and incubated on ice for 15 minutes. Subsequently, the cell lysates were centrifuged at 21,000 x g for 10 minutes at 4°C to pellet chromatins and debris. Finally, the supernatants were transferred to new eppendorf tubes and kept at -20°C until use.

2.1.3.2 Protein quantification

Bicinchoninic acid (BCA) protein assay was used to quantify protein lysate concentrations according to the manufacturer's instructions. This assay reduces Cu^{2+} to Cu^{1+} by protein in an alkaline medium and detects Cu^{1+} by a reagent containing BCA in a colorimetric way. Chelation of one Cu^{1+} ion with two BCA molecules forms purple-coloured reaction product. This product is water soluble and absorbs strongly at 562 nm and its absorbance almost linearly correlates with increasing concentrations from 20 to 2000μg/mL.

Bovine serum albumin (BSA) standards were prepared by serially diluting 2000μg/mL BSA in distilled water. The following BSA concentrations were prepared: 2000, 1500, 1000, 750, 500, 250, 125, 50, 25 and 5μg/mL. These BSA standards were kept at -20°C and used in multiple times. BCA working solution was prepared by mixing reagents A and B (50:1) thoroughly, and then 200μL of BCA working solution was added to each well of a 96-well plate. 10μL of each BSA standards were added to each well in triplicate, and 10μL of protein samples were added in duplicate. Then the plate was incubated at 37°C for 30 minutes and read by an ELISA plate reader for absorbance at 562 nm. Although the colour development continues, following incubation at 37°C the colour development rate is slow enough for the samples to be read. Finally, protein concentrations were calculated according to the BSA standards and equal amounts of protein lysates were loaded for Western blotting.

2.1.3.3 SDS-PAGE

Sodium dodecyl sulphate-polyacrylamide gel electrophoresis (SDS-PAGE) was employed to separate proteins based on their size. After protein quantification, protein lysates were mixed with same volumes of Laemmli 2X sample buffer (supplemented with 5% 2-mercaptoethanol) in a 1.5mL eppendorf tube and heated to 95°C for 10 minutes. SDS, contained within the sample buffer, is a negatively charged anionic detergent. It binds to hydrophobic regions of protein and denatures protein into its primary structure as soluble polypeptide chains. It also applies negative charge to protein molecules in proportion to its mass, leading to migration of protein towards the positive electrode if an electric field is applied.

After short centrifugation, the samples were loaded into a Nupage® Novex® Bis-Tris 4-12% gradient gel. 10μL of Novex® Sharp™ Pre-stained protein standard marker was loaded into a lane for protein size measurement. The gel was run in 1X NuPAGE® MOPS SDS Running Buffer (20X Running Buffer diluted in dH_2O) at 200V for 60 minutes with Invitrogen XCell *SureLock*™ Mini-Cell electrophoresis system. During the electrophoresis, proteins run through a polyacrylamide gel, a polymer meshwork of acrylamide monomers. With electric field applied, proteins with different sizes move at different rates. Smaller proteins run faster that larger ones, leading to separation of proteins according to their size.

2.1.3.4 Transfer to PVDF membrane

After gel electrophoresis, separated proteins on the gel were transferred to a Polyvinylidene fluoride (PVDF) membrane with the XCell II™ Blot Module. The PVDF membrane was soaked in methanol briefly for its activation, and then the membrane was soaked in transfer buffer for several minutes until it is completely wet. The sponges and filter papers were all pre-wet in transfer buffer (2.3.7.7) before use. Then the transfer sandwich was assembled as shown in Figure 2-2. Proteins were transferred at 30V for 60 minutes.

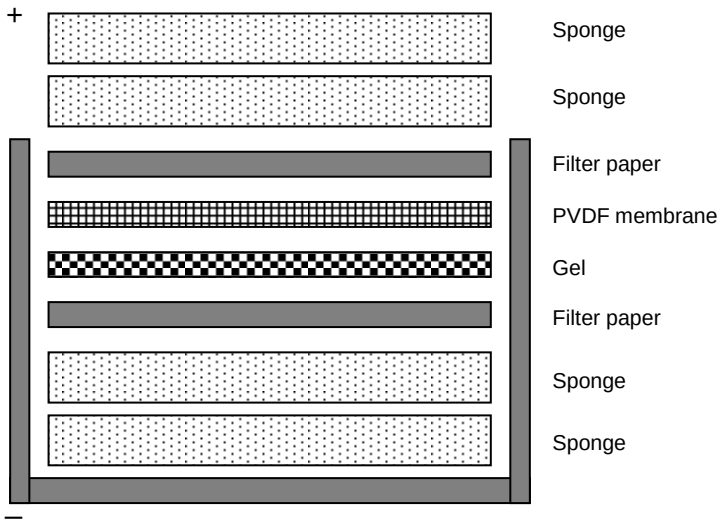

Figure 2-2. Assemble of sandwich for transfer of proteins to PVDF membrane.

10% methanol was included in the transfer buffer, and it has two important functions during the protein transfer. Firstly, methanol can maintain dimensional stability of gels. Polyacrylamide gel is able to absorb water. Thus the gel size increases a lot in water, resulting in loss of protein resolution in transfer. The presence of methanol in transfer buffer can minimize gel swelling. Secondly, methanol is capable of removing SDS from proteins and increase protein binding to the membrane. Since SDS adds a large amount of negative charges to proteins, protein molecules move very fast through the membrane and their interactions with PVDF decrease. Thus, removal of SDS by methanol retains proteins in the membrane.

2.1.3.5 Antibody labelling

After transfer, the PVDF membrane was stained with 0.1% Ponceau S for a minute to visualize protein bands and to examine transfer efficiency. Then the membrane was washed with distilled water several times to de-stain Ponceau S. Following that, the membrane was blocked in the 5% BSA/TBST blocking buffer (5g BSA in 100mL TBST) at room temperature for 1 hour with constant agitation. After blocking, the membrane was incubated with primary antibody solution diluted in the blocking buffer overnight at 4°C with gentle rotation. The next morning, the membrane was washed in the 1X TBST buffer (2.3.7.9) four times (10 minutes each time) to get rid of unbound primary antibody and reduce background. After washes, the membrane was incubated with horseradish peroxidase (HRP)-conjugated secondary antibody dilution for 1 hour at room temperate with agitation. Then the membrane was washed in the 1X TBST buffer four times (10 minutes each time) to remove unbound secondary antibody. Finally, the membrane was developed with the Immuno-Star™ WesternC™ Kit according to the manufacturer's instruction. Briefly, equal amounts of luminol/enhancer solution and peroxide solutions were mixed just prior to use. The membrane was incubated with the mixture for about three minutes. HRP oxidises luminol in the presence of hydrogen peroxide. Then the oxidized luminol goes back to its initial state, and light is emitted. The enhancer increases signal intensity and length. At last, digital pictures of protein bands were taken by the Molecular Imager® ChemiDoc™ XRS machine.

2.1.3.6 Stripping

In order to incubate the PVDF membrane with a different primary antibody, the membrane was incubated in 1X Re-Blot^{TM} Plus Strong Antibody Stripping Solution (diluted with distilled water) for about 15 minutes with constant shaking at room temperature. Then the membrane was washed briefly in TBST and re-blocked in 5% BSA/TBST for 1 hour before incubation with another primary antibody. The stripping solution removes antibodies bound in the membrane without removing proteins.

2.1.4 Immunoprecipitation

Immunoprecipitation is used to concentrate and separate a specific protein from a lysate with lots of different proteins. In the beginning, 1 x 10^7 cells were collected and washed twice with ice-cold PBS, and then the cell pellet was resuspended and lysed with 1mL ice-cold NP-40 lysis buffer, then incubated on ice for 30 minutes with occasional agitation for complete cell lysis. After incubation, the lysate was centrifuged at 21,000 x g for 15 minutes at 4°C to pellet insoluble materials. The supernatant was then transferred to a new eppendorf tube and 1µg of appropriate primary antibody was added followed by overnight incubation at 4°C with constant agitation. In this stage, the primary antibody specifically bound to a particular protein and indirectly to other proteins complexed with that particular protein. After that, 40µL of Protein A-Sepharose beads (50% slurry, pre-washed with NP-40 lysis buffer) was added to the lysate and incubated at 4°C for 2 hours with constant agitation. The primary antibody sticks to the beads during this incubation. Beads complexed with the antibody and proteins were then washed three times with the NP-40 lysis buffer to get

rid of non-specifically bound proteins (1000 x g for 2 minutes). Finally, 40µL of Laemmli 2X sample buffer was added to the beads, and boiled at 95°C for 10 minutes. In this step, proteins were denatured, separated from the beads and were then dissolved in the sample buffer. Finally, the beads were pelleted and the supernatant was subject to analysis by Western blotting.

2.1.5 Immunofluorescence microscopy

Poly-L-lysine coated multi-spot microscope slides were prepared in advance. Briefly, poly-L-lysine solution was diluted 1:10 in distilled water, and multi-spot microscope slides were immersed in the dilution in a coplin jar for 10 minutes. After that, excessive poly-L-lysine dilution was removed from slides, and these slides were air-dried and kept in a box for future use. Poly-L-lysine is adhesive and it facilitates suspension cells binding to glass microscope slides.

CML cells were pipetted onto poly-L-lysine coated multi-spot microscope slides (2 x 10^4 cells/spot) and left for 90 minutes. Then the suspension CML cells should be attached to microscope slides facilitated by poly-L-lysine. Subsequently, culture medium on the cells was removed by blotting with tissue paper without touching the cells. After that cells were fixed by 3.65% formaldehyde in PBS for 15 minutes at room temperature and then permeabilized by 0.5% Triton-X100 in PBS (5µL Triton-X100 in 95µL PBS) for 10 minutes. Formaldehyde fixes cells by cross-linking protein molecules. Triton-X100 is a detergent which can dissolve cellular lipid membranes to allow antibody access of internal proteins.

After permeabilization, cells were incubated with 5% BSA/PBS (5g BSA in 100mL PBS) for one hour at room temperature to block non-specific binding of antibodies. After blocking, cells were incubated with 0.5 µg/mL primary antibodies in 5% BSA/PBS for one hour at room temperature. Isotype control antibodies (class matched with primary antibodies) were used as negative controls. Then the cells were washed four times (5 minutes each time) with PBS to get rid of unbound primary antibodies in a coplin jar, isotype controls were washed in a separate coplin jar to avoid any antibody cross-contamination. After washing, cells were incubated with fluorochrome conjugated secondary antibodies for one hour at room temperature in the dark. After four washes (5 minutes each time) in PBS in a coplin jar, cells were air-dried and mounted in VECTASHIELD® mounting medium containing 4,6-diamidino-2-phenylindole (DAPI) and visualized by a Zeiss Imager M1 fluorescence microscope at 10x100 times magnification using oil immersion. Images were captured with multiple layers from the top to the bottom of cells and with the optimal distance (0.25µM) between adjacent layers. Captured images were subjected to deconvolution to remove non-specific fluorescence and sharpen images. Deconvolution was performed by the deconvolution module of the AxioVision software, the iterative algorithm and clip normalisation method was used.

Alexa Fluor® 488 phalloidin was added (1:250 dilution) into the primary antibody dilution to co-stain F-actin. Phalloidin is a mushroom toxin which binds with F-actin specifically. Alexa Fluor® 488 cholera toxin subunit B (CTxB) conjugate was employed to stain lipid rafts. CTxB is commonly used as a marker for lipid rafts.

Briefly, cells were incubated with the CTxB conjugate (1:500 dilution) at 4°C for 30 minutes before fixation. Then cells were washed with PBS once (5 minutes at 4°C) to get rid of excessive CTxB conjugate and fixed by formaldehyde. The following procedures are as above.

Fluorescence was measured as grey values by ImageJ software. The region of nucleus was selected manually according to the DAPI staining in order to quantify the red fluorescence within the nucleus. In the red channel, mean grey values and area sizes of the nuclear and whole cell were then measured. Mean grey value is the sum of all grey values in the selected area divided by the size of the area. The percentage of nuclear fluorescence was calculated using the equation $F_n\% = 100\% A_n (M_n - M_b)/A_w (M_w - M_b)$. In this equation, M_n, M_b, and M_w represent the nuclear, background, and whole cell mean grey values, respectively. A_n and A_w represent nuclear and whole cell areas, respectively. Three background areas were randomly selected around each cell, and the mean of these background mean grey values was calculated as M_b.

2.1.6 Uptake of sLDL by cell lines and primary cells

Synthesis of sLDL particles was performed by our collaborators in Cancer Research UK Formulation Unit, University of Strathclyde. CML cell line K562 (2.5×10^5 cells/mL) and primary CML patient cells (5×10^5 cells/mL) were incubated in the presence or absence of sLDL particles. At the end of incubation, 5×10^4 cells were sampled from each condition and washed with PBS. Mean fluorescence intensity of

the cells was then measured by flow cytometry in the FITC channel. For fluorescence microscopy, 2 x 10^4 cells from each condition were left on a poly-L-lysine coated multi-spot microscope slide for 90 minutes to allow cell attachment. Then cells were fixed with 3.65% formaldehyde in PBS for 15 minutes at room temperature, and air-dried. Finally, fixed cells were mounted in VECTASHIELD® mounting medium containing DAPI, and examined by the fluorescence microscope.

2.1.7 Polymerise chain reaction (PCR)

PCR is a powerful technique to amplify a single or a few DNA copies to billions of copies. It contains 20-40 thermal cycles, with each cycle consisting of three steps including denaturation of double-stranded DNA into single strands, annealing of primers to the single-stranded DNA and extension of primers by the Taq polymerase.

2.1.7.1 Primer design

Primers were designed with NCBI/Primer-Blast. The cDNA sequences were identified by searches on the Pubmed website, and then the sequences were used to design appropriate primers. The primers were about 20 base pairs with similar melting temperatures between forward and reverse primers, and no internal loops or primer dimers.

2.1.7.2 RNA extraction and cDNA synthesis by reverse transcription

Total cellular RNA was extracted using the RNeasy Mini Kit according to the manufacturer's instructions. The concentration and quality of extracted RNA was

measured with a NanoDrop ND-1000 spectrophotometer. An absorbance at 260nm quantified nucleic acid concentration, and RNA purity was determined by the ratio of 260/280 (1.8 to 2.0) and 260/230 (1.8 or greater). This is because nucleic acid is detected at 260nm, while solvents, salts and protein are detected at 230nm and 280nm.

RNA was reverse transcribed into cDNA by the High Capacity cDNA Reverse Transcription Kit according to the manufacturer's instruction. Briefly, 10μL of the extracted RNA was mixed with 10μL of 2X Reverse Transcription Master Mix (2.3.7.10) in a PCR tube. Then the 20μL mixture was run in a PCR Thermo Cycler. The program was 25°C for 10 minutes, 37°C for 120 minutes and 85°C for 5 seconds. Synthesised cDNA was kept at 4°C for short-term storage or at -20°C for long-term storage.

2.1.7.3 PCR

PCR Mix (2.3.7.11) was prepared in a PCR tube with GeneAmp® RNA PCR Core Kit according to the manufacturer's instruction. The PCR tube was heated to 94°C for 5 minutes at first to denature all the double-stranded cDNA, and then the PCR Thermo Cycler was set up to run 35 cycles of 94°C for 30 seconds, 52°C for 1 minute and 72°C for 1 minute. After all cycles finished, the tubes were heated to 72°C for 5 minutes for final extension, and then held at 4°C.

2.1.7.4 Gel electrophoresis

The PCR products were electrophoresed in gels in order to visualize individual DNA bands. Basically, a 1% agarose gel was prepared with 0.5g agarose powder in 50mL of 1X TBE buffer (2.3.7.12; 10X TBE buffer diluted in dH_2O). It was melted in a conical flask in a microwave until the agarose powder had completely dissolved. When the gel cooled down to about 60°C, 1μL ethidium bromide (10mg/mL) was added and mixed well. Then the gel was poured into a casting tray with a comb inserted to create loading wells. The gel was left to set for about 30 minutes. The comb was removed and the gel was placed in a gel tank with 1X TBE buffer. The TBE buffer should cover the gel and be 2-5 mm higher). 10μL of PCR product mixed with 2μL loading dye (6X) was loaded into each well of the gel (2μL of 100bp DNA ladder was loaded in a separate lane), and then the gel was run at 50V constant voltage. After running, the gel was viewed by a UV transilluminator (ChemiDoc) and photographed.

2.1.8 ROS measurement

Intracellular reactive oxygen species (ROS) was measured with 2'-7'-dichlorofluorescin diacetate (DCFDA). The non-fluorescent DCFDA can be cleaved into green fluorescent 2',7'-dichlorofluorescein (DCF) by intracellular esterases and oxidation. DCFDA is commonly used to detect the generation of ROS in cells. To measure intracellular ROS level with drug treatments, fresh cells were washed with PBS and incubated with 5μM DCFDA / PBS at 37°C in the dark for 30 minutes. Cells were loaded with DCFDA at this stage as DCFDA was cell-permeable. After that,

cells were washed with PBS and plated in fresh medium, and then cells were left to recover in a cell culture incubator for 2 hours. Subsequently, appropriate drugs were added to the cell culture, and at the end of the treatment the level of fluorescent DCF was measured by flow cytometry in the FITC channel. Cells without drug treatment (either unloaded or loaded with DCFDA) were used as negative controls.

2.2 Statistics

The results are shown as the mean ± standard error of the mean (mean ± SEM). Unless otherwise stated, all statistical analyses were performed with the Microsoft Office Excel software using the two-sided unpaired Student's t-test and the assumption of normality was checked. *P*-values less than 0.05 were considered statistically significant.

2.3 Materials

2.3.1 Small molecule inhibitors

Imatinib Mesylate (IM) was provided as a white powder under a Materials Transfer Agreement from Novartis Pharma (Basel, Switzerland). It was dissolved in sterile water and stored as 100mM aliquots at 4°C. Dasatinib, BMS-214662 and BMS-225975 were provided as white powder under Materials Transfer Agreements from Bristol-Myers Squibb (Princeton, USA). They were dissolved in sterile DMSO to give a stock concentration of 20mM, 100mM and 100mM respectively, and stored as

aliquots at −20°C. PP2 and sodium stibogluconate (SSG) were purchased from Calbiochem, Merck Biosciences (Nottingham, UK) as white powder. PP2 was dissolved in DMSO to give a stock concentration of 10mM and stored as aliquots at −20°C. SSG was dissolved in sterile water (10mg/mL) and heat to 75°C until completely dissolved immediately prior to use. All small molecule inhibitors were diluted to the appropriate concentrations prior to use.

2.3.2 Tissue culture materials

Chugai Pharma London, UK	Recombinant human G-CSF
Gilson Middleton, USA	Yellow and Blue pipette tips
Greiner Bio-One Gloucestershire, UK	Cryo.s™ cryotubes Tissue culture flasks (25cm^2, 75cm^2 and 175cm^2) Tissue culture plates (6-well, 12-well, 24-well and 96-well) Pipettes (5mL, 10mL and 25mL)
Invitrogen Paisley, UK	2-mercaptoethanol Foetal calf serum (FCS) L-glutamine 200mM IMDM medium Penicillin-streptomycin solution 5000u/mL RPMI 1640 medium Dulbecco's PBS
Nalgene Labware Roskilde, Denmark	25 and 75cm^3 non-adherent tissue culture flasks Cryo freezing container "Mr. Frosty" Vacubottles
Startorius Hannover, Germany	Minisart 0.2μM Sterile filters Minisart 0.45μM sterile filters

Scottish National Blood Transfusion Glasgow, UK	20% Human Serum Albumin 4.5% human albumin solution (ALBA®)
Sigma-Aldrich Dorset, UK	Bovine serum albumin (BSA) Dimethyl sulphoxide (DMSO) Hydrochloric acid (HCl) Magnesium chloride ($MgCl_2$) PBS tablets Poly-L-lysine Potassium Chloride (KCl) Trypan Blue Solution (0.4%) Trisodium citrate
Stem Cell Technologies British Columbia, Canada	Bovine pancreatic deoxyribonuclease (DNase 1) 1mg/mL Bovine serum albumin/insulin/transferrin (BIT) serum substitute Flt-3 ligand Interleukin-3 (IL-3) Interleukin-6 (IL-6) Stem Cell Factor (SCF)
Sterilin Ltd Hounslow, UK	Pastettes 5mL, 10mL and 25mL disposable pipettes 15 and 50mL sterile plastic falcon tubes
Weber Scientific International West Sussex, UK	Hawksley Neubauer counting chamber

2.3.3 Flow cytometry materials

Becton Dickinson Oxford, UK	Annexin V Binding Buffer (10X) FACS flow FACS clean Mouse anti-human-annexin-V-FITC Mouse anti-human-CD34-APC Mouse anti-human-CD34-PE

	Mouse anti-human-CD38-PE Mouse anti-human-CD45-PE Mouse anti-human-CD133-APC Mouse IgG-APC isotype control Mouse IgG-FITC isotype control Mouse IgG-PE isotype control Via-Probe™
Caltag Laboratories Silverstone, UK	Fix and Perm® A and B
Cell Signaling, New England Biolabs Hitchin, UK	Rabbit anti-p-CrkL antibody
Greiner Bio-One Gloucestershire, UK	FACS tubes
Sigma-Aldrich Dorest, UK	Goat anti-rabbit IgG FITC-linked secondary antibody

2.3.4 Fluorescence microscopy supplies

Abcam Cambridge, UK	Mouse IgG2a isotype control Rabbit IgG isotype control
Carl Zeiss Jena, Germany	AxioVision software Imager 1 fluorescence microscope
Cell Signalling, New England Biolabs Hitchin, UK	Mouse anti-Bcr-Abl (b2a2 junction specific) antibody
Hendley Essex, UK	Multi-spot microscope slides
Invitrogen Paisley, UK	Alexa Fluor® 488 cholera toxin subunit B conjugate Alexa Fluor® 488 goat anti-rabbit IgG Alexa Fluor® 594 goat anti-mouse IgG Alexa Fluor® 488 phalloidin
Santa Cruz Santa Cruz, USA	Rabbit anti-Pan-14-3-3 antibody

Sigma-Aldrich Dorest, UK	Poly-L-lysine solution 0.1 % (w/v) in H_2O Triton-X100
Vector Laboratories Burlingame, CA, USA	VECTASHIELD® mounting medium with DAPI

2.3.5 Molecular biology materials

Lonza Basel, Switzerland	Nucleofector® II Device Amaxa® Cell Line Nucleofector® Kit V
Applied Biosystem Foster City, CA, USA	GeneAmp® RNA PCR Core Kit High Capacity cDNA Reverse Transcription Kit Nuclease free water
Bio-Rad Hercules, CA, USA	Combs for gel casting Gel casting trays Immuno-Blot™ PVDF membrane Immuno-Star™ WesternC™ Kit Laemmli 2X sample buffer Molecular Imager® ChemiDoc™ XRS PVDF membrane
Becton Dickinson Oxford, UK	Anti-PTP1B antibody Anti-SHP1 antibody Anti-SHP2 antibody
Cell Signalling, New England Biolabs Hitchin, UK	Goat anti-mouse IgG HRP-linked secondary antibody Goat anti-rabbit IgG HRP-linked secondary antibody Mouse anti-Bcr-Abl (b2a2 junction specific) antibody Rabbit anti-c-Abl antibody Rabbit anti-GAPDH antibody Rabbit anti-p-CrkL antibody Rabbit anti-Ubiquitin antibody
Chemicon International	Re-Blot™ Plus Strong Antibody Stripping

Temecula, CA, USA	Solution
Chemical Store, University of Glasgow Glasgow, UK	Ethanol Methanol
Eurofins MWG Operon Wolverhampton, UK	PCR Primers
Helena Biosciences Gateshead, UK	Agarose Powder
Invitrogen Paisley, UK	Novex® Sharp™ Pre-stained Protein Standard NuPage® MOPS SDS Running Buffer (20X) Nupage® Novex® Bis-Tris 4-12% gel NuPage® Transfer Buffer (20X) XCell II™ Blot Module XCell *SureLock*™ Mini-Cell electrophoresis system
Labtech International East Sussex, UK	NanoDrop ND-1000 spectrophotometer
Lonza Basel, Switzerland	Amaxa® Cell Line Nucleofector® Kit V Nucleofector® Device
Qiagen West Sussex, UK	RNeasy Mini Kit QIAshredder Kit
Sigma-Aldrich Dorset, UK	0.1% Ponceau S solution 2-glycerophosphate Aprotinin Boric acid Dichlorofluorescin diacetate (DCFDA) Ethylenediaminetetraacetic acid (EDTA) Formaldehyde solution (36.5%) Leupeptin NP-40 PMSF Protein A-Sepharose® 4B Sodium chloride Sodium fluoride Sodium orthovanadate

	Sodium pyrophosphate Tris base TWEEN 20 for electrophoresis
Thermo-Scientific Hertfordshire, UK	Albumin standard BCA™ Protein Assay Kit
SG Wasseraufbereitung und Regenerierstation GmbH Barsbuttel, Germany	Ultra Pure Water system (sterile water)
Upstate (Millipore) Watford, UK	Anti-Phosphotyrosine (4G10®) antibody
Promega, Southampton, UK	100bp DNA ladder PCR loading dye (6X)

2.3.6 PCR primer sequences

Actin Forward	GTGCGTGACATTAAGGAGAA
Actin Reverse	GGAGGGGCCGGACTCGTCA
Bcr-Abl Forward	GATGCTGACCAACTCGTGTG
Bcr-Abl Reverse	AGCAGATACTCAGCGGCATT

2.3.7 Media and solutions

2.3.7.1 RPMI^{++}

RPMI 1640	440mL
FCS	50mL
L-glutamine (200mM)	5mL
Penicillin/streptomycin solution (10,000 UmL^{-1}/ 10,000 gmL^{-1})	5mL

2.3.7.2 'DAMP' solution

DNase I (2 vials at ~2500 U/vial (1mL)	2mL
Magnesium chloride (400X, 1.0 M stock)	1.25mL
Trisodium citrate (0.155M)	53mL
Human Serum Albumin (20%, SNBTS)	25mL
Dulbecco's PBS (magnesium/calcium free)	418.75mL

2.3.7.3 Serum free medium (SFM)

BIT	25mL
L-glutamine (200mM)	1.25mL
Penicillin/streptomycin solution ($10,000\ UmL^{-1}$/ $10,000\ gmL^{-1}$)	1.25mL
2-mercaptoethanol (50mM)	250µL
Low density lipoprotein (10 mg/mL)	500µL
IMDM	97.25mL

Make up in a sterile bottle then filter sterilise using a Vacubottle.

2.3.7.4 SFM supplemented with five growth factors (SFM + 5GFs)

Serum free medium	10mL
IL-3 (50µg/mL)	4µL
IL-6 (50µg/mL)	4µL
G-CSF (20µg/mL)	10µL
Flt3L (50µg/mL)	20µL
SCF (50µg/mL)	20µL

2.3.7.5 SFM supplemented with physiological growth factors (SFM + PGFs)

Serum free medium	10mL
SCF (0.5µg/mL)	4µL
G-SCF (2µg/mL)	5µL
GM-CSF (0.1µg/mL)	20µL
IL6 (5µg/mL)	2µL
LIF (0.1µg/mL)	5µL
MIP-a (0.1µg/mL)	20µL
Filter through 0.22µM filter	

2.3.7.6 NP-40 Protein lysis buffer

dH_2O	8.7mL
NaCl (5M)	300µL
Hepes-NaOH (1M, pH 7.5)	200µL
EDTA (100mM)	200µL
NP-40	50µL
PMSF (100mM)	100µL
Sodium fluoride (500mM)	40µL
Sodium orthovanadate (500mM)	20µL
Sodium pyrophosphate (100mM)	100µL
2-glycerophosphate (1M)	200µL
Leupeptin (1mg/mL)	50µL
Aprotinin (1mg/mL)	22µL

2.3.7.7 Transfer buffer

NuPAGE® Transfer Buffer (20X)	30mL
dH_2O	510mL
Methanol	60mL

2.3.7.8 10X TBS buffer

NaCl	876.6g
Tris	121.1g
dH_2O	10L
Adjust pH to 8.0	

2.3.7.9 1X TBST buffer

10X TBS buffer	1L
TWEEN 20	10mL
dH_2O	8.99L

2.3.7.10 2X Reverse Transcription Master Mix (10μL)

10X RT Buffer	2μL
25X dNTP Mix	0.8μL
10X RT Random Primers	2μL
Reverse Transcriptase	1μL
Nuclease free H_2O	4.2μL

2.3.7.11 PCR Mix (50µL)

10X PCR Buffer	5µL
dNTP Mix (1000µM)	10µL
Taq polymerase	0.25µL
Forward primer (100µM)	0.25µL
Reverse primer (100µM)	0.25µL
$MgCl_2$ (25mM)	5µL
cDNA	1µL
Nuclease free H_2O	28.25µL

2.3.7.12 10X TBE buffer

Boric Acid	55g
EDTA (0.5M, pH8.0)	40mL
Tris Base	108g
dH_2O	1L

3 Results 1: Treatment of CML cells with IM and LMB

3.1 Introduction

Despite the success of TKI in treating CML, *Bcr-Abl* mRNA and DNA are still detectable in CML patients who have achieved CCgR and even CMR (143;182). In addition, the primitive CML stem cell population is insensitive to TKI treatment (201), and may lead to disease relapse. Therefore, new strategies must be developed to eradicate this TKI-insensitive CML stem cell population in order to cure CML.

There are three NLSs and one NES in the Abl protein, and Abl constantly shuttles between the cytoplasm and the nucleus (72;245), and these localisation signals are intact in the Abl portion of the Bcr-Abl fusion protein. However, Bcr-Abl protein is exclusively located in the cytoplasm of expressing fibroblasts and K562 cells (198), but Vigneri and Wang have reported that inhibition of phosphorylation of Bcr-Abl by IM could induce nuclear import of Bcr-Abl protein (198). In their study, nuclear entrapment of Bcr-Abl by LMB resulted in apoptosis of transfected fibroblasts and K562 cells induced by reactivation of Bcr-Abl tyrosine kinase activity in the nucleus (198). In addition, they treated K562 cells with IM and LMB for 72 hours followed by drug washout, and K562 cells were eliminated six days after drug removal, but not with IM or LMB alone treatment (198). These findings suggest that long term drug exposure was not required. However, they did not test this combination in human primary CML cells.

Furthermore, Aloisi *et al* reported that sequential treatment of CML myeloid progenitors with IM then LMB effectively reduced the number of Bcr-Abl$^+$ colonies with limited effects on normal CD34$^+$ cells (246). Their rational was that the initial 12-hour IM treatment inhibited Bcr-Abl tyrosine kinase activity, and induced nuclear localisation of Bcr-Abl protein. The addition of LMB for another 12 hours trapped Bcr-Abl inside the nucleus. Finally, drug washout at the end of the treatment reactivated Bcr-Abl tyrosine kinase in the nucleus, and induced apoptosis via the p73 pathway (198;246). In that report Aloisi *et al* demonstrated a cytostatic effect of the sequential IM and LMB treatment on CML myeloid progenitors by colony-forming assay. However, the cytotoxicity of the sequential regimen on CML cells has not been investigated.

Thus, the aims of this chapter were to investigate the cytotoxic efficacy of 72-hour continuous IM and LMB combined treatment in human primary CML progenitors, and evaluate the cytotoxic effect of the sequential IM and LMB treatment on CML cells.

3.2 IC_{50} of LMB in K562, KCL22 and HL60 cells

In order to assess the cytotoxicity of LMB, the 50% proliferation inhibitory concentrations (IC_{50}) of LMB were investigated in Bcr-Abl$^+$ CML cell lines K562 and KCL22, and in Bcr-Abl$^-$ AML cell line HL60. Cells were treated with LMB with concentrations from 0.625 to 40nM for 24 and 72 hours. The number of viable cells was counted with trypan blue (Figure 3-1), and the IC_{50} values are shown in Table 3-1.

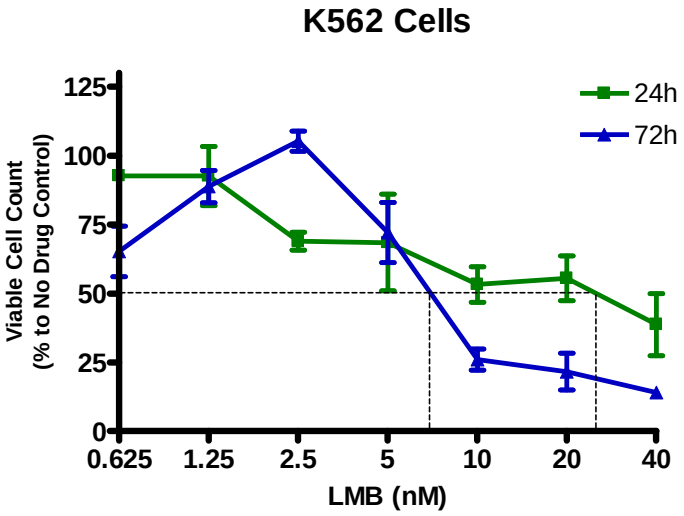

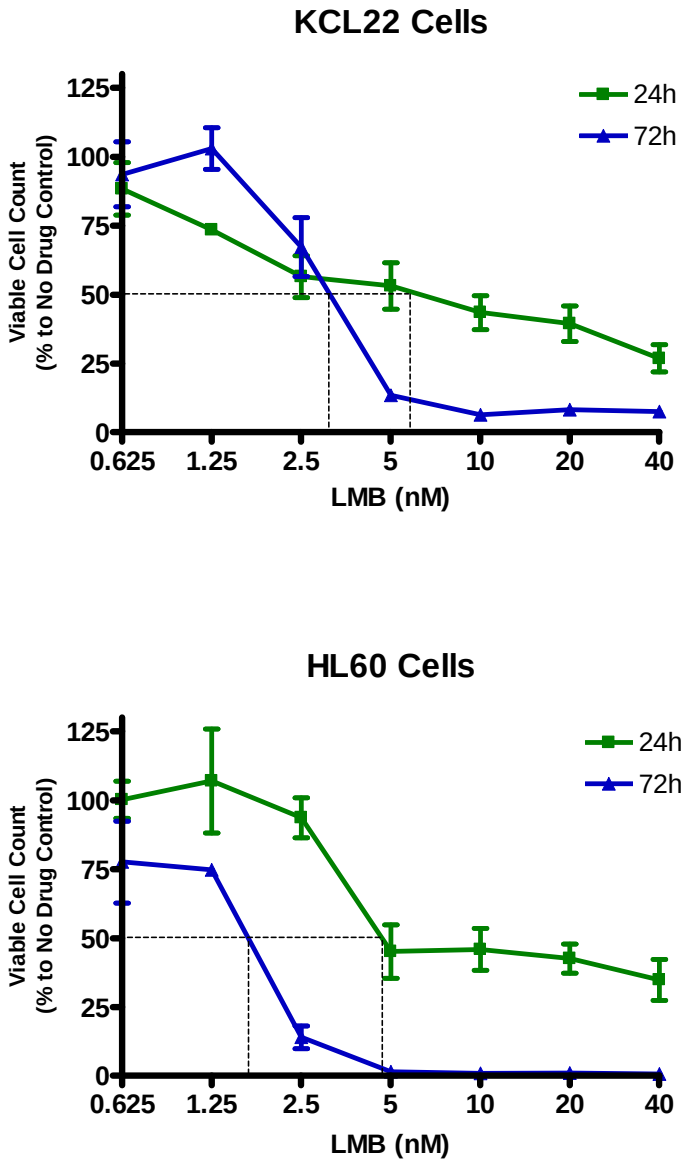

Figure 3-1: Determination of IC_{50} for LMB in K562, KCL22 and HL60 cells.

Viable cells were counted by trypan blue at 24 and 72 hours. The percentage of cells in each treatment compared with no drug control (NDC, 100%, the untreated at each corresponding time-point) were calculated and is presented as mean ± SEM (n=3). LMB concentrations are plotted in Log2 scale.

	Leptomycin B (LMB) IC50 (nM)		
Time (hours)	**K562**	**KCL22**	**HL60**
24	26	7	5
72	7	3	2

Table 3-1: IC_{50} for LMB in K562, KCL22 and HL60 cells at 24 and 72 hours.

Estimated from mean values in the above figure.

Vigneri and Wang used 10μM IM and 10nM LMB in their cell survival assays (198), as did Aloisi *et al* in their colony-forming assays (246). Since the experiments in this chapter were designed as follow-up of their investigations and the observed IC_{50} values for LMB were also in the low nM range, 10μM IM and 10nM LMB were used in the subsequent experiments.

3.3 Continuous treatment of IM and LMB in CML cells

To investigate the cytotoxicity of IM and LMB combined treatment in human primary CML $CD34^+$ progenitors, cells were treated with 10μM IM, 10nM LMB or both drugs continuously for 72 hours. Then drugs were washed out and cells were plated into fresh medium. The number of cells in each treatment was counted with trypan blue every 2 or 3 days. Fresh medium was added after cell counting and cell density was adjusted to the original seeding density if necessary. Dilution factors were calculated every time when fresh media was added, and the total number of counted viable cells

multiplied by the corresponding dilution factors. Non-CML (Lymphoma) $CD34^+$ cells were used as a $Bcr\text{-}Abl^-$ control.

As shown in Figure 3-2A, the 72-hour IM and LMB continuous treatment regimen did not eliminate CML $CD34^+$ cells. Although it caused a one-log reduction of cell counts compared with input three days after drug washout, these cells then recovered and continue to grow. An alternative scheduling regimen of the two drugs, such as sequential treatment, might be effective in killing primary CML $CD34^+$ cells. In addition, the LMB alone arm showed very similar effect as the combined treatment arm in CML $CD34^+$ cells (Figure 3-2A), indicating the combined treatment does not improve cytotoxic effect with respect to LMB alone. Furthermore, LMB inhibited proliferation of non-CML $CD34^+$ cells (Figure 3-2B), demonstrating the non-specific cytotoxicity of this compound. However, CML $CD34^+$ cells did appear to be more sensitive to LMB than non-CML $CD34^+$ cells.

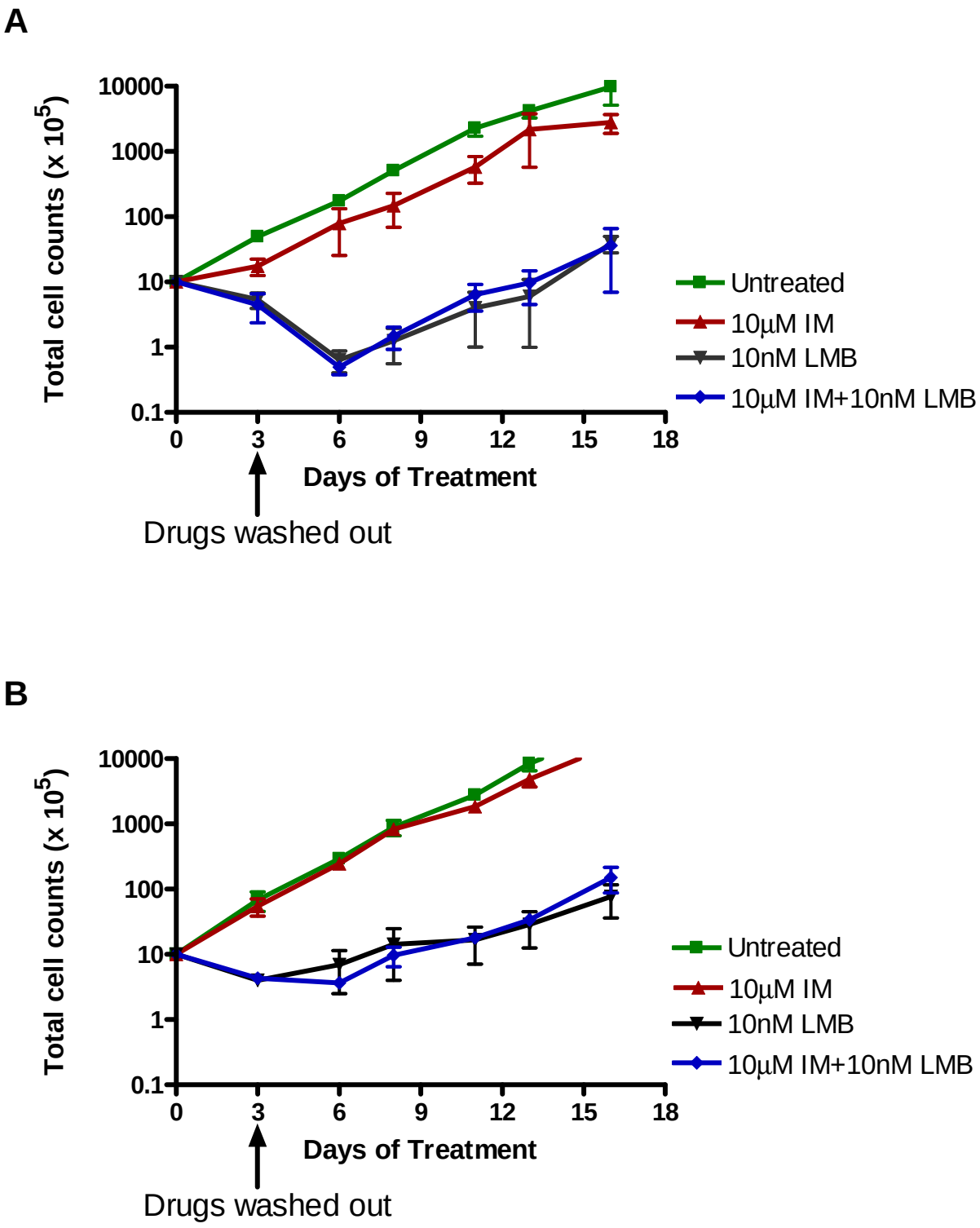

Figure 3-2: IM and LMB 72-hour continuous treatment.

CML CD34$^+$ (A) and non-CML CD34$^+$ (B) cells were treated with 10μM IM, 10nM LMB or both drugs for 72 hours. Drugs were washed out with PBS at the end of 72-hour treatment, and cells were plated in fresh medium. The number of viable cells in each treatment was counted with trypan blue at Day 3, 6, 8, 11, 13 and 16. Cell counts were plotted in log10 scale and presented as mean ± SEM (n=3, CML samples 223, 236 and 255. Non-CML samples 006, 007 and 011). CD34$^+$ cells were plated at 5 X 10^5 cells/mL in 2 mL cultures in SFM + 5GFs medium.

3.4 Sequential treatment of IM and LMB in CML cell lines

After the failure of IM and LMB continuous treatment to eliminate CML progenitors, the effects of IM and LMB sequential treatment were investigated in CML cells, initially in CML cell lines. K562 and KCL22 cells were treated with 10μM IM for 12 hours, and then 10nM LMB was added in without change of culture medium. The cells were incubated with both IM and LMB for another 12 hours, after that, drugs were washed out with PBS and the cells were plated into fresh medium (as illustrated in Figure 3-3A). This sequential regimen was adopted from the report by Aloisi *et al* (246).

The adjusted total cell counts in each treatment are shown in Figure 3-3B and C. It was shown that 10μM IM significantly inhibited proliferation of both K562 and KCL22 cell lines (p<0.05 since Day 3 and p<0.05 since Day 6, respectively; Figure 3-3B and C). In addition, K562 cells, but not KCL22 cells, were eliminated by IM at the end of the experiments, indicating that K562 is more sensitive to IM than KCL22. Although

the IM+LMB treatment arm had lower cell counts than the IM alone arm, the difference was not statistically significant in either K562 or KCL22 cells (p>0.07 at all time-points). This suggested that the sequential IM and LMB treatment did not significantly reduce the proliferation of CML cell line cells compared to IM alone.

A

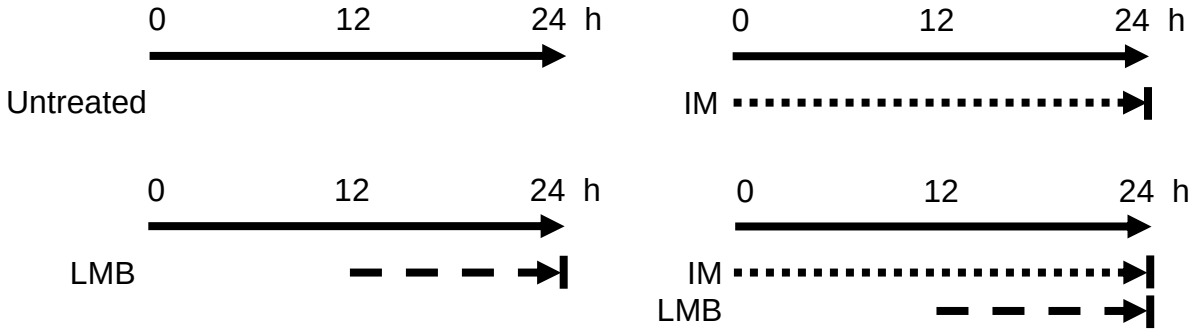

B

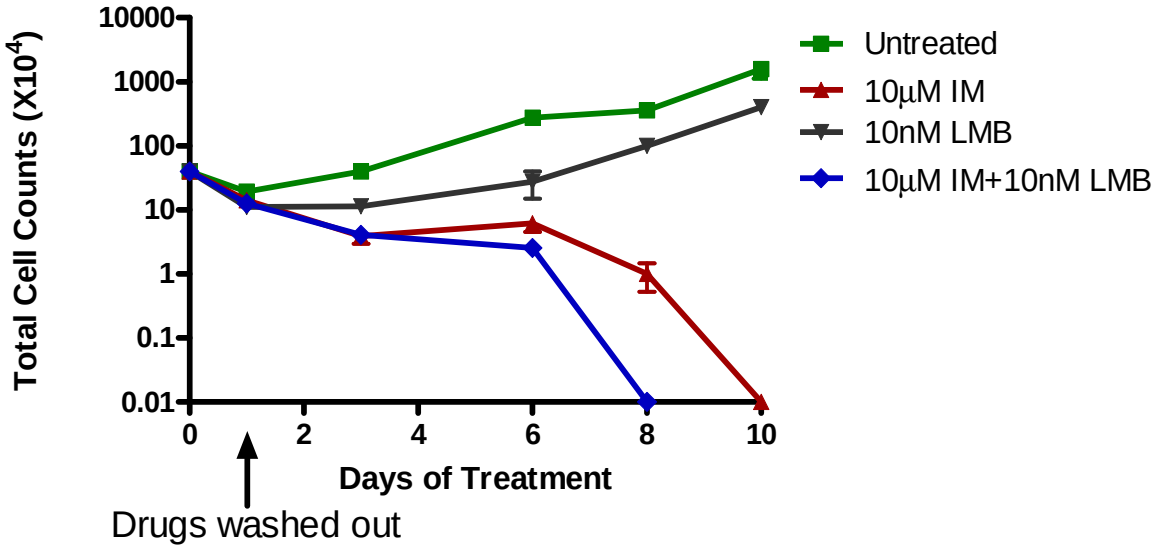

C

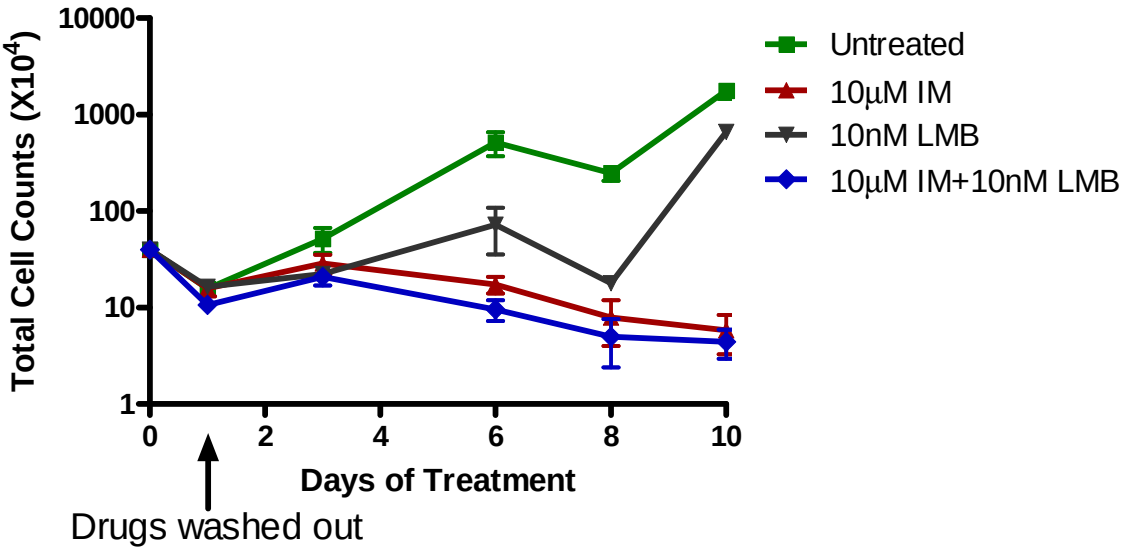

Figure 3-3: IM and LMB scheduling treatment in K562 and KCL22 cells.

Diagram illustrating the scheduling treatment strategy with IM and LMB in CML cells. Drugs were washed out at the end of 24-hour treatment, and cells were plated in fresh medium. The number of viable cells in each treatment was counted with trypan blue at Day 1, 3, 6, 8 and 10. Cell counts were plotted in log10 scale in graph B (K562 cells) and C (KCL22 cells), and presented as mean ± SEM (n=4). Cells were plated at 2 X 10^5 cells/mL in 2 mL cultures.

3.5 Sequential treatment of IM and LMB in BaF3 wild type and Bcr-Abl expressing cells

In order to assess whether sequential IM and LMB treatment differentially affect Bcr-Abl positive and negative cells, the sequential treatment was applied to Ba/F3 wild type and Ba/F3 Bcr-Abl expressing cells (Ba/F3 p210). LMB (10nM) inhibited proliferation of both Ba/F3 wild type and p210 cells by about one log compared to the untreated arm, again showing the non-specific cytotoxicity of this drug. As expected, 10μM IM eliminated Ba/F3 p210 cells at Day 8 (Figure 3-4B), but had mild though significant inhibition of proliferation of Ba/F3 wild type cells compared to the untreated (p<0.05 at every time-point; Figure 3-4A).

However, there was no statistical significant difference between IM+LMB and IM treatment arms in Ba/F3 p210 cells (p>0.07 at every time-point; Figure 3-3B). This result confirms that sequential IM and LMB treatment did not induce more cell death compared to IM only in the Bcr-Abl transduced cell line in a similar way to the Ph^+ CML cell lines.

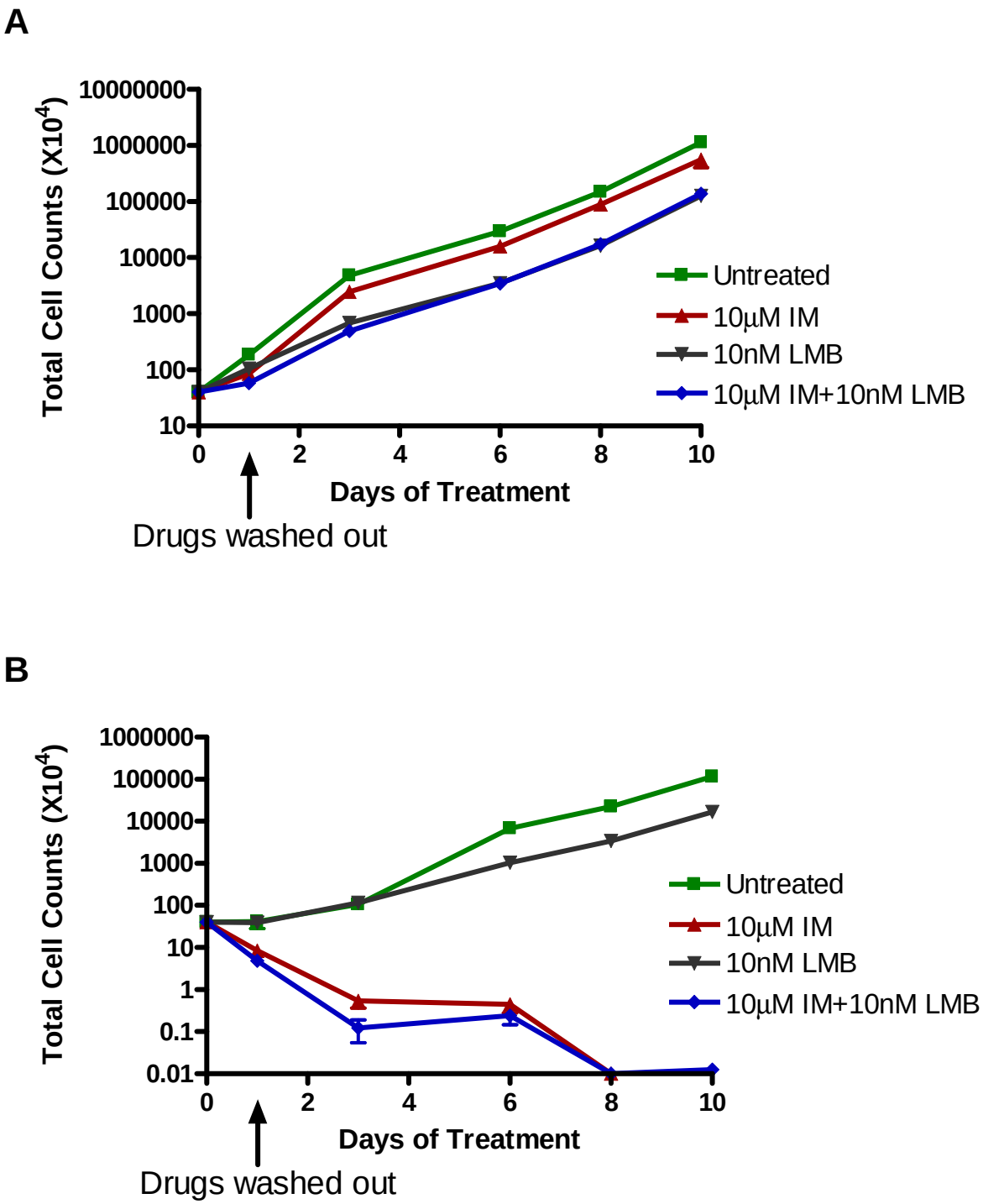

Figure 3-4: IM and LMB scheduling treatment in Ba/F3 cells.

Ba/F3 wild type (A) and Ba/F3 Bcr-Abl expressing cells (B) were treated with IM and LMB in the schedules shown in Figure 3-3A. The number of viable cells in each treatment was counted with trypan blue. Cell counts were plotted in log10 scale, and presented as mean ± SEM (n=4). Cells were plated at 2 X 10^5 cells/mL in 2 mL cultures. 10ng/mL IL-3 was added as a supplement to parental Ba/F3 cell culture medium.

3.6 Sequential treatment of IM and LMB in CML primary cells

In order to test the effect of the sequential treatment on CML progenitors, primary CML $CD34^+$ cells were treated with the same scheduling regimen as in CML cell lines, and it was found that both IM and IM+LMB treatment arms significantly inhibited cell proliferation compared to the untreated arm at Day 3 (p=0.002 and p=0.014, respectively), Day 6 (p=0.004 and p=0.009, respectively) and Day 10 (p=0.05 and p=0.01, respectively). Unlike in CML cell lines, IM and IM+LMB treatment arms did not reduce cell counts of primary $CD34^+$ cells to lower than input at later time-points, showing just a mild cytostatic effect (Figure 3-5A).

On the other hand, there was no statistical significant difference between IM and IM+LMB treatment arms at each time-point (p>0.35 at every time-point; Figure 3-5A), suggesting that sequential IM and LMB treatment did not preferentially inhibit proliferation of primary CML $CD34^+$ cells compared to IM alone.

In addition, the percentage of viable cells in each treatment was measured by flow cytometry of staining cells with Annexin V and Via-Probe (Figure 3-5B). Cells

negative for both Annexin V and Via-Probe staining were considered viable. It showed that the difference between IM+LMB and LMB treatments was not statistically significant (p>0.32 at every time-point), although significant difference was observed between IM+LMB and IM treatments on Day 1 and Day 3 (p=0.028 and p=0.022, respectively). These data suggested that sequential IM and LMB treatment did not further induce apoptosis of primary CML $CD34^+$ cells compared to LMB alone.

A

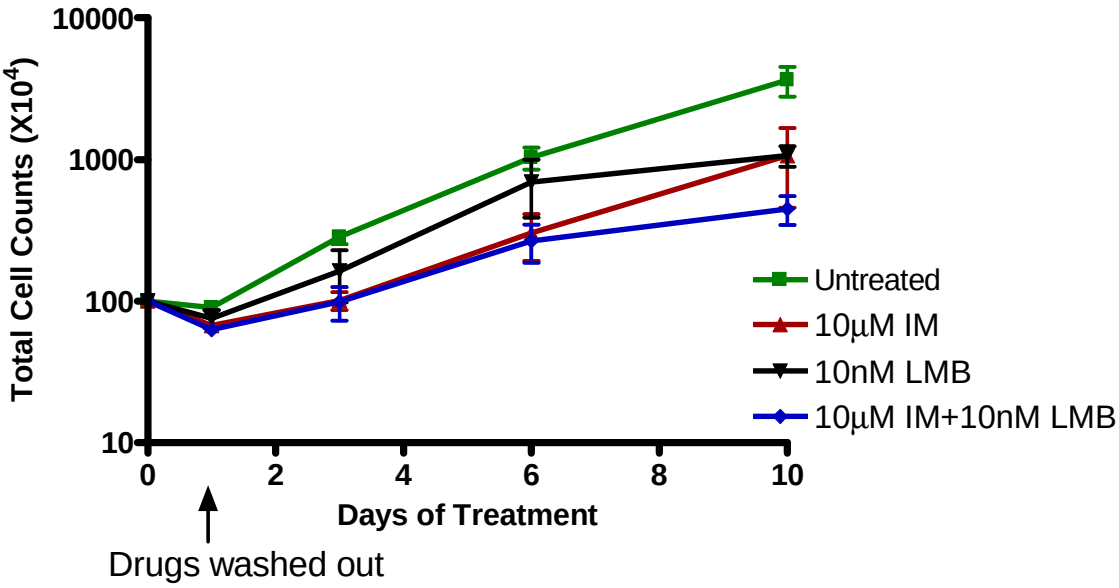

B

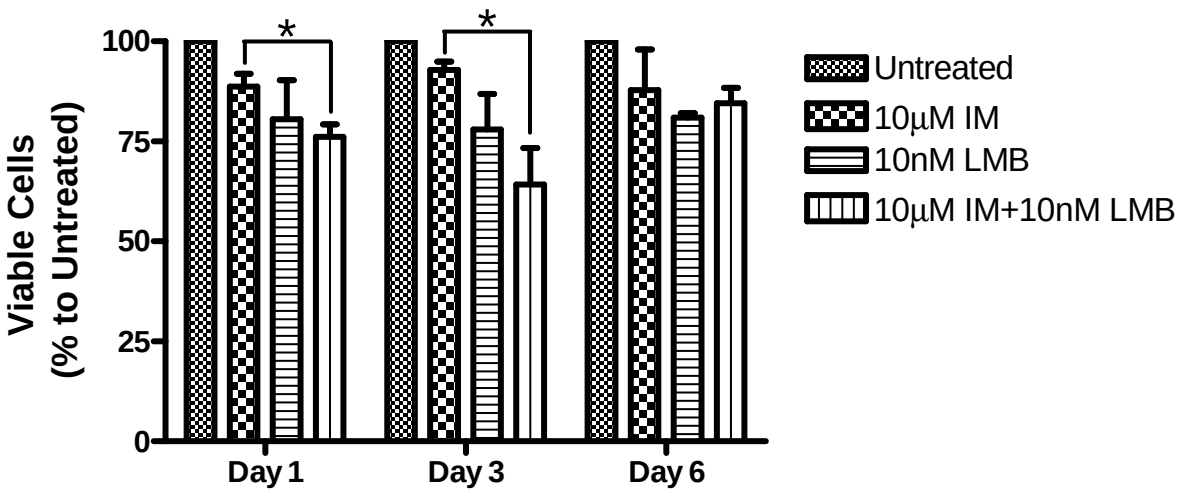

Figure 3-5: IM and LMB scheduling treatment in primary CML CD34$^+$ cells.

(A) Viable cell counts with trypan blue were plotted in log10 scale (B) Percentage of viable cells in each treatment compared with untreated as analyzed by flow cytometry with Annexin V and Via-Probe (mean ± SEM, n=2, CML235 and CML255, each sample was plated in duplicates). Cells were plated at 5 X 10^5 cells/mL in 2 mL cultures in SFM + 5GFs medium. (*p<0.05)

3.7 Nuclear localisation of Bcr-Abl in IM and LMB treated CML cells

To determine whether the Bcr-Abl protein was translocated into cell nucleus after IM and LMB exposure as per the hypothesis, KCL22 cells were treated with 10μM IM and 10nM LMB for 4 hours. Subsequently, cells were stained with a Bcr-Abl b2a2 junction specific antibody and prepared for immunofluorescence microscopy. It was observed that the vast majority of the Bcr-Abl protein was located in the cytoplasm of

untreated KCL22 cells (Figure 3-6). However, after treatment with IM and LMB a significant proportion of Bcr-Abl protein was observed in the nucleus of KCL22 cells.

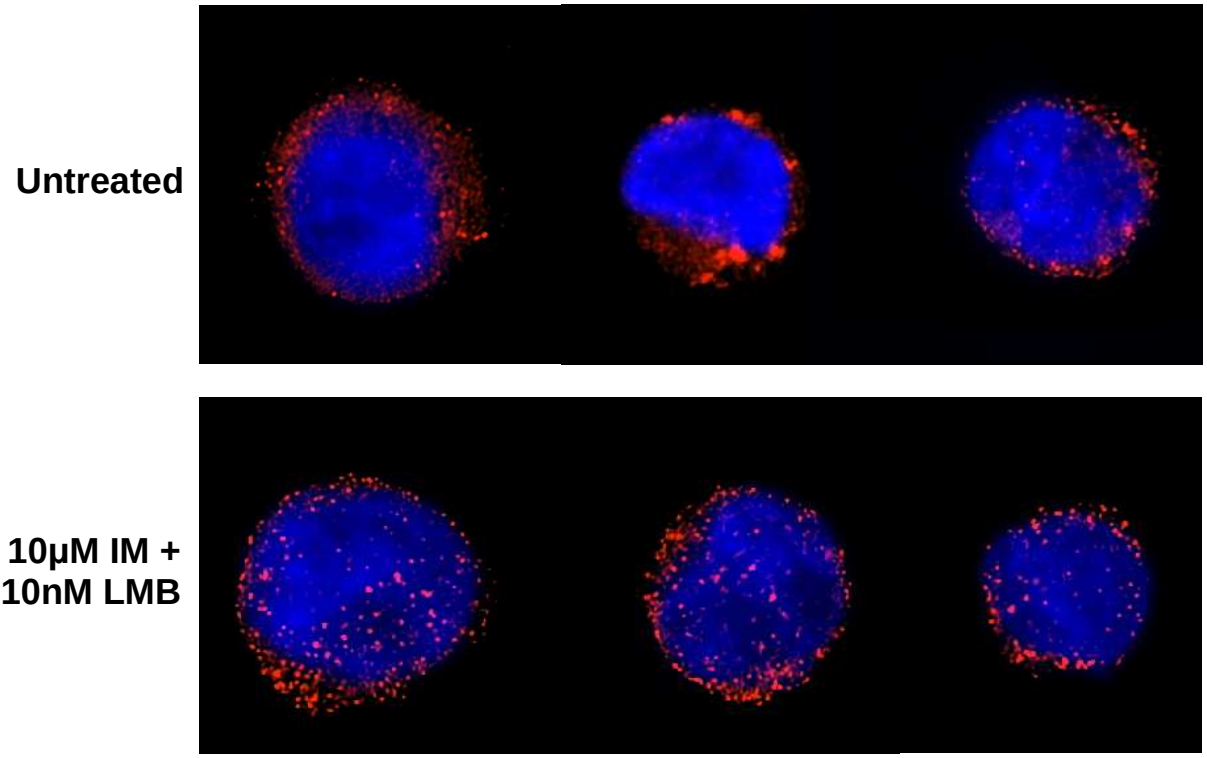

Figure 3-6: Nuclear localisation of Bcr-Abl in KCL22 cells treated with IM and LMB.

KCL22 cells were treated with 10μM IM and 10nM LMB for 4 hours and then stained with Bcr-Abl b2a2 junction specific antibody (Red) for examination by immunofluorescence microscopy. DNA was stained with DAPI (Blue).

3.8 Summary and Discussion

Overall, these findings demonstrated that neither continuous nor sequential regimens with IM and LMB in CML cell lines or primary $CD34^+$ cells significantly increased inhibition of cell proliferation more than IM alone. It was also shown that the sequential treatment did not significantly induce more apoptosis than LMB alone in primary CML $CD34^+$ cells.

Previously researchers showed that 72-hour continuous IM and LMB treatment regimen could preferentially induce apoptosis and eliminate K562 cells (198). However, it is observed in this chapter that the combination strategy does not kill primary CML $CD34^+$ cells more effectively than LMB alone (247). In addition, Aloisi *et al* showed that sequential IM and LMB treatment (as illustrated in Figure 3-3A) had greater reduction in the colony-forming ability of CML myeloid progenitors compared with IM or LMB alone, and the sequential treatment preferentially targeted CML myeloid progenitors compared to their healthy counterparts in terms of clonogenicity (246). Here in this chapter, the cytotoxic effect of the sequential IM and LMB treatment was investigated in CML cell lines and progenitors, and it was determined that the sequential regimen did not improve the cytotoxic effect of IM in Bcr-Abl^+ cell lines and primary CML $CD34^+$ cells, although this regimen demonstrated cytostatic effect by colony-forming assays in CML myeloid progenitors (246).

Patel *et al* showed the presence of Bcr-Abl protein in the nucleus of primary CML $CD34^+$ cells, but not in the nucleus of CML cell line BV173 (248), implying that CML

progenitors are able to tolerate nuclear Bcr-Abl tyrosine kinase to a certain extent. This might explain the ineffectiveness of continuous and sequential IM and LMB treatment in this chapter. Another explanation is the *de novo* synthesis of CRM1 after drug washout, leading to the impairment of LMB effect with subsequent transportation of Bcr-Abl protein back out of the cell nucleus.

In the sequential regimen, cell counts of Bcr-Abl$^+$ cells were reduced to less than input by exposure to IM, and IM eliminated K562 and Ba/F3 p210 cells (Figure 3-3B and C; Figure 3-4B), demonstrating the cytotoxic effect of IM on these cell lines. However, IM showed mild cytostatic effect on CML CD34$^+$ cells in both regimens (Figure 3-2A and Figure 3-5A), demonstrating the persistence/resistance of these progenitor cells to IM. In addition, 72-hour continuous LMB treatment led to a one-log reduction of cell counts three days after drug washout, showing the cytotoxicity of LMB in CML CD34$^+$ cells (Figure 3-2A), while no reduction was observed in the LMB alone treatment arm after drug washout in the sequential treatment (Figure 3-5A). This may be because cells were only treated with LMB for 12 hours in the sequential regimen. Furthermore, since the sequential IM and LMB treatment did not enhance kill of primary CML bulk CD34$^+$ cells compared with IM and LMB alone, the rare, more primitive CD34$^+$CD38$^-$ stem cell subset or normal primary CD34$^+$ cells were not tested with the sequential regimen.

Nuclear accumulation of Bcr-Abl protein was observed in IM and LMB treated KCL22 cells (Figure 3-6), but the majority of Bcr-Abl was still retained in the cytoplasm. This

is consistent with our previous observation (247). We reported increase of nuclear Bcr-Abl protein in K562 cells after 4-hour IM and LMB exposure as measured by Western blotting with nuclear extraction, but the cytoplasmic Bcr-Abl level was maintained as high as the untreated (247). In addition, Vigneri and Wang made similar observations. They demonstrated that only 25-35% Bcr-Abl was trapped in the nucleus of the Bcr-Abl expressing fibroblasts treated with IM and LMB (198).

Copland *et al* reported the resistance of primary CML $CD34^+$ cells to IM treatment, and showed the second generation TKI dasatinib was much more effective in inhibiting Bcr-Abl tyrosine kinase activity in the primitive CML population (163). This led to the speculation that the IM used in the continuous and sequential regimens did not sufficiently block Bcr-Abl tyrosine kinase, and dasatinib may be a better TKI to use in these regimens. However, Vigneri and Wang observed the nuclear fraction of Bcr-Abl was around the same level in kinase-defective Bcr-Abl expressing fibroblasts treated with LMB only, or NES-inactivated Bcr-Abl expressing fibroblasts treated with IM for 24 hours (198), eliminating the possibilities of incomplete inhibition of Bcr-Abl tyrosine kinase activity by IM or nuclear exportation by LMB. These observations indicate other mechanisms apart from Bcr-Abl tyrosine kinase activity retaining Bcr-Abl protein in the cytoplasm of CML cells.

4 Results 2: Subcellular localisation of Bcr-Abl protein in CML progenitor cells

4.1 Introduction

In the previous chapter, it was observed that most of the Bcr-Abl protein was in the cytoplasm of KCL22 cells after IM and LMB exposure, although a fraction of Bcr-Abl was accumulated in the nucleus (Figure 3-6). Retention of Bcr-Abl protein in the cytoplasm of IM and LMB treated K562 cells (247) and Bcr-Abl expressing fibroblasts (198) has also been reported. The mechanism of cytoplasmic retention of Bcr-Abl in CML cells when Bcr-Abl tyrosine kinase activity is inhibited is still not clear. However, cytoplasmic Bcr-Abl is known to promote cell proliferation and survival (44;68), while nuclear Bcr-Abl tyrosine kinase activity induces apoptosis (198). Thus, cytoplasmic retention of Bcr-Abl is a possible survival mechanism in CML cells against TKI treatment, and impairment of Bcr-Abl cytoplasmic retention may provide a novel therapeutic approach to cure CML.

It was hypothesised that the Bcr-Abl protein was retained in the cytoplasm of TKI insensitive primary CML $CD34^+$ cells, and that this retention was caused by its cytoplasmic binding partners. Therefore, the aims of the study in this section were to examine the subcellular localisation of Bcr-Abl protein in human primary CML $CD34^+$ cells with or without TKI treatment, and investigate its cytoplasmic binding partners which potentially retain Bcr-Abl protein in the cytoplasm.

4.2 Validation of the Bcr-Abl b2a2 junction specific antibody

In order to visualize subcellular localisation of Bcr-Abl protein in CML cells, immunofluorescence microscopy was employed with a specific Bcr-Abl antibody. Since the only commercially available Bcr-Abl antibody is b2a2 junction specific and was released onto the market relatively recently, the specificity of this novel antibody was initially tested. Figure 4-1A shows the examination of the specificity of the Bcr-Abl b2a2 junction specific antibody by Western blotting. It is known that KCL22 cells express Bcr-Abl protein with b2a2 junction and K562 cells with b3a2 junction. HL60 cells are Bcr-Abl negative. It was shown that Bcr-Abl protein was detected in KCL22 cell lysate, but not in K562 or HL60 cell lysate (Figure 4-1A), demonstrating the specificity of the Bcr-Abl b2a2 junction specific antibody.

However, the background of the Western blot was high and the Bcr-Abl protein band was quite weak and not very sharp. Thus, immunoprecipitation (IP) was used to concentrate Bcr-Abl protein. As shown in Figure 4-1B, the b2a2 Bcr-Abl protein in KCL22 cell lysate was immunoprecipitated by the b2a2 junction specific Bcr-Abl antibody, but not by its corresponding mouse IgG2a isotype control. In addition, no b3a2 Bcr-Abl protein was pulled down from the K562 cell lysate. These results demonstrated that the Bcr-Abl antibody specifically detected Bcr-Abl protein with b2a2 junction.

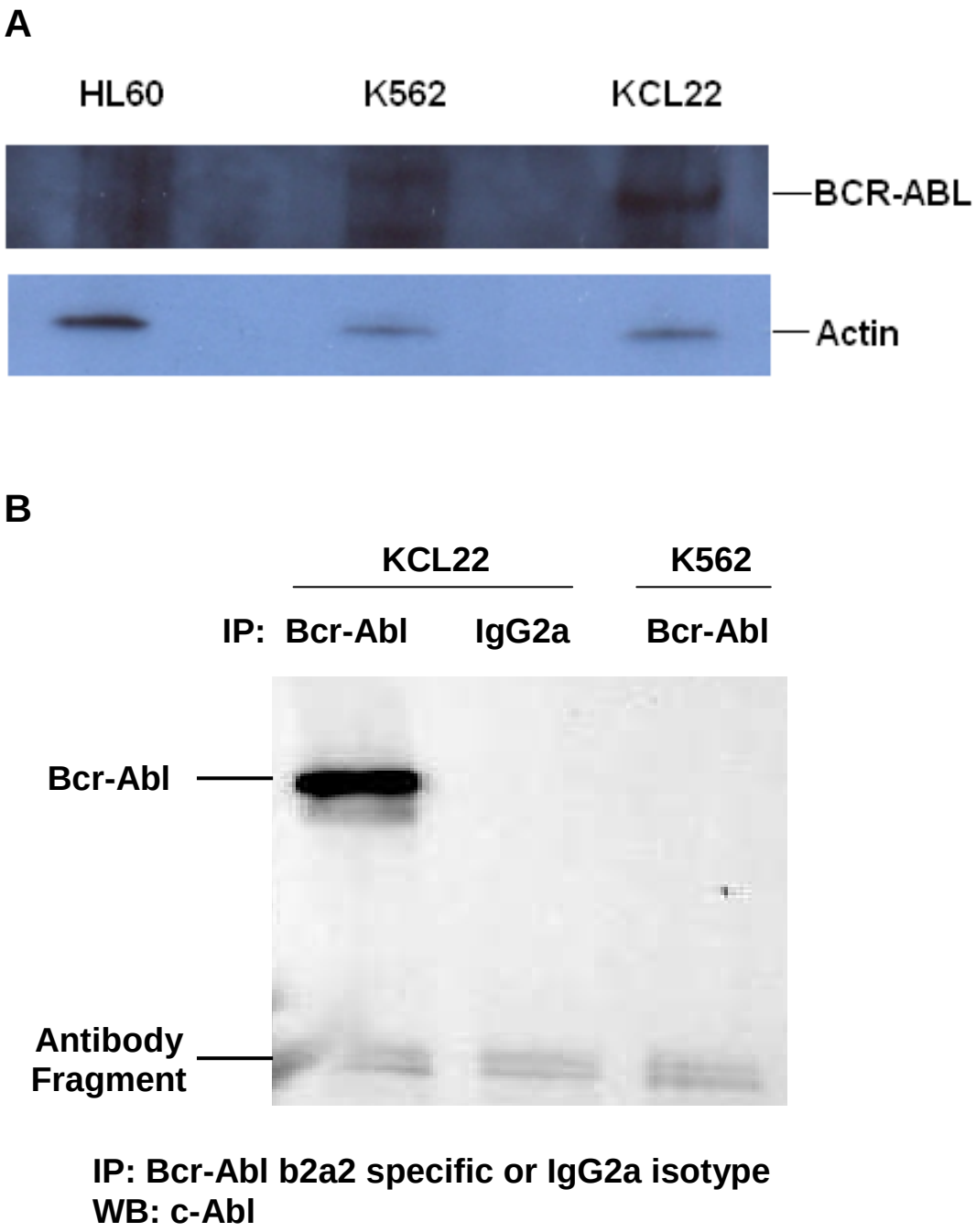

Figure 4-1: Validation of the Bcr-Abl b2a2 junction specific antibody by (A) Western blotting and (B) immunoprecipitation.

(A) Western blotting with K562, KCL22 and HL60 cell lysates, and the blot was probed with the Bcr-Abl b2a2 junction specific antibody. Actin was used as a loading control. (B) Immunoprecipitation with the Bcr-Abl b2a2 junction specific antibody in KCL22 and K562 lysates, as well as mouse IgG2a isotype in KCL22 lysate. The immunoprecipitates were analysed by Western blotting and probed with c-Abl antibody.

Moreover, to investigate subcellular localisation of Bcr-Abl protein, CML cells need to be stained with the Bcr-Abl b2a2 junction specific antibody and observed with a fluorescence microscope. Thus, the specificity of this antibody was examined with fluorescence microscopy as well. KCL22, K562 and HL60 cells were stained with the antibody, and only KCL22 cells showed positive staining (Figure 4-2D, red fluorescence). KCL22 cells stained with mouse IgG2a isotype was negative (Figure 4-2A). This result concludes that the Bcr-Abl antibody is b2a2 junction specific, and it is compatible with fluorescence microscopy.

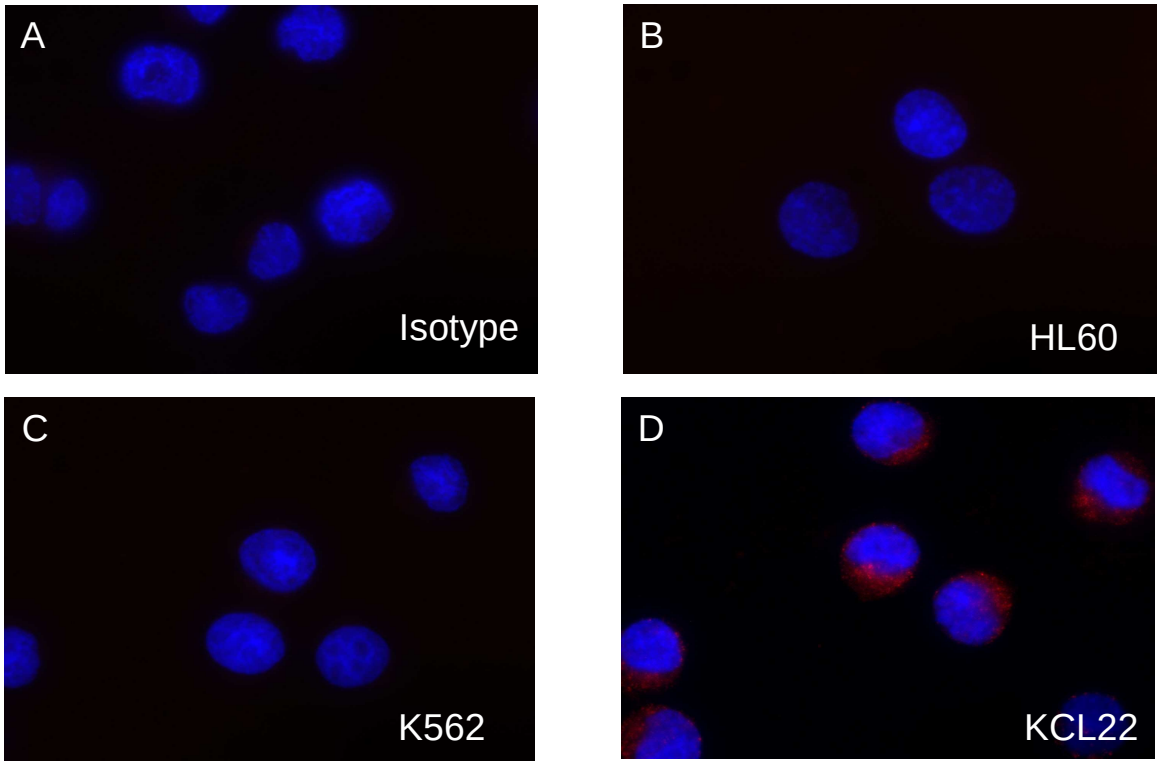

Figure 4-2: Validation of Bcr-Abl b2a2 specific antibody with fluorescence microscopy.

(A) KCL22 cells stained with IgG2a isotype control. (B) HL60 cells, (C) K562 cells and (D) KCL22 cells stained with the Bcr-Abl b2a2 junction specific antibody (Red). Cell nuclei were stained with DAPI (blue).

4.3 Identification of CML CD34$^+$ samples expressing b2a2 Bcr-Abl

In order to stain primary CML CD34$^+$ samples using this Bcr-Abl b2a2 junction specific antibody, CML samples expressing b2a2 Bcr-Abl protein rather than b3a2 need to be identified. A pair of Bcr-Abl primers were designed which spanned the junction region of the *Bcr-Abl* gene (as illustrated in Figure 4-3A). Total mRNA was extracted from primary CML CD34$^+$ cells and reversed transcribed into complementary DNA (cDNA). Polymerase chain reaction (PCR) was performed with the Bcr-Abl primers and the cDNA. In theory, the PCR products are 486 base pairs (bp) with b3a2 *Bcr-Abl* templates, and 411bp with b2a2 *Bcr-Abl* templates. Thus, b3a2 and b2a2 CML samples are able to be distinguished by the size of their PCR products after separation by gel electrophoresis. As shown in Figure 4-3B, primary CML CD34$^+$ samples 250, 273, 274 and 281 were identified as b2a2 Bcr-Abl samples. K562 and KCL22 cells were used as controls, as they were known as b3a2 and b2a2 Bcr-Abl expressing cells respectively.

In addition, the specificity of the Bcr-Abl b2a2 junction specific antibody in these primary b2a2 CML cells was validated by immunoprecipitation. It was demonstrated that Bcr-Abl protein was pulled down by the antibody, as well as c-Abl protein (Figure 4-4). The presence of c-Abl in the pull-down lysate was probably due to the binding of Bcr-Abl with c-Abl in these cells. It was reported that there is a SH2 binding domain in the Bcr part of Bcr-Abl, and the SH2 domain of c-Abl can associate with Bcr-Abl in a phosphotyrosine independent manner (63).

A

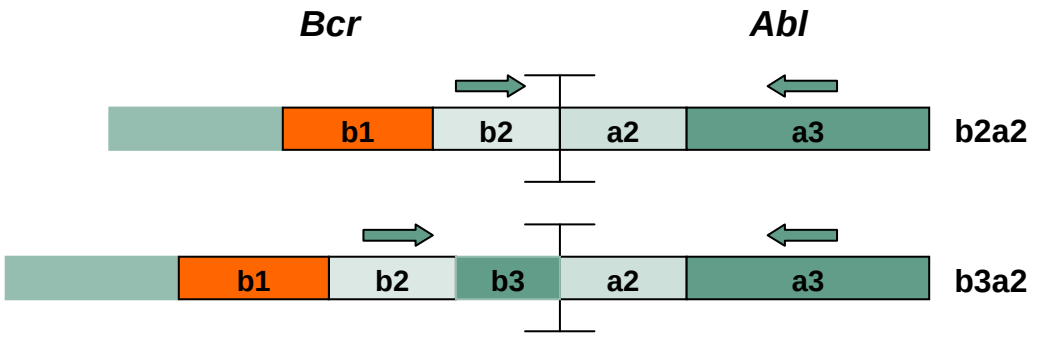

Expected PCR Product Length
b3a2: 486bp
b2a2: 411bp

Forward primer

Reverse primer

B

```
  1 gcgaacaagg gcagcaaagc tacggagagg ctgaagaaga agctgtcgga gcaggagtca
 61 ctgctgctgc ttatgtctcc cagcatggcc ttcagggtgc acagccgcaa cggcaagagt
121 tacacgttcc tgatctcctc tgactatgag cgtgcagagt ggagggagaa catccgggag
181 cagcagaaga agtgtttcag aagcttctcc ctgacatccg tggagctgca gatgctgacc
241 aactcgtgtg tgaaactcca gactgtccac agcattccgc tgaccatcaa taaggaagat
301 gatgagtctc cggggctcta tgggtttctg aatgtcatcg tccactcagc cactggattt
361 aagcagagtt caaaagccct tcagcggcca gtagcatctg actttgagcc tcagggtctg
421 agtgaagccg ctcgttggaa ctccaaggaa aaccttctcg ctggacccag tgaaaatgac
481 cccaaccttt tcgttgcact gtatgatttt gtggccagtg gagataacac tctaagcata
541 actaaaggtg aaaagctccg ggtcttaggc tataatcaca atggggaatg gtgtgaagcc
601 caaaccaaaa atggccaagg ctgggtccca agcaactaca tcacgccagt caacagtctg
661 gagaaacact cctggtacca tgggcctgtg tcccgcaatg ccgctgagta tctgctgagc
721 agcgggatca atggcagctt cttggtgcgt gagagtgaga gcagtcctgg ccagaggtcc
781 atctcgctga gatacgaagg gagggtgtac cattacagga tcaacactgc ttctgatggc
841 aagctctacg tctcctccga gagccgcttc aacaccctgg ccgagttggt tcatcatcat
901 tcaacggtgg ccgacgggct catcaccacg ctccattatc cagccccaaa gcgcaacaag
961 cccactgtct atggtgtgtc ccctaactac gacaagt
```

C

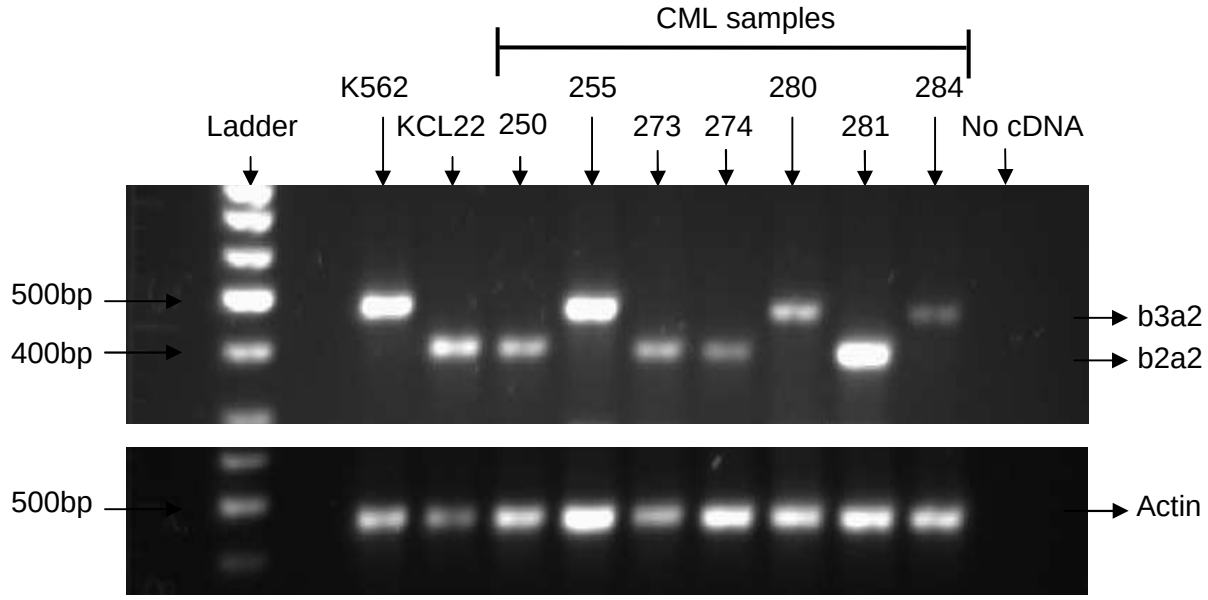

Figure 4-3: Identification of primary CML CD34$^+$ samples with b2a2 *Bcr-Abl* by PCR.

(A) Diagram illustrating the annealing of the primers on b2a2 and b3a3 *Bcr-Abl* templates. (B) Partial mRNA sequence of b3a2 *Bcr-Abl*, showing annealing sites of forward (blue) and reverse (pink) primers. The sequence was obtained from NCBI GenBank with Accession No. AJ131466. (C) Gel electrophoresis of PCR products to identify b2a2 Bcr-Abl samples. Actin was used as a positive control.

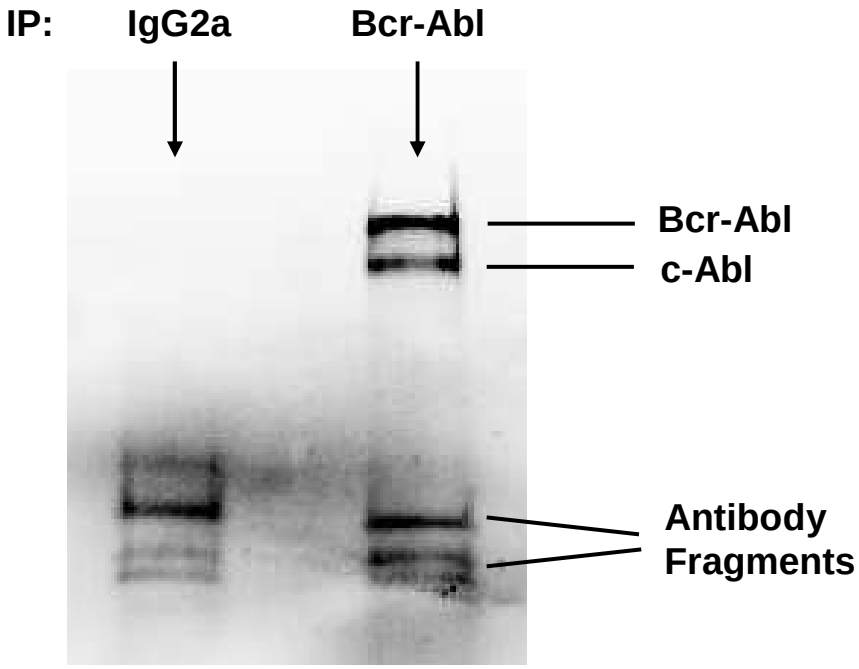

Figure 4-4: Validation of Bcr-Abl b2a2 specific antibody by immunoprecipitation.

The specificity of the Bcr-Abl b2a2 junction specific antibody was validated in the lysates of primary CML CD34^{+} cells expressing b2a2 Bcr-Abl protein. Mouse IgG2a isotype was used as a negative control. The immunoprecipitates were analysed by Western blotting and probed with c-Abl antibody.

4.4 12-Day Dasatinib Treatment of CML CD34$^+$ cells

After identification, b2a2 positive CML samples 250, 273 and 281 were used to investigate the subcellular localisation of Bcr-Abl protein in primary CML CD34$^+$ cells by immunofluorescence microscopy. Hamilton *et al* treated CML CD34$^+$ cells with 150nM dasatinib continuously for 12 days *in vitro*, and found about 10% of CML cells survived (249). This method of drug selection was adopted here in order to get TKI resistant/persistent cells. CML CD34$^+$ cells were thawed and cultured in serum free medium with five growth factors overnight to recover. Then the cells were washed and replated in serum free medium with physiological growth factors, with the addition of 150nM dasatinib (Day 0). Cells were replated with fresh medium and dasatinib every two or three days for 12 days. Physiological growth factors were used to mimic *in vivo* conditions. Cells without dasatinib treatment were also cultured in similar conditions for 12 days as a control.

At the end of treatment, the untreated cells and cells surviving dasatinib treatment were stained with the Bcr-Abl b2a2 junction specific antibody and the subcellular localisation of Bcr-Abl protein was visualized by fluorescence microscopy (Figure 4-5A). The percentages of nuclear Bcr-Abl protein relative to the whole cell were measured by ImageJ software based on the red fluorescence (Figure 4-5B). It was shown that the percentages of nuclear Bcr-Abl protein in the untreated and dasatinib treated CML cells at the end of the 12-day treatment were 41.8 ± 2.2% and 50.5 ± 3.0% respectively (n=18, 6 cells from each CML sample, mean ± SEM), and the difference between them is statistically significant (p=0.024). This indicates that

dasatinib treatment induced a fraction of Bcr-Abl protein to translocate into the cell nucleus from the cytoplasm, but a large proportion (almost half) of Bcr-Abl protein was still located in the cytoplasm of these treated cells.

A

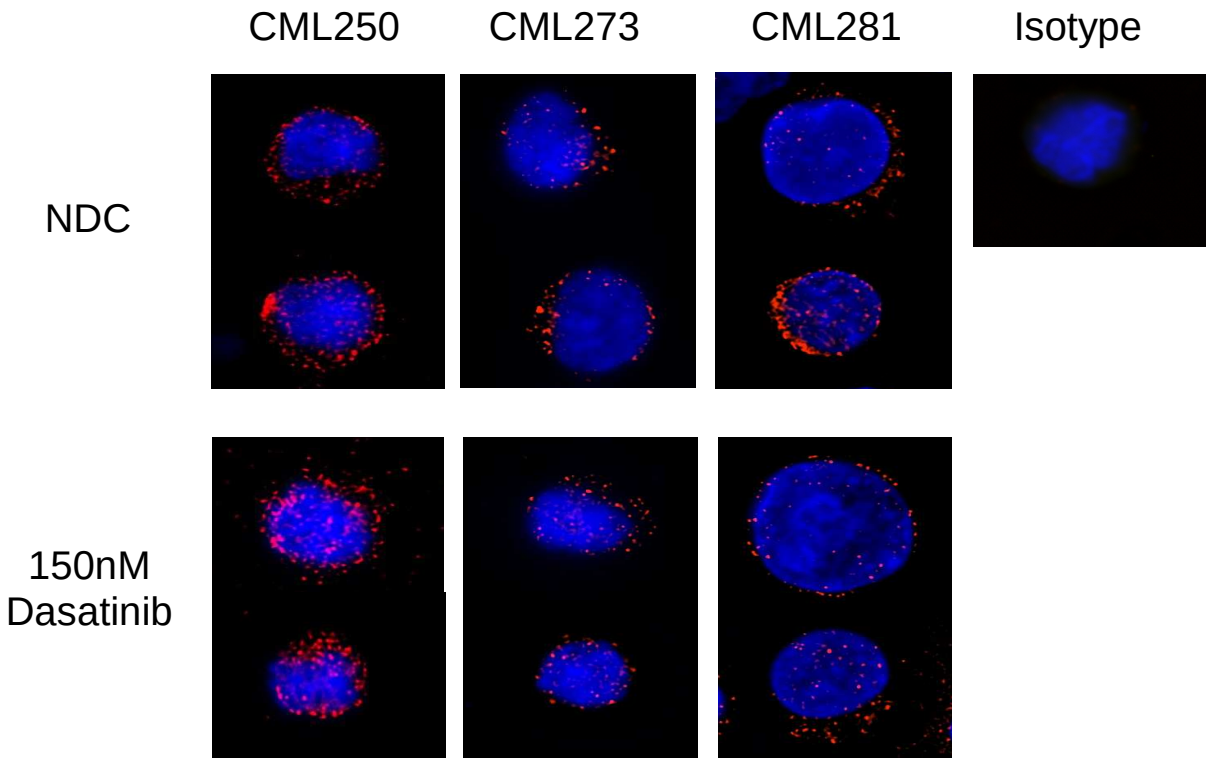

B

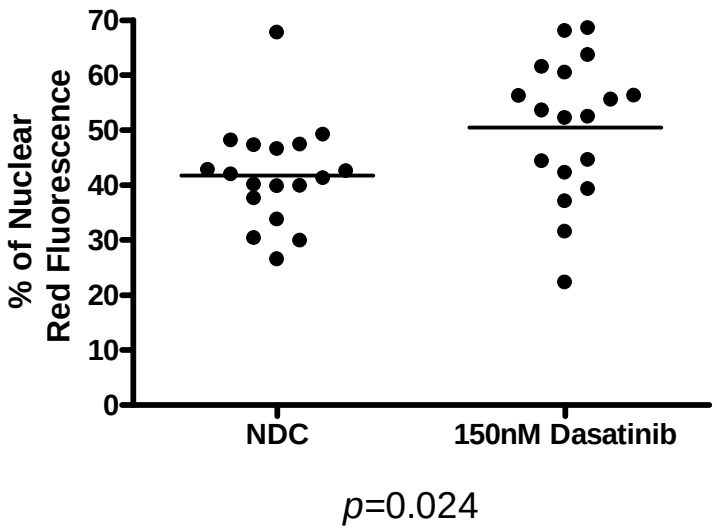

Figure 4-5: Subcellular localisation of Bcr-Abl protein.

(A) Localisation of Bcr-Abl protein in the untreated cells (NDC) and 150nM dasatinib treated primary CML CD34$^+$ cells at Day 12. Bcr-Abl protein was stained with the Bcr-Abl b2a2 junction specific antibody (red) and cell nuclei were stained with DAPI (blue). (B) A scatter plot demonstrating the percentage of nuclear Bcr-Abl protein in NDC and 150nM dasatinib treated primary CML CD34$^+$ cells at Day 12. The nuclear and whole cell red fluorescence intensities were measured with the ImageJ software (n=18, 6 cells from each CML sample), and the percentages of red fluorescence in the nuclei relative to in the whole cells were shown in the scatter plot.

In the mean time, the effectiveness of dasatinib as a TKI in this experiment was examined by measuring p-CrkL level in these cells. p-CrkL is a downstream effector of Bcr-Abl, and has been used as a convenient surrogate marker to measure Bcr-Abl tyrosine kinase activity (161). As shown in Figure 4-6A, p-CrkL completely disappeared in the 150nM dasatinib treated CML $CD34^+$ cells at Day 4 and Day 12, with or without physiological growth factors. This indicates that the tyrosine kinase activity of Bcr-Abl protein was completely inhibited by dasatinib in this experiment.

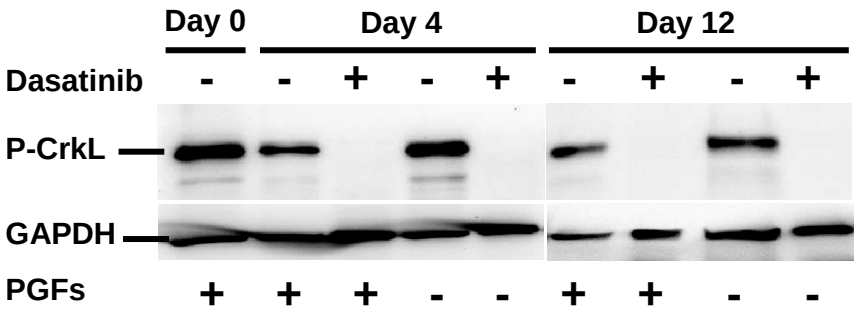

Figure 4-6: A representative Western blot showing the inhibition of CrkL phosphorylation with 150nM dasatinib in primary CML $CD34^+$ cells.

Although the subcellular localisation of Bcr-Abl has been revealed in the surviving cells, it is not clear whether they are still $CD34^+$ and at what stages of maturation they are at. In order to determine the phenotype of cells visualized in Figure 4-5A, the expression of the cell surface markers CD34, CD45 and CD133 were analysed by flow cytometry. CD45 is a common marker of leucocytes (250), CD34 is a marker of

haemopoietic progenitor cells and CD133 is a marker of primitive haemopoietic progenitor cells (251). At Day 0, all the CML cells are $CD34^+$ and $CD45^+$ (Figure 4-7A), indicating all the cells are haemopoietic progenitors at this stage. At the end of 12-day dasatinib treatment, the percentage of $CD34^+$ cells decreased to 7.2 ± 3.5% (n=3, mean ± SEM), while the vast majority of cells are still $CD45^+$. On the other hand, the primitive $CD133^+$ cells decreased from 14.1 ± 1.1% at Day 0 to 3.1 ± 0.21% at Day 12 of dasatinib treatment (Figure 4-7D). These data shows that the surviving cells from 12-day dasatinib treatment are mainly $CD45^+$, $CD34^{low/-}$ and $CD133^{low/-}$. In addition, there is no statistical significant difference between NDC and dasatinib treatment arms regarding percentage of $CD34^+$ cells or $CD133^+$ cells at Day 4 and Day 12 ($p \geq 0.082$, Figure 4-7D).

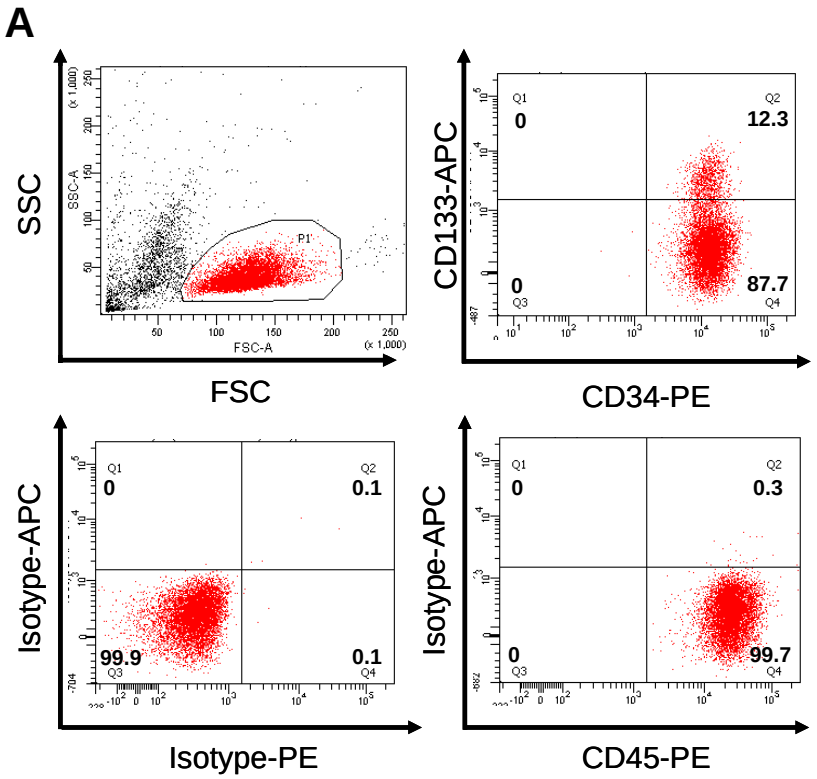

B

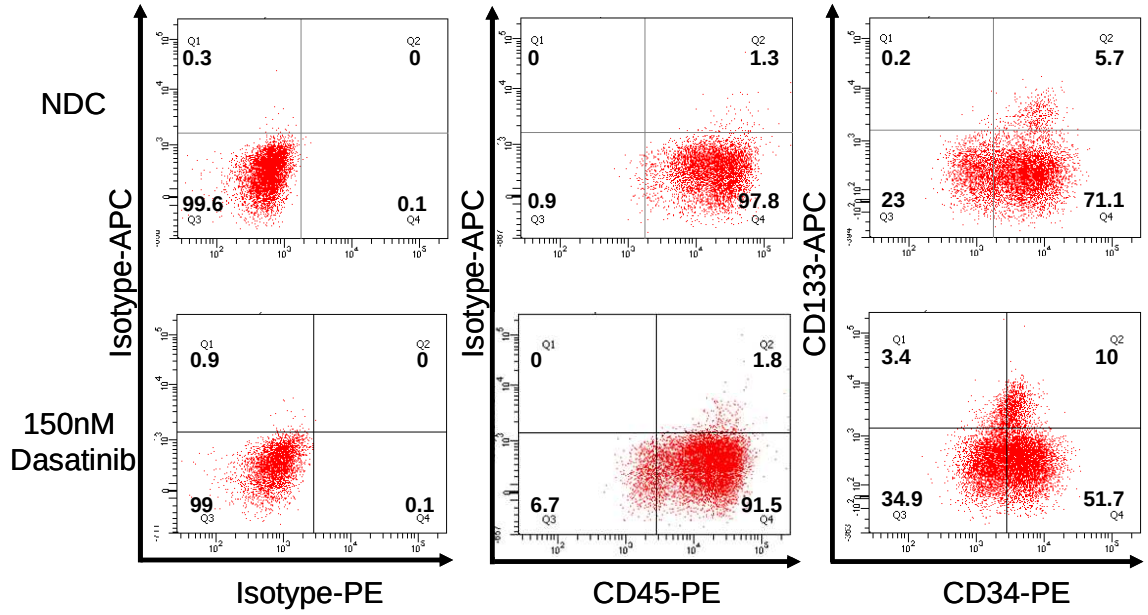
NDC
150nM Dasatinib
Isotype-APC
Isotype-PE
CD45-PE
CD133-APC
CD34-PE
Q1 0.3
Q2 0
Q3 99.6
Q4 0.1
Q1 0
Q2 1.3
Q3 0.9
Q4 97.8
Q1 0.2
Q2 5.7
Q3 23
Q4 71.1
Q1 0.9
Q2 0
Q3 99
Q4 0.1
Q1 0
Q2 1.8
Q3 6.7
Q4 91.5
Q1 3.4
Q2 10
Q3 34.9
Q4 51.7

C

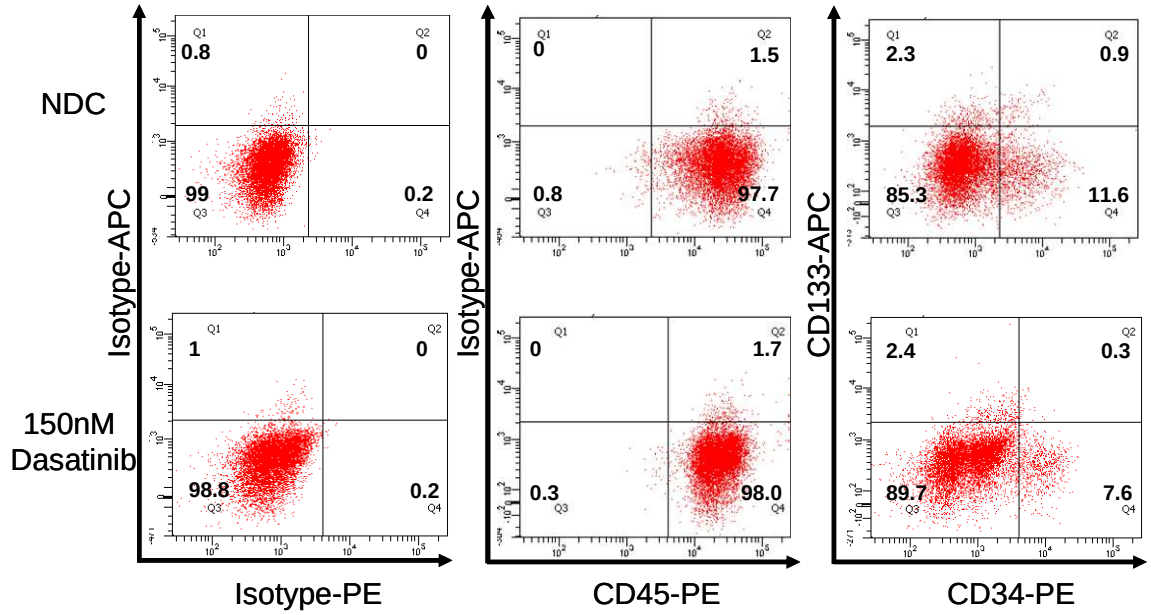
NDC
150nM Dasatinib
Isotype-APC
Isotype-PE
CD45-PE
CD133-APC
CD34-PE
Q1 0.8
Q2 0
Q3 99
Q4 0.2
Q1 0
Q2 1.5
Q3 0.8
Q4 97.7
Q1 2.3
Q2 0.9
Q3 85.3
Q4 11.6
Q1 1
Q2 0
Q3 98.8
Q4 0.2
Q1 0
Q2 1.7
Q3 0.3
Q4 98.0
Q1 2.4
Q2 0.3
Q3 89.7
Q4 7.6

D

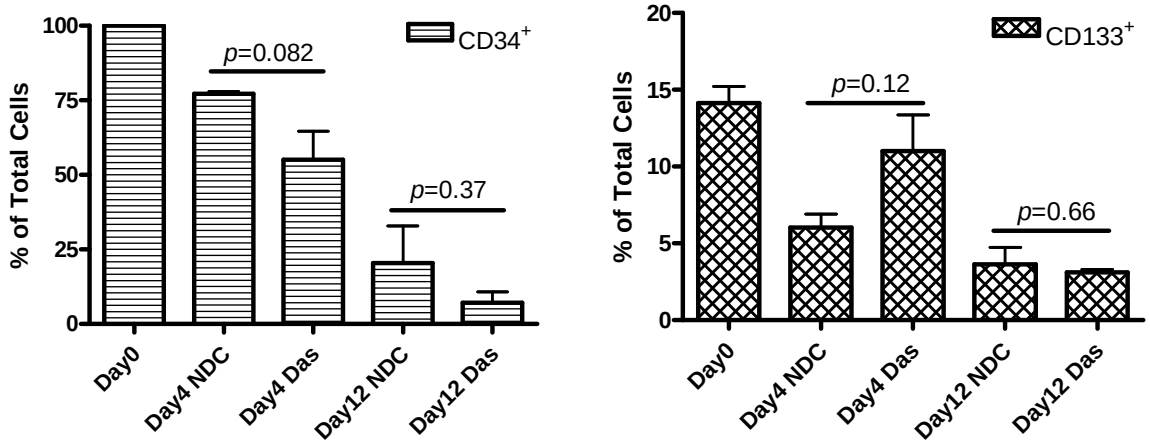

Figure 4-7: Representative flow cytometry plots.

CML281 cells were stained with surface-markers and analyzed at Day 0 (A), Day 4 (B) and Day 12 (C) of 150nM dasatinib treatment. (D) Average percentages of $CD34^+$ cells and $CD133^+$ cells with CML samples 250, 273 and 281 in different treatment conditions.

4.5 Bcr-Abl binding partners

Previously it was shown that 50.5 ± 3.0% of Bcr-Abl protein was in the nucleus of dasatinib treated cells (Figure 4-5), suggesting that about 50% of Bcr-Abl protein was still retained in the cytoplasm of these cells. The cytoplasmic retention of Bcr-Abl may be due to its cytoplasmic binding partners. If these binding partners were identified, disruption of their binding with Bcr-Abl may induce nuclear translocation of the rest of cytoplasmic Bcr-Abl protein. Thus, the co-localisation of Bcr-Abl and its binding partners was investigated in the Day 12 dasatinib treated primary CML $CD34^+$ cells.

F-actin is a known Bcr-Abl binding partner and there is an F-actin binding domain in the C-terminus of Bcr-Abl protein (73). Impairment of F-actin binding has been reported to decrease the transforming ability of Bcr-Abl protein (73). However, the role of F-actin retaining Bcr-Abl in the cytoplasm of TKI-insensitive primary CML cells is not clear. Thus, co-localisation of Bcr-Abl and F-actin was investigated in Day 12 dasatinib treated primary CML $CD34^+$ cells by immunofluorescence microscopy (Figure 4-8). Another possible group of binding partner is the 14-3-3 family it has been reported that nucleocytoplasmic shuttling of c-Abl protein was regulated by 14-3-3 proteins whereby 14-3-3 sequestered c-Abl protein in the cytoplasm by binding to its phosphorylated Thr735 residue (231). Upon DNA damage or oxidative stress, JNK is phosphorylated which in turn phosphorylates 14-3-3, resulting in the release and nuclear translocation of c-Abl (231). Since the Abl part of Bcr-Abl protein contains the 14-3-3 binding site (i.e. Thr735 residue), it could be hypothesized that 14-3-3 associate with Bcr-Abl and sequester it in the cytoplasm. Therefore, Bcr-Abl and 14-3-3 proteins were stained and visualized by immunofluorescence microscopy (Figure 4-9), in order to examine if they co-localised in the Day 12 dasatinib treated primary CML $CD34^+$ cells. It was observed that a small proportion of Bcr-Abl protein co-localised with F-actin or 14-3-3 proteins in both NDC and dasatinib treated cells.

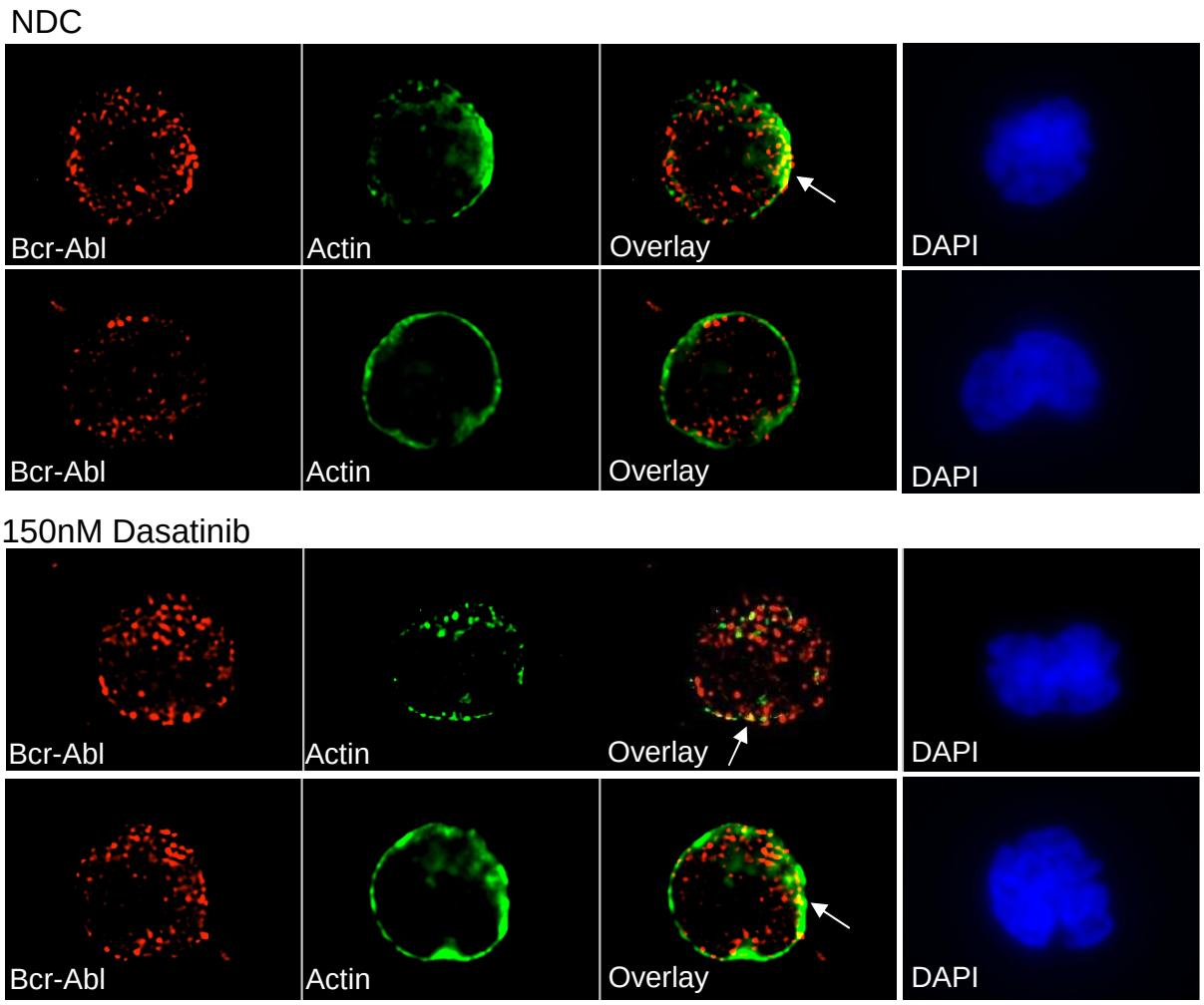

Figure 4-8: Co-staining of Bcr-Abl and F-Actin in 12-Day 150nM dasatinib treated primary CML CD34$^+$ cells, as well as the 12-Day untreated cells (NDC).

Bcr-Abl protein was stained with the Bcr-Abl b2a2 junction specific antibody (red), F-Actin was stained with Alexa Fluor 488® phalloidin (green), and overlay shows the merge of red and green channels. Cell nuclei were stained with DAPI (blue). White arrows indicate some of the co-localised pixels.

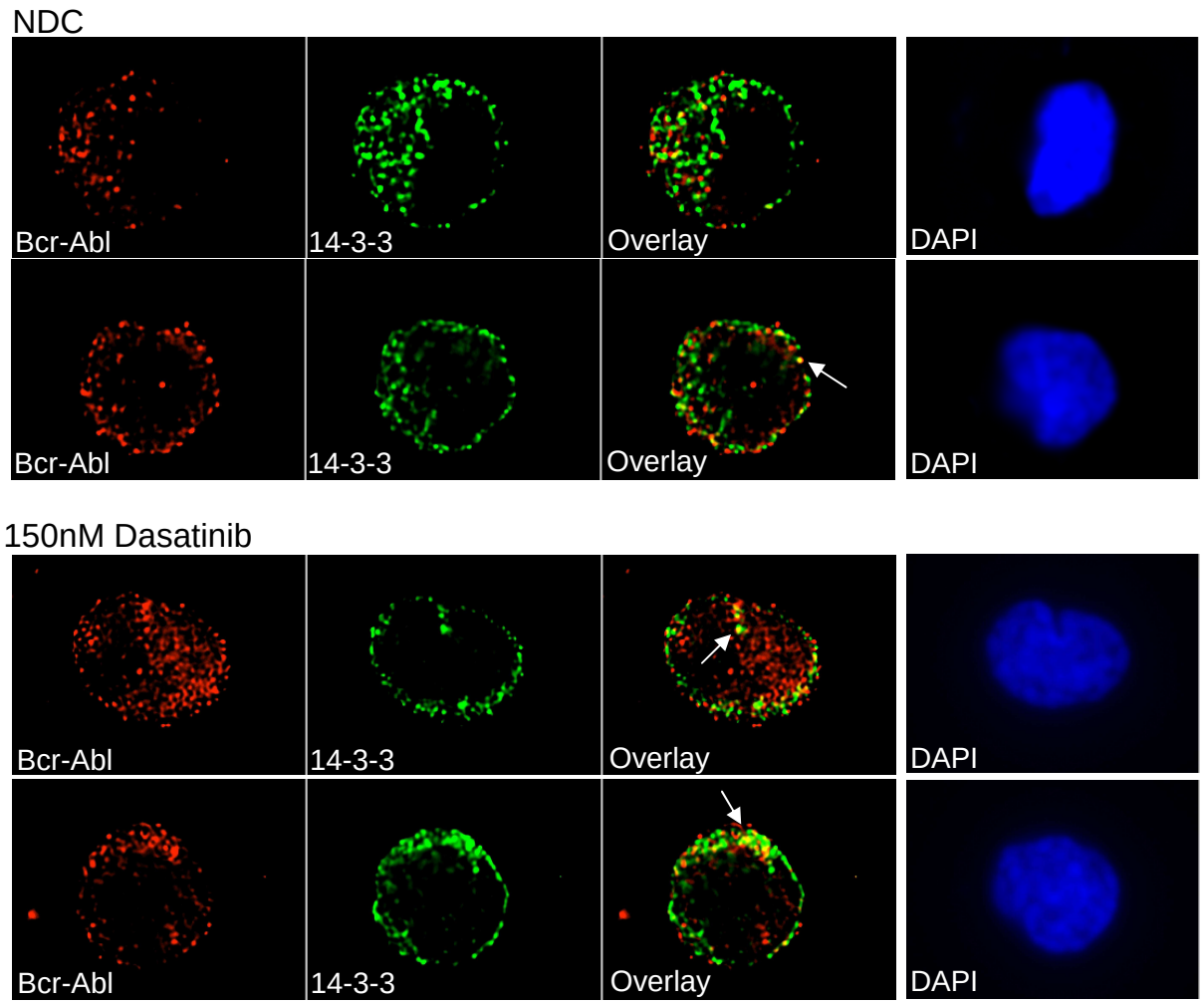

Figure 4-9: Co-staining of Bcr-Abl and 14-3-3 in 12-Day 150nM dasatinib treated primary CML CD34$^+$ cells, as well as the 12-Day untreated cells (NDC).

Bcr-Abl protein was stained with the Bcr-Abl b2a2 junction specific antibody (red), 14-3-3 proteins were stained with a Pan-14-3-3 antibody (green), and overlay shows the merge of red and green channels. Cell nuclei were stained with DAPI (blue). White arrows indicate some of the co-localised pixels.

In order to confirm the association of Bcr-Abl and 14-3-3 proteins in CML cells, and investigate if IM can disrupt their association, Bcr-Abl and 14-3-3 proteins were immunoprecipitated by Bcr-Abl b2a2 junction specific antibody and pan 14-3-3 antibody respectively in KCL22 cells with or without 1μM IM treatment for 2 hours. It was observed that 14-3-3 proteins were detected in the Bcr-Abl immunoprecipitates, and that Bcr-Abl was also detected in the 14-3-3 immunoprecipitates as well (Figure 4-10). This demonstrates the binding of Bcr-Abl and 14-3-3 proteins in KCL22 cells. In addition, Bcr-Abl and 14-3-3 are still associated with each other in the presence of IM (Figure 4-10), indicating that IM treatment in KCL22 cells did not disrupt Bcr-Abl/14-3-3 complex and their association was independent of Bcr-Abl tyrosine kinase activity.

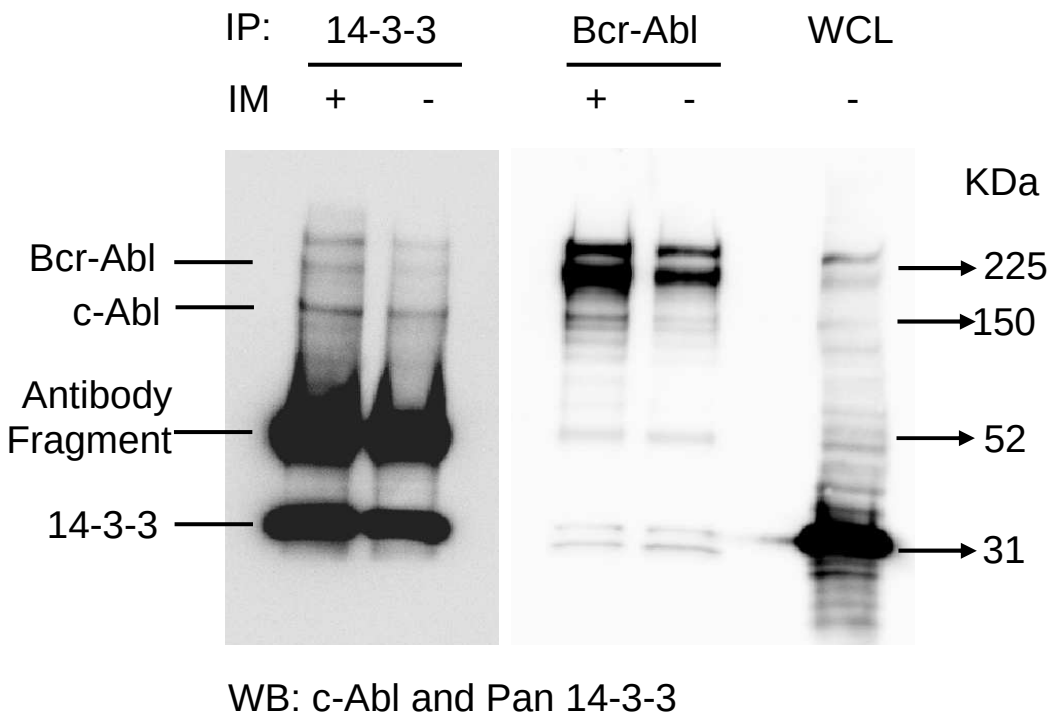

Figure 4-10: Immunoprecipitation showing Bcr-Abl/14-3-3 association in KCL22 cells.

KCL22 cells were treated with or without 1μM IM for 2 hours. Bcr-Abl and 14-3-3 proteins were pulled down by the Bcr-Abl b2a2 junction specific and pan 14-3-3 antibodies respectively. c-Abl and 14-3-3 antibodies were used on Western blotting. WCL: Whole Cell Lysate.

It was observed that some Bcr-Abl protein was located in close proximity to the plasma membrane in CML cells (Figure 4-8 and Figure 4-9). Lipid rafts are glycolipoprotein microdomains in the cytoplasmic membrane, which serve as integrating centres for the assembly of signalling molecules (252). Therefore, it was interesting to investigate if Bcr-Abl associated with lipid rafts as they are both integrators of signalling molecules.

Monosialotetrahexosylganglioside (GM1) is a component of the cytoplasmic membrane and is enriched in lipid rafts, and clustering of GM1 can be used to indicate the presence of lipid rafts (253). Cholera toxin subunit B (CTxB) binds specifically to GM1 and fluorophore-conjugated CTxB is commonly used to detect GM1, and therefore lipid rafts (253). A fraction of Bcr-Abl was found co-localised with GM1 clusters in KCL22 cells and primary CML cells (Figure 4-11, as indicated by white arrows). With 12-day dasatinib treatment, some GM1 aggregates are still co-localised with Bcr-Abl (Figure 4-11B). This indicates that lipid rafts might be involved in the cytoplasmic retention of Bcr-Abl in CML cells.

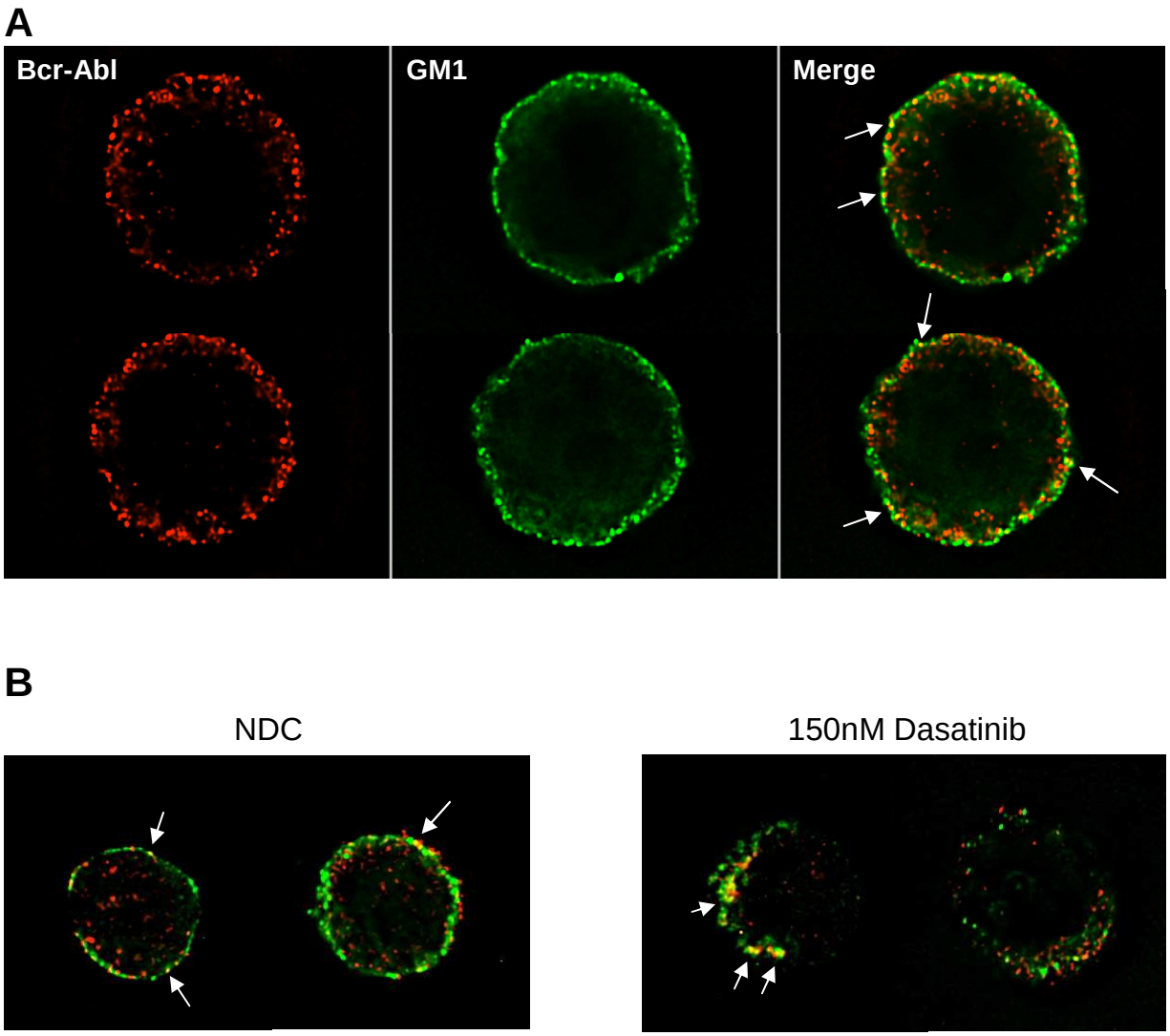

Figure 4-11: Co-staining of Bcr-Abl and GM1.

Bcr-Abl (red) and GM1 (green) were stained in KCL22 cells (A) and CML281 primary cells (B). Bcr-Abl protein was detected by the Bcr-Abl b2a2 junction specific antibody and GM1 was visualized by Alexa Fluor 488 conjugated CTxB. CML281 cells were sampled from the end of 12-Day 150nM dasatinib treatment experiment. White arrows indicate some of the co-localised pixels.

4.6 Summary and discussion

In summary, the specificity of the Bcr-Abl b2a2 junction specific antibody was validated by Western blotting, immunoprecipitation and immunofluorescence microscopy. Then the subcellular localisation of Bcr-Abl protein in TKI resistant/persistent primary CML $CD34^+$ cells was measured by immunofluorescence microscopy. It was shown that there was a significant increase in nuclear Bcr-Abl in 12-Day 150nM dasatinib treated cells with respect to NDC, while about 50% of Bcr-Abl was stilled retained in the cytoplasm of treated cells. Cell surface marker staining showed the surviving cells had greatly reduced CD34 and CD133 surface expression, implying that these cells were losing 'stemness'. In addition, a small proportion of Bcr-Abl protein was found co-localised with F-actin or 14-3-3 proteins in the surviving cells, indicating the cytoplasmic retention of Bcr-Abl might be due to its binding with F-actin or 14-3-3 proteins. The association of Bcr-Abl and 14-3-3 proteins was confirmed by immunoprecipitation in KCL22 cells, while IM treatment did not disrupt their association. Furthermore, the molecular signalling organizing centres, lipid rafts, might be involved in the cytoplasmic retention of Bcr-Abl.

Bcr-Abl protein had been previously found located in the cytoplasm of Bcr-Abl expressing fibroblasts, K562, and BV173 cells (198;248), while nuclear Bcr-Abl was visualized in 12-Day cultured primary CML $CD34^+$ cells which showed a significant increase in nuclear Bcr-Abl on dasatinib treatment (Figure 4-5). This is consistent with report by Patel *et al* where they showed the presence of nuclear Bcr-Abl protein in CML $CD34^+$ cells, and an increase in nuclear Bcr-Abl after IM treatment (248).

However, it is not clear why nuclear Bcr-Abl is absent in Bcr-Abl$^+$ cells lines and fibroblasts, but present in primary CML CD34$^+$ cells. These observations demonstrated that primary CML CD34$^+$ cells are able to tolerate the presence of nuclear Bcr-Abl protein, which could potentially induce apoptosis in these cells. Another consistent finding was the focal distribution of Bcr-Abl protein observed in KCL22 (Figure 3-6) and primary CML CD34$^+$ cells (Figure 4-5A), which was also demonstrated by Patel *et al* (248). They argued that Bcr-Abl foci might be sites for signalling protein assembly, since a proportion of Bcr-Abl foci are co-localised with other proteins such as p-CrkL, Grb2 and Cbl (248).

There is a possibility that at the end of 12-Day dasatinib treatment, point-mutation may occur in the kinase domain of Bcr-Abl protein, conferring resistance to dasatinib treatment and preventing nuclear translocation of Bcr-Abl. However, Figure 4-6A demonstrated complete inhibition of p-CrkL by dasatinib, indicating the Bcr-Abl tyrosine kinase activity was blocked. In addition, Hamilton *et al* showed that at the end of 12-Day 150nM dasatinib treatment there was no *Bcr-Abl* gene mutation (254), and they also observed maximal inhibition of p-CrkL, which is a downstream effector of Bcr-Abl. Thus, it is unlikely that there is TKI resistance induced by Bcr-Abl kinase domain mutation.

It is also possible that the Day 12 surviving cells are Ph$^-$ cells, which could explain their insensitivity to dasatinib treatment. However, immunofluorescence microscopy demonstrated positive Bcr-Abl protein staining in those surviving cells (Figure 4-5A).

In addition, Hamilton *et al* confirmed the presence of Bcr-Abl exclusively within the surviving cells by FISH (249;254), eliminating the possibility of presence of non-CML cells in the Day 12 surviving population. Furthermore, they showed the surviving cells from 12-Day 150nM dasatinib treatment were able to form colonies in LTC-IC (249;254). Since LTC-IC is the most stringent *in vitro* assay to assess stem cell function, it indicated the presence of stem cells in the survived population. However, cell surface staining demonstrated the survived cells are $CD45^{+}$, $CD34^{low/-}$ and $CD133^{low/-}$ (Figure 4-7), indicating most of these cells might not be haematopoietic stem/progenitor cells. One possible explanation, however, is that the human HSCs can be $CD34^{-}$ (255;256). Another explanation is that only a small proportion of the surviving cells are stem cells which form colonies in LTC-IC.

Since there was no LMB to trap Bcr-Abl in the nucleus in this experiment, Bcr-Abl could shuttle freely out of the nucleus via its NES. Wang *et al* demonstrated IM alone did not induce nuclear accumulation of Bcr-Abl protein in the Bcr-Abl expressing fibroblasts, while IM and LMB combination led to accumulation of Bcr-Abl in the nucleus (198). This indicates that although inhibition of tyrosine kinase targeted Bcr-Abl into the nucleus, Bcr-Abl shuttles out of nucleus very quickly in the absence of LMB. In the case of 12-Day dasatinib treated CML cells, nuclear translocated Bcr-Abl protein is quite possible to shuttle back into the cytoplasm quickly. This shuttling potentially explains why only about 50% Bcr-Abl was observed in the nucleus of surviving CML cells as it is a single point in a dynamic system.

Interestingly, ectopically expressed Bcr-Abl protein with four additional NLSs was shown to be able to translocate into the nucleus and induced apoptosis in K562 cells, but not wild type Bcr-Abl or Bcr-Abl with only one additional NLS (257). This indicates that the NLSs of wild type Bcr-Abl may be masked to prevent its nuclear translocation. 14-3-3 proteins sequester proteins in the cytoplasm by blocking their NLSs (258). It was shown that Bcr-Abl and 14-3-3 interacted with each other in CML cells (Figure 4-9 and Figure 4-10). Dong *et al* also demonstrated 14-3-3/Bcr-Abl association by immunoprecipitation (259). Thus, it is quite possible that 14-3-3/Bcr-Abl association masks NLSs of Bcr-Abl, and holds it in the cytoplasm.

Hamilton *et al* showed that, in the surviving CML cells of 12-Day dasatinib treatment in the absence of growth factors, there was maximal inhibition of Bcr-Abl tyrosine kinase as measured by p-CrkL and no Bcr-Abl kinase domain mutation (249;254). This suggests that the survival of CML cells is independent of Bcr-Abl tyrosine kinase activity. The survival mechanisms of CML cells fall into two broad categories, Bcr-Abl dependent and independent mechanisms (157). It was shown that normal human quiescent haemopoietic progenitors could not survive in the absence of IL-3 or GM-CSF in culture (18), while 10% of Bcr-Abl^{+} primary CML CD34^{+} cells survived 12-Day dasatinib treatment in the absence of any growth factor (249;254). This suggests that the survival of CML cells is dependent on the presence of Bcr-Abl protein, but not on the tyrosine kinase activity of Bcr-Abl. The mechanism by which kinase-inhibited Bcr-Abl protein enables CML cells survive in the absence of growth factors is not clear. Since the Bcr-Abl protein retained in the cytoplasm of surviving cells is in focal

formation (Figure 4-5), it is possible that the tyrosine kinase inhibited Bcr-Abl may serve as a scaffolding protein which integrate other signalling molecules in the cytoplasm, and provide a survival mechanism for dasatinib treated CML $CD34^+$ cells. If this is the case, impairment of the cytoplasmic Bcr-Abl retention will lead to increased accumulation of nuclear Bcr-Abl, disruption of its scaffolding role in the cytoplasm, and elimination of resistant/persistent CML progenitor cells. One possible way of doing this is to dissociate Bcr-Abl from its cytoplasmic binding partners. It has been shown here that 14-3-3 proteins complexed with Bcr-Abl in the cytoplasm of Day 12 surviving CML cells (Figure 4-9). It was reported that 14-3-3 proteins were linked to diverse signalling molecules (229), and they interacted with Bcr-Abl (61). Thus, disruption of the association between 14-3-3 and Bcr-Abl may increase nuclear accumulation of Bcr-Abl, and impair cytoplasmic signalling of Bcr-Abl.

BV02, a newly discovered inhibitor of 14-3-3, was reported to be able to dissociate c-Abl from 14-3-3 and induce nuclear translocation of c-Abl (260). BV02 also induced apoptosis in Ba/F3 cells expressing wild type Bcr-Abl or T315I mutant Bcr-Abl. It also demonstrated anti-proliferative effect in $CD34^+$ CML cells sampled from CML patients at BC stage that developed *in vivo* resistance to IM (147). However, it is not clear whether BV02 is able to disrupt 14-3-3/Bcr-Abl complex in CML cells, or if it can increase nuclear accumulation of Bcr-Abl. The combination effect of TKI and BV02 in resistant/persistent CML progenitors is worthy of further investigation.

5 Results 3: p-CrkL is not a surrogate of Bcr-Abl activity in vitro at short time-points

5.1 Introduction

In previous study, CML cells were treated with IM to induce nuclear localisation of Bcr-Abl protein through inhibition of its tyrosine kinase (Figure 3-6). Due to the rapid nature of kinase inhibition and nuclear transportation, an appropriate time-point should be chosen after IM treatment, at which time Bcr-Abl kinase activity is inhibited to allow its nuclear transportation, but cells should not be apoptotic. Thus, studies are required to measure the earliest time-point of inhibition of Bcr-Abl tyrosine kinase by IM.

p-CrkL has been commonly used to assess Bcr-Abl tyrosine kinase activity (160-163), as p-CrkL is a downstream substrate of Bcr-Abl (166) and is the major tyrosine phosphorylated protein in CML cells, but not in normal cells (93). In addition, the level of CrkL phosphorylation correlates well with the level of Bcr-Abl protein in CML cells, while p-CrkL is not detected in Bcr-Abl negative samples (165). Recently, p-CrkL has begun to be used as a surrogate marker of Bcr-Abl tyrosine kinase activity due to its convenience to be detected and low cell number requirement by flow cytometry (161;162).

However, the accuracy of p-CrkL as a reflection of Bcr-Abl tyrosine kinase status at early time-points during *in vitro* TKI treatment has not been examined. Although Bcr-Abl is the prominent driving force of tyrosine phosphorylation in CML cells, p-CrkL level does not necessarily equate to p-Tyr Bcr-Abl level. Therefore, the aims of this chapter were to reveal the kinetic of Bcr-Abl kinase inhibition by measuring p-CrkL and p-Tyr Bcr-Abl levels after TKI treatment, and investigate if p-CrkL is an accurate surrogate marker of Bcr-Abl tyrosine kinase activity in Ph^+ cells at early time-points of TKI treatment.

5.2 Assessment of the accuracy of p-CrkL as a surrogate marker of Bcr-Abl kinase activity in K562 cells after IM treatment at early time-points

IM is currently the first line drug for treating CP CML patients. Its IC_{50} in K562 cells is 600nM as measured by ^{3}H-thymidine uptake proliferation assay at 72 hours (172). In order to investigate if p-CrkL is an accurate surrogate marker of Bcr-Abl kinase activity after IM treatment at early time-points (≤48 hours), K562 cells were treated with 1μM IM. 1μM IM is higher than the IC_{50} concentration in K562 cells, and it was chosen to assure kinase inhibition. At each time-point of IM treatment (0, 0.5, 1, 2, 4, 8, 24, 48 hours), cells were collected and prepared for Western blotting. p-CrkL (Tyrosine 207), tyrosine phosphorylated Bcr-Abl (p-Tyr Bcr-Abl) and Bcr-Abl protein levels were measured. GAPDH was used as a loading control as described in the Materials and Methods.

After 1μM IM treatment, p-Tyr Bcr-Abl level dropped quickly to 24.9 ± 7.7% (n=3, mean ± SEM) of baseline (NDC at 0 time-point) by 1 hour time-point and then plateaued around this level out to the 48 hours time-point. Interestingly, p-CrkL level dropped to 59.3 ± 13.5% at 0.5 hour time-point, but then recovered to 94.4 ± 17.3% at 4 hours time-point (p=0.012, paired t-test), and subsequently declined to 39.0 ± 13.4% at 48 hours time-point. This phasic response of p-CrkL was unexpected and different to the response of Bcr-Abl after IM treatment. This strongly demonstrates that p-CrkL may not mirror the response of Bcr-Abl. The difference between protein

levels of p-CrkL and p-Tyr Bcr-Abl was statistically significant at several time-points (p<0.05 at 4 hours time-point; p<0.01 at 8 hours time-point; p<0.001 at 24 hours time-point).

A

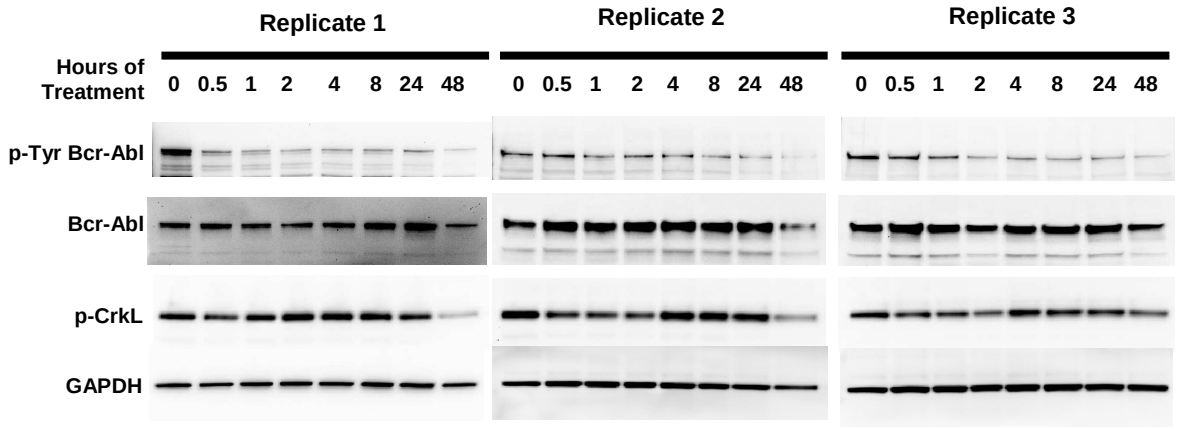

B

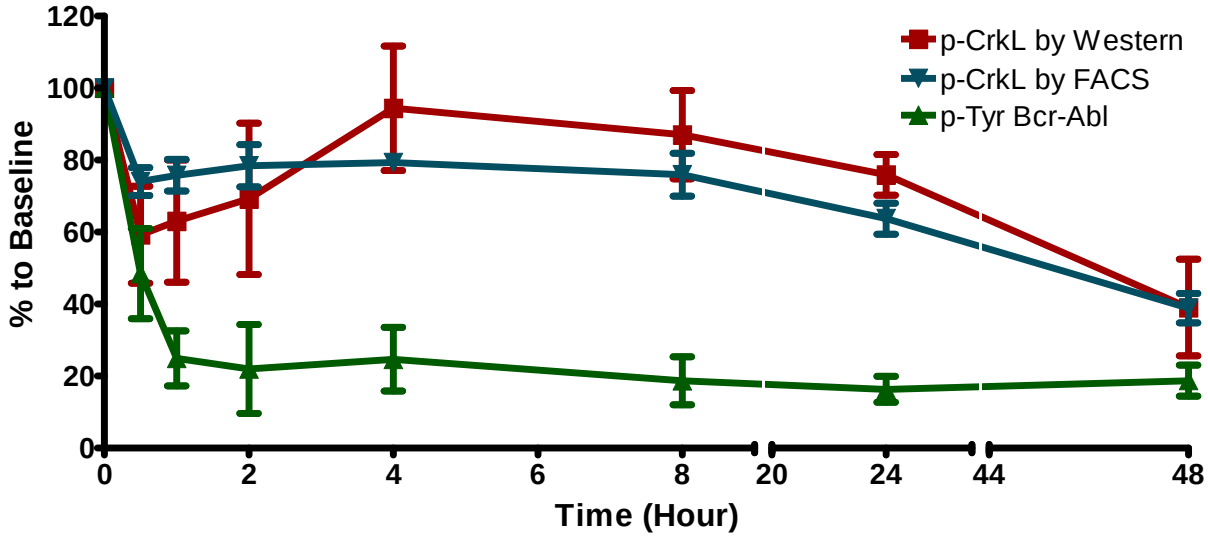

C

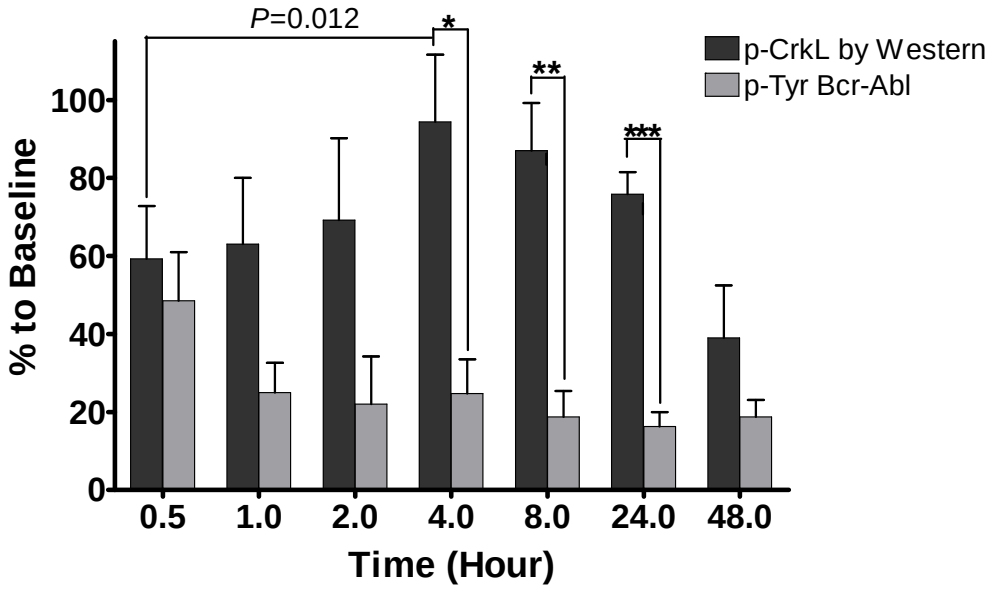

Figure 5-1: Levels of p-Tyr Bcr-Abl, Bcr-Abl, p-CrkL in 1μM IM treated K562 cells.

(A) Western blots showing protein levels of p-Tyr Bcr-Abl, Bcr-Abl, p-CrkL and GAPDH at different time-points (0, 0.5, 1, 2, 4, 8, 24, 48 hours) after IM treatment (n=3). (B) Plots showing normalized densitometry values of Western blot protein bands, as well as p-CrkL levels measured by intracellular flow cytometry. Densitometry was performed on each Western blot protein band to measure pixel intensity. P-Tyr Bcr-Abl, Bcr-Abl and p-CrkL protein band densitometry values were normalised against their corresponding GAPDH values. Values are shown as percentage of baseline. (C) Histograms showing the same percentages as in plot B with p-values indicated (* $p<0.05$, ** $p<0.01$, *** $p<0.001$). Results are shown as mean ± SEM, n=3

These results show that p-CrkL is not an accurate indicator of p-Tyr Bcr-Abl level in K562 cells after 1μM IM treatment at early time-points (≤24 hours). Since Bcr-Abl protein is auto-phosphorylated, p-Tyr Bcr-Abl level is a direct measurement of Bcr-Abl tyrosine kinase activity. Thus, p-CrkL is not an accurate surrogate marker of Bcr-Abl tyrosine kinase activity in this case. In addition, it was observed that the p-Tyr Bcr-Abl level dropped sharply within 0.5 hour of IM treatment in K562 cells (Figure 5-1B), thus it was interesting to investigate further how rapidly p-Tyr Bcr-Abl levels could be reduced and if the p-CrkL response was a surrogate marker of Bcr-Abl tyrosine kinase activity within minutes of IM treatment. K562 cells were treated with 1μM IM, and cells were sampled at very short time-points (0, 1, 5, 10, 15 minutes). Western blotting was employed to measure p-CrkL and p-Tyr Bcr-Abl levels (Figure 5-2A). GAPDH was used as a loading control.

It was observed that there was a rapid reduction of p-Tyr Bcr-Abl to less than 50% of baseline by 10 minutes of 1μM IM treatment in K562 cells, while p-CrkL remained around baseline level during this period (Figure 5-2B). The difference between p-CrkL and p-Tyr Bcr-Abl levels are statistically significant ($p<0.05$ at 5 and 10 minutes; $p<0.01$ at 15 minutes) (Figure 5-2C). These results demonstrate that p-CrkL is not an accurate surrogate marker of Bcr-Abl tyrosine kinase activity after IM treatment at very short time-points in K562 cells (≤ 15 minutes).

A

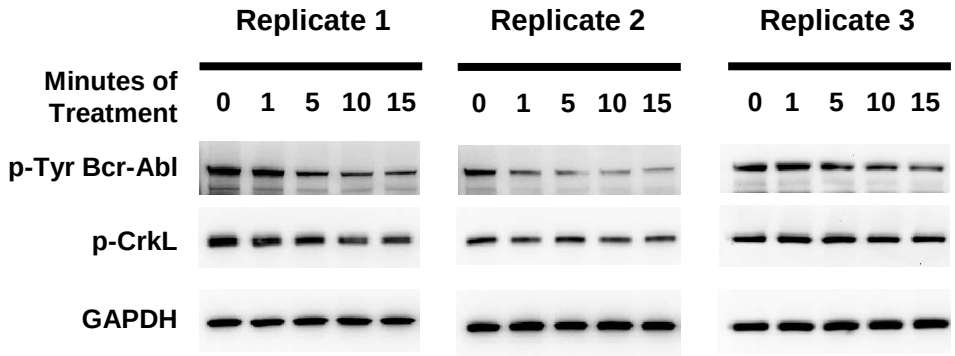
Replicate 1
Replicate 2
Replicate 3
Minutes of Treatment
0 1 5 10 15
0 1 5 10 15
0 1 5 10 15
p-Tyr Bcr-Abl
p-CrkL
GAPDH

B

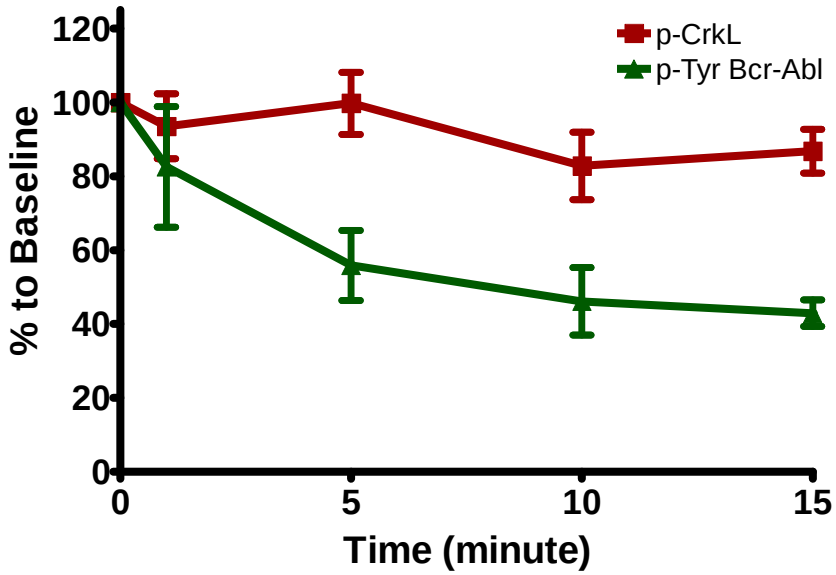
p-CrkL
p-Tyr Bcr-Abl
% to Baseline
120
100
80
60
40
20
0
0
5
10
15
Time (minute)

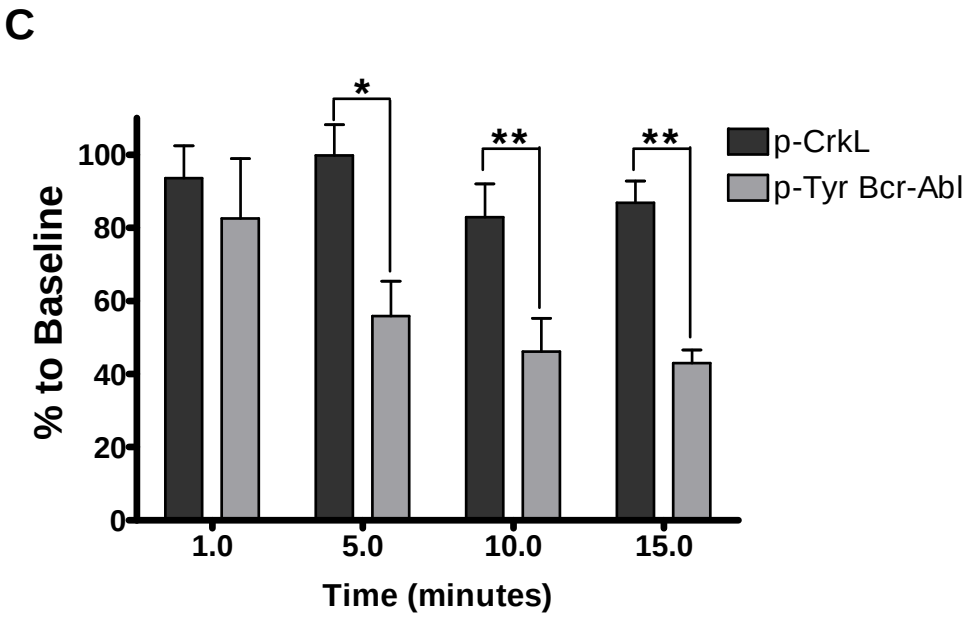

Figure 5-2: p-Tyr Bcr-Abl and p-CrkL levels in 1μM IM treated K562 cells (≤ 15 minutes).

(A) Western blots showing protein levels of p-Tyr Bcr-Abl, p-CrkL and GAPDH at different time-points (0, 1, 5, 10, 15 minutes) after IM treatment (n=3). (B) Plots showing normalized densitometry values of Western blot protein bands. Values are shown as percentage of no drug control. (C) Histograms showing the same percentages as in plot B with P-values indicated (*p<0.05, ** p<0.01). Results are shown as mean ± SEM, n=3.

In the first study (Figure 5-1), K562 cells were centrifuged at low speed (120 x g) and washed with PBS to prepare cell lysates. Since time-points as short as 1 minute were examined in the study above, the preparation of the cells had to be amended and cells were centrifuged at high speed (21,000 x g) without washing in PBS (Figure 5-2). As the responses seen at very short time-points were quite dramatic, it was possible that this change in methodology could have affected the phosphorylation status of CrkL and Bcr-Abl. Therefore, the full time course was repeated with the high speed centrifugation method, and the results are shown in Figure 5-3. Similar to low speed methodology (Figure 5-1), p-Tyr Bcr-Abl level dropped quickly within 1 hour of 1μM IM treatment to 14.5 ± 1.3% (n=3, mean ± SEM) and then plateaued around this level to 24 hours. p-CrkL level dropped to 50.6 ± 3.6% at 0.5 hour time-point, and recovered to 99.3 ± 11.8% at 4 hours time-point (p=0.041), finally dropping slightly at 24 hours time-point. The differences between p-CrkL and p-Tyr Bcr-Abl levels at all time-points are statistically significant (p<0.01 at 0.5, 1, 2, 4, 8 and 24 hours time-points). Taken together, the low speed (Figure 5-1) and high speed (Figure 5-3) methods were very similar to each other. In general, the high speed centrifugation method produced results with smaller error bars, so this method was used in subsequent Western blotting experiments.

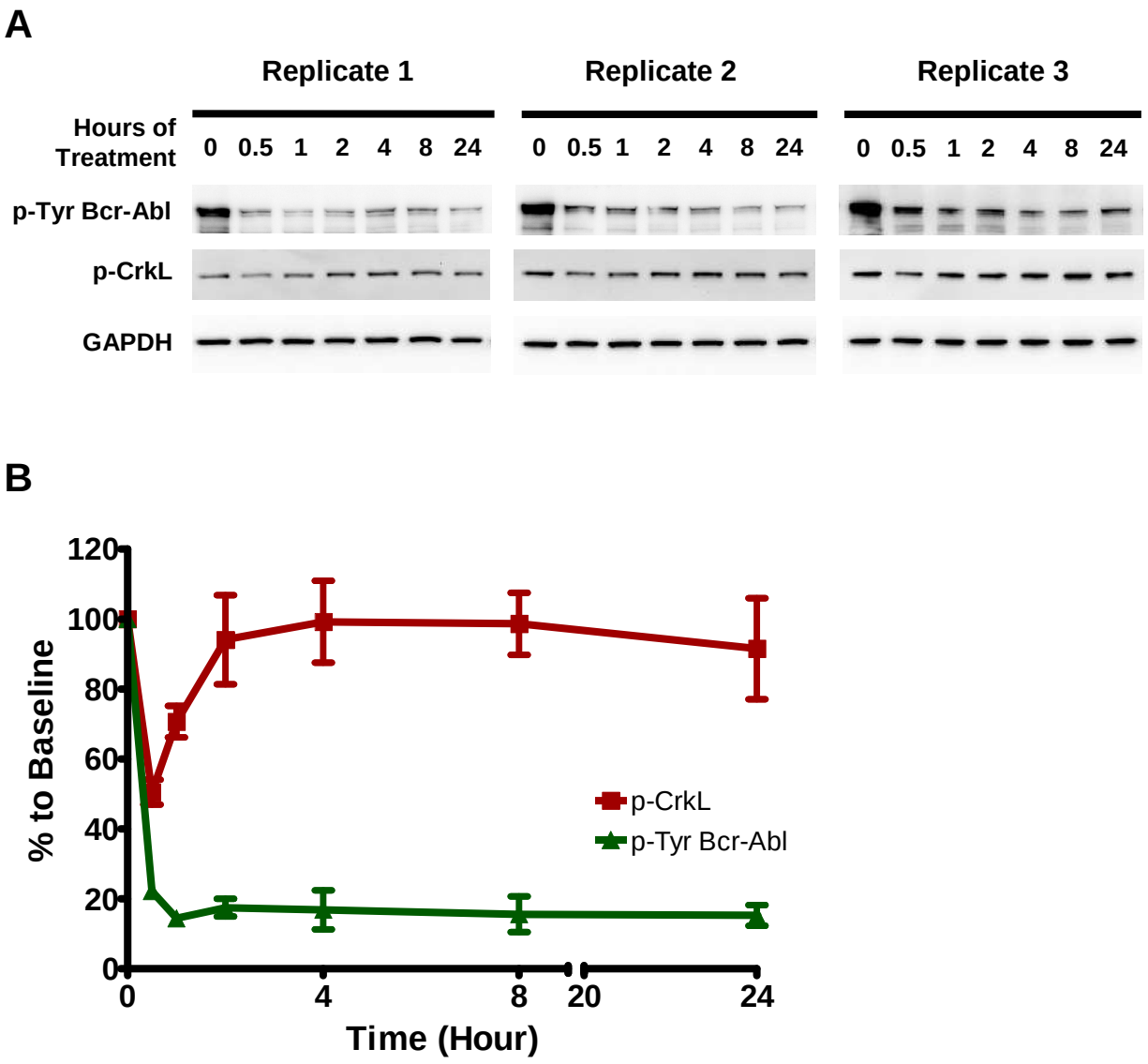

Figure 5-3: p-Tyr Bcr-Abl and p-CrkL levels in 1μM IM treated K562 cells up to 24 hours. Cells were centrifuged at 21,000 x g for 30 seconds at each time-point and then subject to Western blotting analysis. Results are shown as mean ± SEM (n=3).

Based on these observations, a three-phase model was formed to illustrate the level of p-CrkL after 1μM IM treatment. As shown in Figure 5-4, there is a rapid reduction of p-CrkL after IM treatment in the first phase as p-CrkL levels drop to about half of the baseline level at 0.5 hour time-point. In phase two, the p-CrkL level recovers to around the baseline level by 4 hours. Finally, p-CrkL level declines slowly in the third phase.

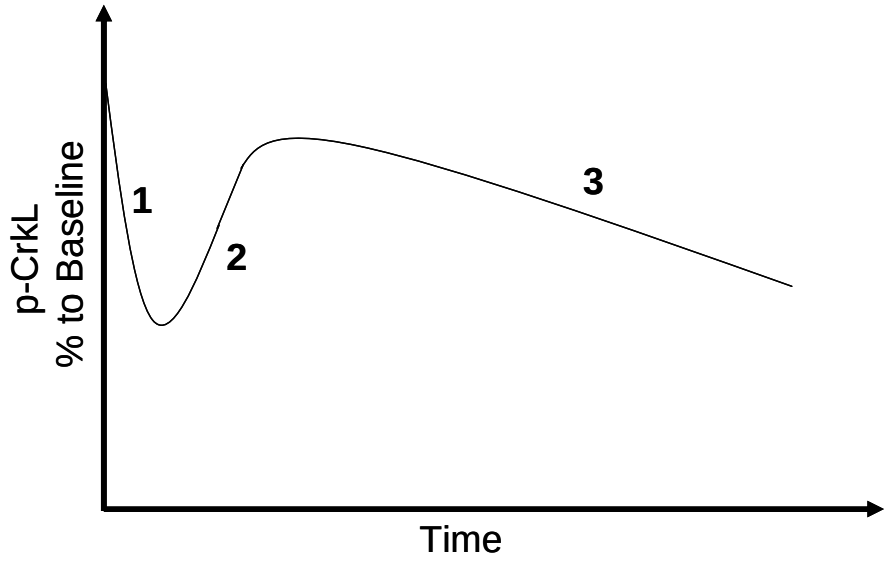

Figure 5-4: Model of p-CrkL level after IM treatment in K562 cells.

(1) A sharp drop of p-CrkL immediately after IM treatment. (2) Re-phosphorylation of CrkL from 0.5 hour to a peak at 4 hours time-point. (3) Gradual decrease of p-CrkL level from 4 hours time-point.

5.3 Investigation of the role of protein tyrosine phosphatases in Bcr-Abl dephosphorylation after IM treatment in K562 cells

5.3.1 Effect of SSG and IM co-treatment on p-Tyr Bcr-Abl in K562 cells

The initial rapid reduction of p-Tyr Bcr-Abl within minutes of TKI treatment suggests there may be an active dephosphorylation of Bcr-Abl protein after TKI treatment, and it was hypothesized the initial sharp drop of p-Tyr Bcr-Abl level after TKI treatment may be due to protein tyrosine phosphatase (PTP) activity. Therefore, K562 cells were treated with both IM and PTP inhibitor, sodium stibogluconate (SSG), which inhibits activity of PTPs including SHP-1, SHP-2 and PTP1B (261). SSG inhibits 99% of SHP-1 activity at 10μg/mL, and inhibits 99% of SHP-2 and PTP1B activities at 100μg/mL with *in vitro* PTP assays (261). Thus, K562 cells were treated with 1μg/mL, 10μg/mL or 100μg/mL SSG with 1μM IM for 1 hour, and it was observed that the combination of IM with 10μg/mL or 100μg/mL SSG resulted in significantly higher levels of p-Tyr Bcr-Abl than IM alone (p=0.007 and p=0.046, respectively), but not as high as the baseline level (Figure 5-5). These results suggest that SSG can partially inhibit the initial drop of p-Tyr Bcr-Abl level caused by IM, indicating PTPs play a role in Bcr-Abl dephosphorylation.

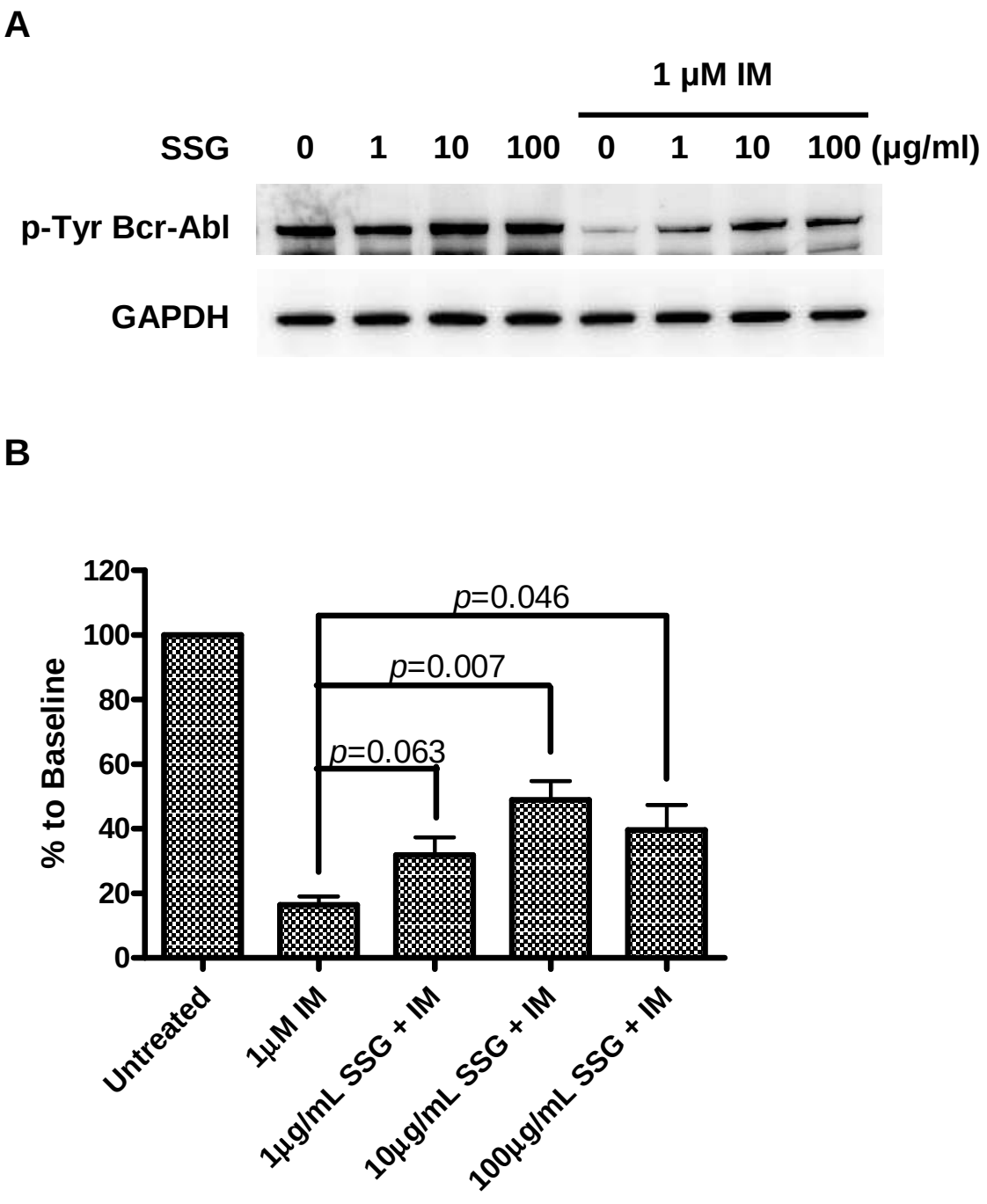

Figure 5-5: Combination treatment of 1μM IM and SSG in K562 cells for 1h.

(A) A representative Western blot showing p-Tyr Bcr-Abl and GAPDH protein levels in these treatments including untreated, SSG alone, 1μM IM alone, IM with 1μg/mL, 10μg/mL and 100μg/mL SSG, and (B) Histograms showing normalized densitometry

values of Western blot protein bands. Values are shown as percentage of no drug control. Results are shown as mean ± SEM (n=3).

5.3.2 Expression of protein tyrosine phoshpatases in K562 cells

Since PTPs are involved in the dephosphorylation of Bcr-Abl protein and SSG targets SHP1, SHP2 and PTP1B, the next aim was to specify which one(s) of the three possible PTPs were relevant in K562 cells. At first, expression of the three PTPs were examined by Western blotting with K562 cell lysate, and it was found that SHP1 was almost absent in K562 cells, while SHP2 and PTP1B proteins were highly expressed (Figure 5-6). This result is consistent with previous reports that K562 cells did not express SHP1 mRNA and protein (214;262). In addition, it has been reported that differentiated K562 cells express SHP1, while expression of both SHP2 and PTP1B is not changed upon differentiation of K562 cells (262).

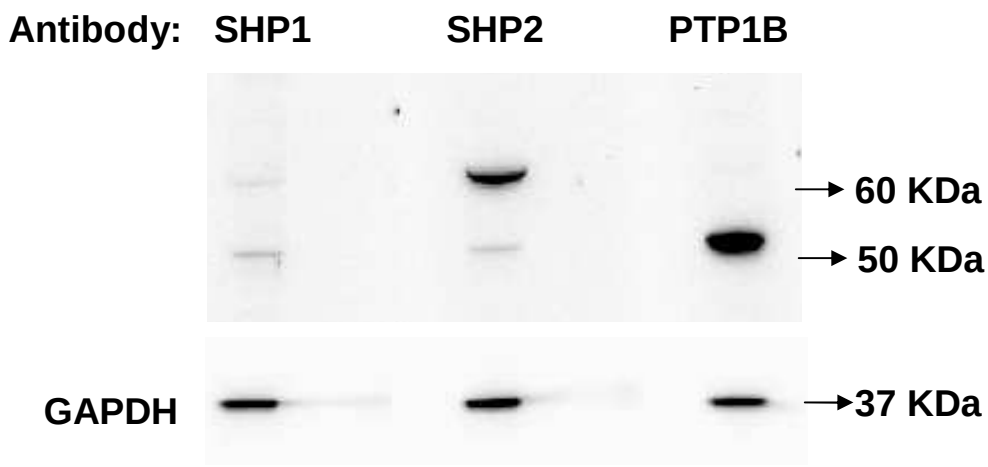

Figure 5-6: Expression of PTPs in K562 cells.

Protein expression of three PTPs, including SHP1, SHP2 and PTP1B, was assessed in K562 cells by Western blotting. K562 whole cell lysates were resolved by SDS-PAGE and incubated with anti-SHP1, anti-SHP2 or anti-PTP1B antibodies individually. GAPDH was used as the loading control.

5.4 Assessment of the accuracy of p-CrkL as a surrogate marker of Bcr-Abl kinase activity in K562 cells after dasatinib treatment at early time-points

Dasatinib is a second line TKI for treating CML. It is a dual Abl/Src inhibitor and 325 times more potent than IM in inhibiting wild type Bcr-Abl activity (173). Thus, it is interesting to study if p-CrkL is a surrogate marker of Bcr-Abl tyrosine kinase activity after dasatinib treatment in K562 cells. Similar to the previous experiments in Chapter

5.2, K562 cells were treated with 10nM dasatinib, and cells were sampled at several time-points (0, 0.5, 1, 2, 4, 8 hours).

It was observed that, with 10nM dasatinib, the p-Tyr Bcr-Abl response was similar to that seen with IM, which dropped rapidly to 14.3 ± 2.0% at 1 hour and then remained around this level. However, unlike IM, dasatinib caused a strong reduction in p-CrkL to 18.8 ± 4.7% by 1 hour, although this reduction slightly recovered to 28.8 ± 6.3% at 4 hours time-point (p=0.035, paired t-test). The difference between p-CrkL and p-Tyr Bcr-Abl are not statistically significant at each time-point (p≥0.070). These results indicate that p-CrkL accurately reflects Bcr-Abl tyrosine kinase activity after 10nM dasatinib treatment in K562 cells, which is quite different from IM treatment. This could be due to the additional inhibition of Src kinases by dasatinib.

A

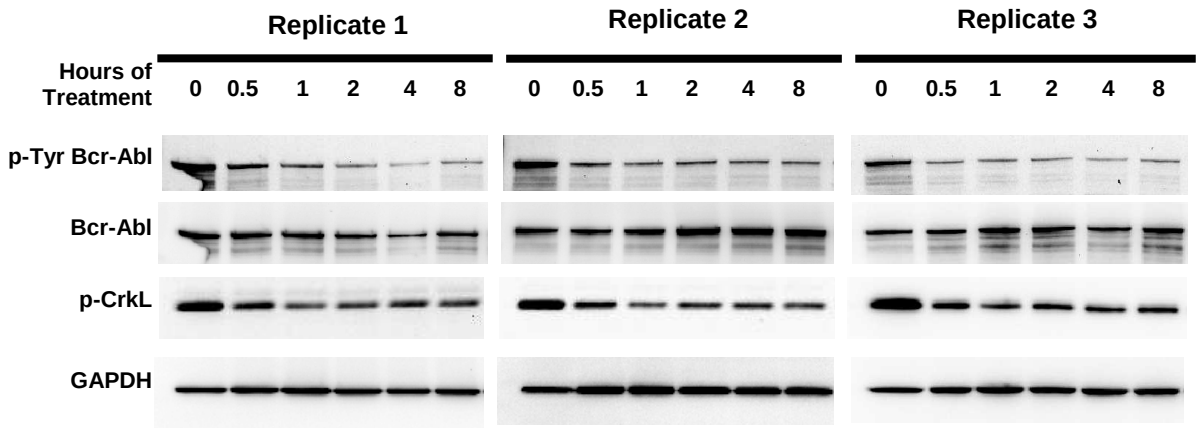

B

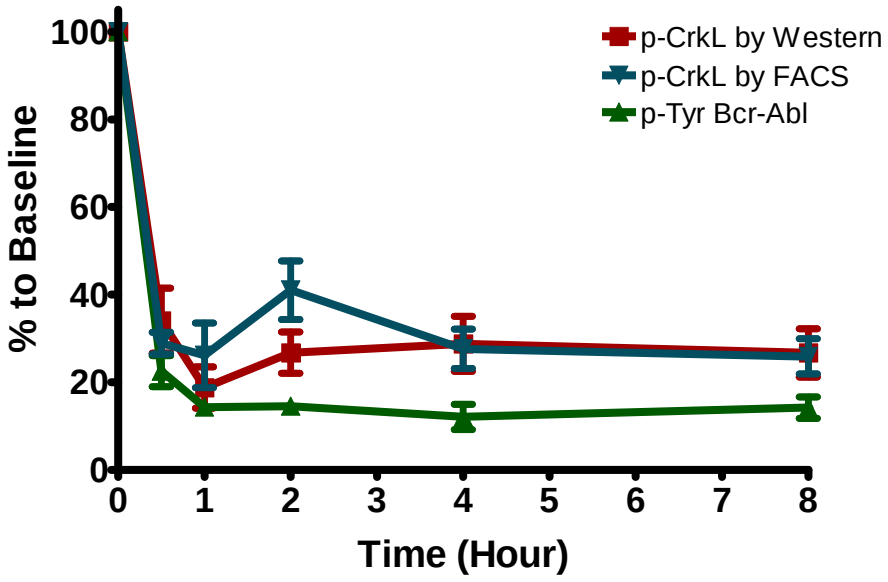

Figure 5-7: Protein levels of p-Tyr Bcr-Abl, Bcr-Abl and p-CrkL in 10nM Dasatinib treated K562 cells up to 8 hours by Western blotting, and p-CrkL level by FACS.

(A) Western blots showing protein levels of p-Tyr Bcr-Abl, Bcr-Abl, p-CrkL and GAPDH at different time-points (0, 0.5, 1, 2, 4, 8 hours) after IM treatment (n=3). (B) Plots showing normalized densitometry values of Western blot protein bands, as well as p-CrkL levels measured by FACS (n=3). Values are shown as percentage of no drug control. Results are shown as mean ± SEM, n=3.

5.5 Effect of PP2 and IM co-treatment on p-Tyr Bcr-Abl and p-CrkL

As shown above, the dual Abl/Src kinase inhibitor dasatinib significantly reduced p-CrkL level in K562 cells, while p-CrkL maintained at high level with IM treatment. Thus, Src kinases could be involved in CrkL phosphorylation. In order to test if Src kinases phosphorylate CrkL, the effects of Src inhibitor PP2 on p-CrkL level with or without IM was assessed in K562 cells.

5.5.1 Measurement of IC_{50} for the Src inhibitor PP2 in K562 cells

PP2 is a potent inhibitor of the Src tyrosine kinase family (263), and it was reported that the IC_{50} of PP2 was 10μM in K562 cells at 72 hours (264). Since the CrkL re-phosphorylation occurred within 24 hours, IC_{50} of PP2 at 24 hours in K562 cells was measured by viable cell count with trypan blue. It was shown that PP2 had an IC_{50} of approximately 30μM (Figure 5-8), which was used in subsequent experiments.

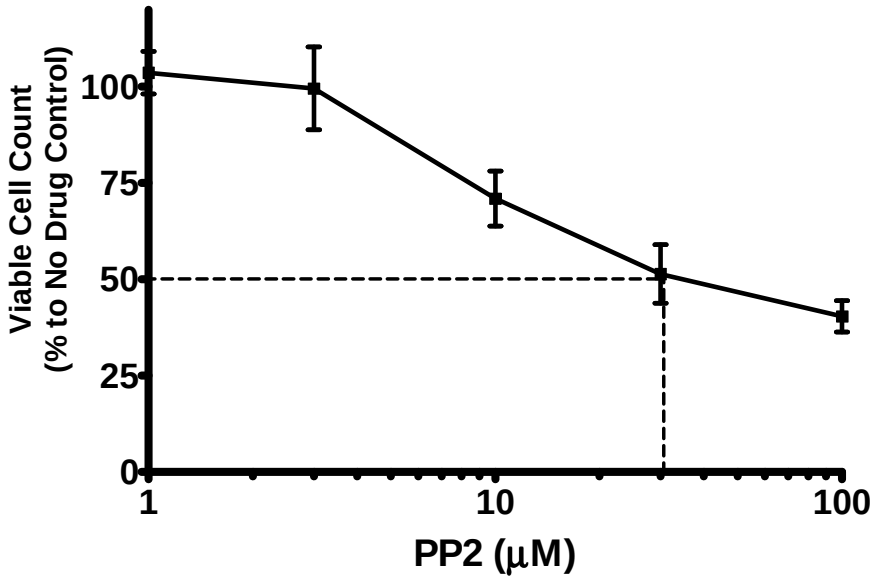

Figure 5-8: Determination of IC_{50} for PP2 in K562 cells at 24 hours.

50% inhibition of K562 cell proliferation was achieved by 30μM PP2 at 24 hours. Viable cells were counted by trypan blue and are shown as percentage to NDC (mean ± SEM, n=3).

5.5.2 PP2 and IM co-treatment in K562 cells

In order to examine the effect of Src inhibition on p-CrkL, K562 cells were treated with 30μM PP2 and 1μM IM. It was observed that (Figure 5-9) p-CrkL level was significantly decreased within 0.5 hour of the IM and PP2 co-treatment, and reached the lowest level of 7.0 ± 0.6% of baseline at 1 hour time-point. The p-CrkL level then recovered to 31.1 ± 5.1% by 8 hours and slightly dropped to 27.8 ± 3.2% at 24 hour time-point. On the other hand, p-Tyr Bcr-Abl level decreased to 24.1 ± 1.8% and

remained around this level. p-CrkL level was significant lower than p-Tyr Bcr-Abl level at 0.5 hour and 1 hour time-points (p=0.006 and p=0.0009, respectively), while there was no significant difference between p-CrkL and p-Tyr Bcr-Abl levels at later time-points. The increase of p-CrkL from 1 hour to 4 hour time-point is statistically significant (p=0.011, paired t-test). The pattern of p-CrkL response in the IM and PP2 co-treatment (Figure 5-9) is similar to the response in dasatinib treatment (Figure 5-7), as they both have an initial strong reduction, followed by a slight but significant recovery of p-CrkL level, and p-CrkL reached similar levels as p-Tyr Bcr-Abl at later time-points.

A

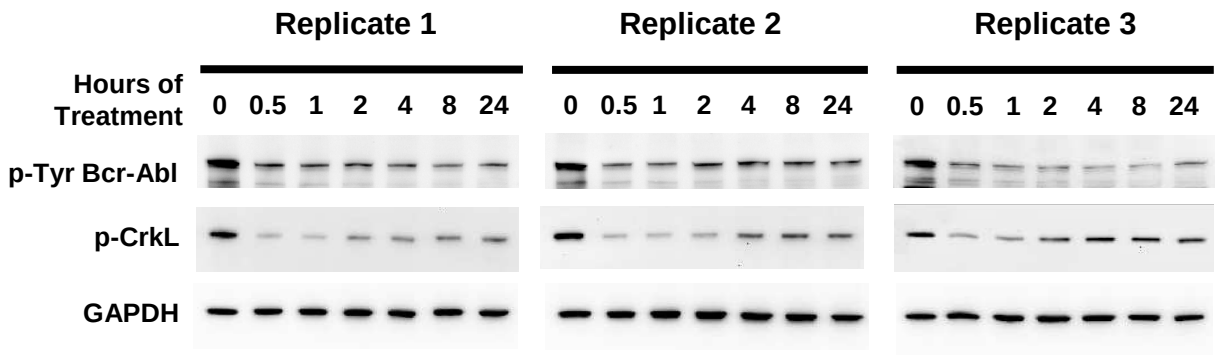

B

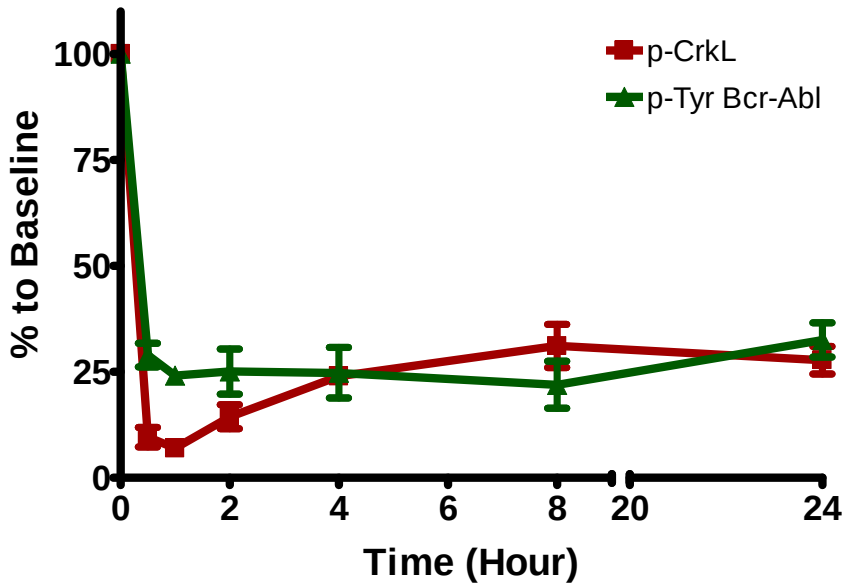

Figure 5-9: Co-treatment of 1μM IM and 30μM PP2 in K562 cells for up to 24 hours.

(A) Western blots showing protein levels of p-Tyr Bcr-Abl, p-CrkL and GAPDH at different time-points (0, 0.5, 1, 2, 4, 8 and 24 hours) after IM and PP2 co-treatment. (B) Plots showing normalized densitometry values of Western blot protein bands as percentage to baseline. Results are shown as mean ± SEM (n=3).

5.6 Effects of hydroxyurea treatment on p-Tyr Bcr-Abl and p-CrkL

It was concerning that the observation of rapid reduction of p-CrkL and p-Tyr Bcr-Abl after TKI treatments, as well as recovery of p-CrkL (Figure 5-1 and Figure 5-3), might be a technical issue. In order to ensure that this was not a technical artefact, a non-Bcr-Abl targeting drug need to be tested with K562 cells to make sure there was no such observation. Hydroxyurea, an inhibitor of DNA synthesis, was used to treat CML patients before the era of IM (135), and it is not known to target Bcr-Abl protein. Therefore, K562 cells were treated with 400μM hydroxyurea, a concentration which is around the proliferation inhibitory IC_{50} as shown in Figure 5-10A. It was found that p-CrkL and p-Tyr Bcr-Abl levels were maintained (Figure 5-10B and C). Cell counts at 24 hours showed hydroxyurea inhibited K562 cell proliferation by about 42% (Figure 5-10A), indicating the hydroxyurea used in this experiment is active. This result eliminates the possibility of technical artefact, such as lack of access of the antibodies to epitope target, in the previous experiments.

A

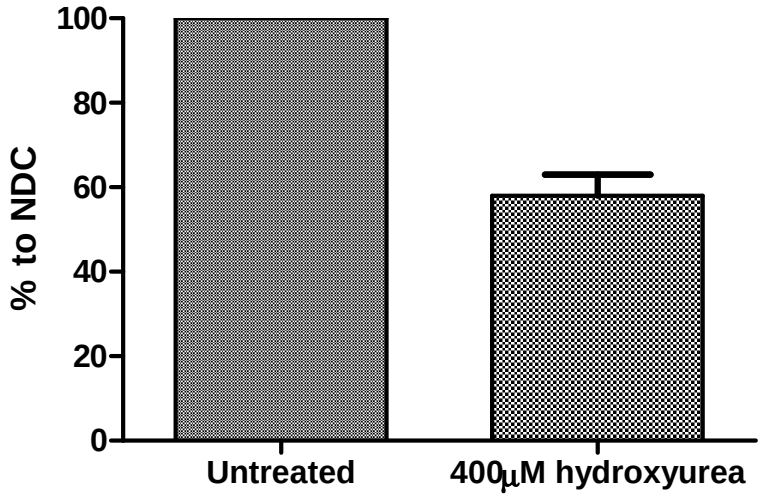
100
80
60
40
20
0
% to NDC
Untreated
400μM hydroxyurea

B

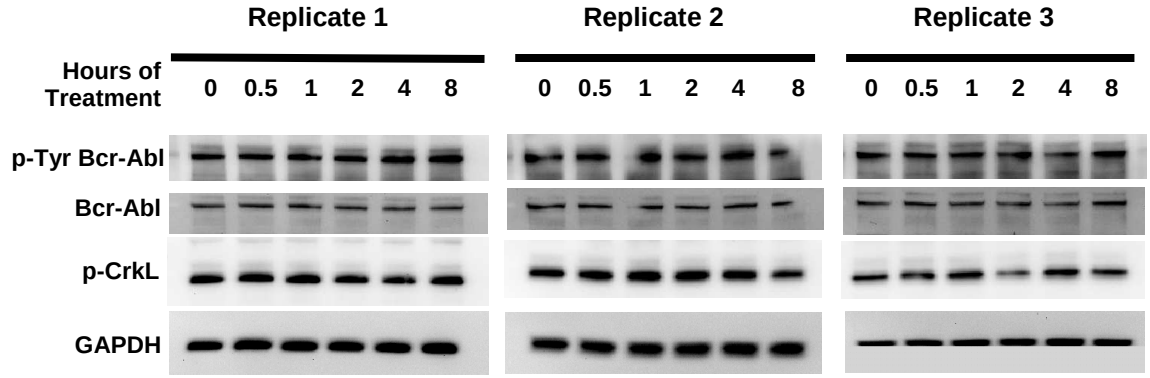
Replicate 1
Replicate 2
Replicate 3
Hours of Treatment
0 0.5 1 2 4 8
0 0.5 1 2 4 8
0 0.5 1 2 4 8
p-Tyr Bcr-Abl
Bcr-Abl
p-CrkL
GAPDH

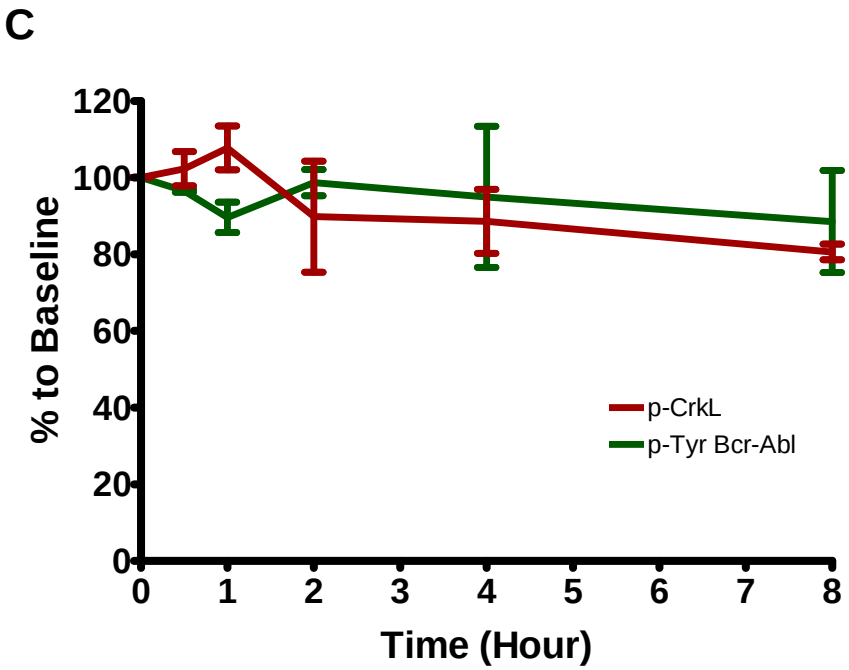

Figure 5-10: p-Tyr Bcr-Abl and p-CrkL levels in K562 cells with 400μM hydroxyurea.

(A) Cell counts by trypan blue dye exclusion at 24-hour 400μM hydroxyurea treatment in K562 cells. (B) Western blots showing protein levels of p-Tyr Bcr-Abl, Bcr-Abl, p-CrkL and GAPDH at different time-points (0, 0.5, 1, 2, 4, 8 hours) after hydroxyurea treatment (n=3). (C) Histograms showing normalized densitometry values of Western blot protein bands. Values are shown as percentage of baseline. All results are shown as mean ± SEM (n=3).

5.7 Summary and Discussion

These results demonstrate that p-CrkL is not a reliable indicator of Bcr-Abl kinase activity within 24 hours of IM treatment and indicate that the early responses to IM and dasatinib differ significantly. Importantly, these data also show that in addition to inhibition of the Bcr-Abl kinase activity there is a rapid and active dephosphorylation of Bcr-Abl within 1 hour of TKI treatment, driven at least in part, by PTP activity. This dephosphorylation is only revealed on switching off Bcr-Abl kinase activity with TKI.

The initial aim was to examine the accuracy of p-CrkL as a surrogate marker of Bcr-Abl tyrosine kinase activity. Thus, p-CrkL and p-Tyr Bcr-Abl levels were compared after IM treatment in K562 cells. It was observed that p-CrkL level dropped to about 39% of baseline level at 48 hours (Figure 5-1), which is consistent with the literature (162), but it was clearly shown that p-CrkL level was significantly different from p-Tyr Bcr-Abl level within 24 hours (Figure 5-1, Figure 5-2 and Figure 5-3). The differences between p-CrkL and p-Tyr Bcr-Abl levels could be due to incomplete inhibition of Bcr-Abl by IM, i.e. a small proportion of active Bcr-Abl protein is sufficient to phosphorylate CrkL. Since IM only targets Bcr-Abl protein in an inactive conformation (146), it is possible that a low level of active Bcr-Abl tyrosine kinase exists after IM treatment. In addition, it was shown by Khorashad *et al* that when $CD34^+$ cells from 5 newly diagnosed CML patients were treated with high concentration IM (5μM) that p-CrkL level decreased dramatically at 2 hour time-point to about 20% of baseline and was maintained around this level out to 16 hours (265). This report indicated that the significant difference between p-CrkL and p-Tyr Bcr-Abl levels after low concentration

IM (1μM) treatment may be abolished by a higher IM dose. This could be due to inhibition of other tyrosine kinases, which might phosphorylate CrkL, by a high dose of IM.

In addition, the differences could result from phosphorylation of CrkL by other kinases other than Bcr-Abl. It was reported that CrkL may be a substrate of Src kinases (266). If this is the case, the dual Abl/Src inhibitor dasatinib should have a better effect on p-CrkL inhibition compared with IM. Indeed, it was observed that there was no significant difference between p-CrkL and p-Tyr Bcr-Abl levels in dasatinib treated K562 cells (Figure 5-7), suggesting Src kinases could be involved in phosphorylating CrkL. In was further demonstrated that treatment of K562 cells with IM and PP2 (an inhibitor of Src kinases) induced rapid reduction of p-CrkL to levels which were significantly lower than p-Tyr Bcr-Abl at early time-points, then CrkL phosphorylation recovered to approximately the same levels as p-Tyr Bcr-Abl at later time-points (Figure 5-9). Co-treatment of K562 cells with IM and PP2 dramatically reduced p-CrkL compared with IM only treatment, indicating that Src kinases play a role in phosphorylating CrkL.

Interestingly, p-CrkL level was significantly recovered after an initial drop with IM treated K562 cells (Figure 5-1 and Figure 5-3), suggesting that there were other kinases phosphorylating CrkL after inhibition of Bcr-Abl kinase activity. At first, this recovery was thought to be mediated by Src kinases, as it was known that CrkL could be a substrate for Src kinases (266). However, there was still a recovery of CrkL

phosphorylation after dasatinib treatment in K562 cells (Figure 5-7), while the degree of recovery is smaller than with IM treatment. Similarly, the recovery of p-CrkL was observed in IM and PP2 co-treatment in K562 cells. These results indicate that there are other kinases that phosphorylate CrkL in addition to Bcr-Abl and Src.

Unexpectedly, it was observed that p-Tyr Bcr-Abl is reduced to a minimum within 1 hour of TKI treatment (Figure 5-1, Figure 5-3 and Figure 5-7), and reduced to less than 50% of baseline level within just 10 minutes of IM treatment (Figure 5-2). The rapid reduction of p-Tyr Bcr-Abl lead to the hypothesis that Bcr-Abl was actively dephosphorylated by PTPs after TKI treatment. It has been reported that Bcr-Abl is a substrate of PTP1B, and co-expression of PTP1B and Bcr-Abl proteins in COS cells resulted in significantly lower level of p-Tyr Bcr-Abl compared with expression of Bcr-Abl only (225). In addition, it was shown that inhibition of PTP1B activity, by expression of a dominant-negative substrate-trapping PTP1B mutant (binding to substrates, but without catalyzing activity), confers resistance to IM treatment in K562 cells (224;264). Therefore, the rapid drop of p-Tyr Bcr-Abl level within 1 hour of TKI treatment may be caused by PTP1B activity in K562 cells, and a future direction to confirm this is to knock down PTP1B in CML cells by siRNA to examine if there is any inhibition of Bcr-Abl dephosphorylation after IM treatment.

Furthermore, since all experiments in this Chapter were performed in the human CML cell line K562 cells, a future perspective is to confirm these findings in human primary CML cells, as primary cells might be different to cell line cells in this regard. Finally,

based on the findings in this Chapter, one could say that high p-CrkL level does not necessarily indicate high Bcr-Abl tyrosine kinase activity in CML cells. Thus, using p-CrkL as a surrogate marker of Bcr-Abl activity can generate false positive results in some cases, and it may be mistaken to conclude that there is high Bcr-Abl activity when high p-CrkL level is observed.

6 Results 4: Does BMS-214662 induce CML cell apoptosis by proteasome inhibition?

6.1 Introduction

BMS-214662 is a FTI, which was developed as an inhibitor of Ras signalling pathway (206). Cytosolic Ras protein is post-translationally modified to enable its membrane association, which is critical for the signalling functions of Ras (206), and farnesylation of the C-terminal cysteine residue of Ras by farnesyltransferase is the key step of this process (208). Therefore, inhibition of the farnesyltransferase activity by FTI prevents membrane association of cytosolic Ras and its signalling function. BMS-214662 has been shown to induce apoptosis potently in tumour cells, but another highly related FTI, BMS-225975, does not (211). Since BMS-214662 and BMS-225975 have very similar FTI activity (211), it is thought that BMS-214662 induces apoptosis in tumour cells by a mechanism apart from its FTI activity. Additionally, BMS-214662 exhibits apoptotic effect in primary CML stem and progenitor cells, making it a potential drug to eradicate CML (212;213), but it is not clear how exactly BMS-214662 activates the intrinsic apoptotic pathway in CML cells.

In the previous chapter, hydroxyurea was tested in K562 cells as a control showing that p-CrkL and p-Tyr Bcr-Abl levels were maintained. In the mean time, BMS-214662 was tested for the same purpose in K562 cells, and surprisingly it was found that BMS-214662 elevated p-Tyr Bcr-Abl and total Bcr-Abl levels (Figure 6-1). It has been

reported that c-Abl and Bcr-Abl protein could be ubiquitinated and degraded by the proteasome pathway (267;268). Thus, inhibition of proteasome activity may lead to the accumulation Bcr-Abl protein, and BMS-214662 may therefore act as a proteasome inhibitor leading to the accumulation of Bcr-Abl protein as observed in Figure 6-1.

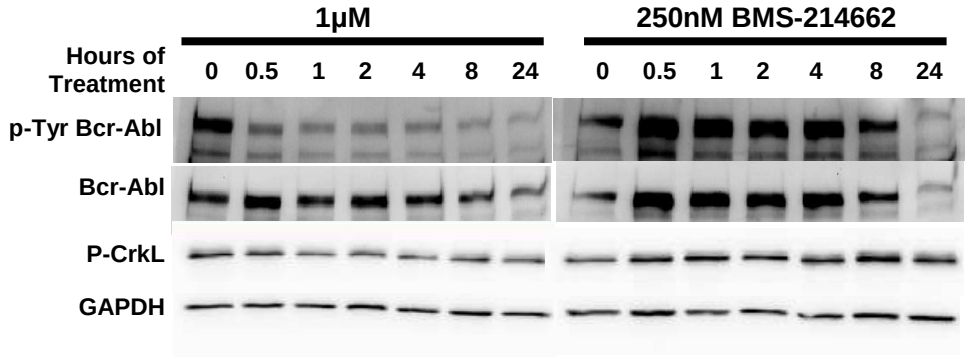

Figure 6-1: Accumulation of p-Tyr Bcr-Abl and total Bcr-Abl protein in K562 cells after BMS-214662 treatment.

It has been reported that Bcr-Abl$^+$ cells had much higher proteasome activity than their normal counterparts (269), suggesting that Bcr-Abl protein increases proteasome activity. In addition, it was reported that intracellular ROS is up-regulated by Bcr-Abl tyrosine kinase (270). Furthermore, inhibition of proteasome elevates intracellular ROS level in leukaemic cells. Therefore, it was hypothesised that if BMS-214662 inhibited proteasome activity, this could result in the accumulation of Bcr-Abl protein and further elevation of intracellular ROS level, which CML cells can not tolerate leading to apoptosis. The aim of study in this section was to examine if

inhibition of proteasome activity is a novel mechanism of action of BMS-214662 which preferentially induces apoptosis in CML cells compared with the related FTI BMS-225975.

6.2 Determination of IC_{50} values in K562 cells

If proteasome inhibition is the novel mechanism of action of BMS-214662 which BMS-225975 does not have, it should induce accumulation of ubiquitinated proteins in CML cells in a similar pattern as a known proteasome inhibitor bortezomib, and different from BMS-225975. Since Bcr-Abl increases proteasome activity (269), inhibition of Bcr-Abl kinase by IM should decrease proteasome activity and accumulate ubiquitinated proteins, which could be measured by Western blotting. Before doing that, the cytotoxicity of these drugs needed to be examined in CML cells and suitable drug concentrations should be chosen. Therefore, the IC_{50} values of BMS-214662, BMS-225975, bortezomib and IM were measured in the CML cell line K562. Cells were treated with various concentrations of each drug for 24 and 72 hours. The number of viable cells in each treatment was counted with trypan blue (Figure 6-2), and the IC_{50} values are shown in Table 6-1.

BMS-214662 has an IC_{50} value about 47 times lower than BMS-225975 in K562 cells at 24 hours, demonstrating a much more potent cytotoxic effect of BMS-214662 and confirming the existence of a non-FTI related mechanism of action of BMS-214662 (Table 6-1). Since the levels of ubiquitinated proteins were measured within 24 hours

of drug treatments, 40μM BMS-214662, which is slightly higher than the IC_{50} at 24 hours, was chosen to be used in the subsequent experiments to make sure the effects of the drug could be seen but before the degree of apoptosis was too great to allow analysis of the cells. As BMS-214662 and BMS-225975 have very similar FTI activity, 40μM BMS-225975 was tested as a negative control. If BMS-214662 treatment arm had a significant difference from BMS-225975 arm, it should be due to the additional mechanism of action of BMS-214662. In addition, the established proteosome inhibitor bortezomib (20nM) was also used as a positive control. Additionally, 1μM IM was used in the following experiments to examine if inhibition of Bcr-Abl tyrosine kinase leads to accumulation of ubiquitinated proteins and down-regulation of intracellular ROS.

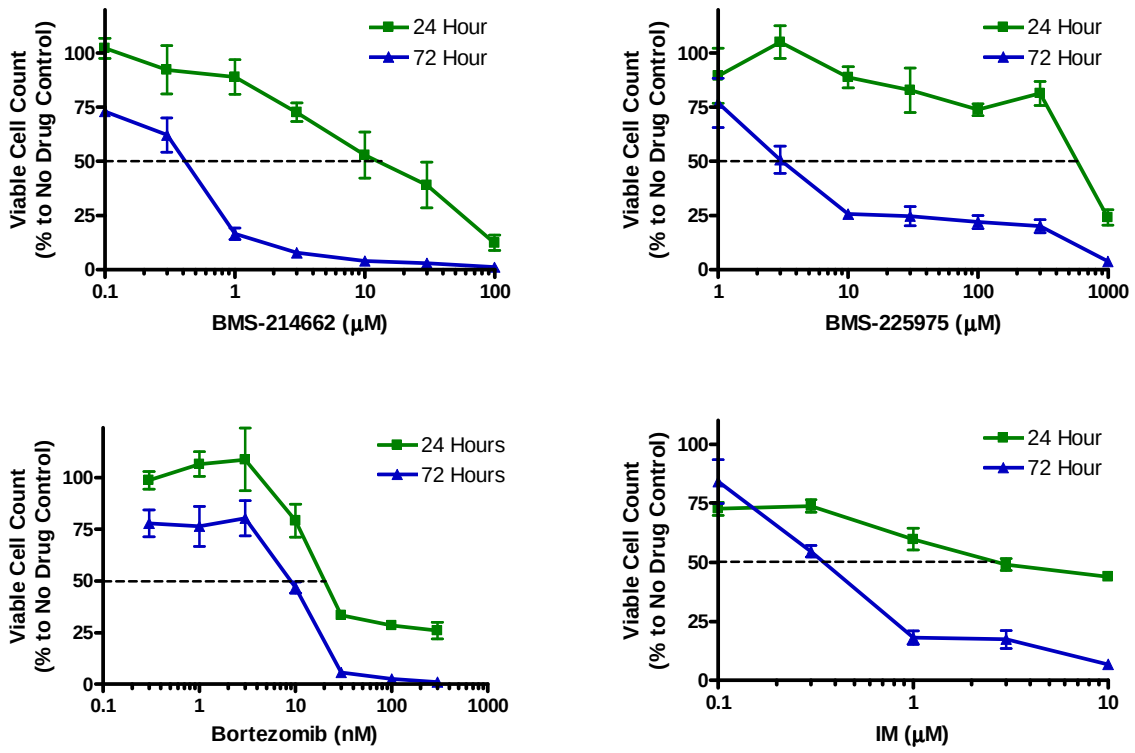

Figure 6-2: IC_{50} for BMS-214662, BMS-225975, bortezomib and IM in K562 cells.

Viable cells were counted by trypan blue at 24 and 72 hours. The percentage of cells in each treatment compared with NDC (100%) were calculated and is presented as mean ± SEM (n=3). Drug concentrations are plotted in Log10 scales.

IC_{50} in K562	BMS-214662 (μM)	BMS-225975 (μM)	Bortezomib (nM)	IM (μM)
24h	14.5	680	22	2.75
72h	0.5	3.4	9.5	0.4

Table 6-1: IC_{50} for BMS-214662, BMS-225975, bortezomib and IM in K562 cells.

Estimated from mean values in the above figure.

6.3 Accumulation of ubiquitinated proteins and Bcr-Abl

To test if BMS-214662 is a proteasome inhibitor, K562 cells were treated with 40μM BMS-214662, 40μM BMS-225975, 20nM bortezomib or 1μM IM. Cells were sampled at various time-points up to 8 hours, and subjected to Western blotting analysis. At first, the total ubiquitinated proteins were examined in each treatment condition (Figure 6-3A). It was observed that BMS-214662 and BMS-225975 accumulated ubiquitinated proteins in a very similar manner, but quite different from bortezomib at later time-points (Figure 6-3B). All three drugs began to up-regulate the level of total ubiquitinated proteins from 0.5 hour time-point, and all reached about 2-fold of baseline level at 1 hour time-point. However, bortezomib accumulated more and more ubiquitinated proteins with increasing time, and reached 5-fold of baseline level at 8 hour time-point. In contrast, the level of ubiquitinated proteins was maintained around or under 2-fold of baseline in BMS-214662 and BMS-225975 treatment arms. There was no statistical significant difference between BMS-214662 and BMS-225975 treatment arms in terms of the level of ubiquitinated proteins at any time-point

(p>0.55). On the other hand, bortezomib treatment arm had a significantly higher level of ubiquitinated proteins than BMS-214662 and BMS-225975 treatment arms at later time-points (p<0.05 at 4 hours time-point, p<0.01 at 8 hours time-point).

There is a gradual accumulation of ubiquitinated proteins in the IM treatment arm, and achieved statistical significance at 4 and 8 hours time-points with respect to baseline (p=0.033 and p=0.046, respectively. Paired t-test). There is also a significant increase of ubiquitinated proteins from 0.5 hour to 4 hours time-point (p=0.026, paired t-test) (Figure 6-3B). This is consistent with the idea that IM reduces proteasome activity by inhibiting Bcr-Abl tyrosine kinase. In addition, there is no statistically significant change in the levels of ubiquitinated proteins in NDC arm compared to baseline (p>0.12, paired t-test), suggesting that the untreated cells did not alter their ubiquitinated-protein levels within the 8 hour of cell culture.

Furthermore, Bcr-Abl protein was accumulated in both BMS-214662 and BMS-225975 treatment arms (Figure 6-3C and D), and there was no statistical significant difference between these treatment arms at any time-points (p>0.20). Since both BMS-214662 and BMS-225975 consistently accumulated total ubiquitinated proteins and Bcr-Abl protein in K562 cells, it is likely that the protein accumulation is due to their common, presumed FTI activity. In the bortezomib treatment arm, Bcr-Abl protein was accumulated in the early time-points, but returned to baseline level at later time-points (Figure 6-3D).

A

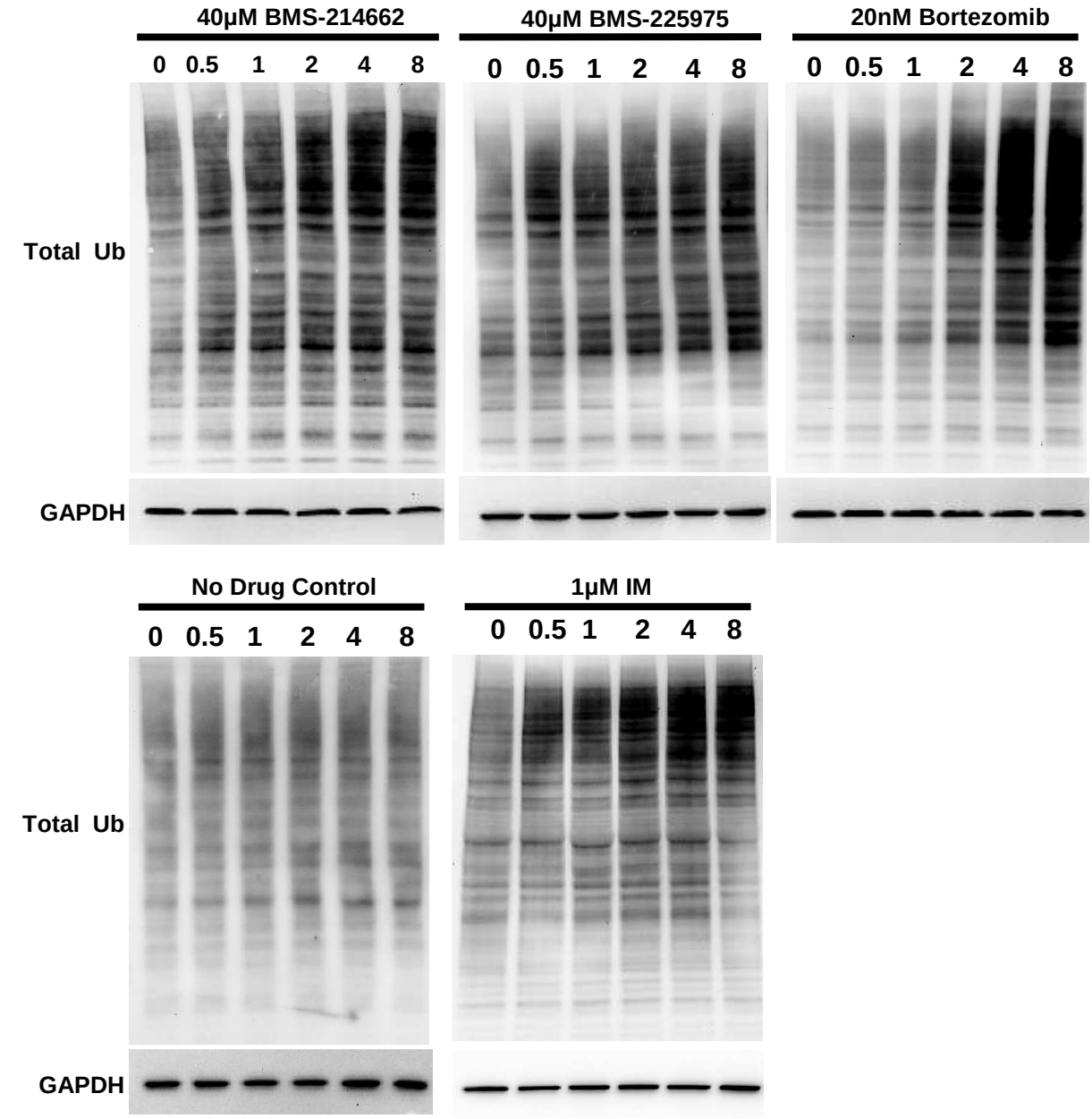
40μM BMS-214662
40μM BMS-225975
20nM Bortezomib
0 0.5 1 2 4 8
Total Ub
GAPDH
No Drug Control
1μM IM
0 0.5 1 2 4 8
Total Ub
GAPDH

B

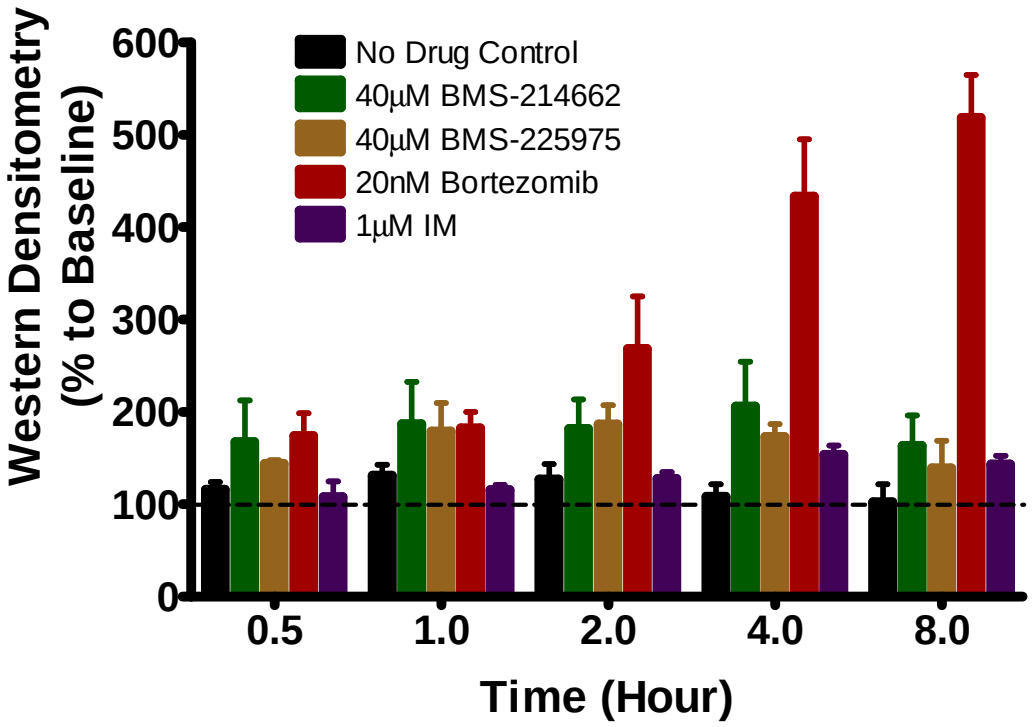
Western Densitometry
(% to Baseline)
600
500
400
300
200
100
0
No Drug Control
40μM BMS-214662
40μM BMS-225975
20nM Bortezomib
1μM IM
0.5
1.0
2.0
4.0
8.0
Time (Hour)

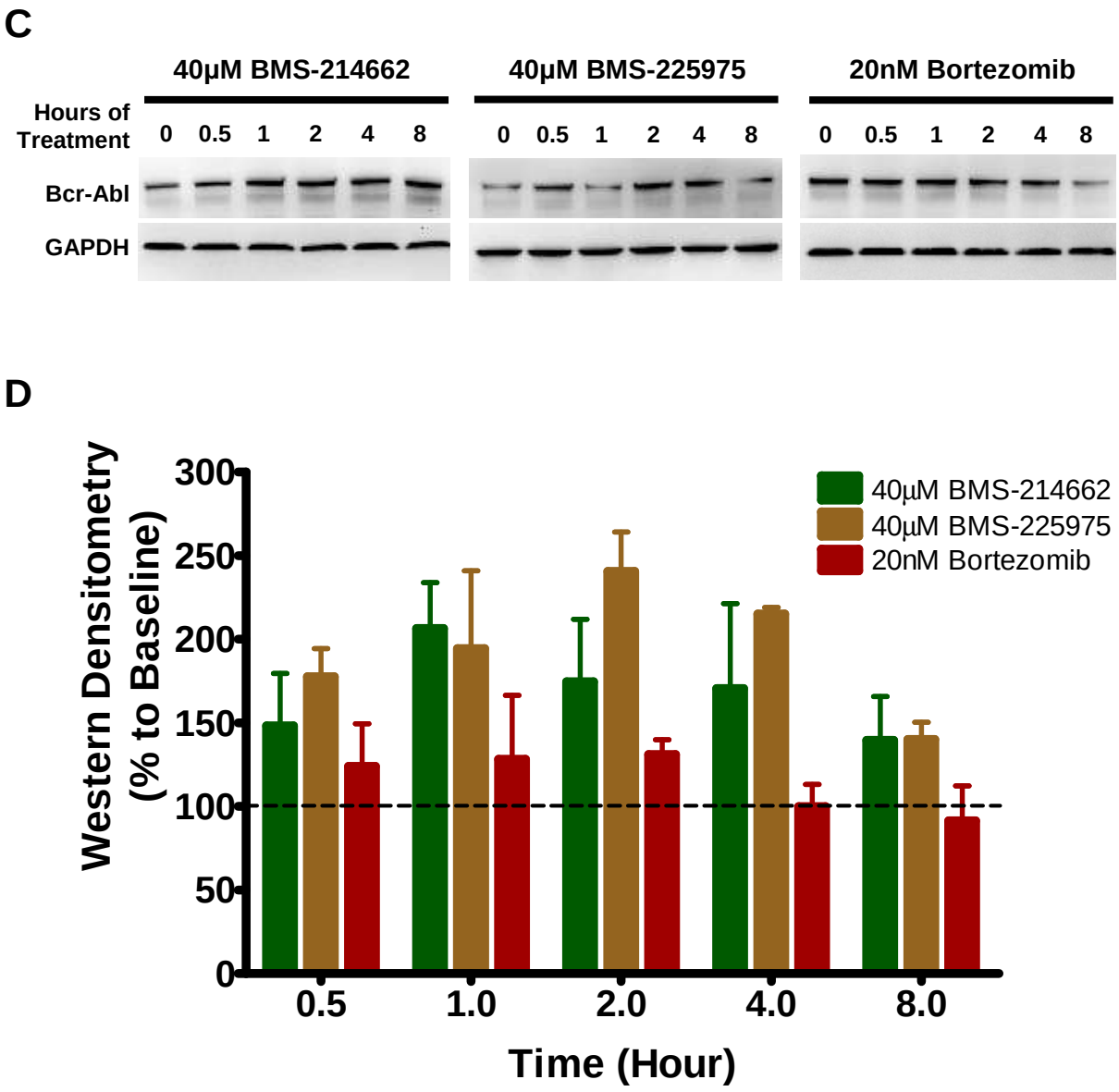

Figure 6-3: Ubiquitination and Bcr-Abl protein levels after BMS-214662, BMS-225975 or Bortezomib treatment in K562 cells.

(A) Western blots showing total ubiquitin levels at each time-point of drug treatments. GAPDH was used as a loading control. (B) Normalized total ubiquitin levels against GAPDH, and plotted as percentage to baseline (NDC at 0 hour time-point). (C) Western blots showing Bcr-Abl protein levels. (D) Normalized Bcr-Abl levels against GAPDH,

and plotted as percentage to baseline. Graphs were plotted as mean ± SEM, n=3. Ub stands for ubiquitin.

6.4 Measurement of ROS in K562 cells

According to the hypothesis, BMS-214662 induced apoptosis of CML cells by elevating intracellular ROS level. In order to test if BMS-214662 increases intracellular ROS level, DCFDA was employed, and was loaded into K562 cells prior to drug treatments. In the presence of ROS, DCFDA is cleaved into DCF, which is a green fluorescent dye and can be detected by flow cytometry in the FITC channel. Thus, the level of DCF fluorescence indicates the level of intracellular ROS. It was shown in Figure 6-4 that the BMS-214662 treatment arm had significantly higher DCF levels with respect to BMS-225975 at 1 hour and 4 hours time-points (p=0.0037 and p=0.00025, respectively). Bortezomib arm had baseline level DCF from 0.5 hour to 4 hour time-points, and had an increase to more than 2-fold of baseline at 8 hour time-point. On the other hand, the DCF level in the IM treatment arm was always around the baseline level at any time-point. In addition, hydrogen peroxide (H_2O_2) was used as a positive control to mimic oxidative stress, and it was observed that the H_2O_2 treatment arm had dramatic increase of DCF fluorescence from the earliest time-point (Figure 6-4).

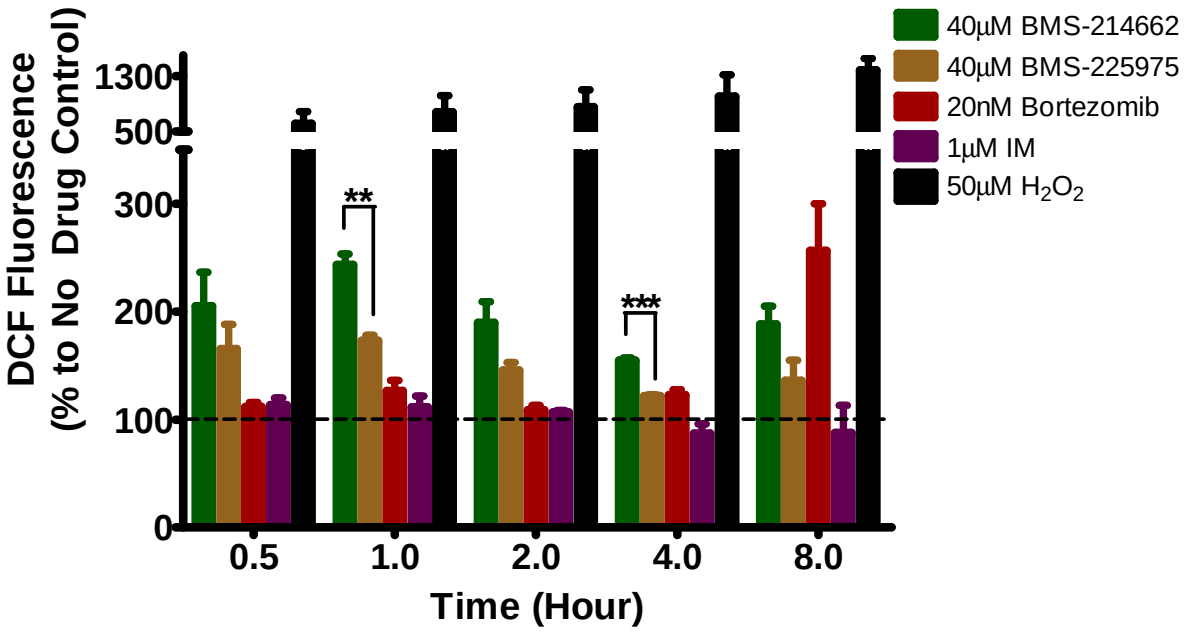

Figure 6-4: Intracellular ROS level in K562 cells after drug treatments.

K562 cells were pre-loaded with DCFDA, and then treated with each drug individually. Cells were sampled at each time-point and analyzed by flow cytometry to measure DCF fluorescence level with the FITC channel. DCF fluorescence was shown as percentage to the NDC at each time-point. Results are shown as mean ± SEM, n=3 (***p*<0.01, *** ***p*<0.001).**

6.5 Determination of IC_{50} values in serum-starved K562 cells

As shown above, BMS-214662 induced significantly higher level of intracellular ROS than BMS-225975 in proliferating K562 cells. It then raised the question if this was the case in quiescent K562 cells. In order to synchronise cell cycle and arrest cell division, K562 cells were starved in serum free medium for 16 hours. Cell counting showed that these serum-starved K562 cells did not proliferate. As shown in Figure 6-5, the serum-starved K562 cells were re-plated and cultured for another 24 hours in serum free medium, and the cell density did not increase compared with input (p=0.23, paired t-test). In contrast, the density of proliferating K562 cells increased about 3-fold when they were cultured in serum-containing medium for 24 hours, and it is significantly different from the density of serum-starved K562 cells (p=0.0012) This demonstrated that the 16-hour serum-starvation had made K562 cells exit the cell cycle and stop proliferating.

Subsequently, IC_{50} values of BMS-214662, BMS-225975, bortezomib and IM were measured in the non-proliferating K562 cells, since they may have different IC_{50} values from proliferating K562 cells. As shown in Table 6-2, the IC_{50} of BMS-214662 at 24 hours is more than 13 times less than BMS-225975, demonstrating the preferential apoptotic effect of BMS-214662 in non-proliferating CML cells. In addition, BMS-214662, BMS-225975 and bortezomib had similar IC_{50} values between proliferating and non-proliferating K562 cells at 24-hour treatment (Table 6-1 and Table 6-2). Thus, the same concentrations of these drugs as used with proliferating K562 cells were used in the subsequent experiment with serum-starved non-

proliferating K562 cells. The IC_{50} of IM in non-proliferating K562 cells at 24 hours is about five times higher than in proliferating K562 cells (Table 6-1 and Table 6-2), demonstrating the resistance of quiescent CML cells to TKI treatment.

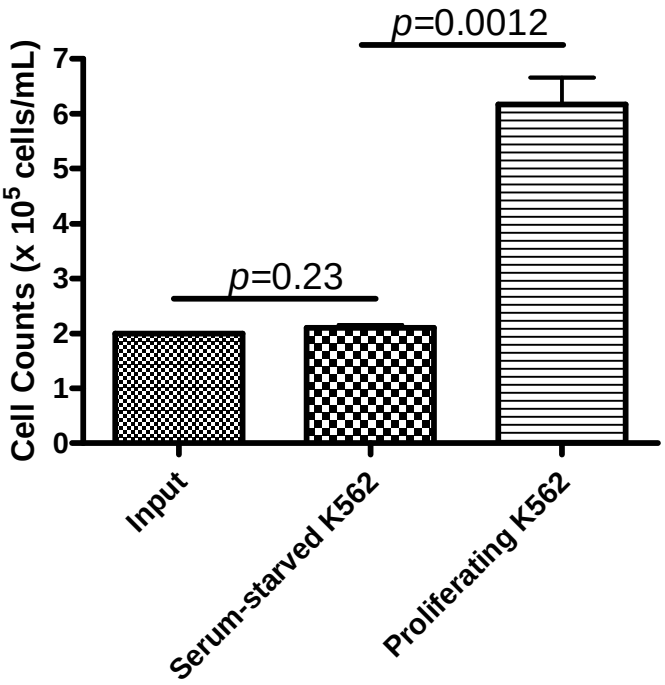

Figure 6-5: Serum-starved K562 cells stopped proliferation.

Proliferating K562 cells were starved in serum free medium for 16 hours to induce cell cycle arrest, and then the cells were re-plated at 2 x 10^5 cells/mL in serum-free medium for another 24 hours. As a control, proliferating K562 cells were plated at 2 x 10^5 cells/mL in serum-containing medium for 24 hours.

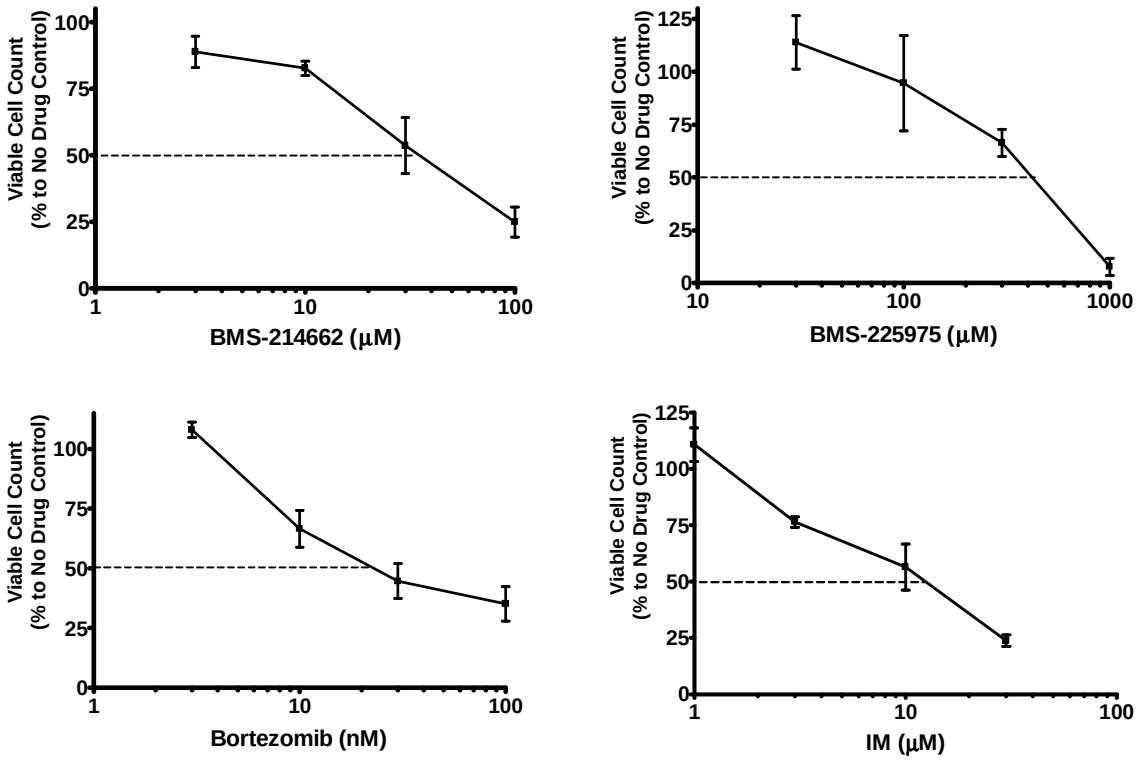

Figure 6-6: Determination of IC_{50} for BMS-214662, BMS-225975, Bortezomib and IM in serum-starved K562 cells by trypan blue viable cell counts at 24 hours.

K562 cells were starved in serum free medium for 16 hours, and then the cells were re-plated and treated with each drug for another 24 hours. The percentage of cells in each treatment compared with NDC were calculated and is presented as mean ± SEM (n=3). Drug concentrations are plotted in Log10 scales.

IC50 in serum-starved K562	BMS-214662 (μM)	BMS-225975 (μM)	Bortezomib (nM)	IM (μM)
24h	37.5	500	25	13

Table 6-2: IC_{50} for BMS-214662, BMS-225975, Bortezomib and IM in starved K562 cells. Estimated from mean values in the above figure.

6.6 Measurement of ROS in serum-starved K562 cells

Intracellular ROS levels were measured in non-proliferating K562 cells to investigate if BMS-214662 preferentially induced generation of intracellular ROS compared with BMS-225975. It was observed that both BMS-214662 and BMS-225975 treatment arms had elevated DCF levels, while BMS-214662 treatment arm generally had higher DCF level than the BMS-225975 arm at each time-point that achieved statistical significance at 8 hours and 24 hours time-points (p=0.0012 and p=0.031, respectively). In contrast, bortezomib did not significantly increase DCF level over baseline (p>0.16, paired t-test) (Figure 6-7).

The DCF level in IM arm is significantly decreased at 24 hours time-point with respect to baseline and 8 hours time-point (p=0.013 and p=0.031, respectively. Paired t-test) (Figure 6-7). H_2O_2 was used as a positive control, and it was observed that the H_2O_2 treatment arm had gradual increase of DCF fluorescence and reached about 2-fold of baseline at 24 hours time-point (Figure 6-7).

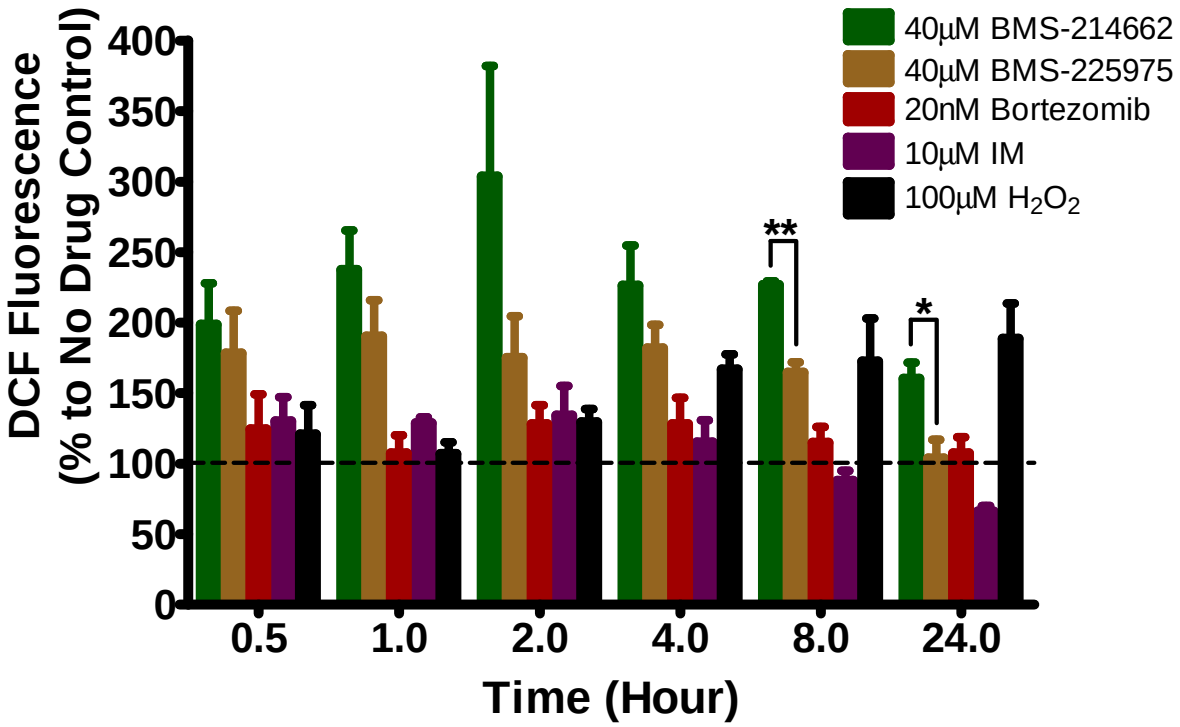

Figure 6-7: Intracellular ROS level in serum-starved K562 cells with drug treatments.

Proliferating K562 cells were cultured in serum free medium for 16 hours, then loaded with DCFDA and treated with each drug in serum free medium. DCF fluorescence was measured by flow cytometry, and shown as percentage to the NDC at each time-point. Results are shown as mean ± SEM, n=3 (*p<0.05, ** p<0.01).

6.7 Summary and Discussion

In summary, these results demonstrated that BMS-214662 is not a proteasome inhibitor like bortezomib. Although BMS-214662 treatment induced accumulation of total ubiquitinated proteins and specifically Bcr-Abl protein in K562 cells, another FTI BMS-225975 had very similar effects. This indicates that accumulation of total ubiquitinated proteins and Bcr-Abl protein is not the novel mechanism of action of BMS-214662 which preferentially induces apoptosis in CML cells. It is likely that the observed protein accumulation results from the common mechanism of BMS-214662 and BMS-225975, which is their FTI activity. On the other hand, BMS-214662 induced significantly higher levels of intracellular ROS in both proliferating and non-proliferating K562 cells than BMS-225975, demonstrating the involvement of significant ROS production in the novel mechanism of action of BMS-214662.

It was shown that the IC_{50} values of BMS-214662 are much lower than BMS-225975 in both proliferating and non-proliferating K562 cells (Table 6-1 and Table 6-2), which is consistent with previous reports that BMS-214662 has a much more potent cytotoxic effect against tumour cells compared with BMS-225975. Manne *et al* demonstrated BMS-214662 preferentially induced apoptosis in tumour cells *in vitro* other than BMS-225975 (211). In addition, BMS-214662 caused dramatic tumour regression *in vivo,* while BMS-225975 only had a mild inhibition of tumour growth (211). Copland *et al* showed that BMS-214662 significantly reduced the number of quiescent CML $CD34^+$ cells, and increased the percentage of caspase-3 positive CML $CD34^+$ cells, but the effects of BMS-225975 was not different from NDC (212).

Since BMS-214662 and BMS-225975 have very similar FTI activity, these reports and observations consolidate the notion that BMS-214662 has a novel mechanism of action against tumour cells, including CML cells.

Pellicano *et al* showed that BMS-214662 increased intracellular ROS level compared with NDC in CML $CD34^+$ cells, but the effect of BMS-225975 on ROS was not studied in their report (213). In this chapter, the induction of ROS by both BMS-214662 and BMS-225975 was studied, and was found that both drugs up-regulated intracellular ROS levels in proliferating and non-proliferating K562 cells, but the level of ROS induced by BMS-214662 was significantly higher than by BMS-225975. This indicates that the FTI activity of BMS-225975 is able to increase intracellular ROS to a certain level, and that the much greater increase of ROS induced by BMS-214662 was due in part to its FTI activity but also by its novel non-FTI related activity.

Bcr-Abl can increase proteasome activity (269). Consistent with this, it was observed that inhibition of Bcr-Abl tyrosine kinase by IM accumulated ubiquitinated proteins in proliferating K562 cells (Figure 6-3A and B), indicating IM decreased proteasome activity by Bcr-Abl inhibition. In addition, Bcr-Abl can up-regulate intracellular ROS level (270), so inhibition of Bcr-Abl tyrosine kinase is supposed to down-regulate ROS level. However, 1μM IM did not significantly decrease ROS level with 8-hour treatment in proliferating K562 cells (Figure 6-4). This may be because the length of treatment or drug concentration is not sufficient. On the other hand, the intracellular

ROS level significantly decreased with 24-hour 10μM IM treatment in non-proliferating K562 cells (Figure 6-7),

Previous reports have shown that BMS-214662 was able to activate JNK signalling pathway (211), and up-regulate PKCβ level (213), whereas BMS-225975 could not activate these signalling pathways. In addition, co-treatment of CML progenitor and stem cells with BMS-214662 and PKCβ inhibitor greatly reduced apoptosis compared to BMS-214662 single treatment (213). In this chapter, it was illustrated that BMS-214662 induced significantly higher level of intracellular ROS compared with BMS-225975 in both proliferating and non-proliferating CML cells. However, further studies are required to link these findings together in order to uncover the novel mechanism of action of BMS-214662 against CML cells, which will facilitate novel drug development to eliminate CML disease.

One possible model to link these observations is that BMS-214662 treatment generated sufficient amount of intracellular ROS to activate JNK (Figure 6-4 and Figure 6-7). It is known that JNK is activated upon exposure to oxidative stress and DNA damage, and then activated JNK phosphorylates 14-3-3 and results in the release of c-Abl (and possibly Bcr-Abl as well in CML cells) from 14-3-3, hence nuclear translocation of c-Abl and induction of apoptosis by Abl tyrosine kinase (231;234). In addition, 14-3-3/PKC association inhibits PKC enzymatic activity, including PKCβ (271), and expression of functionally inactivated 14-3-3 in mice is accompanied with elevated expression of PKCβ2 (272). Additionally, phosphorylating

of 14-3-3 by activated JNK disrupts 14-3-3/ligands association (229). Thus, phosphorylating of 14-3-3 by JNK in response to oxidative stress may lead to 14-3-3/PKCβ dissociation, recovery of PKCβ activity and enhanced expression of PKCβ, which could explain the observations made by Pellicano *et al* (213). Thus, the future perspective is to examine the subcellular localization of c-Abl and Bcr-Abl proteins in BMS-214662 treated CML cells, as well as 14-3-3/PKCβ interaction.

7 Results 5: Targeted drug delivery by sLDL particles

7.1 Introduction

With the failure of efforts so far to eliminate CML stem cells, a new approach was developed based upon one possible explanation of TKI insensitivity, which is that there may be insufficient intracellular drug concentration in insensitive CML stem cells. The expression level and kinase activity of Bcr-Abl is greatly elevated in primitive CML $CD34^{+}CD38^{-}$ cells compared to mature MNC (163). In addition, the clinically achievable steady state peak plasma concentration of IM is about 4.6μM at the standard 400mg once daily dosing (149), and it was demonstrated that this concentration of IM did not significantly reduce CrkL phosphorylation in CML $CD34^{+}38^{-}$ cells *in vitro* (163). Therefore, insufficient inhibition of Bcr-Abl tyrosine kinase activity in the primitive CML $CD34^{+}38^{-}$ cells could be an explanation of IM insensitivity, and an increased intracellular IM concentration may overcome this drug resistance, and kill CML stem cells.

However, simple escalation of IM oral dose may not be the best choice, as the therapeutic window could be lost and side effects become intolerable with high levels of IM. On the other hand, a CML stem cell targeted drug delivery approach may overcome this resistant mechanism with limited toxicity. Natural LDL particles are preferentially uptaken by leukaemic cells (237). sLDL particles are functionally equivalent to LDL and do not have issues associated with natural LDL (240;241).

Therefore, sLDL particles are suitable for targeted drug delivery in CML stem cells. The ultimate aim of this study was to determine if the drug loaded sLDL particles may overcome insufficient intracellular drug levels in CML stem cells. The first step of this investigation, however, was to examine the ability of CML stem cells to uptake unloaded sLDL particles *in vitro*.

7.2 Uptake of sLDL by CML cells

Competent sLDL particles were prepared with a green fluorescence tracer dye dioctadecyloxacarbocyanine (DiO), and synthetic apoprotein B receptor peptide which is recognized by LDLR inducing active cellular uptake. Control particles lacking the Apo-B receptor peptide were also prepared (peptide free sLDL). Since the tracer dye DiO emits green fluorescence, the level of sLDL uptake by CML cells could be measured by flow cytometry in the FITC channel.

In order to study if CML cells were able to uptake sLDL particles and determine an optimal sLDL concentration and incubation time for the subsequent experiments, K562 cells were treated with sLDL for various lengths of time and sLDL concentrations. It was demonstrated that sLDL treated K562 cells (equivalent to 5μg cholesterol/mL culture medium) accumulated sLDL particles with increased incubation time, and there was a one-log elevation of FITC mean fluorescence intensity (MFI) at 24 hours of treatment compared to the untreated cells (Figure 7-1A). In addition, an increased uptake of sLDL by K562 cells with increasing sLDL concentrations at 24 hours of treatment was also observed (Figure 7-1B). Taken together, these data demonstrated firstly the uptake of sLDL particles by K562 cells, and that this uptake was in a time and concentration dependent manner. Treatment for 24 hours with 5μg cholesterol/mL was chosen for the subsequent experiments.

In addition, uptake of sLDL particles by CML $CD34^{+}38^{low/-}$ cells was also examined. Similarly to K562 cells, sLDL treated (equivalent to 5μg cholesterol/mL) CML

$CD34^{+}38^{low/-}$ cells had approximately one-log increase in FITC MFI compared to the untreated cells, demonstrating the uptake of sLDL particles by these cells (Figure 7-2). Cells treated with peptide free sLDL also had a slightly increased FITC MFI, but not as high as the competent sLDL treated cells, indicating a low level of passive sLDL uptake.

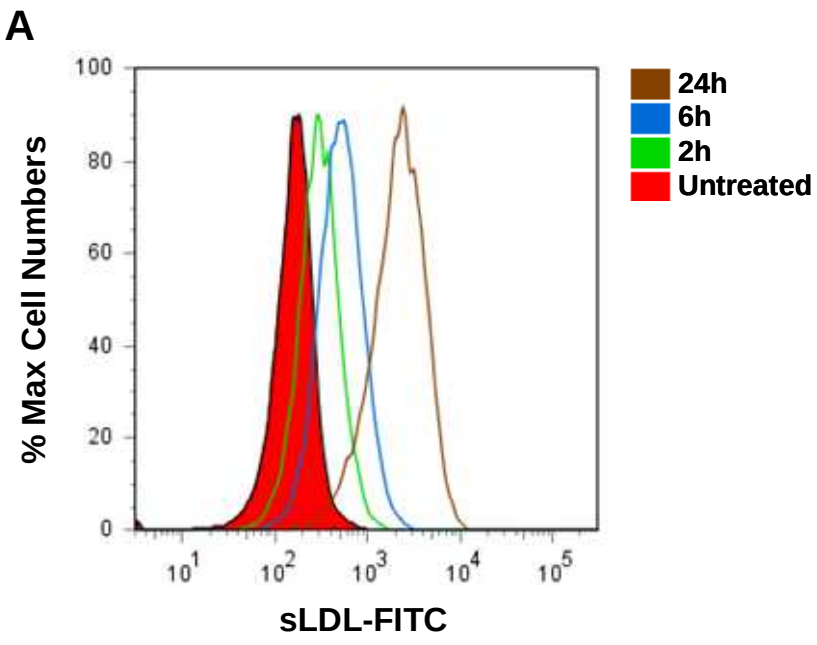

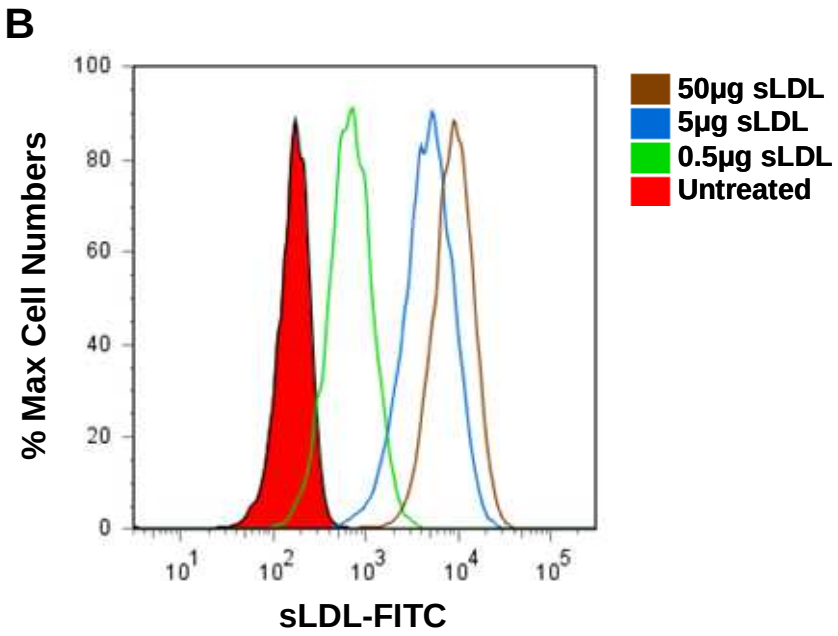

Figure 7-1: Uptake of sLDL particles by K562 cells.

(A) K562 cells were treated with sLDL (5µg cholesterol/mL), and analyzed by flow cytometry at 2, 4 and 24 hours of treatment. (B) K562 cells were treated with 0.5, 5 and 50µg cholesterol/mL, and measured by flow cytometry at 24 hours of treatment.

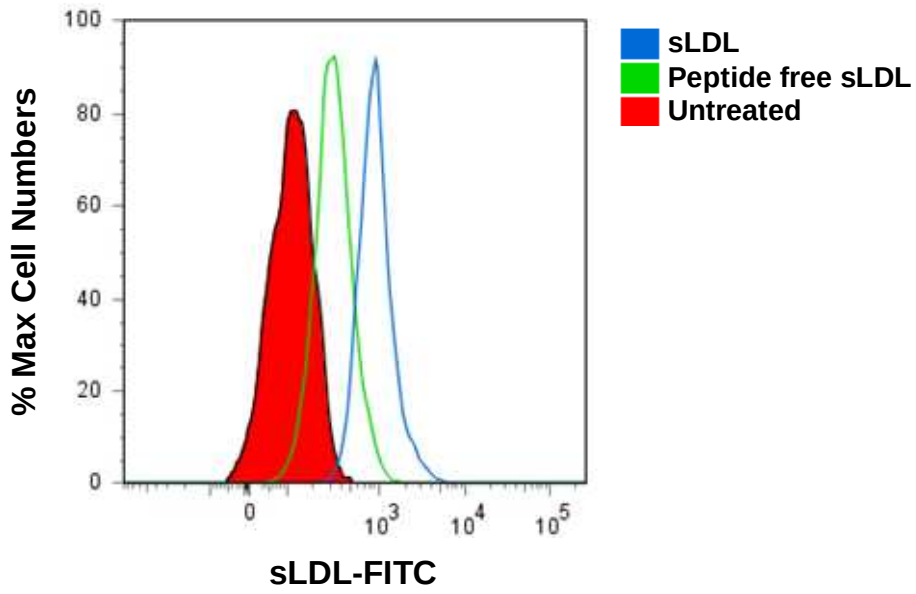

Figure 7-2: Uptake of sLDL particles by CML CD34^{+}38$^{low/-}$ cells.

CD34^{+}38$^{low/-}$ cells were incubated with sLDL or peptide free sLDL (equivalent to 5µg cholesterol/mL) for 24 hours, and then analyzed by flow cytometry.

7.3 Internalization of sLDL by CML cells

It was demonstrated by flow cytometry that sLDL particles were taken up by CML cells. However, a fluorescent signal by flow cytometry does not necessarily mean sLDL particles had been internalized by these cells, since cell surface associated fluorescent dye would be detected by flow cytometry as well. Therefore, deconvolution microscopy was employed to confirm the internalisation of the sLDL particles in CML cells. K562 and CML CD34^{+}38$^{low/-}$ cells were treated with sLDL particles (equivalent to 5µg cholesterol/mL) for 24 hours, and Z-Stack images were taken with multiple slices and then deconvolved to remove non-specific fluorescence.

As shown in Figure 7-3, intracellular sLDL particles were visualized in the cytoplasm of K562 and CML $CD34^{+}38^{low/-}$ cells. The internalised sLDL particles appeared to be associated with cellular organelles such as the endosomes (indicated by white arrows in Figure 7-3). When the cells were treated with apoprotein B peptide-free sLDL particles, very weak green fluorescence was observed in the cytoplasm by fluorescence microscopy, again indicating a low level of passive sLDL uptake. Green fluorescence was not detected in the untreated cells. This result confirmed that the majority of fluorescence signals detected by flow cytometry were intracellular. Furthermore, the internalisation of the sLDL particles was confirmed by transmission electron microscopy (Figure 7-4; pictures were taken by Ms Abraham in the Glasgow Caledonian University).

A

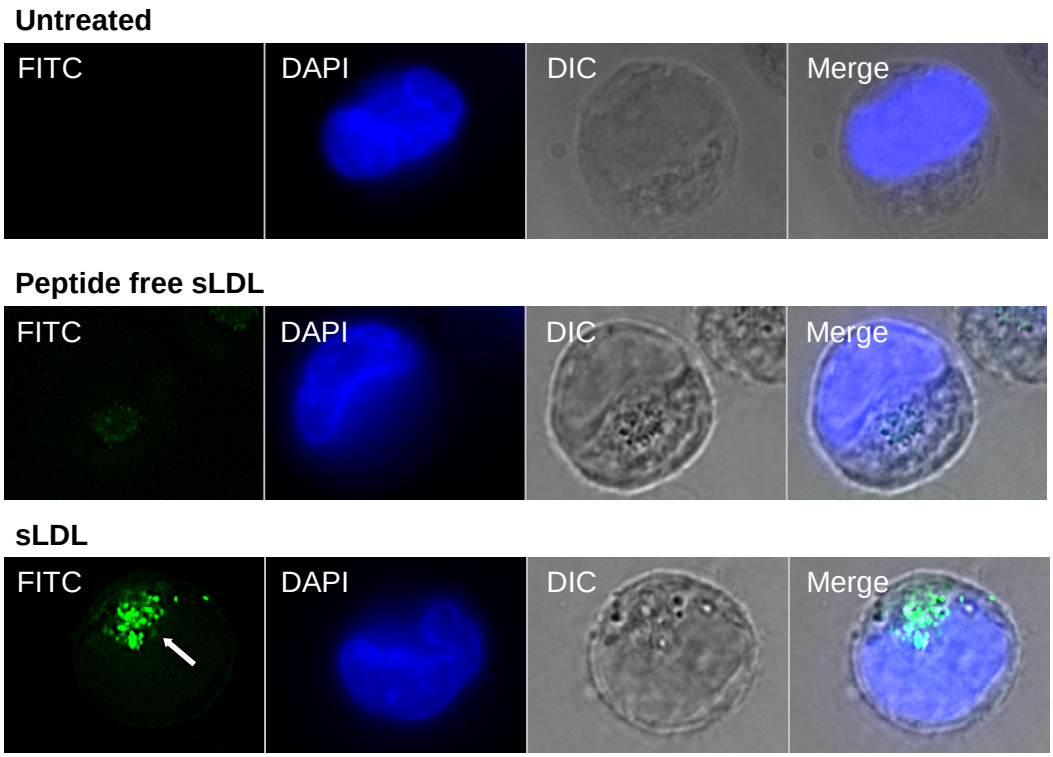

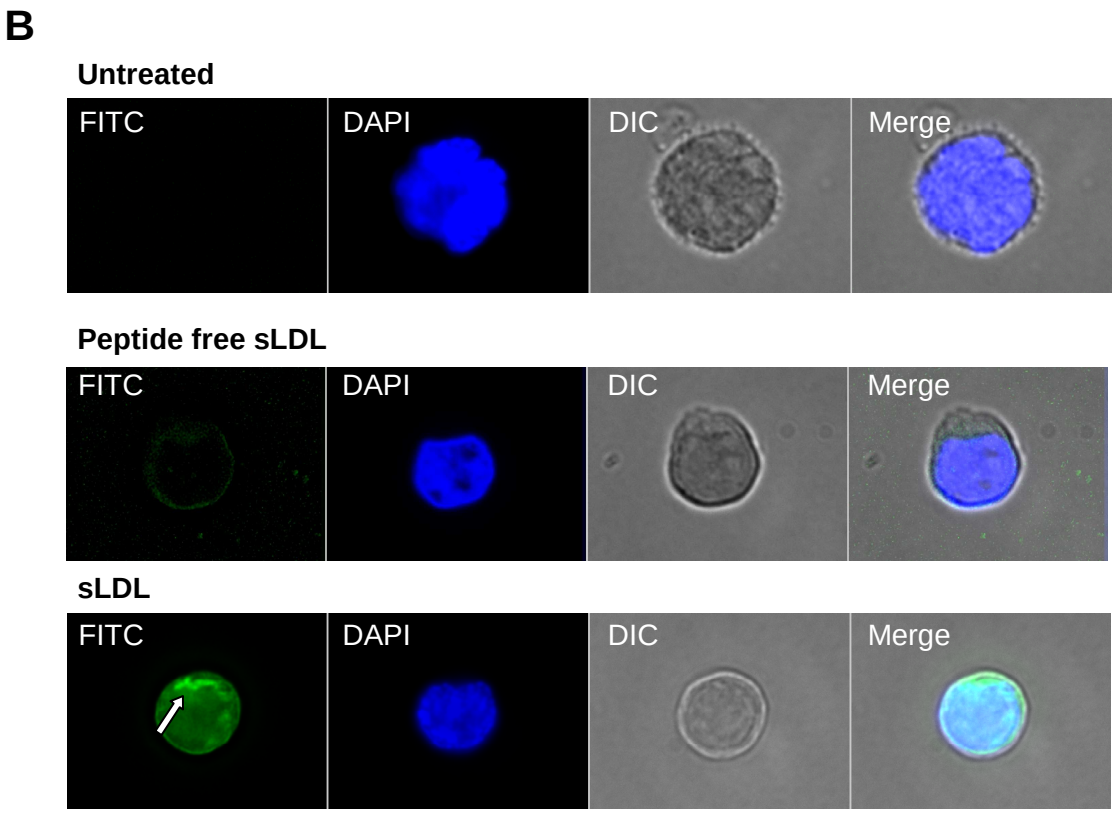

Figure 7-3: Fluorescence microscopy of sLDL.

K562 (A) and CML $CD34^{+}38^{low/-}$ (B) cells were treated with sLDL to confirm the internalization of sLDL particles. Z-stacks were captured then subjected to deconvolution to remove non-specific fluorescence. FITC channel shows sLDL particles (Green), DAPI channel shows cell nucleus (Blue), differential interference contrast (DIC) channel is to show the phase contrast images of cells.

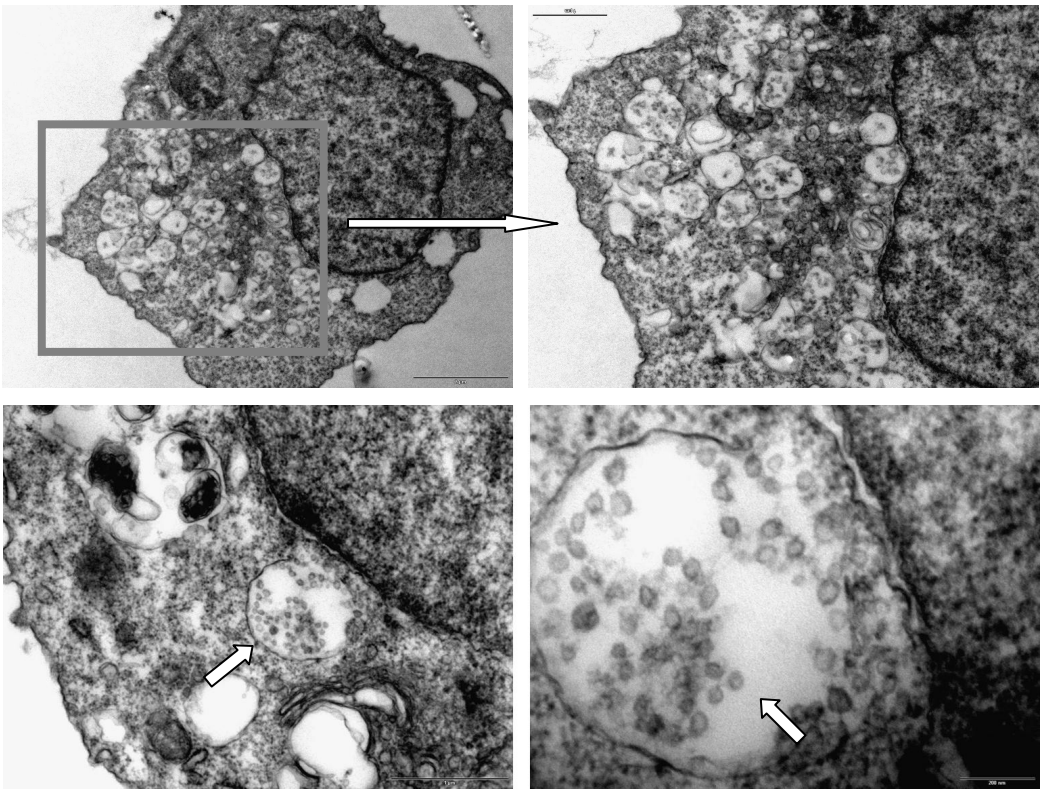

Figure 7-4: Electron microscopy of CML CD34$^+$ cells after treatment with sLDL.

CML CD34$^+$ progenitors were treated with sLDL particles for 24 hours, and then fixed for transmission electron microscopy to confirm the internalisation of sLDL particles. White arrows indicate engulfed sLDL particles within intracellular vesicles/endosomes. Cells were fixed with 2.5% glutaraldehyde and sent to Glasgow Caledonian University for electron microscopy.

7.4 Summary and Discussion

In this study, the cell targeting potential of sLDL particles was assessed. These results demonstrate uptake and internalization of sLDL particles by CML cell line K562 and for the first time by CML stem cells.

Tumour cells were considered to require more cholesterol for increased cell proliferation compared to their normal counterparts. It was reported that cancer patients had significantly decreased serum cholesterol levels than matched normal controls, except breast cancer in women. (273-275). Reports demonstrated elevated uptake of LDL in cancer cells than normal cells (237;239;276). We recently showed that tumour prostate cells uptake significantly more sLDL particles than normal cells *in vitro* (277). These observations support the notion that tumour cells require more cholesterol than normal cells. In addition, we also demonstrated that Ph^+ myeloid cell lines and $CD34^+$ cells uptake significantly more sLDL particles compared to Ph^- myeloid cell lines and $CD34^+$ cells respectively (277). Thus, sLDL particles can be preferentially uptaken by tumour cells and Ph^+ cells, achieving some level of targeted drug delivery when sLDL particles are loaded with specific drug(s).

It might be argued that CML quiescent stem cells do not uptake sLDL particles due to their quiescence, but our observations demonstrated that these cells do uptake sLDL particles. Primary CML $CD34^+38^{low/-}$ cells were shown to take up and internalize sLDL particles in Figure 7-2 and Figure 7-3B. In addition, we demonstrated the primary CML $CD34^+38^{low/-}$ cells took up sLDL particles at about the same level as bulk CML

$CD34^+$ cells, which was significantly higher than non-CML $CD34^+$ cells (277). Furthermore, we also showed CML quiescent stem cells, which were identified by maintenance of maximal CESE fluorescence, also were able to uptake sLDL particles (277). These results showed that sLDL particles could be used as a drug delivery vehicle targeting CML $CD34^+38^{low/-}$ cells.

However, studies revealed that the second generation TKI, dasatinib, was able to inhibit Bcr-Abl tyrosine kinase activities in CML cells, but did not eliminate CML stem cells (157;163). This indicates that there are other mechanisms keeping primitive CML stem cells alive against dasatinib treatment, such as autophagy (186). It was shown that combination of TKI with the autophagy inhibitor chloroquine significantly reduced the number of colonies formed by CML stem cells (186). Therefore, sLDL particles would be used to delivery other drugs together with TKI in order to completely eliminate CML stem cells.

Another potential advantage of using sLDL particle as a drug delivery vehicle is reduction of side effects *in vivo*. TKI cause many side effects in patients and these side effects can lead to intolerance and patient drop-out from TKI treatment (149). In addition, IM was reported to be cardiotoxic and caused heart failure, and this cardiotoxicity was induced by c-Abl inhibition in cardiocytes (278). Nilotinib and dasatinib also exhibited some degree of cardiotoxicity (279). By employment of sLDL as a targeted drug delivery vehicle, these side effects might be reduced. It was reported that LDL-DOX (Doxorubicin) complex exhibited no toxicity to the heart in

nude mice bearing HepG2 cells, whereas DOX only treatment caused cardiotoxicity in the mice while LDL-DOX and DOX had similar anti-proliferative effects on tumour cells (280).

The following step of this study is to incorporate TKI and /or other drugs into the sLDL particles and examine if there is any improvement in inducing apoptosis in leukaemic quiescent stem cells. Hydrophobic drugs can be incorporated into the hydrophobic core of LDL, while hydrophilic drugs can be chemically modified into hydrophobic pro-drugs and then incorporated (244). LDL has been shown to be successfully coupled with several drugs (280-282), indicating the feasibility of coupling sLDL with TKI and/or other drugs. Furthermore, using sLDL as a targeted drug delivery vehicle could potentially benefit treatment of other cancers of stem cell origin besides CML.

8 Final discussion and future perspectives

Overall, these studies provide further insight into how CML cells may be fully eradicated. Although TKIs revolutionized the treatment of CML in the last decade and successfully eliminate differentiated CML cells, primitive quiescent CML stem cells still survive even with maximal inhibition of Bcr-Abl tyrosine kinase activity. In this thesis, we studied alternative strategies to eliminate these TKI-insensitive CML stem cells by addressing the aims specific in the Introduction (Chapter 1.7). Firstly, the efficacy of nuclear entrapment of Bcr-Abl to induce apoptosis in CML cells was investigated, and it was found that neither continuous nor sequential IM and LMB treatment significantly increased the cytotoxic or cytostatic effect of IM in Bcr-Abl$^+$ cell lines and primary CML CD34$^+$ cells. Then the subcellular localisation of Bcr-Abl protein was visualized in TKI-insensitive CML progenitors which survived long-term dasatinib treatment, and it was observed that there was a significant increase in nuclear Bcr-Abl level in these survived cells compared to the NDC and about 50% of Bcr-Abl protein was still retained in the cytoplasm of these survived cells. It was also found that a proportion of Bcr-Abl protein was associated with 14-3-3 proteins in the cytoplasm of these surviving cells, indicating the cytoplasmic retention of Bcr-Abl might be due to its binding with 14-3-3 proteins. In addition, the accuracy of p-CrkL as a surrogate marker of Bcr-Abl tyrosine kinase activity was studied at short time points, and found that p-CrkL was not a reliable indicator of Bcr-Abl kinase activity within 24 hours of IM treatment *in vitro*. It was also observed that there was a rapid and active dephosphorylation of Bcr-Abl within 1 hour of TKI treatment, driven at least in part by

protein tyrosine phosphatase activity. Furthermore, the mechanism of action of the BMS-214662 in inducing apoptosis of CML cells was investigated, and it was demonstrated that the non-FTI mechanism of BMS-214662 was not proteasome inhibition but involved generation of a significant amount of intracellular ROS. Finally, the efficacy of sLDL as a drug delivery vehicle to target primitive CML stem cells was assessed, and it was observed that unloaded sLDL particles were preferentially taken up and internalized by CML cell line K562 and for the first time by CML stem cells, demonstrating the targeting potential of sLDL particles in CML when they are loaded with drugs. Additionally, novel strategies besides TKI treatment have been developed in recent years to target primitive CML stem cells. Examples of these strategies are shown in Table 8-1.

Strategy	**Drugs**	**Reference**
Activation of PP2A	FTY720	(283)
Activation of quiescent CML stem cells	G-CSF or IFN-α	(284;285)
Allosteric inhibitor of Bcr-Abl	GNF-2	(286)
Degradation of PML	AraC and As2O3	(287)
Inhibition of Alox5 pathway	Zileuton	(288)
Inhibition of anti-apoptotic Bcl2 family member – Mcl1	Omacetaxine	(289;290)
Inhibition of autophagy	Hydroxychloroquine	(186)
Inhibition of JAK2 kinase	TG101209	(222)
Inhibition of self-renewal	Cyclopamine	(291)
Targeting of IL-1 receptor accessory protein (IL1RAP)	Anti-IL1RAP antibody	(292)

Table 8-1: Novel therapies of CML.

Neviani *et al* demonstrated that FTY-720 significantly reduced the number of human quiescent CML stem cells *in vitro* and murine Bcr-Abl^{+} LT-HSCs *in vivo* compared to their normal counterparts (283). FTY-720 is an inhibitor of SET, and inhibition of SET restores serine/threonine phosphatase PP2A in CML cells. Activated PP2A then activates tyrosine phosphatase SHP1 which is capable of dephosphorylating Bcr-Abl and JAK2 (217;218). Since both Bcr-Abl and JAK2 are substrates of another tyrosine phosphatase PTP1B (225;293) and it was shown in Chapter 5 that PTP1B could be involved in rapid dephosphorylation of Bcr-Abl after TKI treatment in K562 cells, activation of PTP1B in primitive CML stem cells may dephosphorylate both Bcr-Abl and JAK2 kinases and leads to apoptosis, which is worthy of further investigation.

In addition, Neviani *et al* also demonstrated that although the expression level of Bcr-Abl protein was much higher in quiescent CML CD34^{+} cells than proliferating CML CD34^{+} cell, the activity of Bcr-Abl (as measured by p-Abl level) is much lower in the former population than the latter, suggesting Bcr-Abl may serve a scaffolding role for other proteins that maintain survival of quiescent CML stem cells (283). Furthermore, Copland *et al* also demonstrated higher expression level of Bcr-Abl protein in primitive CML CD34^{+}CD38^{-} cells than total CML CD34^{+} cells (163). However, Copland *et al* observed higher p-CrkL and total phosphorylated tyrosine levels in the former population than the latter (163). This may be explained by the findings in Chapter 5, which is that p-CrkL level does not accurately correlate with Bcr-Abl activity in CML cells.

Hamilton *et al* observed that 10% of primary Bcr-Abl$^+$ CD34$^+$ cells survived long-term dasatinib treatment in the absence of any growth factor (249;254), while normal haemopoietic progenitors were not able to survive in the absence of IL-3 or GM-CSF (18). These observations indicate that it is the presence of Bcr-Abl protein that sustains survival of TKI-insensitive CML cells, but not its tyrosine kinase activity. This further demonstrates that Bcr-Abl may serve as a scaffold in TKI-insensitive CML cells. A possible example of the scaffolding role of Bcr-Abl was shown by Agarwal *et al* that Bcr-Abl aberrantly induced localisation of p27 in the cytoplasm in a kinase-independent manner (294). p27 normally resides in the nucleus and serves as an inhibitor of cyclin dependent kinase, while in the cytoplasm it promotes oncogenesis (294). Thus, cytoplasmic retention of p27 enables Bcr-Abl to promote cell cycle progression.

Neviani *et al* also showed that kinase-deficient Bcr-Abl enhanced JAK2 expression and kinase activity (283). On the other hand, knockdown of Bcr-Abl in primitive CML stem cells significantly reduced JAK2 activity (283). This demonstrates that Bcr-Abl elevates JAK2 activity in a kinase-independent manner. This might be due to mislocalisation of JAK2 which is caused by a non-kinase activity of Bcr-Abl protein. Activated JAK2 upregulates the level of SET and then inhibits PP2A activity, preventing the dephosphorylation of JAK2 (216-218). In addition, JAK2 plays a pivotal role in Bcr-Abl mediated cell signalling (222;223). For example, it activates STAT5 and upregulates anti-apoptotic protein Bcl-xL (114;117). Furthermore, Neviani *et al* observed that inhibition of JAK2 significantly reduced β-catenin expression and its

transcriptional activity (283), suggesting the role of JAK2 in Wnt/β-catenin pathway, which functions to promote self-renewal of CML stem cells (295). Overall, these observations may explain the inability of TKIs in eliminating primitive CML stem cells, as kinase-inhibited Bcr-Abl is still able to promote cell cycle progression, inhibit apoptosis, and induce self-renewal in these stem cells.

Since the presence of Bcr-Abl protein, but not its tyrosine kinase activity, is a relevant therapeutic target in primitive CML stem cells, one strategy is to induce nuclear translocation of Bcr-Abl in these cells in order to kill them. It can be speculated that the pro-survival scaffolding role of Bcr-Abl in the cytoplasm is impaired by inducing nuclear translocation of Bcr-Abl protein in primitive CML stem cells, and then nuclear Bcr-Abl plays a pro-apoptotic role in these cells. It was shown in Chapter 4 that Bcr-Abl associated with 14-3-3 proteins in primary CML progenitors, as well as in TKI-insensitive CML progenitors. It was also shown that about 50% Bcr-Abl protein still retained in the cytoplasm of CML progenitors after long-term TKI treatment. In addition, other investigators demonstrated 14-3-3/Bcr-Abl association as well. For example, 14-3-3 ζ binds with both Bcr and Abl parts of Bcr-Abl (231). Since a 14-3-3 dimer can interact with two molecules at the same time (230) and 14-3-3 ζ is highly dimerized (296), it is possible that a 14-3-3 ζ homodimer can interact with two sites of Bcr-Abl protein simultaneously, with one site at Bcr and another at Abl part of Bcr-Abl. Thus, it is thought that interaction with 14-3-3 is a mechanism of cytoplasmic retention of Bcr-Abl.

R18 is a specific competitive antagonist of 14-3-3 proteins without selectivity for isoforms, which is capable of disrupting 14-3-3/ligand interaction in a phosphorylation independent manner (259;297;298). However, presence of R18 was not able to accumulate Bcr-Abl into the nucleus (299). Dong *et al* also demonstrated that R18 was insufficient to disrupt 14-3-3/Bcr-Abl association in Bcr-Abl expressing BaF/3 cells, while R18 induced apoptosis in Bcr-Abl expressing BaF/3 and K562 cells by disrupting 14-3-3 association with forkhead box O3a (FOXO3a) protein (259). Recently a small molecule competitive antagonist of 14-3-3 proteins, BV02, was identified to be able to disrupt 14-3-3/c-Abl association and induce nuclear translocation of c-Abl (147). BV02 induced apoptosis in Bcr-Abl$^+$ cell lines and CML progenitors (147). However, further study is required to investigate whether BV02 is able to dissociate 14-3-3/Bcr-Abl complex and induce nuclear translocation of Bcr-Abl.

Another strategy is to induce quiescent CML stem cells to cycle, which, once cycling, can then be targeted by TKIs. It was observed that intermittent G-CSF treatment activated quiescent CML cells and enhanced the kill of CML progenitors by IM *in vitro* (284). However, this strategy was not effective in a pilot clinical trial with IM treated CML patients who had achieved CCgR (300). In addition, mathematical modelling predicts that addition of G-CSF may not improve the therapeutic effect of IM in CML patients (301). Furthermore, IFN-α is capable of promoting murine quiescent HSCs into cell cycle and sensitized them to the anti-proliferative drug, 5-FU *in vivo* (302). Some CML patients who switched from IFN-α to IM treatment achieved higher rate of

stable CMR compared to those who were not previously treated with IFN-α (303). This suggests that priming quiescent CML stem cells with IFN-α may activate these cells and sensitize them to IM treatment (285). However, the effectiveness of this strategy with human quiescent CML stem cells requires further investigation.

Overall, despite the success of TKIs in killing the majority of CML cells, primitive quiescent CML stem cells are still insensitive to TKI treatment, causing disease relapse and minimal residual disease. In recent years, studies have been carried out to investigate why primitive CML stem cells resist or persist to TKIs, and possible approaches have been searched to eliminate them. Since most CML cells are dependent on Bcr-Abl tyrosine kinase to survive, TKIs are able to get rid of leukaemic burden. Together with drug(s) targeting primitive CML stem cells, the possibility of eliminating all CML cells is greatly increased. Therefore, combination of TKIs with these approaches, which specifically target leukaemic stem cells, is likely to eradicate CP CML ultimately.

9 Appendix

Characteristics of CML samples used:

Patient number	CML stage	WCC at leucapheresis (x 10^6/mL)	Pre-selection % $CD34^+$	Post selection % $CD34^+$	Method of CD34 selection	% Ph^+ in $CD34^+$ (FISH)
223	Chronic	344	1.01	96.06	CliniMacs	96
235	Chronic	500	3.2	90	CliniMacs	99.2
236	Chronic	323	1.44	98.22	CliniMacs	98
250	Chronic	374	2.8	97.28	CliniMacs	100
255	Chronic	326	22.2	98.4	CliniMacs	100
273	Chronic	400	6.4	96	CliniMacs	98
274	Chronic	200	0.2	100	CliniMacs	98.6
280	Chronic	230	6.3	99.7	CliniMacs	87.5
281	Chronic	357.9	26.2	100	CliniMacs	94
284	Chronic	250	11.2	99.6	CliniMacs	100

Characteristics of non-CML samples used:

Sample number	Disease	WCC at leucapheresis (x 10^6/mL)	Pre-selection % $CD34^+$	Post selection % $CD34^+$	Method of CD34 selection	% Ph^+ in $CD34^+$ (FISH)
006	T-Cell Lymphoma	150	7.31	99.19	CliniMacs	0
007	Follicular NHL	189	2.73	99.04	CliniMacs	0
011	Myeloma	194	3.52	99.7	CliniMacs	0

WCC, white cell count

NHL, non-Hodgkin's Lymphoma

FISH, fluorescence in situ hybridization

10 Bibliography

(1) Morrison SJ, Uchida N, Weissman IL. The biology of hematopoietic stem cells. Annual Review of Cell and Developmental Biology 1995;11:35-71.

(2) Smith DL, Burthem J, Whetton AD. Molecular pathogenesis of chronic myeloid leukaemia. Expert Reviews in Molecular Medicine 2003 Nov 25;5.

(3) Bryder D, Rossi DJ, Weissman IL. Hematopoietic stem cells - The paradigmatic tissue-specific stem cell. American Journal of Pathology 2006 Aug;169(2):338-46.

(4) Marley SB, Gordon MY. Chronic myeloid leukaemia: stem cell derived but progenitor cell driven. Clin Sci (Lond) 2005 Jul;109(1):13-25.

(5) Schofield R. Relationship Between Spleen Colony-Forming Cell and Hematopoietic Stem-Cell - Hypothesis. Blood Cells 1978;4(1-2):7-25.

(6) Wang JCY, Doedens M, Dick JE. Primitive human hematopoietic cells are enriched in cord blood compared with adult bone marrow or mobilized peripheral blood as measured by the quantitative in vivo SCID-repopulating cell assay. Blood 1997 Jun 1;89(11):3919-24.

(7) Sutherland HJ, Eaves CJ, Eaves AC, Dragowska W, Lansdorp PM. Characterization and Partial-Purification of Human Marrow-Cells Capable of Initiating Long-Term Hematopoiesis In vitro. Blood 1989 Oct;74(5):1563-70.

(8) Sutherland HJ, Lansdorp PM, Henkelman DH, Eaves AC, Eaves CJ. Functional-Characterization of Individual Human Hematopoietic Stem-Cells Cultured at Limiting Dilution on Supportive Marrow Stromal Layers. Proceedings of the National Academy of Sciences of the United States of America 1990 May;87(9):3584-8.

(9) Larochelle A, Vormoor J, Hanenberg H, Wang JCY, Bhatia M, Lapidot T, et al. Identification of primitive human hematopoietic cells capable of repopulating NOD/SCID mouse bone marrow: Implications for gene therapy. Nature Medicine 1996 Dec;2(12):1329-37.

(10) Morrison SJ, Weissman IL. The Long-Term Repopulating Subset of Hematopoietic Stem-Cells Is Deterministic and Isolatable by Phenotype. Immunity 1994 Nov;1(8):661-73.

(11) Morrison SJ, Wandycz AM, Hemmati HD, Wright DE, Weissman IL. Identification of a lineage of multipotent hematopoietic progenitors. Development 1997 May;124(10):1929-39.

(12) Kondo M, Weissman IL, Akashi K. Identification of clonogenic common lymphoid progenitors in mouse bone marrow. Cell 1997 Nov 28;91(5):661-72.

(13) Akashi K, Traver D, Miyamoto T, Weissman IL. A clonogenic common myeloid progenitor that gives rise to all myeloid lineages. Nature 2000 Mar 9;404(6774):193-7.

(14) Passegue E, Jamieson CH, Ailles LE, Weissman IL. Normal and leukemic hematopoiesis: are leukemias a stem cell disorder or a reacquisition of stem cell characteristics? Proc Natl Acad Sci U S A 2003 Sep 30;100 Suppl 1:11842-9.

(15) Suda T, Suda J, Ogawa M. Proliferative Kinetics and Differentiation of Murine Blast Cell Colonies in Culture - Evidence for Variable G0-Periods and Constant Doubling Rates of Early Pluripotent Hematopoietic Progenitors. Journal of Cellular Physiology 1983;117(3):308-18.

(16) Leary AG, Hirai Y, Kishimoto T, Clark SC, Ogawa M. Survival of Hematopoietic Progenitors in the G0 Period of the Cell-Cycle Does Not Require Early Hematopoietic Regulators. Proceedings of the National Academy of Sciences of the United States of America 1989 Jun;86(12):4535-8.

(17) Vickers M, Brown GC, Cologne JB, Kyoizumi S. Modelling haemopoietic stem cell division by analysis of mutant red cells. British Journal of Haematology 2000 Jul;110(1):54-62.

(18) Leary AG, Zeng HQ, Clark SC, Ogawa M. Growth factor requirements for survival in G0 and entry into the cell cycle of primitive human hemopoietic progenitors. Proc Natl Acad Sci U S A 1992 May 1;89(9):4013-7.

(19) Lajtha LG. Stem-Cell Concepts. Differentiation 1979;14(1-2):23-34.

(20) Huang S, Terstappen LW. Formation of Hematopoietic Microenvironment and Hematopoietic Stem-Cells from Single Human Bone-Marrow Stem-Cells. Nature 1992 Dec 24;360(6406):745-9.

(21) Link H, Arseniev L, Bahre O, Kadar JG, Diedrich H, Poliwoda H. Transplantation of allogeneic CD34(+) blood cells. Blood 1996 Jun 1;87(11):4903-9.

(22) Krause DS, Fackler MJ, Civin CI, May WS. CD34: Structure, biology, and clinical utility. Blood 1996 Jan 1;87(1):1-13.

(23) Caux C, Favre C, Saeland S, Duvert V, Mannoni P, Durand I, et al. Sequential Loss of CD34 and Class-II MHC Antigens on Purified Cord Blood Hematopoietic Progenitors Cultured with IL-3 - Characterization of CD34-, HLA-DR+ Cells. Blood 1989 Sep;74(4):1287-94.

(24) Andrews RG, Singer JW, Bernstein ID. Monoclonal-Antibody 12-8 Recognizes A 115-Kd Molecule Present on Both Unipotent and Multipotent Hematopoietic Colony-Forming Cells and Their Precursors. Blood 1986 Mar;67(3):842-5.

(25) Gothot A, Pyatt R, McMahel J, Rice S, Srour EF. Functional heterogeneity of human CD34(+) cells isolated in subcompartments of the G(0)/G(1) phase of the cell cycle. Blood 1997 Dec 1;90(11):4384-93.

(26) Bhatia M, Wang JCY, Kapp U, Bonnet D, Dick JE. Purification of primitive human hematopoietic cells capable of repopulating immune-deficient mice. Proceedings of the National Academy of Sciences of the United States of America 1997 May 13;94(10):5320-5.

(27) Hogan CJ, Shpall EJ, Keller G. Differential long-term and multilineage engraftment potential from subfractions of human CD34(+) cord blood cells transplanted into NOD/SCID mice. Proceedings of the National Academy of Sciences of the United States of America 2002 Jan 8;99(1):413-8.

(28) Hao QL, Shah AJ, Thiemann FT, Smogorzewska EM, Crooks GM. A Functional Comparison of Cd34(+)Cd38(-) Cells in Cord-Blood and Bone-Marrow. Blood 1995 Nov 15;86(10):3745-53.

(29) Shah AJ, Smogorzewska EM, Hannum C, Crooks GM. Flt3 ligand induces proliferation of quiescent human bone marrow CD34(+)CD38(-) cells and maintains progenitor cells in vitro. Blood 1996 May 1;87(9):3563-70.

(30) Yahata T, Muguruma Y, Yumino S, Sheng Y, Uno T, Matsuzawa H, et al. Quiescent Human Hematopoietic Stem Cells in the Bone Marrow Niches Organize the Hierarchical Structure of Hematopoiesis. Stem Cells 2008;26(12):3228-36.

(31) Yin AH, Miraglia S, Zanjani ED, AlmeidaPorada G, Ogawa M, Leary AG, et al. AC133, a novel marker for human hematopoietic stem and progenitor cells. Blood 1997 Dec 15;90(12):5002-12.

(32) Handgretinger R, Gordon PR, Leimig T, Chen X, Buhring HJ, Niethammer D, et al. Biology and plasticity of CD133+ hematopoietic stem cells. Ann N Y Acad Sci 2003 May;996:141-51.

(33) Freund D, Oswald J, Feldmann S, Ehninger G, Corbeil D, Bornhauser M. Comparative analysis of proliferative potential and clonogenicity of MACS-immunomagnetic isolated CD34+ and CD133+ blood stem cells derived from a single donor. Cell Prolif 2006 Aug;39(4):325-32.

(34) Gordon PR, Leimig T, Babarin-Dorner A, Houston J, Holladay M, Mueller I, et al. Large-scale isolation of CD133+ progenitor cells from G-CSF mobilized peripheral blood stem cells. Bone Marrow Transplant 2003 Jan;31(1):17-22.

(35) Reya T, Morrison SJ, Clarke MF, Weissman IL. Stem cells, cancer, and cancer stem cells. Nature 2001 Nov 1;414(6859):105-11.

(36) Park CH, Bergsagel DE, McCulloch EA. Mouse myeloma tumor stem cells: a primary cell culture assay. J Natl Cancer Inst 1971 Feb;46(2):411-22.

(37) BRUCE WR, VAN DER GAAG. A quantitative assay for the number of murine lymphoma cells capable of proliferation in vivo. Nature 1963 Jul 6;199:79-80.

(38) Bonnet D, Dick JE. Human acute myeloid leukemia is organized as a hierarchy that originates from a primitive hematopoietic cell. Nat Med 1997 Jul;3(7):730-7.

(39) Fialkow PJ, Jacobson RJ, Papayannopoulou T. Chronic Myelocytic-Leukemia - Clonal Origin in A Stem-Cell Common to Granulocyte, Erythrocyte, Platelet and Monocyte-Macrophage. American Journal of Medicine 1977;63(1):125-30.

(40) Fialkow PJ, Gartler SM, Yoshida A. Clonal origin of chronic myelocytic leukemia in man. Proc Natl Acad Sci U S A 1967 Oct;58(4):1468-71.

(41) Faderl S., Talpaz M., Estrov Z., O'Brien S., Kurzrock R., Kantarjian HM. The biology of chronic myeloid leukemia. New England Journal of Medicine 1999;341(3):164-72.

(42) Rowley JD. A new consistent chromosomal abnormality in chronic myelogenous leukaemia identified by quinacrine fluorescence and Giemsa staining. Nature 1973;243:290-3.

(43) Kurzrock R, Gutterman JU, Talpaz M. The molecular genetics of Philadelphia chromosome-positive leukemias. N Engl J Med 1988 Oct 13;319(15):990-8.

(44) Jørgensen HG, Holyoake TL. A comparison of normal and leukemic stem cell biology in Chronic Myeloid Leukemia. Hematological Oncology 2001 Sep;19(3):89-106.

(45) Faderl S, Talpaz M, Estrov Z, Kantarjian HM. Chronic myelogenous leukemia: Biology and therapy. Annals of Internal Medicine 1999 Aug 3;131(3):207-19.

(46) Savage DG, Szydlo RM, Goldman JM. Clinical features at diagnosis in 430 patients with chronic myeloid leukaemia seen at a referral centre over a 16-year period. Br J Haematol 1997 Jan;96(1):111-6.

(47) Wong S, Witte ON. Modeling Philadelphia chromosome positive leukemias. Oncogene 2001 Sep 10;20(40):5644-59.

(48) Sessions J. Monitoring your patients with chronic myeloid leukemia. Am J Health Syst Pharm 2006 Dec 1;63(23 Suppl 8):S5-S9.

(49) Deininger MWN, Druker BJ. Specific targeted therapy of chronic myelogenous leukemia with imatinib. Pharmacological Reviews 2003 Sep;55(3):401-23.

(50) Kantarjian HM, Dixon D, Keating MJ, Talpaz M, Walters RS, McCredie KB, et al. Characteristics of accelerated disease in chronic myelogenous leukemia. Cancer 1988 Apr 1;61(7):1441-6.

(51) Mitelman F. The cytogenetic scenario of chronic myeloid leukemia. Leuk Lymphoma 1993;11 Suppl 1:11-5.

(52) Vardiman JW, Harris NL, Brunning RD. The World Health Organization (WHO) classification of the myeloid neoplasms. Blood 2002 Oct 1;100(7):2292-302.

(53) Nowell PC, Hungerford DA. A minute chromosome in human chronic granulocytic leukemia. Science 1960 Nov 18;132:1497.

(54) Rowley JD. Letter: A new consistent chromosomal abnormality in chronic myelogenous leukaemia identified by quinacrine fluorescence and Giemsa staining. Nature 1973 Jun 1;243(5405):290-3.

(55) Groffen J, Stephenson JR, Heisterkamp N, Bartram C, de KA, Grosveld G. The human c-abl oncogene in the Philadelphia translocation. J Cell Physiol Suppl 1984;3:179-91.

(56) Elefanty AG, Hariharan IK, Cory S. Bcr-Abl, the hallmark of chronic myeloid leukaemia in man, induces multiple haemopoietic neoplasms in mice. EMBO J 1990;**9**(4):1069-78.

(57) Kelliher MA, McLaughlin J, Witte ON, Rosenberg N. Induction of A Chronic Myelogenous Leukemia-Like Syndrome in Mice with V-Abl and Bcr/Abl. Proceedings of the National Academy of Sciences of the United States of America 1990 Sep;87(17):6649-53.

(58) Pear WS, Miller JP, Xu L, Pui JC, Soffer B, Quackenbush RC, et al. Efficient and rapid induction of a chronic myelogenous leukemia-like myeloproliferative disease in mice receiving P210 bcr/abl-transduced bone marrow. Blood 1998 Nov 15;92(10):3780-92.

(59) Laneuville P, Sun G, Timm M, Vekemans M. Clonal evolution in a myeloid cell line transformed to interleukin-3 independent growth by retroviral transduction and expression of p210bcr/abl. Blood 1992 Oct 1;80(7):1788-97.

(60) Salloukh HF, Laneuville P. Increase in mutant frequencies in mice expressing the BCR-ABL activated tyrosine kinase. Leukemia 2000 Aug;14(8):1401-4.

(61) Reuther GW, Fu H, Cripe LD, Collier RJ, Pendergast AM. Association of the Protein-Kinases c-Bcr and Bcr-Abl with Proteins of the 14-3-3-Family. Science 1994 Oct 7;266(5182):129-33.

(62) Mcwhirter JR, Galasso DL, Wang JYJ. A Coiled-Coil Oligomerization Domain of Bcr Is Essential for the Transforming Function of Bcr-Abl Oncoproteins. Molecular and Cellular Biology 1993 Dec;13(12):7587-95.

(63) Pendergast AM, Muller AJ, Havlik MH, Maru Y, Witte ON. Bcr Sequences Essential for Transformation by the Bcr-Abl Oncogene Bind to the Abl-SH2 Regulatory Domain in A Non-Phosphotyrosine-Dependent Manner. Cell 1991 Jul 12;66(1):161-71.

(64) Maru Y, Witte ON. The Bcr Gene Encodes A Novel Serine Threonine Kinase-Activity Within A Single Exon. Cell 1991 Nov 1;67(3):459-68.

(65) Diekmann D, Brill S, Garrett MD, Totty N, Hsuan J, Monfries C, et al. Bcr Encodes A GTPase-Activating Protein for P21Rac. Nature 1991 May 30;351(6325):400-2.

(66) Ron D, Zannini M, Lewis M, Wickner RB, Hunt LT, Graziani G, et al. A Region of Proto-Dbl Essential for Its Transforming Activity Shows Sequence Similarity to A Yeast-Cell Cycle Gene, Cdc24, and the Human Breakpoint Cluster Gene, Bcr. New Biologist 1991 Apr;3(4):372-9.

(67) Shtivelman E, Lifshitz B, Gale RP, Roe BA, Canaani E. Alternative splicing of RNAs transcribed from the human abl gene and from the bcr-abl fused gene. Cell 1986 Oct 24;47(2):277-84.

(68) Raitano AB, Whang YE, Sawyers CL. Signal transduction by wild-type and leukemogenic Abl proteins. Biochimica et Biophysica Acta-Reviews on Cancer 1997 Dec 9;1333(3):F201-F216.

(69) Feller SM, Ren R, Hanafusa H, Baltimore D. SH2 and SH3 domains as molecular adhesives: the interactions of Crk and Abl. Trends Biochem Sci 1994 Nov;19(11):453-8.

(70) Franz WM, Berger P, Wang JY. Deletion of an N-terminal regulatory domain of the c-abl tyrosine kinase activates its oncogenic potential. EMBO J 1989 Jan;8(1):137-47.

(71) Mayer BJ, Jackson PK, Van Etten RA, Baltimore D. Point mutations in the abl SH2 domain coordinately impair phosphotyrosine binding in vitro and transforming activity in vivo. Mol Cell Biol 1992 Feb;12(2):609-18.

(72) Taagepera S, McDonald D, Loeb JE, Whitaker LL, McElroy AK, Wang JYJ, et al. Nuclear-cytoplasmic shuttling of C-ABL tyrosine kinase. Proceedings of the National Academy of Sciences of the United States of America 1998 Jun 23;95(13):7457-62.

(73) Mcwhirter JR, Wang JYJ. An Actin-Binding Function Contributes to Transformation by the Bcr-Abl Oncoprotein of Philadelphia Chromosome-Positive Human Leukemias. Embo Journal 1993 Apr;12(4):1533-46.

(74) Wetzler M, Talpaz M, Van Etten RA, Hirsh-Ginsberg C, Beran M, Kurzrock R. Subcellular localization of Bcr, Abl, and Bcr-Abl proteins in normal and leukemic cells and correlation of expression with myeloid differentiation. J Clin Invest 1993 Oct;92(4):1925-39.

(75) Van Etten RA, Jackson P, Baltimore D. The mouse type IV c-abl gene product is a nuclear protein, and activation of transforming ability is associated with cytoplasmic localization. Cell 1989 Aug 25;58(4):669-78.

(76) Pendergast AM, Muller AJ, Havlik MH, Clark R, Mccormick F, Witte ON. Evidence for regulation of the human ABL tyrosine kinase by a cellular inhibitor. Proc Natl Acad Sci U S A 1991 Jul 1;88(13):5927-31.

(77) Duyster J, Baskaran R, Wang JY. Src homology 2 domain as a specificity determinant in the c-Abl-mediated tyrosine phosphorylation of the RNA polymerase II carboxyl-terminal repeated domain. Proc Natl Acad Sci U S A 1995 Feb 28;92(5):1555-9.

(78) White E, Prives C. DNA damage enables p73. Nature 1999 Jun 24;399(6738):734-5, 737.

(79) Lewis JM, Baskaran R, Taagepera S, Schwartz MA, Wang JY. Integrin regulation of c-Abl tyrosine kinase activity and cytoplasmic-nuclear transport. Proc Natl Acad Sci U S A 1996 Dec 24;93(26):15174-9.

(80) Renshaw MW, Lewis JM, Schwartz MA. The c-Abl tyrosine kinase contributes to the transient activation of MAP kinase in cells plated on fibronectin. Oncogene 2000 Jun 29;19(28):3216-9.

(81) Ren R. Mechanisms of BCR-ABL in the pathogenesis of chronic myelogenous leukaemia. Nature Reviews Cancer 2005 Mar;5(3):172-83.

(82) Mcwhirter JR, Wang JYJ. Activation of Tyrosine Kinase and Microfilament-Binding Functions of C-Abl by Bcr Sequences in Bcr/Abl Fusion Proteins. Molecular and Cellular Biology 1991 Mar;11(3):1553-65.

(83) Beissert T, Hundertmark A, Kaburova V, Travaglini L, Mian AA, Nervi C, et al. Targeting of the N-terminal coiled coil oligomerization interface by a Helix-2 peptide inhibits unmutated and imatinib-resistant BCR/ABL. International Journal of Cancer 2008 Jun 15;122(12):2744-52.

(84) Liu J, Wu Y, Ma GZ, Lu D, Haataja L, Heisterkamp N, et al. Inhibition of Bcr serine kinase by tyrosine phosphorylation. Mol Cell Biol 1996 Mar;16(3):998-1005.

(85) Liu J, Wu Y, Arlinghaus RB. Sequences within the first exon of BCR inhibit the activated tyrosine kinases of c-Abl and the Bcr-Abl oncoprotein. Cancer Res 1996 Nov 15;56(22):5120-4.

(86) Steelman LS, Pohnert SC, Shelton JG, Franklin RA, Bertrand FE, McCubrey JA. JAK/STAT, Raf/MEK/ERK, PI3K/Akt and Bcr-Abl in Cell Cycle Progression and Leukemogenesis. Leukemia 2004 Feb;18(2):189-218.

(87) Pendergast AM, Quilliam LA, Cripe LD, Bassing CH, Dai ZH, Li NX, et al. Bcr-Abl-Induced Oncogenesis Is Mediated by Direct Interaction with the SH2 Domain of the Grb-2 Adapter Protein. Cell 1993 Oct 8;75(1):175-85.

(88) Skorski T, Bellacosa A, NieborowskaSkorska M, Majewski M, Martinez R, Choi JK, et al. Transformation of hematopoietic cells by BCR/ABL requires

activation of a PI-3k/Akt-dependent pathway. Embo Journal 1997 Oct 15;16(20):6151-61.

(89) Neshat MS, Raitano AB, Wang HG, Reed JC, Sawyers CL. The survival function of the Bcr-Abl oncogene is mediated by Bad-dependent and -independent pathways: Roles for phosphatidylinositol 3-kinase and Raf. Molecular and Cellular Biology 2000 Feb;20(4):1179-86.

(90) Amarante-Mendes GP, McGahon AJ, Nishioka WK, Afar DE, Witte ON, Green DR. Bcl-2-independent Bcr-Abl-mediated resistance to apoptosis: protection is correlated with up regulation of Bcl-xL. Oncogene 1998 Mar;16(11):1383-90.

(91) deJong R, Tenhoeve J, Heisterkamp N, Groffen J. Crkl Is Complexed with Tyrosine-Phosphorylated Cbl in Ph-Positive Leukemia. Journal of Biological Chemistry 1995 Sep 15;270(37):21468-71.

(92) Feller SM, Knudsen B, Hanafusa H. C-Abl Kinase Regulates the Protein-Binding Activity of C-Crk. Embo Journal 1994 May 15;13(10):2341-51.

(93) Oda T, Heaney C, Hagopian JR, Okuda K, Griffin JD, Druker BJ. Crkl Is the Major Tyrosine-Phosphorylated Protein in Neutrophils from Patients with Chronic Myelogenous Leukemia. Journal of Biological Chemistry 1994 Sep 16;269(37):22925-8.

(94) Gotoh A, Miyazawa K, Ohyashiki K, Tauchi T, Boswell HS, Broxmeyer HE, et al. Tyrosine Phosphorylation and Activation of Focal Adhesion Kinase (P125(Fak)) by Bcr-Abl Oncoprotein. Experimental Hematology 1995 Oct;23(11):1153-9.

(95) Skorski T, Kanakaraj P, NieborowskaSkorska M, Ratajczak MZ, Wen SC, Zon G, et al. Phosphatidylinositol-3 Kinase-Activity Is Regulated by Bcr/Abl and Is Required for the Growth of Philadelphia-Chromosome-Positive Cells. Blood 1995 Jul 15;86(2):726-36.

(96) Gotoh A, Miyazawa K, Ohyashiki K, Toyama K. Potential molecules implicated in downstream signaling pathways of p185BCR-ABL in Ph+ ALL involve GTPase-activating protein, phospholipase C-gamma 1, and phosphatidylinositol 3'-kinase. Leukemia 1994 Jan;8(1):115-20.

(97) Skorski T, NieborowskaSkorska M, Szczylik C, Kanakaraj P, Perrotti D, Zon G, et al. C-Raf-1 Serine Threonine Kinase Is Required in Bcr/Abl-Dependent and Normal Hematopoiesis. Cancer Research 1995 Jun 1;55(11):2275-8.

(98) Mandanas RA, Leibowitz DS, Gharehbaghi K, Tauchi T, Burgess GS, Miyazawa K, et al. Role of P21 Ras in P210 Bcr-Abl Transformation of Murine Myeloid Cells. Blood 1993 Sep 15;82(6):1838-47.

(99) Druker B, Okuda K, Matulonis U, Salgia R, Roberts T, Griffin JD. Tyrosine Phosphorylation of RasGAP and Associated Proteins in Chronic Myelogenous Leukemia-Cell Lines. Blood 1992 May 1;79(9):2215-20.

(100) Matsuguchi T, Salgia R, Hallek M, Eder M, Druker B, Ernst TJ, et al. Shc Phosphorylation in Myeloid Cells Is Regulated by Granulocyte-Macrophage Colony-Stimulating Factor, Interleukin-3, and Steel Factor and Is Constitutively Increased by P210(Bcr/Abl). Journal of Biological Chemistry 1994 Feb 18;269(7):5016-21.

(101) Puil L, Liu J, Gish G, Mbamalu G, Bowtell D, Pelicci PG, et al. Bcr-Abl oncoproteins bind directly to activators of the Ras signalling pathway. Embo Journal 1994 Feb;13(4):764-73.

(102) Carlesso N, Frank DA, Griffin JD. Tyrosyl phosphorylation and DNA binding activity of signal transducers and activators of transcription (STAT) proteins in hematopoietic cell lines transformed by Bcr/Abl. Journal of Experimental Medicine 1996 Mar 1;183(3):811-20.

(103) Hoover RR, Gerlach MJ, Koh EY, Daley GQ. Cooperative and redundant effects of STAT5 and Ras signaling in BCR/ABL transformed hematopoietic cells. Oncogene 2001 Sep 13;20(41):5826-35.

(104) Tauchi T, Feng GS, Shen R, Song HY, Donner D, Pawson T, et al. SH2-Containing Phosphotyrosine Phosphatase Syp Is A Target of P210Bcr-Abl Tyrosine Kinase. Journal of Biological Chemistry 1994 May 27;269(21):15381-7.

(105) Inamdar GS, Madhunapantula SV, Robertson GP. Targeting the MAPK pathway in melanoma: Why some approaches succeed and other fail. Biochemical Pharmacology 2010 Sep 1;80(5):624-37.

(106) Sawyers CL, McLaughlin J, Witte ON, Sawyers CL, McLaughlin J, Witte ON. Genetic requirement for Ras in the transformation of fibroblasts and hematopoietic cells by the Bcr-Abl oncogene. Journal of Experimental Medicine 1995 Jan 1;181(1):307-13.

(107) Kardinal C, Konkol B, Lin H, Eulitz M, Schmidt EK, Estrov Z, et al. Chronic myelogenous leukemia blast cell proliferation is inhibited by peptides that disrupt Grb2-SoS complexes. Blood 2001 Sep 15;98(6):1773-81.

(108) Aichberger KJ, Mayerhofer M, Krauth MT, Skvara H, Florian S, Sonneck K, et al. Identification of mcl-1 as a BCR/ABL-dependent target in chronic myeloid leukemia (CML): evidence for cooperative antileukemic effects of imatinib and mcl-1 antisense oligonucleotides. Blood 2005 Apr 15;105(8):3303-11.

(109) Bedi A, Barber JP, Bedi GC, el-Deiry WS, Sidransky D, Vala MS, et al. BCR-ABL-mediated inhibition of apoptosis with delay of G2/M transition after DNA damage: a mechanism of resistance to multiple anticancer agents. Blood 1995 Aug 1;86(3):1148-58.

(110) del PL, Gonzalez-Garcia M, Page C, Herrera R, Nunez G. Interleukin-3-induced phosphorylation of BAD through the protein kinase Akt. Science 1997 Oct 24;278(5338):687-9.

(111) Goetz AW, van der Kuip H, Maya R, Oren M, Aulitzky WE. Requirement for Mdm2 in the survival effects of Bcr-Abl and interleukin 3 in hematopoietic cells. Cancer Res 2001 Oct 15;61(20):7635-41.

(112) Chai SK, Nichols GL, Rothman P. Constitutive activation of JAKs and STATs in BCR-Abl-expressing cell lines and peripheral blood cells derived from leukemic patients. J Immunol 1997 Nov 15;159(10):4720-8.

(113) Shuai K, Halpern J, ten HJ, Rao X, Sawyers CL. Constitutive activation of STAT5 by the BCR-ABL oncogene in chronic myelogenous leukemia. Oncogene 1996 Jul 18;13(2):247-54.

(114) Chuang PY, He JC. JAK/STAT signaling in renal diseases. Kidney Int 2010 Aug;78(3):231-4.

(115) de Groot RP, Raaijmakers JA, Lammers JW, Jove R, Koenderman L. STAT5 activation by BCR-Abl contributes to transformation of K562 leukemia cells. Blood 1999 Aug 1;94(3):1108-12.

(116) Sillaber C, Gesbert F, Frank DA, Sattler M, Griffin JD. STAT5 activation contributes to growth and viability in Bcr/Abl-transformed cells. Blood 2000 Mar 15;95(6):2118-25.

(117) Gesbert F, Griffin JD. Bcr/Abl activates transcription of the Bcl-X gene through STAT5. Blood 2000 Sep 15;96(6):2269-76.

(118) Horita M, Andreu EJ, Benito A, Arbona C, Sanz C, Benet I, et al. Blockade of the Bcr-Abl kinase activity induces apoptosis of chronic myelogenous leukemia cells by suppressing signal transducer and activator of transcription 5-dependent expression of Bcl-xL. J Exp Med 2000 Mar 20;191(6):977-84.

(119) Klejman A, Schreiner SJ, Nieborowska-Skorska M, Slupianek A, Wilson M, Smithgall TE, et al. The Src family kinase Hck couples BCR/ABL to STAT5 activation in myeloid leukemia cells. EMBO J 2002 Nov 1;21(21):5766-74.

(120) Daley GQ, Baltimore D. Transformation of an interleukin 3-dependent hematopoietic cell line by the chronic myelogenous leukemia-specific P210bcr/abl protein. Proc Natl Acad Sci U S A 1988 Dec;85(23):9312-6.

(121) Holyoake TL, Jiang X, Jorgensen HG, Graham S, Alcorn MJ, Laird C, et al. Primitive quiescent leukemic cells from patients with chronic myeloid leukemia spontaneously initiate factor-independent growth in vitro in association with up-regulation of expression of interleukin-3. Blood 2001 Feb 1;97(3):720-8.

(122) Jiang X, Lopez A, Holyoake T, Eaves A, Eaves C. Autocrine production and action of IL-3 and granulocyte colony-stimulating factor in chronic myeloid leukemia. Proc Natl Acad Sci U S A 1999 Oct 26;96(22):12804-9.

(123) Holyoake TL, Jiang X, Drummond MW, Eaves AC, Eaves CJ. Elucidating critical mechanisms of deregulated stem cell turnover in the chronic phase of chronic myeloid leukemia. Leukemia 2002 Apr;16(4):549-58.

(124) Roberts AW. G-CSF: a key regulator of neutrophil production, but that's not all! Growth Factors 2005 Mar;23(1):33-41.

(125) Teixido J, Hemler ME, Greenberger JS, Anklesaria P. Role of beta 1 and beta 2 integrins in the adhesion of human CD34hi stem cells to bone marrow stroma. J Clin Invest 1992 Aug;90(2):358-67.

(126) Hurley RW, McCarthy JB, Verfaillie CM. Direct adhesion to bone marrow stroma via fibronectin receptors inhibits hematopoietic progenitor proliferation. J Clin Invest 1995 Jul;96(1):511-9.

(127) Verfaillie CM, Hurley R, Lundell BI, Zhao C, Bhatia R. Integrin-mediated regulation of hematopoiesis: do BCR/ABL-induced defects in integrin function underlie the abnormal circulation and proliferation of CML progenitors? Acta Haematol 1997;97(1-2):40-52.

(128) Salesse S, Verfaillie CM. Mechanisms underlying abnormal trafficking and expansion of malignant progenitors in CML: BCR/ABL-induced defects in integrin function in CML. Oncogene 2002 Dec 9;21(56):8605-11.

(129) Gordon MY, Dowding CR, Riley GP, Goldman JM, Greaves MF. Altered adhesive interactions with marrow stroma of haematopoietic progenitor cells in chronic myeloid leukaemia. Nature 1987 Jul 23;328(6128):342-4.

(130) Verfaillie CM, McCarthy JB, Mcglave PB. Mechanisms underlying abnormal trafficking of malignant progenitors in chronic myelogenous leukemia. Decreased adhesion to stroma and fibronectin but increased adhesion to the basement membrane components laminin and collagen type IV. J Clin Invest 1992 Oct;90(4):1232-41.

(131) Bazzoni G, Carlesso N, Griffin JD, Hemler ME. Bcr/Abl expression stimulates integrin function in hematopoietic cell lines. J Clin Invest 1996 Jul 15;98(2):521-8.

(132) Fierro FA, Taubenberger A, Puech PH, Ehninger G, Bornhauser M, Muller DJ, et al. BCR/ABL expression of myeloid progenitors increases beta1-integrin mediated adhesion to stromal cells. J Mol Biol 2008 Apr 4;377(4):1082-93.

(133) Bhatia R, Wayner EA, Mcglave PB, Verfaillie CM. Interferon-Alpha Restores Normal Adhesion of Chronic Myelogenous Leukemia Hematopoietic Progenitors to Bone-Marrow Stroma by Correcting Impaired Beta-1 Integrin Receptor Function. Journal of Clinical Investigation 1994 Jul;94(1):384-91.

(134) GALTON DA. Myleran in chronic myeloid leukaemia; results of treatment. Lancet 1953 Jan 31;264(6753):208-13.

(135) Kennedy BJ. Hydroxyurea therapy in chronic myelogenous leukemia. Cancer 1972 Apr;29(4):1052-6.

(136) Kantarjian HM, Giles FJ, O'Brien SM, Talpaz M. Clinical course and therapy of chronic myelogenous leukemia with interferon-alpha and chemotherapy. Hematol Oncol Clin North Am 1998 Feb;12(1):31-80.

(137) Garcia-Manero G, Faderl S, O'Brien S, Cortes J, Talpaz M, Kantarjian HM. Chronic myelogenous leukemia: a review and update of therapeutic strategies. Cancer 2003 Aug 1;98(3):437-57.

(138) Gratwohl A, Hermans J, Goldman JM, Arcese W, Carreras E, Devergie A, et al. Risk assessment for patients with chronic myeloid leukaemia before allogeneic blood or marrow transplantation. Chronic Leukemia Working Party of the European Group for Blood and Marrow Transplantation. Lancet 1998 Oct 3;352(9134):1087-92.

(139) Goldman J. Hematopoietic stem cell transplantation. Curr Opin Hematol 1998 Nov;5(6):417-8.

(140) Kujawski LA, Talpaz M. The role of interferon-alpha in the treatment of chronic myeloid leukemia. Cytokine Growth Factor Rev 2007 Oct;18(5-6):459-71.

(141) Guilhot F, Chastang C, Michallet M, Guerci A, Harousseau JL, Maloisel F, et al. Interferon alfa-2b combined with cytarabine versus interferon alone in chronic myelogenous leukemia. French Chronic Myeloid Leukemia Study Group. N Engl J Med 1997 Jul 24;337(4):223-9.

(142) Tothova E, Fricova M, Kafkova A, Stecova N, Guman T, Raffac S, et al. Hematological and cytogenetic response of interferon alpha 2b alone and

combined interferon alpha plus cytarabine as a first-line treatment in chronic myeloid leukemia. Neoplasma 2000;47(2):125-8.

(143) Druker BJ, Guilhot F, O'Brien SG, Gathmann I, Kantarjian H, Gattermann N, et al. Five-year follow-up of patients receiving imatinib for chronic myeloid leukemia. New England Journal of Medicine 2006 Dec 7;355(23):2408-17.

(144) le Coutre P, Mologni L, Cleris L, Marchesi E, Buchdunger E, Giardini R, et al. In vivo eradication of human BCR/ABL-positive leukemia cells with an ABL kinase inhibitor. Journal of the National Cancer Institute 1999 Jan 20;91(2):163-8.

(145) Druker BJ, Tamura S, Buchdunger E, Ohno S, Segal GM, Fanning S, et al. Effects of a selective inhibitor of the Abl tyrosine kinase on the growth of Bcr-Abl positive cells. Nat Med 1996 May;2(5):561-6.

(146) Schindler T, Bornmann W, Pellicena P, Miller WT, Clarkson B, Kuriyan J. Structural mechanism for STI-571 inhibition of abelson tyrosine kinase. Science 2000 Sep 15;289(5486):1938-42.

(147) Corradi V, Mancini M, Manetti F, Petta S, Santucci MA, Botta M. Identification of the first non-peptidic small molecule inhibitor of the c-Abl/14-3-3 protein-protein interactions able to drive sensitive and Imatinib-resistant leukemia cells to apoptosis. Bioorganic & Medicinal Chemistry Letters 2010 Oct 15;20(20):6133-7.

(148) Deininger MWN, Goldman JM, Lydon N, Melo JV. The tyrosine kinase inhibitor CGP57148B selectively inhibits the growth of BCR-ABL-positive cells. Blood 1997 Nov 1;90(9):3691-8.

(149) Druker BJ, Talpaz M, Resta DJ, Peng B, Buchdunger E, Ford JM, et al. Efficacy and safety of a specific inhibitor of the BCR-ABL tyrosine kinase in chronic myeloid leukemia. N Engl J Med 2001 Apr 5;344(14):1031-7.

(150) Kantarjian H, Sawyers C, Hochhaus A, Guilhot F, Schiffer C, Gambacorti-Passerini C, et al. Hematologic and cytogenetic responses to imatinib mesylate in chronic myelogenous leukemia. N Engl J Med 2002 Feb 28;346(9):645-52.

(151) Talpaz M, Silver RT, Druker BJ, Goldman JM, Gambacorti-Passerini C, Guilhot F, et al. Imatinib induces durable hematologic and cytogenetic responses in patients with accelerated phase chronic myeloid leukemia: results of a phase 2 study. Blood 2002 Mar 15;99(6):1928-37.

(152) Sawyers CL, Hochhaus A, Feldman E, Goldman JM, Miller CB, Ottmann OG, et al. Imatinib induces hematologic and cytogenetic responses in patients with chronic myelogenous leukemia in myeloid blast crisis: results of a phase II study. Blood 2002 May 15;99(10):3530-9.

(153) O'Brien SG, Guilhot F, Larson RA, Gathmann I, Baccarani M, Cervantes F, et al. Imatinib compared with interferon and low-dose cytarabine for newly diagnosed chronic-phase chronic myeloid leukemia. N Engl J Med 2003 Mar 13;348(11):994-1004.

(154) O'Brien SG, Deininger MW. Imatinib in patients with newly diagnosed chronic-phase chronic myeloid leukemia. Semin Hematol 2003 Apr;40(2 Suppl 2):26-30.

(155) Hochhaus A, O'Brien SG, Guilhot F, Druker BJ, Branford S, Foroni L, et al. Six-year follow-up of patients receiving imatinib for the first-line treatment of chronic myeloid leukemia. Leukemia 2009 Jun;23(6):1054-61.

(156) Milojkovic D, Apperley J. State-of-the-art in the treatment of chronic myeloid leukaemia. Current Opinion in Oncology 2008 Jan;20(1):112-21.

(157) Copland M, Jorgensen HG, Holyoake TL. Evolving molecular therapy for chronic myeloid leukaemia - are we on target? Hematology 2005 Oct;10(5):349-59.

(158) Baccarani M, Castagnetti F, Gugliotta G, Palandri F, Soverini S. Response definitions and European Leukemianet Management recommendations. Best Pract Res Clin Haematol 2009 Sep;22(3):331-41.

(159) Tokarski JS, Newitt JA, Chang CY, Cheng JD, Wittekind M, Kiefer SE, et al. The structure of Dasatinib (BMS-354825) bound to activated ABL kinase domain elucidates its inhibitory activity against imatinib-resistant ABL mutants. Cancer Res 2006 Jun 1;66(11):5790-7.

(160) White D, Saunders V, Lyons AB, Branford S, Grigg A, To LB, et al. In vitro sensitivity to imatinib-induced inhibition of ABL kinase activity is predictive of molecular response in patients with de novo CML. Blood 2005 Oct 1;106(7):2520-6.

(161) Hamilton A, Elrick L, Myssina S, Copland M, Jorgensen H, Melo JV, et al. BCR-ABL activity and its response to drugs can be determined in CD34(+) CML stem cells by CrkL phosphorylation status using flow cytometry. Leukemia 2006 Jun;20(6):1035-9.

(162) Hamilton A, Alhashimi F, Myssina S, Jorgensen HG, Holyoake TL. Optimization of methods for the detection of BCR-ABL activity in Philadelphia-positive cells. Experimental Hematology 2009 Mar;37(3):395-401.

(163) Copland M, Hamilton A, Elrick LJ, Baird JW, Allan EK, Jordanides N, et al. Dasatinib (BMS-354825) targets an earlier progenitor population than imatinib in primary CML but does not eliminate the quiescent fraction. Blood 2006 Jun 1;107(11):4532-9.

(164) Tenhoeve J, Morris C, Heisterkamp N, Groffen J. Isolation and Chromosomal Localization of Crkl, A Human Crk-Like Gene. Oncogene 1993 Sep;8(9):2469-74.

(165) Tenhoeve J, Arlinghaus RB, Guo JQ, Heisterkamp N, Groffen J. Tyrosine Phosphorylation of Crkl in Philadelphia(+) Leukemia. Blood 1994 Sep 15;84(6):1731-6.

(166) Tenhoeve J, Kaartinen V, Fioretos T, Haataja L, Voncken JW, Heisterkamp N, et al. Cellular Interactions of Crkl, An Sh2-Sh3 Adapter Protein. Cancer Research 1994 May 15;54(10):2563-7.

(167) deJong R, Tenhoeve J, Heisterkamp N, Groffen J. Tyrosine 207 in CRKL is the BCR/ABL phosphorylation site. Oncogene 1997 Feb 6;14(5):507-13.

(168) Weisberg E, Manley P, Mestan J, Cowan-Jacob S, Ray A, Griffin JD. AMN107 (nilotinib): a novel and selective inhibitor of BCR-ABL. Br J Cancer 2006 Jun 19;94(12):1765-9.

(169) Weisberg E, Manley PW, Breitenstein W, Bruggen J, Cowan-Jacob SW, Ray A, et al. Characterization of AMN107, a selective inhibitor of native and mutant Bcr-Abl. Cancer Cell 2005 Feb;7(2):129-41.

(170) Golemovic M, Verstovsek S, Giles F, Cortes J, Manshouri T, Manley PW, et al. AMN107, a novel aminopyrimidine inhibitor of Bcr-Abl, has in vitro activity against imatinib-resistant chronic myeloid leukemia. Clin Cancer Res 2005 Jul 1;11(13):4941-7.

(171) Deremer DL, Ustun C, Natarajan K. Nilotinib: a second-generation tyrosine kinase inhibitor for the treatment of chronic myelogenous leukemia. Clin Ther 2008 Nov;30(11):1956-75.

(172) Jorgensen HG, Allan EK, Jordanides NE, Mountford JC, Holyoake TL. Nilotinib exerts equipotent antiproliferative effects to imatinib and does not induce apoptosis in CD34(+) CML cells. Blood 2007 May 1;109(9):4016-9.

(173) O'Hare T, Walters DK, Stoffregen EP, Jia TP, Manley PW, Mestan J, et al. In vitro activity of Bcr-Abl inhibitors AMN107 and BMS-354825 against clinically relevant imatinib-resistant Abl kinase domain mutants. Cancer Research 2005 Jun 1;65(11):4500-5.

(174) Kantarjian H, Giles F, Wunderle L, Bhalla K, O'Brien S, Wassmann B, et al. Nilotinib in imatinib-resistant CML and Philadelphia chromosome-positive ALL. N Engl J Med 2006 Jun 15;354(24):2542-51.

(175) Kantarjian HM, Giles F, Gattermann N, Bhalla K, Alimena G, Palandri F, et al. Nilotinib (formerly AMN107), a highly selective BCR-ABL tyrosine kinase inhibitor, is effective in patients with Philadelphia chromosome-positive chronic myelogenous leukemia in chronic phase following imatinib resistance and intolerance. Blood 2007 Nov 15;110(10):3540-6.

(176) US National Institutes of Health NCI. FDA Approval for Nilotinib. http://www.cancer.gov/cancertopics/druginfo/fda-nilotinib Last Updated: 18 Jan 2011. Access Date: 22 Jan 2011.

(177) Lombardo LJ, Lee FY, Chen P, Norris D, Barrish JC, Behnia K, et al. Discovery of N-(2-chloro-6-methyl- phenyl)-2-(6-(4-(2-hydroxyethyl)- piperazin-1-yl)-2-

methylpyrimidin-4- ylamino)thiazole-5-carboxamide (BMS-354825), a dual Src/Abl kinase inhibitor with potent antitumor activity in preclinical assays. J Med Chem 2004 Dec 30;47(27):6658-61.

(178) Hochhaus A, Baccarani M, Deininger M, Apperley JF, Lipton JH, Goldberg SL, et al. Dasatinib induces durable cytogenetic responses in patients with chronic myelogenous leukemia in chronic phase with resistance or intolerance to imatinib. Leukemia 2008 Jun;22(6):1200-6.

(179) Guilhot F, Apperley J, Kim DW, Bullorsky EO, Baccarani M, Roboz GJ, et al. Dasatinib induces significant hematologic and cytogenetic responses in patients with imatinib-resistant or -intolerant chronic myeloid leukemia in accelerated phase. Blood 2007 May 15;109(10):4143-50.

(180) Cortes J, Rousselot P, Kim DW, Ritchie E, Hamerschlak N, Coutre S, et al. Dasatinib induces complete hematologic and cytogenetic responses in patients with imatinib-resistant or -intolerant chronic myeloid leukemia in blast crisis. Blood 2007 Apr 15;109(8):3207-13.

(181) US National Institutes of Health NCI. FDA Approval for Dasatinib. http://www.cancer.gov/cancertopics/druginfo/fda-dasatinib Last Updated: 29 Oct 2010. Access Date: 22 Jan 2011.

(182) Ross DM, Branford S, Seymour JF, Schwarer AP, Arthur C, Bartley PA, et al. Patients with chronic myeloid leukemia who maintain a complete molecular response after stopping imatinib treatment have evidence of persistent leukemia by DNA PCR. Leukemia 2010 Oct;24(10):1719-24.

(183) Wang Y, Cai D, Brendel C, Barett C, Erben P, Manley PW, et al. Adaptive secretion of granulocyte-macrophage colony-stimulating factor (GM-CSF) mediates imatinib and nilotinib resistance in BCR/ABL+ progenitors via JAK-2/STAT-5 pathway activation. Blood 2007 Mar 1;109(5):2147-55.

(184) Shi P, Chandra J, Sun X, Gergely M, Cortes JE, Garcia-Manero G, et al. Inhibition of IGF-IR tyrosine kinase induces apoptosis and cell cycle arrest in imatinib-resistant chronic myeloid leukaemia cells. J Cell Mol Med 2010 Jun;14(6B):1777-92.

(185) Carew JS, Nawrocki ST, Giles FJ, Cleveland JL. Targeting autophagy: a novel anticancer strategy with therapeutic implications for imatinib resistance. Biologics 2008 Jun;2(2):201-4.

(186) Bellodi C, Lidonnici MR, Hamilton A, Helgason GV, Soliera AR, Ronchetti M, et al. Targeting autophagy potentiates tyrosine kinase inhibitor-induced cell death in Philadelphia chromosome-positive cells, including primary CML stem cells. Journal of Clinical Investigation 2009 May;119(5):1109-23.

(187) Shah NP, Nicoll JM, Nagar B, Gorre ME, Paquette RL, Kuriyan J, et al. Multiple BCR-ABL kinase domain mutations confer polyclonal resistance to the tyrosine kinase inhibitor imatinib (STI571) in chronic phase and blast crisis chronic myeloid leukemia. Cancer Cell 2002 Aug;2(2):117-25.

(188) Bradeen HA, Eide CA, O'Hare T, Johnson KJ, Willis SG, Lee FY, et al. Comparison of imatinib mesylate, dasatinib (BMS-354825), and nilotinib (AMN107) in an N-ethyl-N-nitrosourea (ENU)-based mutagenesis screen: high efficacy of drug combinations. Blood 2006 Oct 1;108(7):2332-8.

(189) O'Hare T, Eide CA, Deininger MW. Bcr-Abl kinase domain mutations, drug resistance, and the road to a cure for chronic myeloid leukemia. Blood 2007 Oct 1;110(7):2242-9.

(190) Borst P, Elferink RO. Mammalian ABC transporters in health and disease. Annu Rev Biochem 2002;71:537-92.

(191) Mahon FX, Belloc F, Lagarde V, Chollet C, Moreau-Gaudry F, Reiffers J, et al. MDR1 gene overexpression confers resistance to imatinib mesylate in leukemia cell line models. Blood 2003 Mar 15;101(6):2368-73.

(192) Hatziieremia S, Jordanides NE, Holyoake TL, Mountford JC, Jorgensen HG. Inhibition of MDR1 does not sensitize primitive chronic myeloid leukemia CD34+ cells to imatinib. Exp Hematol 2009 Jun;37(6):692-700.

(193) Burger H, van TH, Boersma AW, Brok M, Wiemer EA, Stoter G, et al. Imatinib mesylate (STI571) is a substrate for the breast cancer resistance protein (BCRP)/ABCG2 drug pump. Blood 2004 Nov 1;104(9):2940-2.

(194) Brendel C, Scharenberg C, Dohse M, Robey RW, Bates SE, Shukla S, et al. Imatinib mesylate and nilotinib (AMN107) exhibit high-affinity interaction with ABCG2 on primitive hematopoietic stem cells. Leukemia 2007 Jun;21(6):1267-75.

(195) Jordanides NE, Jorgensen HG, Holyoake TL, Mountford JC. Functional ABCG2 is overexpressed on primary CML CD34+ cells and is inhibited by imatinib mesylate. Blood 2006 Aug 15;108(4):1370-3.

(196) Tiwari AK, Sodani K, Wang SR, Kuang YH, Ashby CR, Jr., Chen X, et al. Nilotinib (AMN107, Tasigna) reverses multidrug resistance by inhibiting the activity of the ABCB1/Pgp and ABCG2/BCRP/MXR transporters. Biochem Pharmacol 2009 Jul 15;78(2):153-61.

(197) Davies A, Jordanides NE, Giannoudis A, Lucas CM, Hatziieremia S, Harris RJ, et al. Nilotinib concentration in cell lines and primary CD34(+) chronic myeloid leukemia cells is not mediated by active uptake or efflux by major drug transporters. Leukemia 2009 Nov;23(11):1999-2006.

(198) Vigneri P, Wang JYJ. Induction of apoptosis in chronic myelogenous leukemia cells through nuclear entrapment of BCR-ABL tyrosine kinase. Nature Medicine 2001 Feb;7(2):228-34.

(199) Fornerod M, Ohno M, Yoshida M, Mattaj IW. CRM1 is an export receptor for leucine-rich nuclear export signals. Cell 1997 Sep 19;90(6):1051-60.

(200) Wang JYJ. Regulation of cell death by the Abl tyrosine kinase. Oncogene 2000 Nov 20;19(49):5643-50.

(201) Graham SM, Jorgensen HG, Allan E, Pearson C, Alcorn MJ, Richmond L, et al. Primitive, quiescent, Philadelphia-positive stem cells from patients with chronic myeloid leukemia are insensitive to STI571 in vitro. Blood 2002 Jan 1;99(1):319-25.

(202) Jorgensen HG, Allan EK, Graham SM, Godden JL, Richmond L, Elliott MA, et al. Lonafarnib reduces the resistance of primitive quiescent CML cells to imatinib mesylate in vitro. Leukemia 2005 Jul;19(7):1184-91.

(203) Holtz MS, Forman SJ, Bhatia R. Nonproliferating CML CD34(+) progenitors are resistant to apoptosis induced by a wide range of proapoptotic stimuli. Leukemia 2005 Jun;19(6):1034-41.

(204) Barbacid M. Ras Genes. Annual Review of Biochemistry 1987;56:779-827.

(205) Downward J. Regulatory Mechanisms for Ras Proteins. Bioessays 1992 Mar;14(3):177-84.

(206) Hunt JT, Ding CZ, Batorsky R, Bednarz M, Bhide R, Cho Y, et al. Discovery of (R)-7-cyano-2,3,4,5-tetrahydro-1-(1H-imidazol-4-ylmethyl)-3-(phenylmethyl)-4-(2-thienylsulfonyl)-1H-1,4-benzodiazepine (BMS-214662), a farnesyltransferase inhibitor with potent preclinical antitumor activity. Journal of Medicinal Chemistry 2000 Oct 5;43(20):3587-95.

(207) Gibbs JB. Ras C-Terminal Processing Enzymes - Minireview New Drug Targets. Cell 1991 Apr 5;65(1):1-4.

(208) Kato K, Cox AD, Hisaka MM, Graham SM, Buss JE, Der CJ. Isoprenoid Addition to Ras Protein Is the Critical Modification for Its Membrane Association and Transforming Activity. Proceedings of the National Academy of Sciences of the United States of America 1992 Jul 15;89(14):6403-7.

(209) Kohl NE, Wilson FR, Mosser SD, Giuliani E, Desolms SJ, Conner MW, et al. Protein Farnesyltransferase Inhibitors Block the Growth of Ras-Dependent Tumors in Nude-Mice. Proceedings of the National Academy of Sciences of the United States of America 1994 Sep 13;91(19):9141-5.

(210) Bos JL. Ras Oncogenes in Human Cancer - A Review. Cancer Research 1989 Sep 1;49(17):4682-9.

(211) Manne V, Lee FYF, Bol DK, Gullo-Brown J, Fairchild CR, Lombardo LJ, et al. Apoptotic and cytostatic farnesyltransferase inhibitors have distinct pharmacology and efficacy profiles in tumor models. Cancer Research 2004 Jun 1;64(11):3974-80.

(212) Copland M, Pellicano F, Richmond L, Allan EK, Hamilton A, Lee FY, et al. BMS-214662 potently induces apoptosis of chronic myeloid leukemia stem and

progenitor cells and synergizes with tyrosine kinase inhibitors. Blood 2008 Mar 1;111(5):2843-53.

(213) Pellicano F, Copland M, Jorgensen HG, Mountford J, Leber B, Holyoake TL. BMS-214662 induces mitochondrial apoptosis in chronic myeloid leukemia (CML) stem/progenitor cells, including CD34(+)38(-) cells, through activation of protein kinase C beta. Blood 2009 Nov 5;114(19):4186-96.

(214) Amin HM, Hoshino K, Yang H, Lin Q, La R, Garcia-Manero G. Decreased expression level of SH2 domain-containing protein tyrosine phosphatase-I (ShpI) is associated with progression of chronic myeloid leukaemia. Journal of Pathology 2007 Aug;212(4):402-10.

(215) Xu F, Xu MJ, Zhao R, Guerrah A, Zeng F, Zhao ZJ. Tyrosine phosphatases SHP-1 and SHP-2 are associated with distinct tyrosine-phosphorylated proteins. Exp Cell Res 2002 Jan 1;272(1):75-83.

(216) Samanta AK, Chakraborty SN, Wang Y, Kantarjian H, Sun X, Hood J, et al. Jak2 inhibition deactivates Lyn kinase through the SET-PP2A-SHP1 pathway, causing apoptosis in drug-resistant cells from chronic myelogenous leukemia patients. Oncogene 2009 Apr 9;28(14):1669-81.

(217) Neviani P, Santhanam R, Trotta R, Notari M, Blaser BW, Liu S, et al. The tumor suppressor PP2A is functionally inactivated in blast crisis CML through the inhibitory activity of the BCR/ABL-regulated SET protein. Cancer Cell 2005 Nov;8(5):355-68.

(218) Li M, Makkinje A, Damuni Z. The myeloid leukemia-associated protein SET is a potent inhibitor of protein phosphatase 2A. J Biol Chem 1996 May 10;271(19):11059-62.

(219) Tsui HW, Siminovitch KA, de SL, Tsui FW. Motheaten and viable motheaten mice have mutations in the haematopoietic cell phosphatase gene. Nat Genet 1993 Jun;4(2):124-9.

(220) Jiao H, Berrada K, Yang W, Tabrizi M, Platanias LC, Yi T. Direct association with and dephosphorylation of Jak2 kinase by the SH2-domain-containing protein tyrosine phosphatase SHP-1. Mol Cell Biol 1996 Dec;16(12):6985-92.

(221) Wu C, Guan Q, Wang Y, Zhao ZJ, Zhou GW. SHP-1 suppresses cancer cell growth by promoting degradation of JAK kinases. J Cell Biochem 2003 Dec 1;90(5):1026-37.

(222) Samanta A, Perazzona B, Chakraborty S, Sun X, Modi H, Bhatia R, et al. Janus kinase 2 regulates Bcr-Abl signaling in chronic myeloid leukemia. Leukemia 2010 Dec 24.

(223) Samanta AK, Lin H, Sun T, Kantarjian H, Arlinghaus RB. Janus kinase 2: a critical target in chronic myelogenous leukemia. Cancer Res 2006 Jul 1;66(13):6468-72.

(224) Koyama N, Koschmieder S, Tyagi S, Portero-Robles I, Chromic J, Myloch S, et al. Inhibition of phosphotyrosine phosphatase 1B causes resistance in BCR-ABL-positive leukemia cells to the ABL kinase inhibitor STI571. Clinical Cancer Research 2006 Apr 1;12(7):2025-31.

(225) LaMontagne KR, Flint AJ, Franza BR, Pendergast AM, Tonks NK. Protein tyrosine phosphatase 1B antagonizes signalling by oncoprotein tyrosine kinase p210 bcr-abl in vivo. Molecular and Cellular Biology 1998 May;18(5):2965-75.

(226) LaMontagne KR, Jr., Hannon G, Tonks NK. Protein tyrosine phosphatase PTP1B suppresses p210 bcr-abl-induced transformation of rat-1 fibroblasts and promotes differentiation of K562 cells. Proc Natl Acad Sci U S A 1998 Nov 24;95(24):14094-9.

(227) Hantschel O, Wiesner S, Guttler T, Mackereth CD, Rix LL, Mikes Z, et al. Structural basis for the cytoskeletal association of Bcr-Abl/c-Abl. Mol Cell 2005 Aug 19;19(4):461-73.

(228) Hu GK, Feng H, Zhang T, Yan YH, Wu B, Jiang Q, et al. Molecular cloning of cDNAs for 14-3-3 and its protein interactions in a white-rot fungus Phanerochaete chrysosporium. Annals of Microbiology 2006;56(3):191-6.

(229) Morrison DK. The 14-3-3 proteins: integrators of diverse signaling cues that impact cell fate and cancer development. Trends in Cell Biology 2009 Jan;19(1):16-23.

(230) Aitken A, Baxter H, Dubois T, Clokie S, Mackie S, Mitchell K, et al. Specificity of 14-3-3 isoform dimer interactions and phosphorylation. Biochemical Society Transactions 2002 Aug;30:351-60.

(231) Yoshida K, Yamaguchi T, Natsume T, Kufe D, Miki Y. JNK phosphorylation of 14-3-3 proteins regulates nuclear targeting of c-Abl in the apoptotic response to DNA damage. Nature Cell Biology 2005 Mar;7(3):278-U97.

(232) Braselmann S, Mccormick F. Bcr and Raf Form A Complex In-Vivo Via 14-3-3-Proteins. Embo Journal 1995 Oct 2;14(19):4839-48.

(233) Clokie SJ, Cheung KY, Mackie S, Marquez R, Peden AH, Aitken A. BCR kinase phosphorylates 14-3-3 Tau on residue 233. Febs Journal 2005 Aug;272(15):3767-76.

(234) Pendergast AM. Stress and death: breaking up the c-Abl/14-3-3 complex in apoptosis. Nature Cell Biology 2005 Mar;7(3):213-4.

(235) Goldstein JL, Brown MS. Lipoprotein Receptors, Cholesterol-Metabolism, and Atherosclerosis. Archives of Pathology 1975;99(4):181-4.

(236) Brown MS, Goldstein JL. A receptor-mediated pathway for cholesterol homeostasis. Science 1986 Apr 4;232(4746):34-47.

(237) Vitols S, Gahrton G, Ost A, Peterson C. Elevated Low-Density Lipoprotein Receptor Activity in Leukemic-Cells with Monocytic Differentiation. Blood 1984;63(5):1186-93.

(238) Brown MS, Goldstein JL. Receptor-mediated endocytosis: insights from the lipoprotein receptor system. Proc Natl Acad Sci U S A 1979 Jul;76(7):3330-7.

(239) Gal D, Ohashi M, Macdonald PC, Buchsbaum HJ, Simpson ER. Low-Density Lipoprotein As A Potential Vehicle for Chemotherapeutic-Agents and Radionucleotides in the Management of Gynecologic Neoplasms. American Journal of Obstetrics and Gynecology 1981;139(8):877-85.

(240) Baillie G, Owens MD, Halbert GW. A synthetic low density lipoprotein particle capable of supporting U937 proliferation in vitro. Journal of Lipid Research 2002 Jan;43(1):69-73.

(241) Owens MD, Baillie G, Halbert GW. Physicochemical properties of microemulsion analogues of low density lipoprotein containing amphiphatic apoprotein B receptor sequences. International Journal of Pharmaceutics 2001 Oct 9;228(1-2):109-17.

(242) Hayavi S, Halbert GW. Synthetic low-density lipoprotein, a novel biomimetic lipid supplement for serum-free tissue culture. Biotechnology Progress 2005 Jul;21(4):1262-8.

(243) Halbert GW, Stuart JFB, Florence AT. The Incorporation of Lipid-Soluble Antineoplastic Agents Into Microemulsions Protein-Free Analogs of Low-Density Lipoprotein. International Journal of Pharmaceutics 1984;21(2):219-32.

(244) Nikanjam M, Blakely EA, Bjornstad KA, Shu X, Budinger TF, Forte TM. Synthetic nano-low density lipoprotein as targeted drug delivery vehicle for glioblastoma multiforme. International Journal of Pharmaceutics 2007 Jan 2;328(1):86-94.

(245) Wen ST, Jackson PK, VanEtten RA. The cytostatic function of c-Abl is controlled by multiple nuclear localization signals and requires the p53 and Rb tumor suppressor gene products. Embo Journal 1996 Apr 1;15(7):1583-95.

(246) Aloisi A, Di Gregorio S, Stagno F, Guglielmo P, Mannino F, Sormani MP, et al. BCR-ABL nuclear entrapment kills human CMIL cells: ex vivo study on 35 patients with the combination of imatinib mesylate and leptomycin B. Blood 2006 Feb 15;107(4):1591-8.

(247) Allan EK, Hamilton A, Hatziieremia S, Zhou P, Jorgensen HG, Vigneri P, et al. Nuclear entrapment of BCR-ABL by combining imatinib mesylate with leptomycin B does not eliminate CD34(+) chronic myeloid leukaemia cells. Leukemia 2009 May;23(5):1006-8.

(248) Patel H, Marley SB, Greener L, Gordon MY. Subcellular distribution of p210(BCR-ABL) in CML cell lines and primary CD34(+) CML cells. Leukemia 2008 Mar;22(3):559-71.

(249) Hamilton A, Alcorn M, Allan E, Helgasson GV, Nicolini F, Blair A, et al. Despite treatment with high dose dasatinib in the absence of growth factors, CML stem

cells survive for 12 days in vitro. British Journal of Haematology 2008 Apr;141:47.

(250) Poppema S, Lai R, Visser L, Yan XJ. CD45 (leucocyte common antigen) expression in T and B lymphocyte subsets. Leuk Lymphoma 1996 Jan;20(3-4):217-22.

(251) Ye J, Song YS, Kang SH, Yao K, Kim JC. Involvement of bone marrow-derived stem and progenitor cells in the pathogenesis of pterygium. Eye (Lond) 2004 Aug;18(8):839-43.

(252) Brown DA, London E. Functions of lipid rafts in biological membranes. Annual Review of Cell and Developmental Biology 1998;14:111-36.

(253) Brown DA, London E. Structure and function of sphingolipid- and cholesterol-rich membrane rafts. J Biol Chem 2000 Jun 9;275(23):17221-4.

(254) Hamilton A, Allan E, Alcorn M, Nicolini F, Blair A, Schemionek M, et al. Growth Factor Deprivation Combined with Prolonged Inhibition of BCR-ABL Does Not Eradicate Functional CML Stem Cells. Blood (ASH Annual Meeting Abstracts) 2008 Nov 16;112(11).

(255) Kuci S, Wessels JT, Buhring HJ, Schilbach K, Schumm M, Seitz G, et al. Identification of a novel class of human adherent CD34(-) stem cells that give rise to SCID-repopulating cells. Blood 2003 Feb 1;101(3):869-76.

(256) Gallacher L, Murdoch B, Wu DM, Karanu FN, Keeney M, Bhatia M. Isolation and characterization of human CD34(-)Lin(-) and CD34(+)Lin(-) hematopoietic stem cells using cell surface markers AC133 and CD7. Blood 2000 May 1;95(9):2813-20.

(257) Dixon AS, Kakar M, Schneider KMH, Constance JE, Paullin BC, Lim CS. Controlling subcellular localization to alter function: Sending oncogenic Bcr-Abl to the nucleus causes apoptosis. Journal of controlled release 2009 Dec 16;140(3):245-9.

(258) Muslin AJ, Xing HM. 14-3-3 proteins: regulation of subcellular localization by molecular interference. Cellular Signalling 2000 Dec;12(11-12):703-9.

(259) Dong S, Kang S, Lonial S, Khoury HJ, Viallet J, Chen J. Targeting 14-3-3 sensitizes native and mutant BCR-ABL to inhibition with U0126, rapamycin and Bcl-2 inhibitor GX15-070. Leukemia 2008 Mar;22(3):572-7.

(260) Corradi V, Mancini M, Manetti F, Petta S, Santucci MA, Botta M. Identification of the first non-peptidic small molecule inhibitor of the c-Abl/14-3-3 protein-protein interactions able to drive sensitive and Imatinib-resistant leukemia cells to apoptosis. Bioorganic & Medicinal Chemistry Letters 2010 Oct 15;20(20):6133-7.

(261) Pathak MK, Yi TL. Sodium stibogluconate is a potent inhibitor of protein tyrosine phosphatases and augments cytokine responses in hemopoietic cell lines. Journal of Immunology 2001 Sep 15;167(6):3391-7.

(262) Bruecher-Encke B, Griffin JD, Neel BG, Lorenz U. Role of the tyrosine phosphatase SHP-1 in K562 cell differentiation. Leukemia 2001 Sep;15(9):1424-32.

(263) Hanke JH, Gardner JP, Dow RL, Changelian PS, Brissette WH, Weringer EJ, et al. Discovery of a novel, potent, and Src family-selective tyrosine kinase inhibitor - Study of Lck- and FynT-dependent T cell activation. Journal of Biological Chemistry 1996 Jan 12;271(2):695-701.

(264) Wilson MB, Schreiner SJ, Choi HJ, Kamens J, Smithgall TE. Selective pyrrolo-pyrimidine inhibitors reveal a necessary role for Src family kinases in Bcr-Abl signal transduction and oncogenesis. Oncogene 2002 Nov 21;21(53):8075-88.

(265) Khorashad JS, Wagner S, Greener L, Marin D, Reid A, Milojkovic D, et al. The level of BCR-ABL1 kinase activity before treatment does not identify chronic myeloid leukemia patients who fail to achieve a complete cytogenetic response on imatinib. Haematologica-the Hematology Journal 2009 Jun;94(6):861-4.

(266) Qiao YF, Molina H, Pandey A, Zhang J, Cole PA. Chemical rescue of a mutant enzyme in living cells. Science 2006 Mar 3;311(5765):1293-7.

(267) Mao JH, Sun XY, Zhang QY, Huang QH, Liu P, Xie YY, et al. E3 Ligase c-CBL Mediates Ubiquitination-Proteasomal Degradation of BCR-ABL and

Therapeutic Effects against BCR-ABL Leukemia. Blood 2009 Nov 20;114(22):1261.

(268) Echarri A, Pendergast AM. Activated c-Abl is degraded by the ubiquitin-dependent proteasome pathway. Current Biology 2001 Nov 13;11(22):1759-65.

(269) Magill L, Lynas J, Morris TCM, Walker B, Irvine AE. Proteasome proteolytic activity in hematopoietic cells from patients with chronic myeloid leukemia and multiple myeloma. Haematologica 2004 Dec;89(12):1428-33.

(270) Sattler M, Verma S, Shrikhande G, Byrne CH, Pride YB, Winkler T, et al. The BCR/ABL tyrosine kinase induces production of reactive oxygen species in hematopoietic cells. Journal of Biological Chemistry 2000 Aug 11;275(32):24273-8.

(271) Robinson K, Jones D, Patel Y, Martin H, Madrazo J, Martin S, et al. Mechanism of Inhibition of Protein-Kinase-C by 14-3-3-Isoforms - 14-3-3-Isoforms do Not Have Phospholipase A(2) Activity. Biochemical Journal 1994 May 1;299:853-61.

(272) Gurusamy N, Watanabe K, Ma ML, Zhang SS, Muslin AJ, Kodama M, et al. Inactivation of 14-3-3 protein exacerbates cardiac hypertrophy and fibrosis through enhanced expression of protein kinase C beta 2 in experimental diabetes. Biological & Pharmaceutical Bulletin 2005 Jun;28(6):957-62.

(273) Alexopoulos CG, Blatsios B, Avgerinos A. Serum-Lipids and Lipoprotein Disorders in Cancer-Patients. Cancer 1987 Dec 15;60(12):3065-70.

(274) Williams RR, Sorlie PD, Feinleib M, Mcnamara PM, Kannel WB, Dawber TR. Cancer Incidence by Levels of Cholesterol. Jama-Journal of the American Medical Association 1981;245(3):247-52.

(275) Fiorenza AM, Branchi A, Sommariva D. Serum lipoprotein profile in patients with cancer. A comparison with non-cancer subjects. International Journal of Clinical & Laboratory Research 2000 Sep;30(3):141-5.

(276) Ho YK, Smith RG, Brown MS, Goldstein JL. Low-Density Lipoprotein (Ldl) Receptor Activity in Human Acute Myelogenous Leukemia-Cells. Blood 1978;52(6):1099-114.

(277) Zhou P, Hatziieremia S, Elliott MA, Scobie L, Crossan C, Michie AM, et al. Uptake of synthetic Low Density Lipoprotein by leukemic stem cells — a potential stem cell targeted drug delivery strategy. Journal of controlled release 2010 Dec 20;148(3):380-7.

(278) Kerkela R, Grazette L, Yacobi R, Iliescu C, Patten R, Beahm C, et al. Cardiotoxicity of the cancer therapeutic agent imatinib mesylate. Nature Medicine 2006 Aug;12(8):908-16.

(279) Hasinoff BB. The cardiotoxicity and myocyte damage caused by small molecule anticancer tyrosine kinase inhibitors is correlated with lack of target specificity. Toxicology and Applied Pharmacology 2010 Apr 15;244(2):190-5.

(280) Chu ACY, Tsang SY, Lo EHK, Fung KP. Low density lipoprotein as a targeted carrier for doxorubicin in nude mice bearing human hepatoma HepG2 cells. Life Sciences 2001 Dec 21;70(5):591-601.

(281) Rudling MJ, Collins VP, Peterson CO. Delivery of Aclacinomycin-A to Human Glioma-Cells Invitro by the Low-Density Lipoprotein Pathway. Cancer Research 1983;43(10):4600-5.

(282) Laster BH, Kahl SB, Popenoe EA, Pate DW, Fairchild RG. Biological Efficacy of Boronated Low-Density-Lipoprotein for Boron Neutron-Capture Therapy As Measured in Cell-Culture. Cancer Research 1991 Sep 1;51(17):4588-93.

(283) Neviani P, Harb JG, Oaks JJ, Walker C, Santhanam R, Paisie C, et al. BCR-ABL1 Kinase Activity but Not Its Expression Is Dispensable for Ph+ Quiescent Stem Cell Survival Which Depends on the PP2A-Controlled Jak2 Activation and Is Sensitive to FTY720 Treatment. Blood (ASH Annual Meeting Abstracts) 2010 Nov 19;116(21).

(284) Jorgensen HG, Copland M, Allan EK, Jiang X, Eaves A, Eaves C, et al. Intermittent exposure of primitive quiescent chronic myeloid leukemia cells to

granulocyte-colony stimulating factor in vitro promotes their elimination by imatinib mesylate. Clin Cancer Res 2006 Jan 15;12(2):626-33.

(285) Passegue E, Ernst P. IFN-alpha wakes up sleeping hematopoietic stem cells. Nat Med 2009 Jun;15(6):612-3.

(286) Zhang J, Adrian FJ, Jahnke W, Cowan-Jacob SW, Li AG, Iacob RE, et al. Targeting Bcr-Abl by combining allosteric with ATP-binding-site inhibitors. Nature 2010 Jan 28;463(7280):501-6.

(287) Ito K, Bernardi R, Morotti A, Matsuoka S, Saglio G, Ikeda Y, et al. PML targeting eradicates quiescent leukaemia-initiating cells. Nature 2008 Jun 19;453(7198):1072-8.

(288) Chen Y, Hu Y, Zhang H, Peng C, Li S. Loss of the Alox5 gene impairs leukemia stem cells and prevents chronic myeloid leukemia. Nat Genet 2009 Jul;41(7):783-92.

(289) Quintas-Cardama A, Cortes J. Omacetaxine mepesuccinate--a semisynthetic formulation of the natural antitumoral alkaloid homoharringtonine, for chronic myelocytic leukemia and other myeloid malignancies. IDrugs 2008 May;11(5):356-72.

(290) Chen Y, Hu Y, Michaels S, Segal D, Brown D, Li S. Inhibitory effects of omacetaxine on leukemic stem cells and BCR-ABL-induced chronic myeloid leukemia and acute lymphoblastic leukemia in mice. Leukemia 2009 Aug;23(8):1446-54.

(291) Zhao C, Chen A, Jamieson CH, Fereshteh M, Abrahamsson A, Blum J, et al. Hedgehog signalling is essential for maintenance of cancer stem cells in myeloid leukaemia. Nature 2009 Apr 9;458(7239):776-9.

(292) Jaras M, Johnels P, Hansen N, Agerstam H, Tsapogas P, Rissler M, et al. Isolation and killing of candidate chronic myeloid leukemia stem cells by antibody targeting of IL-1 receptor accessory protein. Proc Natl Acad Sci U S A 2010 Sep 14;107(37):16280-5.

(293) Myers MP, Andersen JN, Cheng A, Tremblay ML, Horvath CM, Parisien JP, et al. TYK2 and JAK2 are substrates of protein-tyrosine phosphatase 1B. J Biol Chem 2001 Dec 21;276(51):47771-4.

(294) Agarwal A, Meckenzie RJ, O'Hare T, Vasudevan KB, LaTocha DH, Loriaux MM, et al. p27 Is Mislocalized to the Cytoplasm by BCR-ABL In a Kinase-Independent Manner and Contributes to Leukemogenesis. Blood (ASH Annual Meeting Abstracts) 2010 Nov 19;116(21).

(295) Zhao C, Blum J, Chen A, Kwon HY, Jung SH, Cook JM, et al. Loss of beta-catenin impairs the renewal of normal and CML stem cells in vivo. Cancer Cell 2007 Dec;12(6):528-41.

(296) Liu D, Bienkowska J, Petosa C, Collier RJ, Fu H, Liddington R. Crystal-Structure of the Zeta-Isoform of the 14-3-3 Protein. Nature 1995 Jul 13;376(6536):191-4.

(297) Wang BC, Yang HZ, Liu YC, Jelinek T, Zhang LX, Ruoslahti E, et al. Isolation of high-affinity peptide antagonists of 14-3-3 proteins by phage display. Biochemistry 1999 Sep 21;38(38):12499-504.

(298) Masters SC, Fu H. 14-3-3 proteins mediate an essential anti-apoptotic signal. Journal of Biological Chemistry 2001 Nov 30;276(48):45193-200.

(299) Mancini M, Veljkovic N, Corradi V, Zuffa E, Corrado P, Pagnotta E, et al. 14-3-3 Ligand Prevents Nuclear Import of c-ABL Protein in Chronic Myeloid Leukemia. Traffic 2009 Jun;10(6):637-47.

(300) Drummond MW, Heaney N, Kaeda J, Nicolini FE, Clark RE, Wilson G, et al. A pilot study of continuous imatinib vs pulsed imatinib with or without G-CSF in CML patients who have achieved a complete cytogenetic response. Leukemia 2009 Jun;23(6):1199-201.

(301) Foo J, Drummond MW, Clarkson B, Holyoake T, Michor F. Eradication of chronic myeloid leukemia stem cells: a novel mathematical model predicts no therapeutic benefit of adding G-CSF to imatinib. PLoS Comput Biol 2009 Sep;5(9):e1000503.

(302) Essers MA, Offner S, Blanco-Bose WE, Waibler Z, Kalinke U, Duchosal MA, et al. IFNalpha activates dormant haematopoietic stem cells in vivo. Nature 2009 Apr 16;458(7240):904-8.

(303) Alimena G, Breccia M, Luciano L, Quarantelli F, Diverio D, Izzo B, et al. Imatinib mesylate therapy in chronic myeloid leukemia patients in stable complete cytogenic response after interferon-alpha results in a very high complete molecular response rate. Leuk Res 2008 Feb;32(2):255-61.